

https://dspace.org/

Application of integrated methods to assess and characterise the hydrogeology of coastal aquifers in parts of Lagos, Southwest, Nigeria

Yusuf, Mumeen Adebayo

2020

https://hdl.handle.net/10539/30986

Downloaded from a DSpace repository. https://dspace.org/

`APPLICATION OF INTEGRATED METHODS TO ASSESS AND CHARACTERISE THE HYDROGEOLOGY OF COASTAL AQUIFERS IN PARTS OF LAGOS, SOUTHWEST, NIGERIA

Mumeen Adebayo Yusuf

Student Number: 1536672

A Thesis submitted to the Faculty of Science, University of the Witwatersrand, Johannesburg, in fulfilment of the requirements for the degree of Doctor of Philosophy in Geology (Hydrogeology)



WITS
UNIVERSITY

School of Geosciences

Supervisor: Professor Tamiru Abiye

Johannesburg, 2020

DECLARATION

I declare that this Thesis is my own, unaided work. It is being submitted for the degree of Doctor of Philosophy at the University of the Witwatersrand, Johannesburg, South Africa. It has not been submitted before for any degree or examination at any other university.

..... 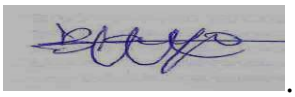 .....

Mumeen Adebayo Yusuf

Signed on the 5th day of November 2020 at Johannesburg.

ABSTRACT

The scope of this Thesis was to apply integrated methods to characterise the groundwater systems of the Lagos Coastal Basin. Like every coastal area in the world, saline intrusion has been the major challenge threatening the fresh groundwater aquifers of the study area over the last couple of decades, and thus, necessitating its assessment. Environmental isotopes, being a reliable and standard tool in hydrological investigation, was employed in combination with geophysical and hydrogeochemical methods to study the coastal aquifer systems.

Geophysical probing of the subsurface revealed an alternating sequence of clay and sand, constituting the major lithological units in the study area. The basin aquifers are hosted essentially by sands and clayey sand, while the modes of aquifer occurrences are unconfined to semi-confined and confined for shallow and deep aquifers, respectively.

Hydrochemical interpretation identified a surficial thin layer of fresh groundwater overlying the main zone of saline intrusion, which essentially comprises Ca-HCO_3 and Ca-Mg-HCO_3, Ca-Mg-HCO_3 and Ca-Mg-Cl-SO_4 hydrochemical facies for both dry and wet seasons, whereas the surface waters are characterised by Mg-Cl and Na-Cl water types for the lagoon and the ocean, respectively. The evaluation of the chemical processes revealed the dominance of carbonate weathering in the shallow aquifer. Hydrochemical, statistical and geochemical model analyses identified that the groundwater chemistry is significantly controlled by water–rock interaction and ion exchange processes as well as anthropogenic activities.

Stable isotopes revealed precipitation as the main source of recharge into the basin aquifer systems. Analyses of the ^{3}H and ^{14}C activities were in agreement, revealing an interesting fact about the increase in the groundwater residence time from the surface through deeper depths deducible from ^{3}H values range between 0.1 TU and 2.8TU; 0.0 TU and 0.3 TU; and ^{14}C age range from 4350±10 to 1050±10 years and between 12030±69 and 7400±50 years for the shallow and deep aquifers, respectively. The mean residence time was supported by the aquifer systems' recharge which took place in Holocene for the shallow aquifer and Late Pleistocene–early Holocene for the deep aquifers evident from the calculated ambient temperature, ^{18}O and ^{14}C plots.

The hydrogeological conceptual models showed that saline incursion severely impacted the second aquifer from a depth ≥20 m to 170 m in the western and central parts of the study.

However, the observed local saline occurrence in places <20 m was attributed to groundwater overexploitation.

Conclusively, the hydrological systems of the Lagos coastal basin is continually being modified by both anthropogenic and natural activities that constitute not only a major threat to the groundwater sustainability of the Lagos coastal basin but can also consume the entire study area.

OUTPUTS OF THE THESIS

Publication 1 (Chapter 6)

Yusuf, M.A., Abiye, T.A., Butler, M.J. and Ibrahim, K.O. (2018) Origin and residence time of shallow groundwater resources in Lagos coastal basin, south-west Nigeria: An isotopic approach. *Journal of Heliyon*, 4(11): e00932. doi:10.1016/j.heliyon.2018.e00932. Impact factor

Publication 2 (Chapter 5)

Yusuf, M.A. and Abiye, T.A. (2019) Risks of groundwater pollution in the coastal areas of Lagos, southwestern Nigeria. *Journal of Groundwater for Sustainable Development*, 9:100222. doi.org/10.1016/j.gsd.100222.

Publication 3 (Chapter 5 and 8): Submitted to Journal of Environmental Earth Sciences

Yusuf, M.A., Abiye, T.A; Ibrahim, K.O. and Ojulari, B.A. (2019) Geo-environmental studies from borehole logs in the Lagos coastal region, Nigeria. It is currently under second review in the Springer *Journal of Environmental Earth Sciences* (manuscript number ENGE-D-18-02360 R2).

Publication 4 (Chapter 7): Submitted to Journal of Heliyon

Yusuf, M.A., Abiye, T.A; Ibrahim, K.O. and Abubakar, H.O. (2020) Hydrogeochemical and salinity appraisal of surficial lens of freshwater aquifer along Lagos Coastal Belt, South West, Nigeria. It is currently under second review in the Elsevier *Journal of Heliyon* (manuscript number HELIYON-D-20-02360 R2).

Publication 5 (Chapter 6): Submitted to Journal of groundwater for sustainable development

Yusuf, M.A., Abiye, T.A; and Butler, M.J. (2020) Application of environmental isotopes in sustainability assessment of the groundwater resources of Lagos Coastal Basin (LCB), south-west, Nigeria It is currently under review in the *Elsevier Journal of Groundwater for Sustainable Development* (manuscript number GSD_2020_357 R1).

DEDICATION

This project is dedicated to my wife, Miniat,

and my children,

Ryhanah, Uwais, Kamaldeen, Muhammad and Yusuf

ACKNOWLEDGEMENTS

In the name of Allah, the beneficent, the most merciful. All praises, glorification and adoration are due to him who made possible this research work.

First and foremost, I am most grateful to my supervisor, Prof. T.A. Abiye, for giving me the opportunity to conduct my doctoral research under his supervision and guidance. This research would not have been possible without his invaluable advice, technical guidance, encouragement, and moral support throughout the research. I will forever remain indebted, Sir. I would also like to thank Mike Butler of i-Themba Labs, Witwatersrand, for the isotope analyses. I thank the Tertiary Education Trust Fund (TETFUND) for their financial support towards realisation of this dream.

I am very thankful to the management and staff of Lagos State Ministry of Energy and Mineral Resources, Lagos State Water Corporation, and Groundwater and Geophysical Services Limited for sharing their data with me. Without your cooperation, this thesis would not have come to light. Special thanks are also expressed to the private well owners for granting access to their wells. I also sincerely appreciate the kind gesture of my host in South Africa, Mr and Mrs Fashola.

The critical comments of my fellow geologists, Prof. Bale, Mr Ojulari, Dr Olojoku and Dr Adeshina, who helped to improve the quality of this work. I am grateful to all the people of the 'Hydrogeology group' under Prof. Abiye, with whom I had the pleasure to meet and share knowledge during the past years, among whom are Khuliso, Khahilso and Joy. I am very grateful to Jamiu, Abdullah and Saefullah, for their assistance during the exhaustive field campaigns. I appreciate the great time we had together in the field. I am grateful to the head of the Department of Geology and Mineral Sciences, University of Ilorin, and the entire departmental staff for their prayers, support, and encouragement.

Lastly, I would like to thank all my family, friends and well-wishers who have become my pillar of support throughout my studies.

TABLE OF CONTENTS

Declaration ..... **ii**

Abstract ..... **iii**

Outputs of the Thesis ..... **v**

Dedication ..... **vi**

Acknowledgements ..... **vii**

Table of Contents ..... **viii**

List of Figures ..... **xii**

List of Tables ..... **xvi**

Abbreviations and Acronyms ..... **xvii**

List of Symbols and Units of Measure ..... **xviii**

Chapter 1
Introduction **1**

1.1 Background to the Research 1

1.2 Research Aim and Objectives 3

1.3 Thesis Structure 3

Chapter 2
Description of the Study Area **6**

2.1 Introduction 6

2.2 Location 6

2.3 Climate, Topography, and Drainage 8

2.4 Population and Land Use 14

2.5 Population and Water Use 14

2.6 Vegetation and Land Cover 15

2.7 Geological Setting of Dahomey Basin 16

2.8 Stratigraphic Setting of Dahomey Basin 17

2.8.1 Abeokuta Group: Neocomian to Maastrichtian (Cretaceous Sequence) 18

2.8.2 Ewekoro Formation – Paleocene (Tertiary sequence) 19

2.8.3 Akinbo Formation – Upper Paleocene to Lower Eocene 19

2.8.4 Oshosun Formation – Lower Eocene to Middle Eocene 19

2.8.5 Ilaro Formation – Upper Eocene 20

2.8.6 Coastal Plain Sands / Benin Formation 20

2.8.7 Recent sediments / alluvial deposits 20

2.9 Geological Setting of Lagos State 21

2.10 Hydrogeological Setting 23

Chapter 3
Literature Review 26

3.1 The State of Research on Groundwater Studies in the Lagos Coastal Basin 26

3.2 Geophysical Methods 30

3.2.1 Electrical resistivity 30
3.2.2 Borehole geophysical logging 32
3.2.3 Dar Zarrouk parameters 32

3.3 Environmental Isotope Analyses 36

3.3.1 Stable isotopes 36
3.3.2 Radio isotopes 39
3.3.3 Carbon isotopes 40

Chapter 4
Methods and Materials 41

4.1 Desktop Review / Data Acquisition 41

4.2 Field Measurements, Sampling Procedures, and Analyses 41

4.2.1 Hydrochemical on-site measurements 43
4.2.2 Laboratory analysis 44

4.3 Geophysical Field Data Acquisition and Processing 45

4.3.1 Data acquisition 45
4.3.1.1 Vertical electrical sounding 45
4.3.1.2 Electrical resistivity tomography 46
4.3.1.3 Borehole geophysical logs 47
4.3.2 Data processing 48
4.3.2.1 Tools used for processing and interpretation 48

4.4 Field Limitations/Constraints 50

Chapter 5
Hydrogeological Units and Hydraulic Characterisation of the Coastal Basin 52

5.1 Introduction 52

5.2 Hydrogeological Units and Hydraulic Properties of the Aquifers 52

5.3 Geophysical Characterisation of the South Lagos Coastal Basin 54

5.3.1 Vertical electrical sounding 55
5.3.2 Estimation of the protective capacity of the shallow aquifers in the study area 63
5.3.2.1 Longitudinal conductance 63
5.3.2.2 Transverse resistance 67
5.3.2.3 Coefficient of anisotropy 67
5.3.3 Estimation of the shallow aquifer potential in the study area 67
5.3.4 Aquifer longitudinal conductance and aquifer conductivity 73

5.3.5 Electrical resistivity tomography 74
5.3.6 Geophysical borehole logs 79

Chapter 6
Isotope Characterisation of the Basin 86

6.1 Introduction 86
6.2 Deuterium (^{2}H) and Oxygen-18 88
6.3 Tritium content 96
6.4 Carbon-14 and ^{13}C 98

Chapter 7
Hydrochemistry of the Shallow Groundwater Aquifer in Lagos Coastal Basin 104

7.1 Introduction 104
7.2 Physicochemical Parameter Evaluation 109
7.2.1 pH and temperature 109
7.2.2 Electrical conductivity 109
7.2.3 Total dissolved solids 111
7.2.4 Microbial counts 112
7.3 Major Ion Chemistry 112
7.4 Metals 115
7.4.1 The heavy metal pollution index 117
7.5 Hydrogeochemical Evaluation 120
7.5.1 Hydrogeochemical facies 120
7.5.2 Hydrochemical evolution 121
7.5.2.1 Dry season water types 122
7.5.2.2 Wet season water types 123
7.5.3 Hydrogeochemical processes 125
7.5.3.1 Chemical weathering 126
7.5.3.2 Ion exchange processes 129
7.5.3.3 Evaporation effect 131
7.5.4 Ionic ratio to evaluate marine impacts 135
7.6 Geostatistical Analysis of the Results 140
7.7 Geochemical Modelling 148

Chapter 8
Hydrogeological Conceptual Modelling of Parts of the Lagos Coastal Basin Systems 151

8.1 General Statement 151
8.2 Local Groundwater Flow Direction 152
8.3 Geological Conceptual Model for the Lagos Coastal Basin System 154
8.4 Model Limitations 159

Chapter 9
Synthesis and Contributions to Knowledge 161
9.1 Synthesis 161
9.2 Research contributions to knowledge 167
9.2.1 Specific contributions 167
9.3 General contributions 168
Chapter 10
Conclusions and Recommendations 169
10.1 Conclusions 169
10.2 Recommendations 171
Reference List 173
Appendix A:
Sampling of water from the lagoons 199
Appendix B:
Groundwater sampling from wells 200
Appendix C:
Carbon sampling steps, Stable isotopes of oxygen-18 and deuterium 201
Appendix D:
I-Geophysical profiling 202
Appendix E:
Complete analytical results for the physicochemical parameters for the wet season 210
Appendix F:
Complete analytical results of heavy metal analysis in THE wet season 212
Appendix G:
Complete analytical results of the physicochemical parameters in the dry season 214
Appendix H:
Wet Season Hydrochemical Facies and Some Ionic Ratios of a Shallow Unconfined Aquifer in the Lagos Coastal Basin 216
Appendix I:
Dry Season Hydrochemical Facies and Some Ionic Ratios of a Shallow Unconfined Aquifer in the Lagos Coastal Basin 218
Appendix J:
Distribution of Water Types in the Lagos Coastal Basin 220
Appendix K:
Published articles 221
Appendix L:
Submitted manuscripts 223

LIST OF FIGURES

Figure 2.1: Generalised geological map of Nigeria showing Lagos State 7

Figure 2.2 Location map of the study area 8

Figure 2.3: (a) Flooded highways in Lekki, Lagos; (b) Flooded street at Apapa residential area 11

Figure 2.4: Twenty years' annual rainfall pattern of Lagos Ijebu-Ode, and Abeokuta in the Dahomey Basin 11

Figure 2.5: A map of rivers draining into the Atlantic through Lagos 13

Figure 2.6: Percentage of land cover changes in the study area: 1984–2006 16

Figure 2.7: Generalised geology map of the Dahomey Basin 17

Figure 2.8: Generalised stratigraphy of the Dahomey Basin 21

Figure 2.9: Geological map of Lagos State 22

Figure 2.10: Schematic hydrogeological cross-section of the study area 24

Figure 3.1: Cross section in a homogeneous and isotropic earth through an electric field which is set up by a two-current electrode configuration indicated by C1 and C2 31

Figure 3.2: Common electrode configurations used to measure apparent resistivity of the subsurface 32

Figure 3.3: Examples of the relationship between deuterium and Oxygen-18 in meteoric water, evaporating water and interactions with rock 38

Figure 3.4: Slope of the radioactive decay curve of tritium 39

Figure 4.1: Work flow chart showing the summary of methods and analyses adopted in this research 42

Figure 4.2: Diagram of resistivity curve types in layered structures 48

Figure 5.1: Map of the study area showing VES and ERT points 56

Figure 5.2a: Base map of the study area showing the projected ERT lines at Elegushi 57

Figure 5.2b: Base map of the study area showing the projected ERT lines at Oniru 58

Figure 5.2c: Base map of the study area showing the projected ERT lines at Adeniji Adele 59

Figure 5.3: Representative resistivity curve from the study area 62

Figure 5.4: First aquifer protective capacity map 66

Figure 5.5: Second aquifer protective capacity map 66

Figure 5.6: (a) Aquifer transverse resistance – T=h.ρa (Ω m) contour map; (b) Aquifer transverse resistance profile; (c) Three-dimensional surface view of aquifer transverse resistance 70

Figure 5.7: (a) Aquifer transmissivity – Tr=K×S (m^2/day) contour map; (b) Aquifer transmissivity profile; (c) Three-dimensional surface view of aquifer transmissivity 70

Figure 5.8: (a) Aquifer resistivity–ρa (Ω m) contour map; (b) Aquifer resistivity profile 71

Figure 5.9: (a) Aquifer thickness (h=m) contour map; (b and c) Aquifer thickness in profiles in north–south and west–east directions 71

Figure 5.10: (a) Aquifer hydraulic conductivity–K (m/day) contour map; (b) Aquifer hydraulic profile 72

Figure 5.11: (a) Aquifer longitudinal conductance – S=h/ρa (Ω^{-1}) contour map; (b) Aquifer longitudinal conductance profile; (c) Three-dimensional surface view of aquifer longitudinal profile 72

Figure 5.12: (a) Aquifer conductivity – σ=1/ρa; (b) Aquifer conductivity profile 73

Figure 5.13: Earth Imager Inverted Resistivity – Depth models for the ERT lines for Elegushi traverses a, b and c 76

Figure 5.14: Earth Imager Inverted Resistivity Depth models for the ERT lines for Oniru traverses a, b and c 77

Figure 5.15: Earth Imager Inverted Resistivity Depth models for the ERT lines for Adeniji Adele (Ilubinrin) traverses a and b 79

Figure 5.16: Typical fresh/saline water interfaces along the A-axis using natural gamma ray logs 82

Figure 5.17: Typical fresh/saline water interfaces along the B-axis using natural gamma ray logs 83

Figure 6.1: Location of sampled wells, boreholes, and surface water 86

Figure 6.2: Plot of δ^2H vs $\delta^{18}O$ (‰) for shallow groundwater in wet and dry seasons, deep wells, surface water and rainwater in the Lagos Coastal Basin 91

Figure 6.3: Plot of d-excess vs ^{18}O in groundwater samples in the study area 93

Figure 6.4: Plot of ^3H vs $\delta^{18}O$ (‰), differentiating groundwater into old water and young water 97

Figure 6.5: Plot of ^{14}C vs ^3H for groundwater in the study area 98

Figure 6.6: ^3H–14C relation of selected deep and shallow groundwater samples in the Lagos Coastal Basin 100

Figure 6.7: The ^{18}O relationship with air temperature 101

Figure 6.8: Plot of annual temperature variation vs ^{14}C ages during Holocene and Pleistocene for groundwater in the study area 102

Figure 6.9: Plot $\delta^{18}O$ (‰) vs ^{14}C activity (22 ± 1.7 pMC) as Holocene and Late Pleistocene boundary for groundwater in the study area 103

Figure 7.1: Location map of the study area showing the sampling points for hydrochemical analysis 106

Figure 7.2: Graphical representation of a statistical summary of physical parameters in groundwater: (a) wet season (b) dry season (c) surface waters.....108

Figure 7.3: Spatial distribution map of electrical conductivity in groundwater.....110

Figure 7.4: Graphical representation of electrical conductivity trend from west to east in groundwater.....111

Figure 7.5: Total dissolved solid distribution (west to east) in groundwater across the study area.....112

Figure 7.6: Statistical summary of groundwater major ions in (a) the wet season, (b) dry season and (c) surface water.....115

Figure 7.7: High concentration of metals in groundwater at the western axis of the study between GWI and GW7 (Industrial zone).....117

Figure 7.8: Percentage contributed by significant metals to HPI in groundwater.....118

Figure 7.9: ***3D view of spatial distribution of EC across the study area.*** 119

Figure 7.10: ***3D view of spatial distribution of NO_3 across the study area.***.....119

Figure 7.11: Piper plot showing the types of water of the Lagos Coastal Basin in the wet and dry seasons.....121

Figure 7.12: Percentage composition of mean occurrence of major ions in groundwater 122

Figure 7.13: Schoeller plot showing water types of the Lagos Coastal Basin in wet and dry seasons.....125

Figure 7.14: $Ca^{2+}+Mg^{2+}$ vs total cations showing carbonate dissolution 127

Figure 7.15: Bivariate plot Ca^{2+}/Na^{+} vs HCO_3^{-}/Ca^{2+} and Ca^{2+}/Na^{+} vs HCO_3^{-}/Ca^{2+} to identify the dominant chemical weathering in the groundwater of study area.....129

Figure 7.16: Durov plot depicting hydrochemical processes involved.....131

Figure 7.17: Shows scatter diagram indicating evaporation influence 132

Figure 7.18: Proposed modified Gibbs diagram showing groundwater evolution in the basin 134

Figure 7.19: Showing the prevalent climatic condition that recharged the shallow groundwater in the study area.....135

Figure 7.20: Ionic plots showing marine impact evaluation.....137

Figure 7.21: Ionic plots indicating the mixing of seawater with fresh water.....138

Figure 7.22: Loading plot of F2, F3 and F5 on F1 showing essentially geogenic contributions during the wet and dry seasons.....147

Figure 7.23: The saturation index of minerals in wet and dry seasons.....149

Figure 8.1: Groundwater level map showing groundwater flow direction in the study area: Dry season 153

Figure 8.2: Three-dimensional view of the subsurface topographical features controlling groundwater flow direction in the study area: Dry season 154

Figure 8.3: Conceptual cross-section model parallel to the ocean and lagoon 156

Figure 8.4: Conceptual cross-section model perpendicular to the ocean and lagoon 158
Figure 8.5: General conceptual model for surface water and groundwater interaction in the study area.....159

LIST OF TABLES

Table 2.1: Twenty years' rainfall data of three major cities in the Dahomey Basin 10

Table 2.2: Importance of groundwater to Lagos residents 15

Table 2.3: Descriptive characteristics of Lagos aquifers 25

Table 4.1: Major ions, metals and microbial count analyses and number of samples analysed for groundwater and surface waters 43

Table 4.2: Environmental isotope analyses and number of samples analysed for groundwater, surface waters and rainwater 44

Table 4.3: Longitudinal conductance/protective capacity rating 49

Table 4.4: Resistivity values for water and sediment rock 50

Table 5.1: Hydraulic characteristics of the different aquifer units present in the study area (compiled from various sources) 54

Table 5.2: Summary of vertical electrical sounding results 60

Table 5.3: Estimation of D-Z parameters and its protective capacity: First aquifer 64

Table 5.4: Estimation of D-Z parameters and its protective capacity: Second aquifer 64

Table 5.5: Dar Zarrouk estimated hydraulic parameters for shallow aquifers 68

Table 5.6: Ranges of freshwater–saltwater interface thicknesses and corresponding resistivities and freshwater zones 84

Table 6.1: Analytical results for rainy season water samples in the Lagos Coastal Basin 87

Table 6.2: Analytical results for dry season water samples in the Lagos Coastal Basin 88

Table 6.3: Analytical results for tritium and carbon in water samples of the study area 95

Table 7.1: Summary of physicochemical, major ions, microbial population in groundwater obtained for the wet and dry seasons in the study area 106

Table 7.2: Summary of physical, bacteriological and macro-element contents of surface water obtained in the study area 107

Table 7.3: Summary of metal concentrations 116

Table 7.4: Statistical summary of dry season analysis of physicochemical parameters 140

Table 7.5: Summary of the rainy season physicochemical (macro and micro) variables statistical analysis in the study area 141

Table 7.6: Factor loading and communalities for groundwater chemistry in the wet season 142

Table 7.7: Saturation indices of aquifer rock minerals in both wet and dry seasons 149

Table 8.1: Model parameters for parallel conceptual model 155

Table 8.2: Model parameters for vertical conceptual model 156

ABBREVIATIONS AND ACRONYMS

2D	Two-dimensional
App	Apapa
BH	Borehole
CPS	Coastal Plain Sands
DGW	Deep groundwater
D-Z	Dar Zarrouk
EC	Electrical Conductivity
ERT	Electrical Resistivity Tomography
GMWL	Global meteoric water line
GNIP	Global Networks of Isotopes in Precipitations
GW	Groundwater
HPI	Heavy metal pollution index
IAEA	International Atomic Energy Agency
LCB	Lagos Coastal Basin
LMWL	Local meteoric water line
LWC	Lagos Water Corporation
MRT	Mean Residence Time
pMC	Percent Modern Carbon
RW	Rainwater
S	Longitudinal conductance
SI	Saturation indices
SPSS	Statistical Package for Social Sciences
SW	Surface water
T	Transverse resistance
Tr	Transmissivity
TDS	Total Dissolved Solids
TU	Tritium Unit
TZ	Total Cation
VES	Vertical Electrical Sounding
WHO	World Health Organization

LIST OF SYMBOLS AND UNITS OF MEASURE

‰	Per-mille
Ω m	Ohm metre
δ	Delta
δ^2H	Change in deuterium from the standard
^2H	Deuterium
^3H	Tritium
$\delta^{18}O$	Change in oxygen from the standard
ϕ	Aquifer porosity
ʎ	Anisotropy
µS/cm	microSiemens per centimetre
p.a.	per annum
Bq/kg	Becquerel per kilogram
d-excess	Deuterium excess
F	Formation factor
E. coli	Faecal coliform
Hz	Hertz
mS	Layer thickness/resistivity
ρ	apparent resistivity
ρL	Longitudinal resistivity
ρT	Transverse resistivity
Rr	Recharge rating

Chapter 1
INTRODUCTION

1.1 Background to the Research

Nigeria is situated in West Africa between Sahel in the north and the Atlantic Ocean in the south. It experiences differential precipitation due to its location in the tropical region. The climate varies from equatorial in the south to tropical in the middle belt and the north. The rainfall distribution in Nigeria is not only variable in time but also in space, being highest in the coastal zones, while decreasing inland. This makes the northern part vulnerable to drought and water shortages, while the southern region is prone to floods and inundation of coastal aquifers by saline water induced by climatic variability and human activities (Yusuf and Abiye, 2019).

In developing countries such as Nigeria, efforts on urban water supply were initially focused on surface water, while groundwater was only meant for rural supply. However, increasing demand for water resources due to high population growth and urbanisation has resulted in an unprecedented dependence on groundwater as a major source of water supply. Groundwater aquifers are known to host approximately 99% of the global available liquid freshwater (Gabriel and Khan, 2010) and at least 25% of the world's population depends on it to fulfil its water demands (Jackson et al., 2001). The heavy reliance on groundwater globally, particularly in urban areas, exposed the aquifers to increasing pressure and accelerated environmental degradation. Like many other countries in the world, the authorities of Nigeria realised that potable groundwater resources are limited and vulnerable. Thus, the management and utilisation of this finite and vulnerable resource are of immense importance to maintain the life, environment, and development of the country (Martins, 2001). However, efforts have been made to prepare all stakeholders for this acute situation. Though the problem of saltwater intrusion was not only limited to Nigeria, it has become a major concern worldwide (Batayneh, 2006). It constitutes the commonest of all the pollutants to fresh groundwater that threatens the sustainable development and economic well-being of dwellers in any coastal area (Urish and Frohlich, 1990).

The southern part of the country, especially in the Lagos region, where this research study was undertaken, is currently grappling with essentially two major threats to groundwater

degradation, namely saltwater intrusion due to the rise in the sea level and over-abstraction, and contamination generated from inland activities. The situation is more aggravated when surface water, which ought to complement groundwater abstraction in many parts of the city, is in itself rendered unusable due to large pollution attendants, leaving groundwater as the only viable option for the users (Adelana et al., 2003; Yusuf et al., 2014). The provision of potable water, however, appears to be crucial for residents, both now and in the future. Longe et al. (1987) estimated that over 45 460.90 m^3 of water is being extracted per day via boreholes from the multilayered aquifers that exist in the coastal city of Lagos. However, a recent study asserts that Lagos State extracts over 818 296.2 m^3 of groundwater per day (Majolagbe and Osinbajo, 2012). This implies a significant increase in the rate of groundwater exploitation by over 170 % within a short period of 25 years, which consequently induces saltwater intrusion into fresh groundwater. The consequences become evident in most of the boreholes drilled in the coastal area of Lagos, which in most cases are abandoned after a few months due to severe saltwater intrusion into the aquifers.

Although seawater intrusion has been affirmed to be an inevitable problem of coastal freshwater aquifers associated with urban areas, the future safety of these aquifers and the potential for shallow aquifer water migrating to deeper aquifers, need to be evaluated and fully understood before making policy and financial investments (Hwang et al., 2004). Apparently, studies on the groundwater resources of the Lagos State have covered many parts of the city and its environs and these studies have contributed a lot to the development and management of groundwater resources (Oteri and Atolagbe, 2003; Oladapo et al., 2013). However, the studies are limited to a narrow area of hydrogeology, studies such as isotope analyses, geochemical modelling, and dynamism associated with groundwater flow systems are not yet known to this basin. As noted by Okagbue (1988), a complete appraisal of groundwater involves the integration of geophysical and hydrogeochemical studies. In order to make an adequate and improved characterisation of hydrogeology in complex multilayered aquifer systems, it is imperative to adopt an integrated approach to enhance an understanding of the groundwater resources.

In light of the above, this study provides an insight into the characterisation and assessment of groundwater resources through an integrated application of different methodologies, which include geophysics, hydrochemistry, environmental isotopes, hydrochemical models, and multivariate statistical techniques. Although groundwater was the major focus of this research, attention was also given to surface water draining the areas, due to potential

interactions with groundwater. The result from this study is not only pivotal to understanding the human interaction and hydrological cycle but also contributes to a detailed understanding of the coastal aquifer system, allowing for better planning and management of groundwater resources. Besides, the results will also guide decision-makers to take precautionary measures towards formulating policies that will control the indiscriminate discharges of contaminants, provide adequate implementable future plans, and protect the aquifer from further deterioration.

1.2 Research Aim and Objectives

The main aim of this forensic research was to apply an integrated approach to investigate and characterise the hydrogeology of the coastal aquifer in the city of Lagos. This involved the collection of relevant data from the government, agencies, individuals, and literature to complement the acquired field data as well as the various analyses. To achieve this laudable aim, the following specific objectives were considered:

- To establish the depth to the water table as well as aquifer thickness, to delineate formations bearing fresh and saline water, distinguish between the sandy and clay layers, establish the depth to the freshwater and saltwater interface, and groundwater flow direction.
- To identify and determine the source of aquifer recharge and Mean Residence Time of groundwater.
- To assess the status or trend of groundwater pollution in the study area.
- To develop a hydrogeochemical model for the study area.
- To recommend optimal and reliable mitigation or control measures for groundwater protection from contamination for future planning and policy formulation.

1.3 Thesis Structure

This thesis is divided into ten chapters. The contents of each chapter are summarised as follows:

Chapter 1 presents the general background of the research including the rationalisation of the research, the research aim and objectives, and the structure of the thesis.

Chapter 2 describes the study area, including location, climate, relief and drainage, population and land use, population and water use, vegetation and land cover, geological setting, stratigraphic setting, and hydrogeological setting.

Chapter 3 reviews the state of research in the Lagos Coastal Basin (LCB) including, the geological, hydrogeological, hydrochemical, geophysical and environmental isotopes techniques. This chapter also offers a background to the processes involved in all the methods adopted for aquifer characterisation.

Chapter 4 details the research approaches, methodology, and materials used in the study to collect, analyse, and present various data.

Chapter 5 investigates and characterises the subsurface of the coastal basin with the aid of geophysical methods. This involves the application of a geoelectrical method and resistivity log interpretation to delineate lithological units, estimation of layer thickness, depth to the aquifer, and the freshwater–saltwater interface. The work was presented at the 15th Biennial Conference of Groundwater Division in Stellenbosch, South Africa, in October 2017, as well as at the 54th Annual International Conference of the Nigerian Mining and Geosciences Society in Kano, Nigeria, in January 2018. Parts of this chapter had been published in the Elsevier *Journal of Groundwater for Sustainable Development* (Yusuf and Abiye, 2019), and the other parts are currently under review in the Springer *Journal of Environmental Earth Sciences* (manuscript number ENGE-D-18-02360 R2).

Chapter 6 presents the results of the environmental isotopes of surface water, groundwater, and rainwater in the LCB. Part of this chapter had been published in the Elsevier *Journal of Heliyon* (Yusuf et al., 2018), while the other part is currently under review in the Elsevier *Journal of Groundwater for Sustainable Development* (GSD-20-357 R1).

Chapter 7 presents the geochemical modelling and hydrochemical characteristics of the LCB. Part of this chapter is presently under review for publication in the Elsevier *Journal of Heliyon* (HELIYON-2020-02205 R2).

Chapter 8 presents both the general and specific conceptual models for the aquifer systems of the study area.

Chapter 9 synthesises all the findings and enumerates the significant contributions of the thesis to knowledge.

Chapter 10 completes and highlights the main conclusions and recommendations from the overall findings of this research work.

Chapter 2
DESCRIPTION OF THE STUDY AREA

2.1 Introduction

The study area is situated within the coastal domain of Dahomey Basin, and thus an integral part of it. Dahomey Basin is a marginal basin forming parts of the Gulf of Guinea, extending from south-eastern Ghana through Togo and the Benin Republic to the western limit of the Niger Delta in Nigeria (Billman, 1976). It is a shelf depositional environment sedimentary basin constituting a thick sequence of sedimentary rocks underlying the Earth surface. The basin acts as host to many mineral resources of economic importance such as oil, gold, coal, and natural gas, some of which have been explored for their resource value. Furthermore, it also plays host to large volumes of groundwater resources that are essentially tapped for human needs. Hence, since groundwater assumes to be the only vital source of freshwater for the coastal inhabitants, studies involving sedimentary basins are of prime importance.

For this study, it becomes necessary to discuss the regional and local physiographic setting, including the geology and geography of the area being investigated. A thorough understanding of the climatic condition and geology of the basin is indispensable in the process of assessing and characterising the groundwater resources of the region.

2.2 Location

The geology of Nigeria consists mainly of basement complexes and sedimentary basins. The port city of Lagos is, however, located in the sedimentary segment of the south-western part of Nigeria, a zone of coastal creeks and lagoons (Elueze and Nton, 2004). It lies approximately between longitudes 2°30' E to 4°30' E and latitudes 6°15' N to 7°00' N (Oladapo et al., 2013). The Lagos State is bounded in the south by the 180 km long Atlantic coastline, while it is bordered in the northern and eastern ends by the Ogun State, and sharing a boundary with the Benin Republic at the western limit (Odumosu et al., 1999) (Figure 2.1). Its land size is about 3 577 km^2; about 22 % of which is a water-covered area (Odumosu et al., 1999). It is the smallest state in the federation in terms of landmass. Until 1991, Lagos was the Federal Capital of Nigeria and still is the commercial capital and economic hub of the

nation (Adelana et al., 2008). Lagos accounts for over 60 % of the industrial and commercial activities of the nation (Nwagwu and Oni, 2015).

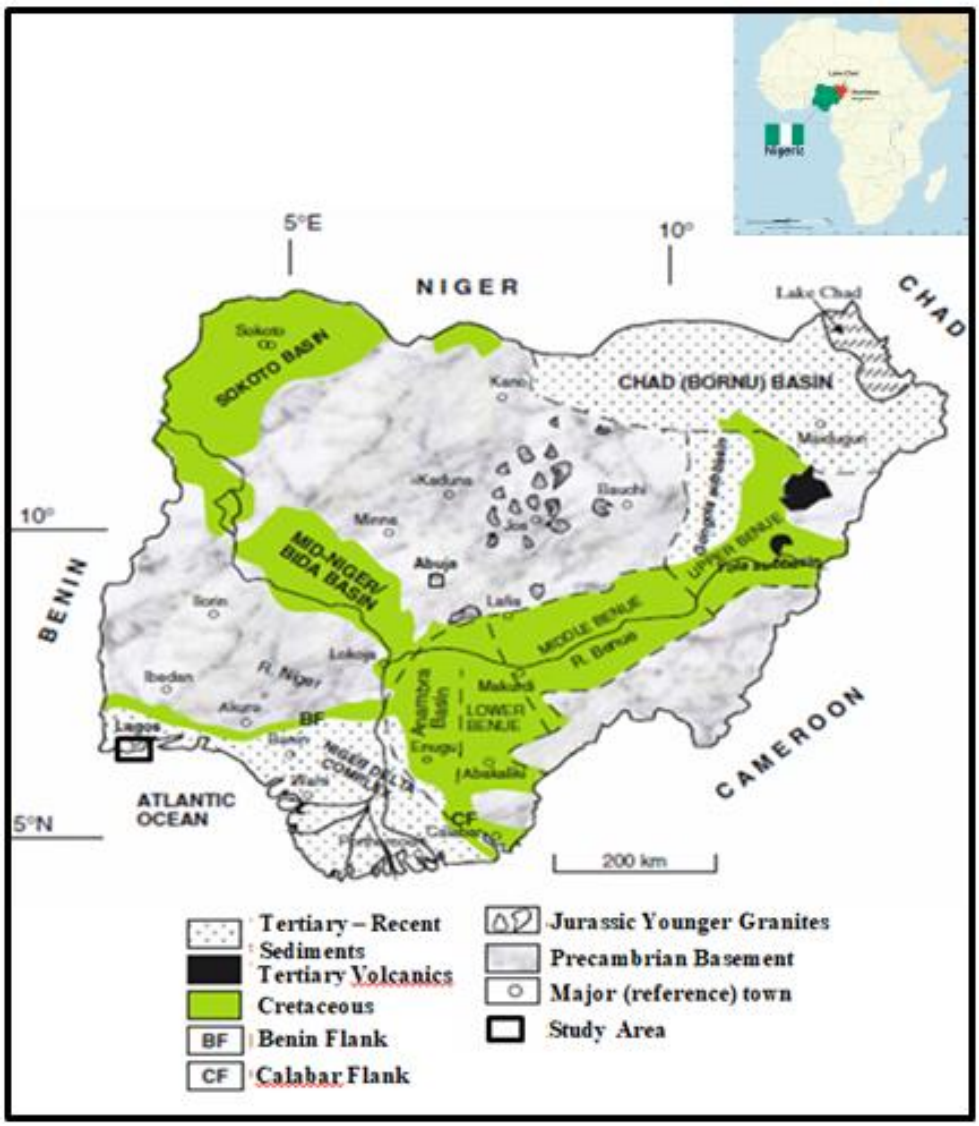

Source: Modified after Obaje (2009)

Figure 2.1: Generalised geological map of Nigeria showing Lagos State

The study area, comprising parts of the Lagos coastal belt, is situated within the coastal plain sand (CPS) aquifer of Lagos and lies approximately between longitudes 3°18' E to 3°54' E and latitudes 6°20' N to 6°32' N It is bordered in the east by Ibeju-Lekki, in the west by Apapa, in the north by lagoon, and in the south by the Atlantic Ocean (Figure 2.2). It is situated on stratified series of sedimentary rocks composed of siltstone, claystone, peat, or coal associated with sandstone deposition. The total area of study was estimated to be approximately 200 km^2. The research area is surrounded by water bodies, the Atlantic Ocean, a lagoon, and creeks, forming a large tract of land from the central area towards the eastern

limit of the study. These surface water bodies are of tremendous ecological importance to neighbouring communities and play host to a large variety of flora and fauna.

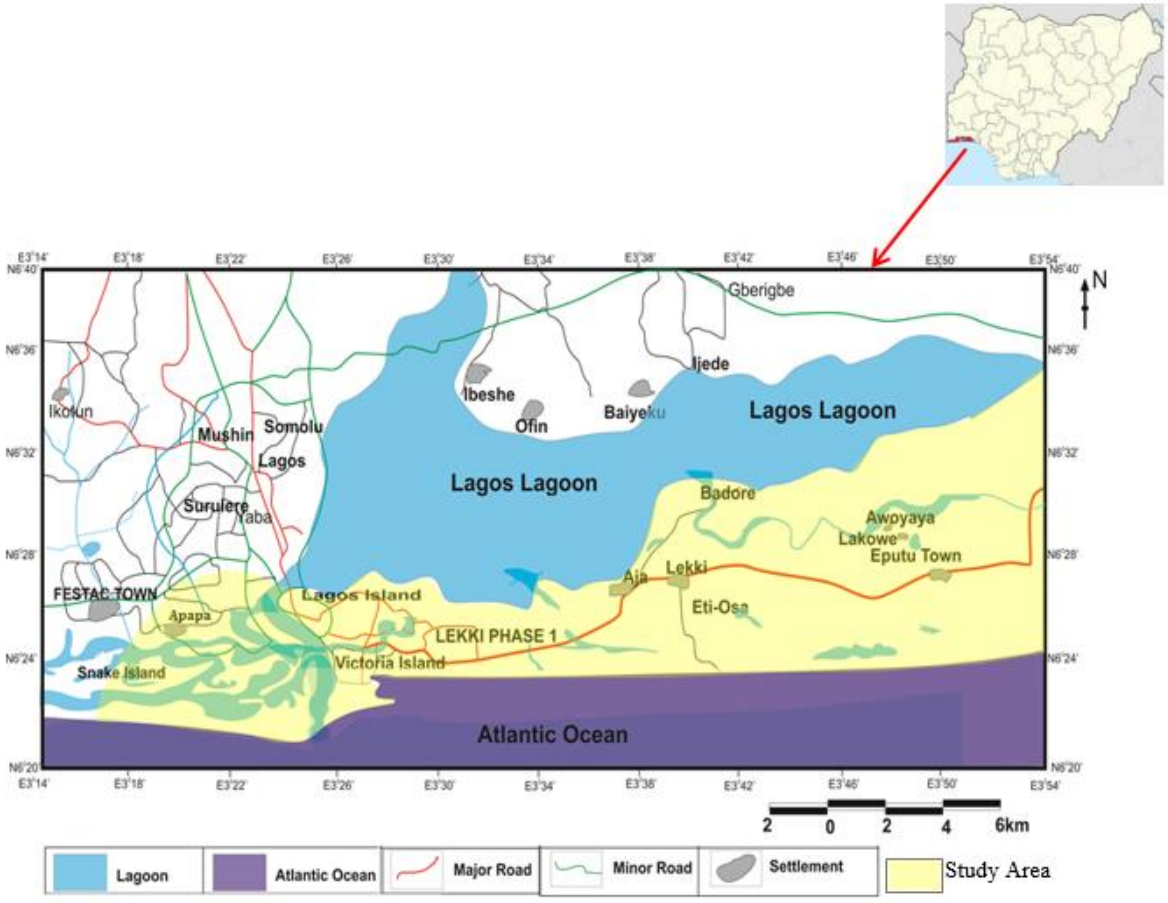

Source: Modified after Yusuf et al. (2018)

Figure 2.2 Location map of the study area

2.3 Climate, Topography, and Drainage

Climate is a major factor influencing the availability of water resources of the coastal region. This is due to the fact that both the surface water and groundwater in the coastal area are in direct response to the local climatic conditions (Yusuf et al., 2018). The system is essentially recharged through precipitation, while evapotranspiration causes the depletion of surface and subsurface moisture. Hydrological processes such as surface run-off and groundwater recharge rates are strongly influenced by rainfall frequency and intensity. Adequate knowledge of local prevalent weather conditions is paramount for hydrological studies.

Lagos, unlike the northern parts of the country, is very humid with an average relative humidity of above 70 % throughout the year (Ogundele, 2012). The region falls into a humid

tropical climatic region characterised by the hot and wet conditions associated with the movement of the Inter-Tropical Convergent Zone north and south of the equator (Adelana et al., 2008). The direction of the wind is synchronous to the season's positions in the Inter-Tropical Convergent Zone. During the wet season, the south-western winds prevail as the front moves to the north. However, as from October/November when the front moves southwards, the northeast winds sweep in the dry season. Lagos State, however, experiences a predominantly south-westerly wind and sea breeze throughout the year (Ogundele, 2012). In Lagos, the annual average temperature is about 27 °C (Adepelumi et al., 2008). Since there is a slight variation in temperature, rainfall distribution over space and time becomes the single most important factor in differentiating the seasons and climatic regions (Adelana et al., 2008).

The area is characterised by torrential rainfall and governed essentially by two major seasons: the wet season spans between April and November, while the dry season covers the months of December to March. Oke (2015) reported an average annual rainfall of 1 800 mm (70 inches) for Lagos, as indicated in Table 2.1. Eighty percent of the annual rainfall (1 440 mm) falls during the southwest Monsoon (April to October) and the remaining twenty percent (360 mm) falls during the northeast Monsoon (November to March). The recent rainfall data shows a slight increase in precipitation in the area when compared to the 1 700 mm per annum reported by Adelana et al. (2008) for the same region. Extreme rainfall events occur when occasional tropical cyclones over the Atlantic Ocean make landfall. Generally, precipitation increases from north to south in the Dahomey Basin. This is reflected in the high rainfall recorded in the southern part of the Dahomey Basin in Lagos, rather than in the northern end at Abeokuta (inland). The average annual recharge estimate varies from 1 800 mm for Lagos, 1 600 mm for Ijebu-Ode and 1 200 mm for Abeokuta (Table 2.1). The stormy and sporadic patterns characterising the heavy downpours, sometimes running for as long as a week, usually subject the coastal basin to frequent flooding, thereby increasing the threat on groundwater, particularly the shallow aquifer.

Table 2.1: Twenty years' rainfall data of three major cities in the Dahomey Basin

Year	Lagos (mm)	Ijebu-Ode (mm)	Abeokuta (mm)
1987	2 057.0	1 501.9	1 277.1
1988	2 432.1	1 653.2	1 604.4
1989	1 702.6	1 445.5	1 401.0
1990	2 030.2	1 713.8	1 111.0
1991	1 722.9	1 646.9	1 173.1
1992	1 357.6	1 611.8	1 076.7
1993	1 828.2	1 456.9	1 193.6
1994	1 602.3	1 556.9	712.2
1995	2 025.3	1 643.8	1 177.5
1996	2 535.9	2 032.4	1 471.6
1997	1 936.8	1 705.7	1 354.9
1998	1 232.9	1 172.8	1 118.4
1999	2 056.9	1 819.4	1 530.4
2000	1 458.9	1 655.0	1 201.9
2001	1 110.0	1 462.3	849.2
2002	1 523.2	1 426.5	1 235.1
2003	1 549.0	1 572.0	1 214.7
2004	2 117.4	1 766.6	1 153.3
2005	1 745.6	1 473.3	917.5
2006	1 996.2	2 043.6	1 157.2
Average	1 801.05	1 618.015	1 196.54

Source: Oke et al. (2016)

Flooding of the Lagos coastal strip occurs during the rainy season, May to October, and is more serious when rains coincide with astronomically high tides (Awosika et al., 2000). In mid-2011, the Lagos State experienced one of the worst and most devastating flood events that claimed 20 lives with thousands of people displaced from their homes (National Emergency Management Agency). The devastation resulted from heavy downpour aided by blockage of water channels and drainages, indiscriminate refuse dumping and building of houses along channels (Stearns, 2011). According to Kalu (2011), it rained for 17 hours, while the Nigeria Institute of Oceanography and Marine Research affirmed that the supposed rainfall of 264 mm for one full month was recorded in one day. From the above submission, the calculated average of 0.37 mm/hour, or 8.8 mm/day, maybe proposed as the threshold for the study area beyond which floods will occur. A comparison of this threshold with the average of 15.53 mm/hour that it rained in less than a day in 2011, was 42 times more than the threshold value. It is, therefore, not surprising that the National Emergency Management

Agency tagged the event as the most devastating flood occurrence in the Lagos State. Figure 2.3 shows the floods in the Lekki and Apapa residential areas in Lagos.



Source: Alegba (2019) Source: Slaughter and Odume (2017)

Figure 2.3: (a) Flooded highways in Lekki, Lagos; (b) Flooded street at Apapa residential area

Figure 2.4 shows the rainfall pattern over twenty years, obtained from Nigeria's Meteorological Agency for Lagos and two notable cities located in the immediate vicinity of the study area within the Dahomey Basin.

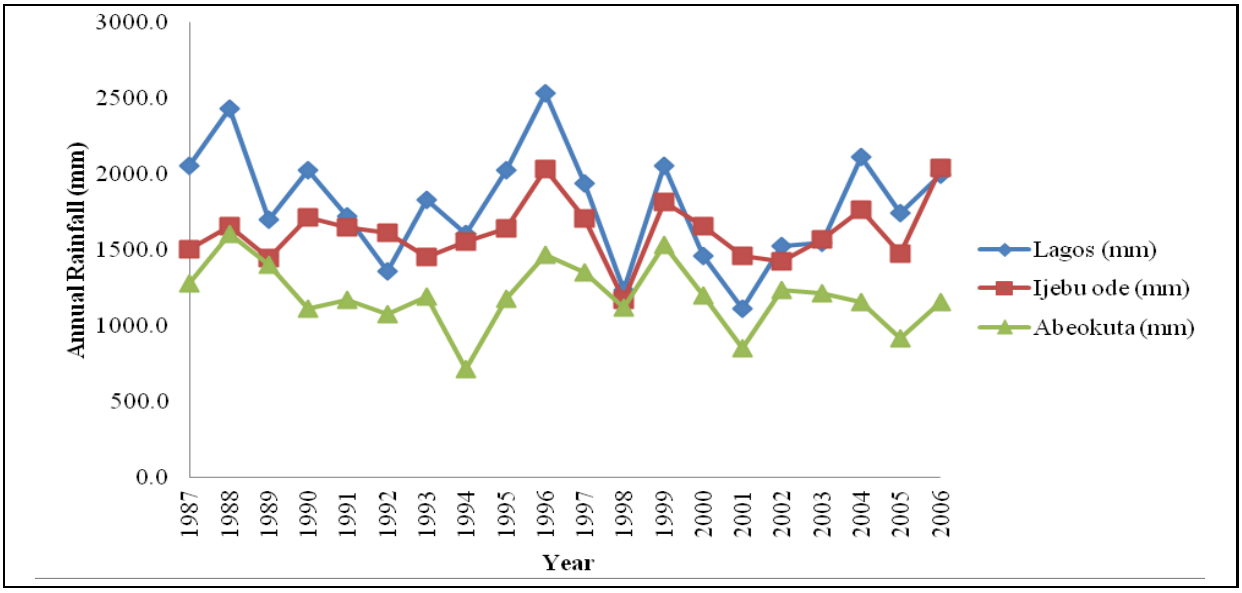

Note: Data as in Table 2.1; Source: Oke et al. (2016)

Figure 2.4: Twenty years' annual rainfall pattern of Lagos Ijebu-Ode, and Abeokuta in the Dahomey Basin

Temperatures also reflected variations; however, more subdued than rainfall. Temperatures peaked in the dry season with the maximum records ranging between 29 °C and 34 °C and lowest in the wet season with the minimum records ranging between 24 °C and 28 °C (Ogundele, 2012).

The topography of the area is generally characterised by the low-lying alluvial plain. It is roughly about 35 m above sea level, with a shallow water table (as shallow as 0.2 m). Some depressions were observed in places along the coastal belt which are prone to flooding, as they are apparently below the surface of the lagoon (Oyedele and Momoh, 2009). The sandy nature of the area, coupled with relatively flat topography and shallow water table, enhances the close relationship between the surface water and groundwater. This association is evident as the groundwater becomes saline, particularly in proximity to the saline sources (Ayolabi et al., 2013; Yusuf et al., 2018). The groundwater level in the study area is sensitive to prevalent local weather conditions and responds directly to rainfall and seasonal cycles. Coastal wetlands, sandy barrier islands, beaches, low-lying tidal flats, and estuaries are typical landforms that characterise the area (Adepelumi et al., 2008). The Cretaceous sediments are unconformably overlain by relatively thin, discontinuous, shallow marine and beach deposits, while the Quaternary sediments of a variety of depositional environments constitute the surface sediments for most of the coastal plain (Hobday, 1979). Due to the high permeability of these sediments, rapid recharge to the aquifer, and strong interactions with wetlands in the basin are promoted.

The drainage system consists of the Lagos and Lekki lagoons, fed by the Oni, Osun and Sunmoge Rivers in the north-eastern region and by the Ogbere and Ogun Rivers in the north-central and north-western parts of the lagoon (Emmanuel and Chukwu, 2010), while the Badagry creek is being fed by the Yewa River. The Lagos lagoon is the only one with significant surface drainage with which other connected tributaries are linked to the ocean (Figure 2.5 and Figure 2.8). The Lagos Metropolitan Area constitutes about 33 % of Lagos State, with 455 km^2 of the metropolis being waterbodies, wetlands, and mangrove swamps (George, 2009).

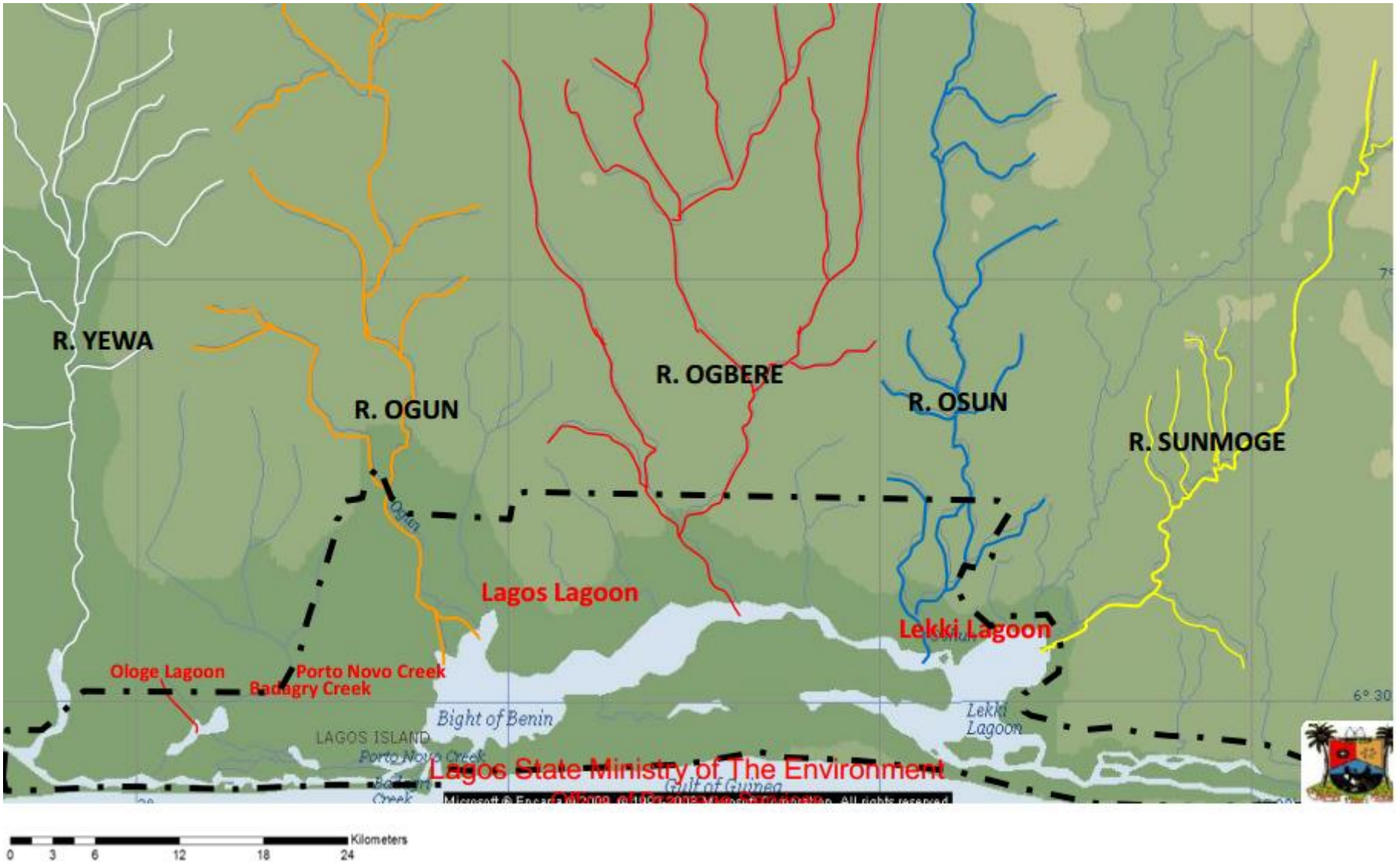

Source: Expectant Leaders Fundaytion (2014: Online)

Figure 2.5: A map of rivers draining into the Atlantic through Lagos

2.4 Population and Land Use

Lagos is known to be one of the fastest-growing and emerging coastal cities in sub-Sahara Africa (Sojobi et al., 2016). With the recent rural-urban migration, the present population of Lagos based on estimates by Bloch et al. (2015) can be conservatively estimated to be around 17.5 million. However, the population of the metropolis was estimated at 14 million in the year 2000 (Boomie, 2001). It is clear that whatever the size, and however the city is defined, Lagos is the centre of one of the largest urban areas in the world. With a population of perhaps 1.4 million in 1970, its growth has been enormous. The rate of population growth is about 300 000 persons per annum, with an average density of about 1 308 persons per square kilometre, whereas the average density in the built-up urban areas of the city is 20 000 persons per square kilometre (Adelana et al., 2005).

Lagos Metropolitan Area, with a total land area of 3 600 km^2 and an annual growth of 4 %, was rated as one of the world's five megacities in 2015. Besides, Lagos is a highly industrialised state, which accounts for over 60 % of the nation's total industrial investment (Atakpo et al., 2011). There are over 2 000 industries located across the length and breadth of the city (Japan International Cooperation Agency, 1999). The industries include manufacturing, major ship berthing port complexes, scores of petrol stations and over 50 tank farms, situated along the coastline, all of which portends a threat to the environment, especially the groundwater resources. The state's three main settlement components are urban, peri-urban, and riverine, while industrial, peri-urban agriculture, commercial activities and fishing are the major activities in the Lagos Metropolitan Area. It is important to note that the rapid growth in population and industrialisation in the Lagos Metropolitan Area further increases pressure on the already stressed groundwater resource.

2.5 Population and Water Use

Lagos is faced with the challenge of acute shortages of municipal water supply resulting from a tremendous increase in the population of the city, with an estimated 17.5 million people in the year 2015. This demographic expansion had great consequences on the municipal water supply system and increased the problem of waste management within the city (Adelana et al., 2008). The supply of drinking water to the residents of Lagos is drawn from both surface water and groundwater resources. To date, the Lagos Water Corporation (LWC) harnesses water essentially from three surface waters, namely Iju, Ishasi, and Adiyan (major

waterworks) and 48 mini and micro waterworks from groundwater. The major and mini/micro waterworks have a total capacity of 119 and 91 million gallons per day, respectively (LWC, 2009). Despite the high total daily production, the water supply in Lagos is becoming more critical in response to the population explosion in the Metropolitan Area. According to Fasona et al. (2005) and the LWC (2009), a supply of 340 million litres per day, which accounts for about 47.6 % of the total domestic water distributed throughout the state is being sourced from the surface rivers, while the remaining 52.4 % (374 million litres per day) was produced through groundwater. The importance of groundwater to the residents of Lagos was further elucidated by Sample et al., (2013) as illustrated in Table 2.2 where the high-income category utilises 95 % groundwater, while the low-income sector focuses on dug wells (59 %).

Table 2.2: Importance of groundwater to Lagos residents

Class	Borehole utilisation (%)	Dug-well utilisation (%)
High income	95	–
Medium income	54	38
Low income	36	59

Source: Sample et al. (2013)

It is important to note that the type of water sourced depends largely on price, quality, and proximity. Due to the steady population growth of the coastal city, the water demand has outpaced the supply over the years. The State faced a demand gap of 330 million gallons per day in 2011 (LWC, 2011), which is continuing until these days. In order to meet the water demand, the solution by residents was sinking private boreholes, water supply via tankers and water carts, boreholes and wells which provide 70 % of the water consumed (LWC, 2011). This is in tandem with the assertion of LWC (2009) that water supplies in Lagos State have only succeeded in meeting less than 40 % of the water demand. This thus confirms that groundwater resources are heavily relied upon in Lagos to equal the water need of the inhabitants. Furthermore, it has been projected that between 2010 and 2020, the demand for potable water is expected to grow from 600 to about 800 million gallons per day (LWC, 2011).

2.6 Vegetation and Land Cover

The Dahomey Basin vegetation varies from a rainforest belt, which characterises the northern-most end, to prevailing swampy mangrove vegetation in the south. Rivers, streams, creeks, and lagoons dominate the southern limit of the basin, particularly in Nigeria and the

Benin Republic where most parts of the basin are water-logged. However, the vegetation of Lagos is dominated by freshwater swamp forests, brackish water swamp forests and riparian forests (Federal Environmental Protection Agency, 1997). The vegetation is influenced by a high rainfall pattern that characterises the region and makes the environment a perpetual wetland domain. Consequent to land reclamation orchestrated by the population explosion, industrialisation and urbanisation, this natural ecosystem had been greatly distorted and degenerated. According to Obiefuna et al. (2013), the mangroves decreased by 77 %, from 88.51 km^2 to 19.92 km^2, at an average loss of 3.12 km^2 per year, while swamps were depleted by about 52 %, from 344.74 km^2 to 165.37 km^2, at an 8.15 km^2 per year deficit between 1984 and 2006 due to urbanisation (Figure 2.6).

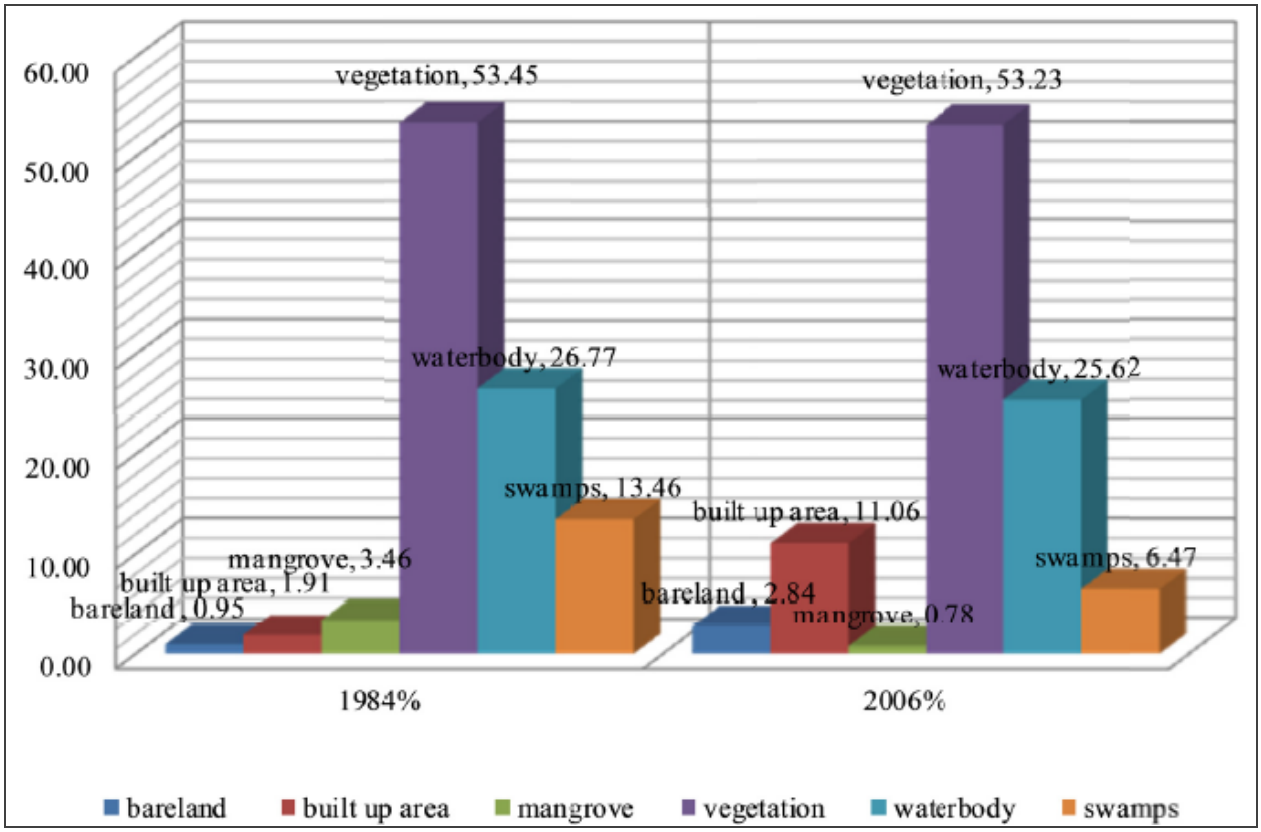

Source: Obiefuna et al. (2013)

Figure 2.6: Percentage of land cover changes in the study area: 1984–2006

2.7 Geological Setting of Dahomey Basin

Regionally, Lagos State is an integral component of the Dahomey Basin. The evolution of Dahomey Basin was attributed to the transcurrent movements on the oceanic fracture systems, especially the Romanche, Chain and Charcot fractures during the drifting stages of separation of South America and Africa in the Campania to Tertiary. It is a marginal sag

basin or marginal pull-apart basin (Kingston et al., 1983), in which the eastern half occurs in the Nigerian territory within which the present study area is located. The basin is composed of an extensive wedge of Cretaceous, Paleocene and Neocene sediments. These are marked with decreasing thickness from the onshore margin (north) of the basin where the Cretaceous clastic sediments rest on the Basement complex, towards the offshore (south) where thick, finer-grained Cenozoic sediments obscure the Cretaceous rocks developed in Leptogeoclinal basins (Whiteman, 1982).

The sequence of Cretaceous has been subdivided into three Formations, namely the Ise, Afowo, and Araromi Formations, formerly known as the Abeokuta Group (Jones and Hockey 1964; Omatsola and Adegoke, 1981). The Upper Cretaceous rocks, which are largely Maestrichtian, are predominantly of sandy facies and were probably laid down during the first post-Santonian sedimentary cycle (Murat, 1972). The oldest known Cenozoic Formation in Nigeria (Dahomey Basin) is the Akinbo shale, while the youngest is the Benin Formation and alluvial deposits. The Cenozoic Formation sequence exposed in the Nigerian parts of the Dahomey basin is Akinbo Shale, Ewekoro Formation, Oshosun Formation, Ilaro Formation, and alluvium CPS (Figure 2.7).

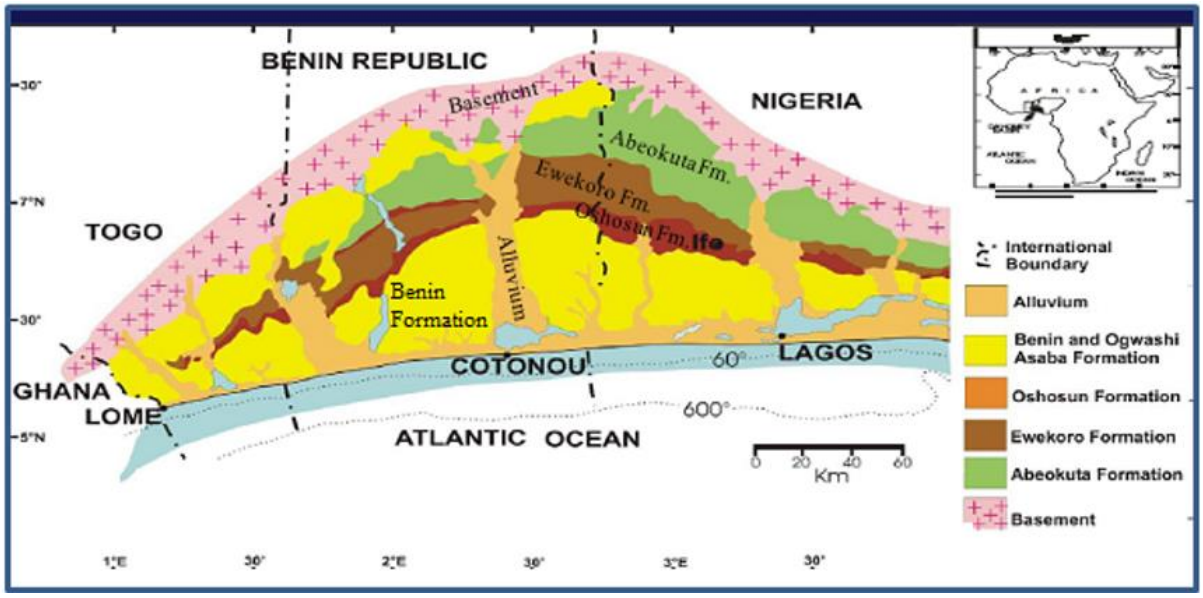

Source: Modified after Billman (1976)

Figure 2.7: Generalised geology map of the Dahomey Basin

2.8 Stratigraphic Setting of Dahomey Basin

Several detailed studies have been carried out on the stratigraphic setting of the Lagos Metropolitan Area and environs by researchers such as Ako et al. (1981), Omatsola and

Adegoke (1981), Okosun (1990) and Adekeye (2005). Five lithostratigraphic Formations, ranging from the Cretaceous to Tertiary ages, were identified. The succession from the oldest to the youngest includes the Abeokuta Group (Cretaceous), Ewekoro Formation (Paleocene), Akinbo Formation (Late Paleocene–early Eocene), Ilaro Formation (Eocene), CPS, and Recent sediments (Table 2.1). Despite the extensive research on the basin, researchers are yet to agree on many issues, including the age of these Formations. They do, however, all recognise their successions (Nton, 2001).

2.8.1 Abeokuta Group: Neocomian to Maastrichtian (Cretaceous Sequence)

The oldest sedimentary succession in the Dahomey Basin constitutes the Abeokuta Group (Figure 2.8). This succession covers the whole of the basin with varying thicknesses. The formation consists mainly of siltstone, poorly sorted ferruginous grit siltstone, and mudstone with shale-clay layers that were deposited in a turbulent shallow sea during a humid tropical climate. The origin of the formations is marine, partly brackish water and freshwater (Kogbe, 1974). The Abeokuta Group was divided into three recognisable sub-Formations: the Ise Formation, Afowo Formation and Araromi Formation (Omatsola and Adegoke, 1981).

- **Ise Formation: Neocomian – Albian**: This Formation consists of basal conglomerate with grits overlying the basement complex and the conglomerate, in turn, is overlain by coarse to medium-grained loose sands, sandstones, and grits with interbedded kaolinite. The conglomerates are unimbricated with ironstones occurrence in places. The cross-bedding azimuth of sandstone and the pebble alignments point to a north-eastern paleocurrent system (Nton, 2001). This formation marked the end of the regressive phase of Benue Trough during Albian, and conformably overlies the basement rocks of southwest Nigeria. Ise Formation is highly prolific with respect to groundwater due to the high amount of pore spaces characterising the conglomerate.

- **Afowo Formation – Turonian**: The Afowo Formation overlies the Ise Formation and is composed of coarse to medium-grained sandstones with a variable proportion of siltstones, clays, and interbedded shales in its upper part. The shale component increases from bottom to top, and the lower parts of the formation are transitional with mixed brackish to marine horizons, alternating with well-sorted, sub-rounded, clean, loose fluviatile sands (Billman, 1976). This indicates the littoral or estuarine nearshore environment of deposition, where there is a rapid fluctuation of the water level. This

formation conformably overlies the Ise Formation, but sometimes overlies the basement complex in some locality (Adekeye, 2005).

- **Araromi Formation – Maestrichtian**: This Formation is equivalent to the unit informally called the Araromi shale by Reyment (1965). The Araromi Formation is the youngest of the Abeokuta Group and comprises the basal fine- to medium-grained sandstones that are overlain by shale and siltstone beds with thin interbedded limestones and marls (Ogbe, 1970; Omatsola and Adegoke, 1981). The light grey/black coloured shale is mostly of marine origin (Billman, 1976).

2.8.2 Ewekoro Formation – Paleocene (Tertiary sequence)

The Ewekoro Formation is underlain by the Abeokuta Group conformably, and consists of fossiliferous limestone (Adegoke, 1969). It is over 30 m thick in the Sagamu quarry (Adegoke et al., 1980). The formation becomes marl, with increasing arenaceous content towards the base and grades into the underlying predominantly sandy Abeokuta Group (Jones and Hockey, 1964). According to Ogbe (1970), the Ewekoro Formation is an extensive limestone body that is traceable over a distance of about 320 km from Ghana in an easterly direction towards the eastern margin of the Dahomey Basin in Nigeria (Adekeye et al., 2005). Evidence indicates a shallow marine environment of deposition (Adegoke et al., 1980). The formation extends to the Benin Republic and Togo where it is referred to as calcareous atogocyamus. The Ewekoro Formation is not only mined on a commercial scale in Nigeria but also in the Benin Republic for cement production.

2.8.3 Akinbo Formation – Upper Paleocene to Lower Eocene

The Akinbo Formation unconformably overlies the Ewekoro Formation and its base was recognised by the presence of a glauconitic rock-band above the Ewekoro Formation. The top of the Akinbo Formation is identified by pure grey, gritty sand, lacking red mottling, and with minor clay. Shears and cracks observed in the shale of this formation can be a preferential pathway for groundwater movement and may also be responsible for the frequent collapsing of boreholes in areas underlain by this formation (Oke et al., 2016).

2.8.4 Oshosun Formation – Lower Eocene to Middle Eocene

Overlying the Akinbo Formation is the Oshosun Formation. It comprises greenish-grey or beige clays, light greyish, white to purple clay, and unconsolidated clayey shale with

interbedded sandstone. The shale is well-laminated and glauconitic (Okosun, 1998). The formation exhibits significant lateral and vertical lithological variations and probably marine throughout its thickness. This is contrary to the lagoon swampy environment postulated by Russ (1924). The top is an unconsolidated and friable mixture of sandstone and clay which serves as the unconfined aquifer bed, while the basal bed comprises facies of sandstone, mudstone, claystone, and shales. This Formation is compositionally phosphorite (Nton, 2001).

2.8.5 Ilaro Formation – Upper Eocene

The Ilaro Formation consists essentially of coarse sandstone of the marine, deltaic and continental environment with lateral facies variations. This Formation occurs above the Oshosun beds and is referred to as the Ilaro Formation (Slansky, 1962). The texture of the sands indicates a beach or shoreline and nearshore environment (Jones and Hockey, 1964). The sedimentation of the Oshosun Formation and consequent marine regression resulted in the deposition of sandstone units at the Ilaro Formation. This formation is well-known for its aquiferous potential with an average thickness range of 30 m–60 m (Oke et al., 2016).

2.8.6 Coastal Plain Sands / Benin Formation

The CPS is the youngest stratigraphic succession in the Dahomey Basin. The formation exists as both unconformable and conformable units upon the Ilaro Formation. It consists of poorly sorted sands, clay lenses, and rare thin lignites, and frequently contains pyritic fragments. They are cross-bedded and reflect more of the continental characteristics. The formation is assigned age ranges from Oligocene to Recent (Reyment, 1965). With exception of the recent alluvium sediment that was deposited along the shore, the Benin Formation underlies the entire Lagos Metropolitan Area. The thickness increases from north to south and a thickness of as much as 400 m was reported towards the coast (Agagu, 1985). The CPS is well-noted for its groundwater resource; however, this resource is vulnerable, particularly the upper aquifer.

2.8.7 Recent sediments / alluvial deposits

The recent sediments occur along the coastal belt and as alluvial deposits of the major rivers. The sediments consist of unconsolidated sands, clays, and muds along with the coastal areas, while the alluvial deposits consist of coarse, clayey, unsorted sands with clay lenses and

occasional pebble beds. This deposit hosts the most vulnerable phreatic aquifer along the coastline. Figure 2.8 shows the generalised stratigraphy of the Dahomey Basin.

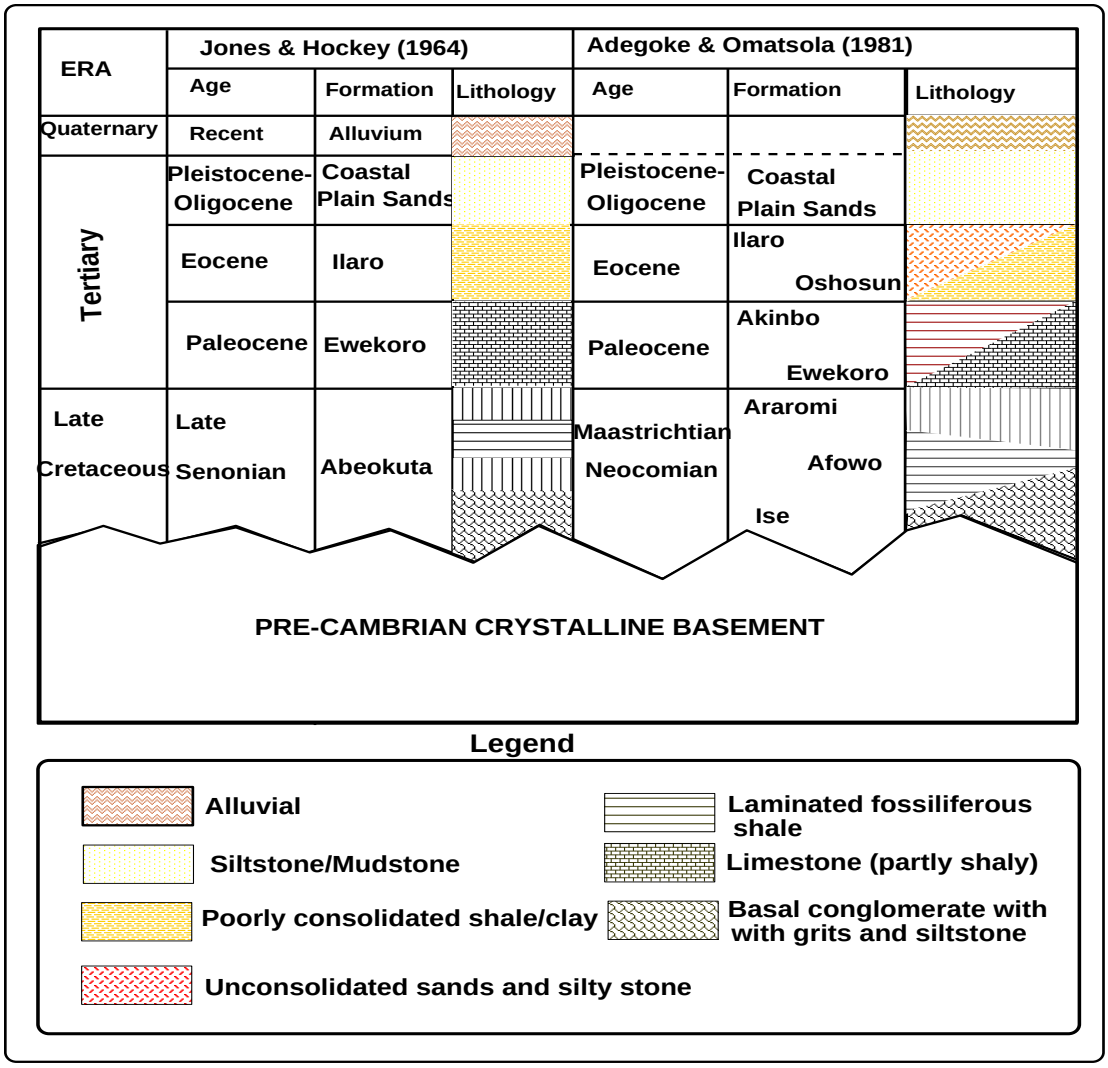

Source: Adapted from Oke et al. (2016)

Figure 2.8: Generalised stratigraphy of the Dahomey Basin

2.9 Geological Setting of the Lagos State

The geology of the Lagos State is a mainly sedimentary sequence of the Tertiary and Quaternary deposits. The entire coastal city of Lagos is underlain by the Benin Formation and consists of highly porous sandy gravels with thin interbedded shale/clay (Oteri and Atolagbe, 2003). The sediments are composed of silt, clay, and sand of various grain sizes and mineralogy without any basement outcrop. The area is developed by barrier beaches associated with sand deposits (Ogbe, 1970). The near-surface Quaternary geology includes recent littoral sandy alluvium and lagoon/CPS (Jones and Hockey, 1964; Longe et al., 1987).

The subsurface geology reveals two basic lithologies: clay and sand units. These deposits are interbedded in places with clayey sand or sandy clay and occasionally with vegetable remains and peat. The Lagos-Osse Basin, in the eastern sector of the Benin Basin, underlies the western low-lying coastal zone, where rock exposures are poor due to the thick soil cover. The coastal belt varies in thickness from about 8 km around the Republic of Benin's border to 24 km towards the eastern end of the Lagos lagoon (Nton, 2001). Figure 2.9 shows the geological map of Lagos State.

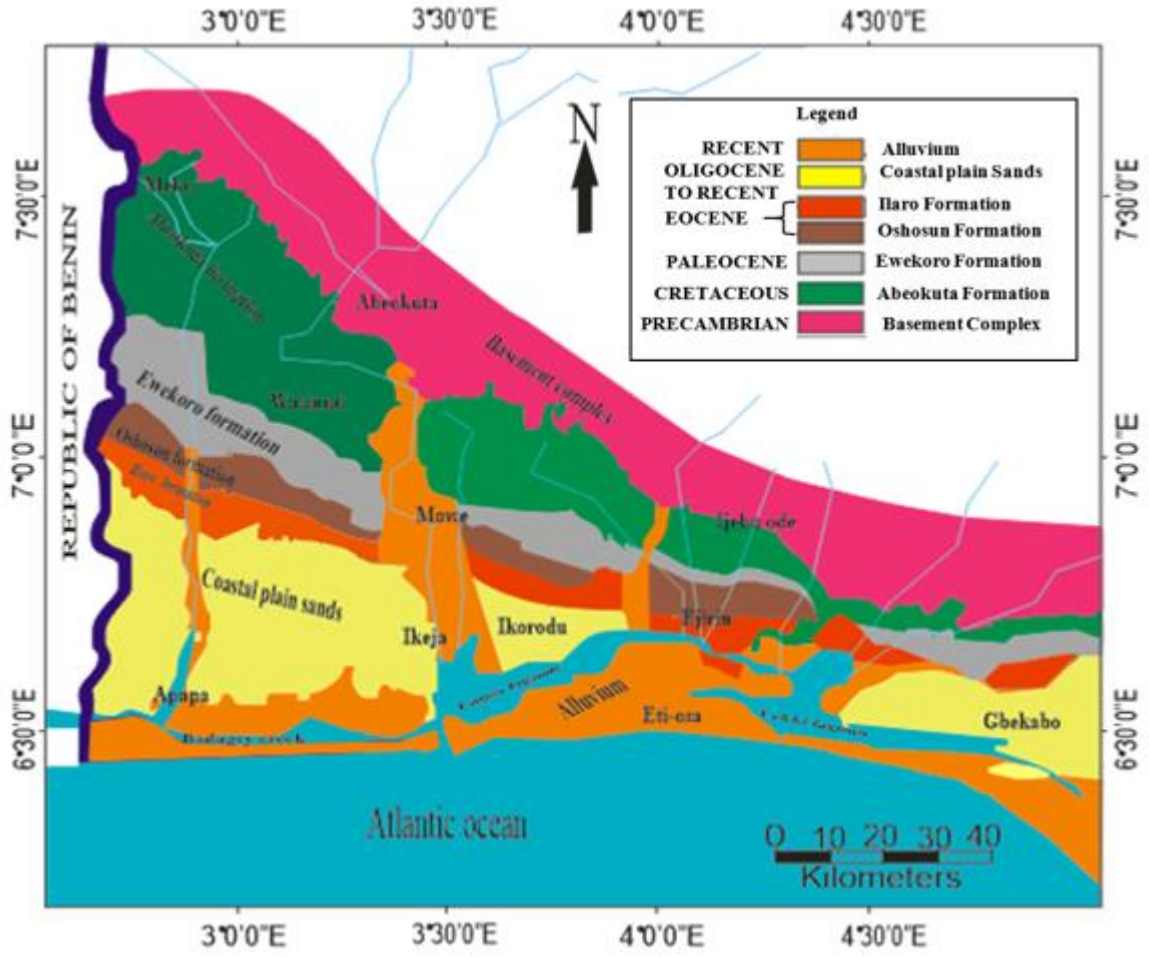

Source: Modified after Billman (1976)

Figure 2.9: Geological map of Lagos State

The entire geology of the coastal basin was formed in the recent geological time (post-Cretaceous). The surface geology includes the Benin Formation (Miocene to Recent), recent littoral alluvial, lagoon and CPS deposits (Longe et al., 1987). The sediments consist of an admixture of coarse to medium grains, clean white loose sandy-soil that graded into one another towards the lagoon and near the mouth of larger rivers (Oyeyemi et al., 2015). The sub-surface is made up of semi-permeable to impermeable geological formations (Akoteyon

et al., 2011). The CPS in a zone between Lekki and Akodo around Lakowe (south-east of this study area), and estimated to be about 20 km wide, consists predominantly of clay with only about 60 m of sand overlying about 240 m of clay, unlike the other areas of the basin where sand represents between 70 % and 95 % of about 300 m thick horizon (Oteri and Atolagbe, 2003).

2.10 Hydrogeological Setting

The basic physical features of the Lagos coastal aquifer are controlled by the nature of the geological strata, while its physical and chemical characteristics are influenced by both natural (geological) and anthropogenic processes (Longe et al., 1987). Generally, the good and major aquifers in the coastal zone of western Nigeria occur in Tertiary and Quaternary sediment deposits, while shale and clays form the impermeable horizons (Longe et al., 1987). An unconfined shallow aquifer also exists at less than 30 m in much of the near coastal area (United Nations, 1988). The water-bearing strata of Lagos State consist of sand, gravel, or admixtures from fine through medium to coarse sand gravel (Adeleye, 1975). Although opinion may differ among various authors with respect to the thickness and depth of a particular aquifer, it is unanimously agreed that the LCB consists of the multilayered aquifers hosted within the Dahomey Basin.

The notable aquifers are distinctly divided into four types. The CPS is the most accessible and most exploited aquifer through boreholes and hand-dug wells in the Lagos Metropolitan Area. This forms a multilayered aquifer system consisting of three aquifer horizons separated by silty or clayey layers (Kampsax-Kruger and Sshwed Associates, 1977; Longe et al., 1987). The first aquifer comprises recent alluvial sediments, while the second and third are the upper and lower CPS aquifers, respectively. The Ilaro and Ewekoro Formations are not key aquifers in Lagos as they are predominantly composed of shale/clay. The only source of hydraulic information on the Ilaro Formation was obtained at Lakowe where no freshwater horizon was intercepted. It has not been possible to differentiate the Ewekoro as a target aquifer in any boreholes or existing wells in the metropolis. The unit represents a minor groundwater resource in Lagos. The fourth is the Abeokuta Formation (Longe, 2011), which is represented by siltstone, poorly-sorted ferruginous grit siltstone, and mudstone with a shale clay layer. Figure 2.10 shows the hydrogeological cross-section.

Based on Jones and Hockey (1964), the first aquifer extends from the ground level to roughly 12 m below the ground layers of clay and sand. This upper aquifer is of minor importance for large water supply purposes and it is prone to pollution because of its limited depth. The second aquifer is intercepted between 20 m and 100 m below sea level and it can be found around the Igando axis. The third aquifer is encountered in the central part of Lagos at a depth ranging from 130 m to 160 m below sea level. The fourth aquifer is located at an elevation of approximately 450 m below sea level and it is separated from the third aquifer by a rather thick layer of shale of the Ewekoro Formation. Only a few boreholes tap water form this aquifer (Jones and Hockey, 1964).

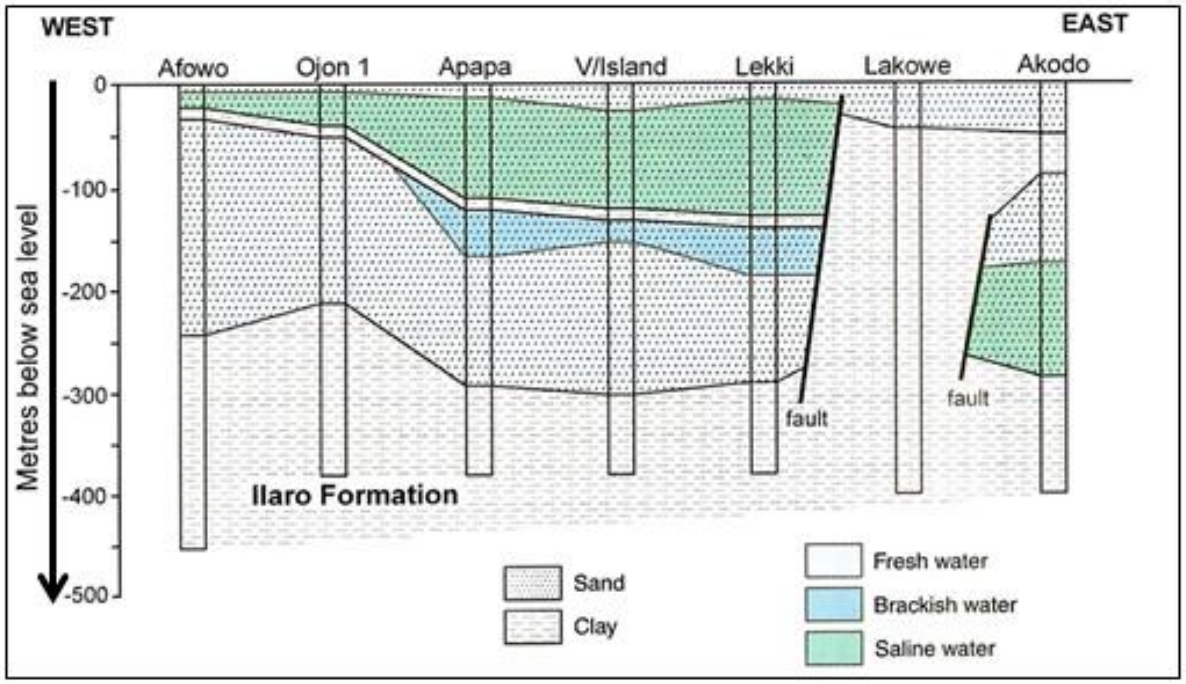

Source: Modified after Adelana et al. (2008)

Figure 2.10: Schematic hydrogeological cross-section of the study area

The Abeokuta Formation constitutes a deep aquifer only within the northern parts of Lagos city (Ikeja area) where boreholes are about 750 m deep. Similarly, Longe et al. (1987) described a succession of a 4 m thick lateritic cover (localised occurrence) that is underlain by alternating thin sands and clays in the part of Oregun, Ikeja. The first aquifer of loose, medium to coarse sands with an average thickness of about 10 m underlies this sequence. This water table aquifer is tapped by shallow boreholes and dug-wells for domestic water supplies and its thickness of 10 m separates the first aquifer horizon from the second sandy aquiferous zone. The second aquifer zone is a very vital groundwater source for private, commercial, and industrial supplies and exists between 20 m and 70 m (Longe et al., 1987).

This aquifer is confined with average values of transmissivity and storage coefficient of 1 120 m^2 per day and 3.77×10^4, respectively, have been reported (Longe, 2011). A third major aquifer zone, ranging from 15 m to 30 m in thickness, occurs at a greater depth in the Benin Formation. Encountered in central Lagos Metropolitan Area at depths ranging between 118 m and 166 m below sea level, this aquifer underlies much of Lagos State and dips towards the coast (Longe et al., 1987).

The Abeokuta Group aquifer is thick, extensive, contains water with recorded temperatures of up to 80 °C (Kampsax-Kruger and Sshwed Associates, 1977). This aquifer is relatively deep and as such expensive to exploit; it is tapped only by very few industrial boreholes. The general characteristics of Lagos aquifers were documented by Kampsax-Kruger and Sshwed Associates (1977) (Table 2.3).

Table 2.3: Descriptive characteristics of Lagos aquifers

T_r-intervals* ($m^2/s\times10^{-3}$)	Category of aquifer yield	Discharge (m^3/hour)	Drawdown (m)
T < 1	Poor	20	9–12
1 ≤T <5	Medium	30–50	5–8
5 ≤T <10	Good	50–100	3–10
10 ≤T	Very good	150	2–7

*T_r=transmissivity

It was equally noted across the coast that there is a progressive increase in aquifer thickness from its outcrop area in the north of the city to the coast in the south, and the sand percentage in the formation also varies from north to south (Longe et al., 1987). Generally, north to south groundwater flow was exhibited with two small cones of depression in Ikeja and Apapa due to intense groundwater abstraction (Coode Blizzard, 1997; Oteri and Atolagbe, 2003). The salinity level in the aquifer changes from north to south. The northern and central parts of the State are characterised by the freshwater-bearing aquifer, while the saltwater-bearing aquifer occurs in the southern coastal part of the State (Coode Blizzard, 1997; Oteri and Atolagbe, 2003).

Chapter 3
LITERATURE REVIEW

3.1 The State of Research on Groundwater Studies in the Lagos Coastal Basin

Over the years, several researchers have carried out various degrees of investigations (published and unpublished) on both groundwater and surface water in industrial and residential areas of almost entire parts of Lagos State. Among the prominent early research on the basin characterisation are those carried out by Jones and Hockey (1964), Kampsax-Kruger and Sshwed Associates (1977), Omatsola and Adegoke (1981), Oteri (1977, 1986), and Omosuyi et al. (1999).

Some recent publications that used conventional hydrochemical methods to investigate the groundwater of Lagos include Ikem et al. (2002), Adelana et al. (2003), Adelana and Olasehinde (2004), Adelana et al. (2005), Adelana et al. (2008), Adewuyi et al. (2010), Balogun and Akoteyon (2012), Akoteyon (2013) and Odukoya et al. (2013). These studies presented detailed information about the hydrogeological and hydrochemical characterisation of water in the northern parts relative to the study area. They all reported elevated concentrations of at least an element in fresh groundwater above the recommended limit for potable water by the World Health Organization and that contamination due to high total dissolved solids (TDS), nitrate, sulphate, and chloride that occur essentially around dumpsites and residential zones. Adelana et al. (2008) studied nitrate content in groundwater in different parts of Nigeria from pre-1970 to 2004 where they synthesized hydrochemical data of about 2,120 boreholes across the country. They reported a gradual increase in the nitrate content of groundwater from 1960 to date, and that about 33 % of the wells produced water above the WHO guide limit of 45 mg NO_3 /L, while 52 % was observed to exceed the permissible limit of WHO in the Lagos-Osse basin. This nitrate anomaly was suggested to be associated with anthropogenic activities. Akoteyon (2013) and Soladoye and Ajibade (2014) both made an overall state-wide analysis of selected hand-dug wells in order to access their water quality. They assert that there is no sampling point that did not have at least one parameter exceeding the WHO standards and thus none of the sampled wells can be considered ‘pure’, which indicates deterioration of water quality.

More recent investigations on hydrochemical assessment to the western side of the study area were documented by Adebo and Adetoyinbo (2009), Babatunde et al. (2009), Odukoya and Abimbola (2010) and Balogun and Akoteyon (2012). Oyeku and Eludoyin (2010) studied groundwater for heavy metals, bacteriological, and virological contents in industrial areas and near dumpsites in parts of Lagos. The anomalous occurrence of bacteriological content and at least one metal in all the water analysed required urgent attention. Adebo and Adetoyinbo (2009) recorded an elevated concentration of chloride in an unconsolidated aquifer in coastal parts of Lagos and this is traced to saltwater intrusion, while the water type delineated include (Fe-Ca-Mg-SO4), (Fe-Cl-HCO_3) and (Mg-Cl). Similarly, Ikem et al. (2002) evaluated groundwater quality close to a waste site in Lagos and found a concentration of NO_3, NH_3, COD, Al, Cd, Cr, Fe, Pb, and total coliform to exceed WHO recommended value. Longe and Enekwechi (2007); Babatunde et al. (2009); Odukoya and Abimbola (2010); and Odukoya (2010) studied groundwater quality near dumpsites in various parts of Lagos such as Isolo, Ojota, Festac, Ilupeju and Agbara. Elevated concentration of NO_3, Cl, SO_4, PO_4, Fe, Mg, and Coliform was detected at Isolo, Ojota and Festac. This is attributable to the leachate impact. While high cadmium, antimony, barium, tellurium, tungsten, copper, lead and nickel recorded at Agbara was linked to industrial effluent. Oyeku and Eludoyin (2010) assessed heavy metal pollution of groundwater resources in Ojota area with high level of metals such Pb, Cu, and Fe recorded in the hand-dug well. They submitted that this may be due to uncontrolled disposal of lead batteries, spent petroleum products and that, the spatial and seasonal variation in the level suggests point source pollution. Meanwhile, Soladoye and Ajibade (2014) carried out random groundwater quality study of Lagos state taken (30) representative samples from a shallow well in all the 27-LGAs and affirmed from their study that there was no sampling point that did not have at least one parameter exceeding WHO set standards. Hence, none of the sampled wells could be considered "pure", which indicates deterioration. He then concluded that groundwater within the Lagos environment cannot be said to be potable. A similar study in the southern coastline conducted by Balogun and Akoteyon (2012) in an unconsolidated aquifer, indicated seawater intrusion and industrial wastes as the major sources of pollution of the groundwater in the area.

Studies on the quality and hydrochemical characteristics of groundwater are widely reported worldwide (For example, Coetsiers and Walravens, 2006; Banoeng-Yakubo et al., 2009; Yidana et al., 2012; Abiye et al., 2018). These studies ascertained that the variation in the geochemistry of the groundwater is largely dependent on the interactions between

groundwater and geological materials through which water flows (rock-water interaction). Although, rock weathering process is an important factor in the hydrochemistry of surface and groundwater resources, evaluation of the dominant chemical process in groundwater of the LCB is scarce, if at all available.

A study by Oyedele (2001) employed both geophysical and geochemical analyses to show the presence of seawater intrusion in Victoria Island and Iwaya in Lagos State. It was suggested that the freshwater–saltwater interface is relatively shallow and water withdrawals are from depths close to the freshwater–saltwater interface. Also, excessive groundwater withdrawals can increase the incidence of seawater intrusion. Similar studies to demarcate saltwater intrusion zones in freshwater aquifers in coastal areas were undertaken by Oteri and Atolagbe (2003), Adelana and Olasehinde (2004), Adelana et al. (2008), Adepelumi et al. (2008), Ayolabi et al. (2009), and Adeoti et al. (2010) which further supported the presence of saltwater intrusion in the coastal area. In a similar study, Ayolabi et al. (2013) examined the saline water intrusion into wells at the University of Lagos using geophysical and geochemical analyses. The result revealed that the coastal aquifer had been affected by saltwater from the adjacent lagoon, as observed from the increasing electrical conductivity (EC) values from mainland aquifers towards the lagoon. In the study by Oladapo et al. (2013), the result showed the occurrence of saline water of varying depths and thicknesses from the surface along the coastal strip. The depths and the zones of intrusions increased with distance away from the west to the east. Also, Oyeyemi et al. (2015) investigated saline water intrusion in Oworo, a coastal alluvial terrain in Lagos. The study revealed that the intrusion occurred as lateral and upconing within the aquifer system.

In addition, the use of geophysical methods to delineate saltwater intrusion has attracted the overwhelming attention of researchers all over the world. An example from South Korea is giving in Lee and Song (2007); from southern Australia in Barret et al (2002) and Frohlich and Urish (2002) from Rhodes Island, USA. Particularly, Nowroozi et al. (1999) delineated the saltwater/freshwater interface in the geological setting of the eastern shore of Virginia. Furthermore, Urish and Frohlich (1990) and Frohlich et al. (1994) observed that the discharge of a large volume of groundwater may induce saltwater intrusion into the freshwater aquifers. Several researchers have adopted a variety of approaches to study the interactions between surface water and groundwater. These include experimental determination and estimation through numerical modeling (Mondal et al., 2010); geophysical surveys (Lee and Song, 2007); Isotopic signatures (Ne´grel and Casanova, 2005); and multivariate statistical

techniques (Liu et al., 2008). Although, the issue of interaction between freshwater and saline water has received fairly considerable attention, to further improve and enhance characterisation of the subsurface coastal aquifer, this research work employed the use of conceptual models, isotope studies and multivariate statistical methods that have not been adopted previously in the study area.

Furthermore, the use of isotopes have not received considerable attention in Nigeria especially in the southern parts of the country. Only a few researchers (Kehinde, 1993; Goni and Edmunds, 2001; Adelana et al., 2005) have used stable and environmental isotopes to investigate the origin, age, flow path, and recharge estimate of groundwater in the northern and central parts. Tijani et al. (1996) used hydrochemical and stable isotope compositions to deduce halite dissolution as the source of salinity of groundwater in the Benue trough in southeast Nigeria.

On a global perspective, environmental stable isotopes of hydrogen and oxygen are used to determine groundwater origin, and have been used to understand the mechanism by which groundwater is recharged and groundwater dynamics (Herczeg et al., 1991). Tredoux and Talma (2008) used isotopes of nitrogen and oxygen (^{15}N, ^{18}O) to deduce various sources of nitrate in groundwater in parts of South Africa. Vogel and Urk (1975) gave an additional example of the application of environmental isotopes in recharge studies in South Africa. The use of environmental isotopes (of ^{18}O, ^{2}H, ^{3}H) was adopted by Alemayehu et al. (2008) to deduce recharge source of groundwater and also to study interactions of different water bodies in Addis Ababa, Ethiopia.

In Summary, it is evident from the brief literature review that groundwater quality assessment has received considerable attention with respect to conventional physico-chemical, geophysical and pathogenic analyses. However, it is surprising that scanty studies have been conducted with respect to the aquifer evaluation through models and isotope perspectives (scientifically adjudged most qualitative indicator to study groundwater) of groundwater particularly in the southwestern part of the country, the location of the present study. The need for this research became imperative not only because of the increase in demand for water supply as a result of sporadic growth in population but also because of the dynamic and complex nature of the contaminants being generated (anthropogenic and natural) and which necessitate periodic scientific monitoring before the situation becomes worsen, uncontrollable and catastrophic.

3.2 Geophysical Methods

Geophysics remains the most viable tool for groundwater exploration and aquifer delineation. It is highly effective and records significant success rates in probing the subsurface for groundwater. There are well-known geophysical techniques that are available for ground-water exploration in both sedimentary and basement complex terrains. These include electrical resistivity, electromagnetic and seismic refraction. Other occasionally deployed methods are gravity, magnetic, and self (spontaneous) potential methods. The prominent geophysical method that is being used for groundwater prospecting is the electrical resistivity method. This is due to its adaptability for qualitative, semi-quantitative and quantitative usage for groundwater evaluation.

3.2.1 Electrical resistivity

The ability of electrical current to flow through materials is known as resistivity, which is an intrinsic property measured in units of ohm metres (Ω m). The method involves the intro-duction of a time-varying direct current or very low frequency (<1 Hz) electric current into the ground through two current electrodes, while the potential gradient (voltage) is measured across another pair of electrodes (potential electrodes), which may or may not be within the current electrodes, depending on the configuration. The current flow lines are perpendicular to the generated equipotential surfaces. As the distance between electrodes increases, the percentage of the current flowing at depth increases. In a homogeneous and isotropic formation, at a depth equal to the electrode spacing, 70% of the current flow is above a plane (Burger, 1992), that is, the distance between C1 and C2 (Figure 3.1).

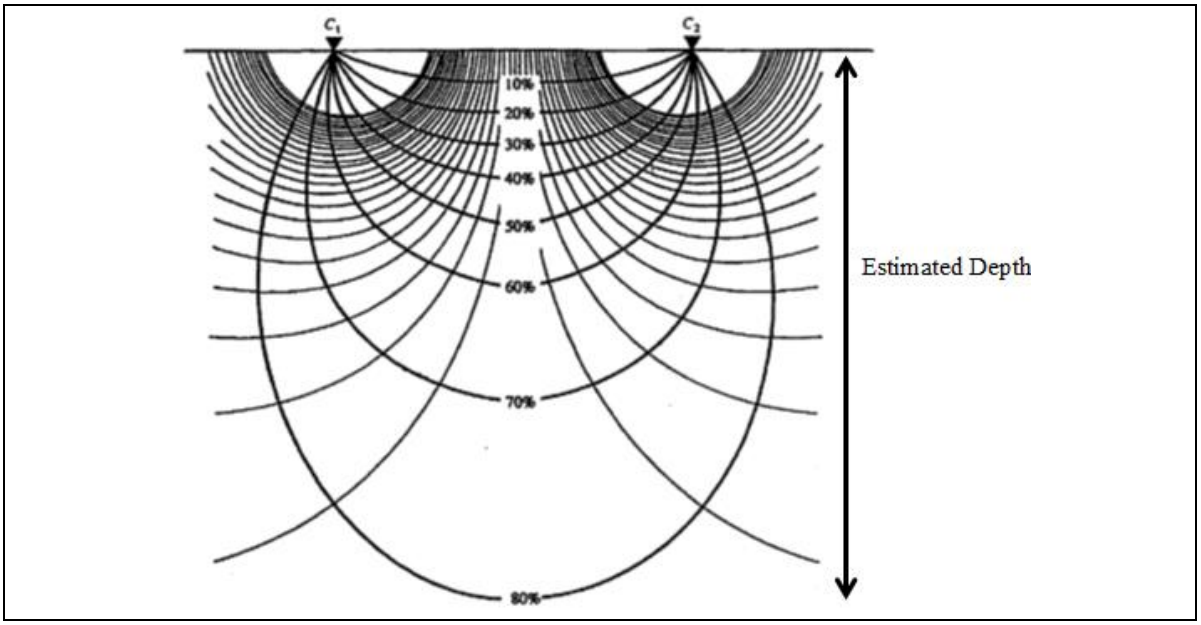

Source: Modified after Burger (1992)

Figure 3.1: Cross-section in a homogeneous and isotropic earth through an electric field which is set up by a two-current electrode configuration indicated by C1 and C2

In a multilayer system, the proportion of current that penetrate a particular depth is dependent largely on the electrode spacing, depth to the interface, and the material resistivities above and below the interface (Van Nostrand and Cook, 1966). The apparent resistivity of the subsurface is calculated from the measured resistance.

The apparent resistivity is the bulk average resistivity of all soils and rocks influencing the current; it is calculated by multiplying the recorded resistance (that is, the measured potential difference divided by the input current, automatically calculated by the measuring unit adopted for this study) by a geometric factor specific to the electrode configuration that has been adopted. Based on the geologic setting and the objective to suitably characterise the subsurface aquifer of the study area, Vertical Electrical Sounding (VES), two-dimensional electrical resistivity tomography (2D ERT), and borehole geophysical logs were the techniques employed. The most common electrode configurations used to measure apparent resistivity of the subsurface are Wenner, Schlumberger and dipole-dipole (Figure 3.2).

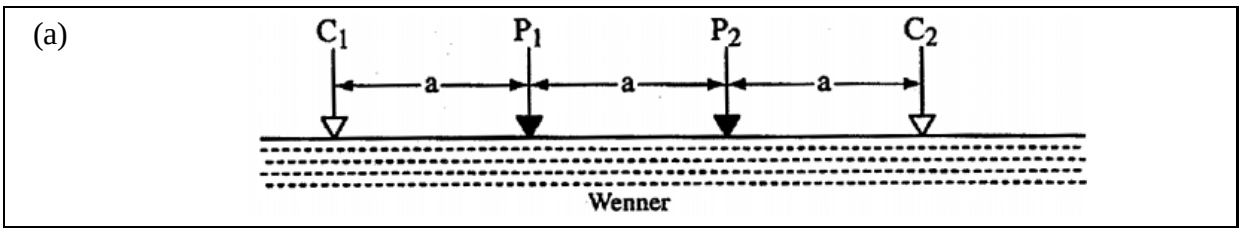

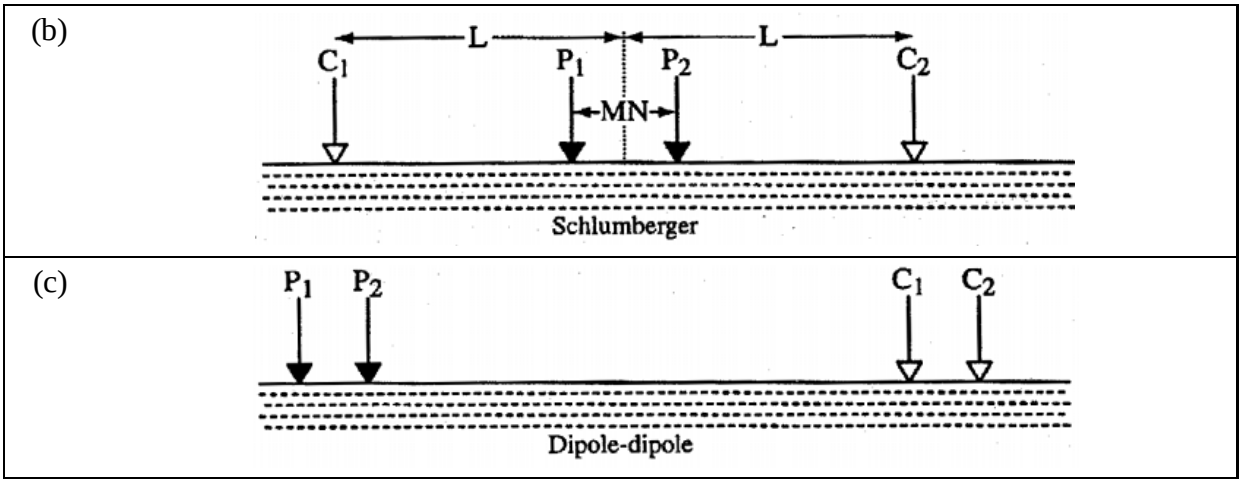

Figure 3.2: Common electrode configurations used to measure apparent resistivity of the subsurface

3.2.2 Borehole geophysical logging

Borehole logging is a process that involves measuring of physical, chemical, and structural properties of penetrated geological formations using logging tools, namely transducers (probes and detectors) that are lowered into a borehole on a wireline cable. The equipment, field application, and interpretation methods have been discussed by researchers such as Hallenburg (1987, 1992), Keys (1990), Yearsley and Crowder (1990) as well as Samworth (1992). Applications of geophysical well logging methods in shallow boreholes have been carried out by a number of researchers over the years for different purposes: geological investigations (Doveton and Prensky, 1992); determination of physical properties (Hearst et al., 2000), hydrogeological studies (Repsold, 1989; Mares et al., 1994; Jorgensen and Petricola, 1995; Kobr et al., 2005); delineation of coastal aquifers and freshwater–saltwater boundaries (Buckley et al., 2001; Hwang et al., 2004); and environmental investigations (Taylor et al., 1990; Keys, 1997; Krammer, 1997).

3.2.3 Dar Zarrouk parameters

The term 'Dar Zarrouk' (D-Z) was initiated on electrical prospecting by Maillet (1947) for describing a relationship between the longitudinal unit conductance and the transverse unit resistance. The D-Z was calculated from the VES values obtained in the field, from where longitudinal conductance (S), transverse resistance (T), and coefficient of anisotropy are derived using the following formula: Consider a multilayer resistivity interpreted model consisting of a layer of apparent resistivities, thickness and depth. Other derivatives are convolved to generate different geoelectric parameters. These identify electrical boundaries

separating layers of different resistivities (Zohdy et al., 1990). Geoelectric layers may be described based on two fundamental parameters, namely apparent resistivity (ρ) and thickness (h). D-Z parameters are derived based on apparent resistivity and thickness. These parameters are longitudinal conductance (S), mS = [layer thickness/resistivity], and transverse resistance (T) Ω m^2 = [layer thickness × resistivity]. The parameters T and S were termed the 'Dar-Zarrouk parameters' by Maillet (1947).

Consider a section consisting of 'N' layers with thickness h1, h2, h3…hn and a resistivity ρ1, ρ2, ρ3…ρn for the block unit area and thickness (H):

$$H = \sum_{i=1}^{N} hi \dots\dots\dots\dots\dots\dots\dots\dots\dots\dots (3.1)$$

The longitudinal conductance (S) is given by:

$$S = \frac{h}{\rho a} \dots\dots\dots\dots\dots\dots\dots\dots\dots\dots (3.2)$$

Total longitudinal unit conductance: It is the geoelectric parameter used to study variations in thickness of low resistivity material. Variation in S from one place to the other has been used in a qualitative sense to document changes in the total thickness of low resistivity materials (Henriet, 1976; Zohdy, 1989):

$$S_L = \sum_{i=1}^{n} \left(\frac{hi}{\rho i}\right) = \frac{h1}{\rho 1} + \frac{h2}{\rho 2} + \frac{h3}{\rho 3} + \cdots\dots\dots + \frac{hn}{\rho n} \dots\dots\dots (3.3)$$

While transverse resistance (T) is given by Equation 3.4.

$$T = h.\rho a \dots\dots\dots\dots\dots\dots\dots\dots\dots (3.4)$$

The total transverse resistance unit is used to study variations in the thickness of high resistivity materials as well as their transverse resistance (Zohdy, 1989; Batayneh, 2013).

Increasing Tr-values are indicative of an increase in the thickness of the high resistivity materials and has a direct relation with transmissivity (Equation 3.5).

$$T_L = \sum_{i=1}^{n} (hi.\rho i) = h1.\rho 1 + h2.\rho 2 + h3.\rho 3 + \cdots\dots\dots + hn.\rho n \dots\dots\dots (3.5)$$

The average longitudinal resistivity is (Equation 3.6).

$$\rho L = \frac{H}{S} = \frac{\sum hi}{\sum\left(\frac{hi}{\rho i}\right)} \ldots\ldots\ldots\

$$K\ (m/day) = 60 \times 60 \times 24 \times [k\ in\ (m/s)] \quad \ldots\ldots\ldots 3.10$$

Transmissivity is expressed as the product of the hydraulic conductivity and layer thickness and can be written as:

$$Tr = K \times h\ (m^2/day) \ldots\ldots\ldots\ldots\ldots\ldots 3.11$$

Where:

Tr = Transmissivity of the aquifer

K = hydraulic conductivity of the aquifer (m/day)

h = Layer thickness (m)

Porosity of an aquifer and could be related to the formation-factor by the formula below deduced from Archie's experiment.

$$F = a/\phi^m \ldots\ldots\ldots\ldots\ldots\ldots 3.12$$

$$\phi = [a/F]^{1/m} \ldots\ldots\ldots\ldots\ldots\ldots 3.13$$

The formation factor is further related to the hydraulic conductivity as written below:

$$F = [K/a]^{1/m} \ldots\ldots\ldots\ldots\ldots 3.14$$

Where:

F = Formation factor;

ϕ = aquifer porosity;

a = 0.62 (Tortuosity factor for unconsolidated sands)

m = 2.15 (cementation exponent)

The interpreted longitudinal conductance and measured water level data were contoured in order to observe the protective capacity and groundwater flow direction, while the aquifer transverse resistance, aquifer longitudinal conductance, aquifer resistivity, aquifer thickness and aquifer transmissivity were all contoured for groundwater characterisation. The SURFER© 13 software was used in producing the maps and profiles.

3.3 Environmental Isotope Analyses

3.3.1 Stable isotopes

Environmental stable isotopes of hydrogen and oxygen are used to determine groundwater origin and have been used to understand the mechanisms by which groundwater is recharged as well as groundwater dynamics (Herczeg et al., 1992).

An isotope refers to the atomic nuclei of an element containing different numbers of neutrons. Isotopic differentiation is produced when physical processes, for example, evaporation, condensation, and melting, separated isotopes into the light and heavy fractions (Fetter, 2001). The chemical or physical processes in compounds or phases present in the same system produced variations in the isotopic composition known as isotopic fractionation (Geyh, 2000). The stable isotopes of ^{2}H and ^{18}O occur naturally in precipitation and provide a seasonal meteoric signal in temperate, continental systems that are often attenuated in shallow groundwater (Clark and Fritz, 1997; Abiye, 2013). Isotopes of hydrogen (^{1}H) and oxygen-16 (^{16}O) contained in water molecules are lighter than the water-containing molecules of deuterium (^{2}H) and oxygen-18 (^{18}O).

Heavy storm precipitations are characterised by depleted heavy isotopes relative to the mean ocean water. Conversely, during condensation, the heavy isotopes condense first, leading to an early isotopically enriched rainfall and subsequently depleted cloud moisture (International Atomic Energy Agency [IAEA], 2012). Moreover, precipitation originating from a lower altitude is isotopically more enriched in ^{2}H and ^{18}O than precipitation at higher altitudes. Environmental isotopes (stable and radiogenic) as a tool for hydrogeological studies are gaining popularity in recent times and have been used to gain some insight into the subsurface flow and recharge conditions (Abiye, 2011; Abiye et al., 2011). Naturally occurring stable (^{2}H, ^{18}O) and radiogenic (^{3}H and ^{14}C) isotopes of waters have been widely employed over the past 40 years to solve problems related to groundwater recharge and its residence time (Fontes, 1980; Gonfiantini, 1986; Clark and Fritz, 1997; Chen et al., 2006). Among these isotopes, ^{2}H and ^{18}O are the most widely used in solving hydrogeological problems. The analyses of oxygen-18 and deuterium are the determination of the high precision of stable isotopes ratio of oxygen $^{18}O/^{16}O$ and $^{2}H/^{1}H$ in water molecules, respectively. The stable isotopic composition of a water sample is denoted by δ notation:

$$\delta = \left(\frac{R_{sam} - R_{std}}{R_{std}}\right).1000$$

Where R = $^{2}H/^{1}H$ or $^{18}O/^{16}O$ and all values are reported in per million with reference to Vienna Standard Mean Ocean Water (Gonfiantini, 1978). A negative and positive value connotes depletion and enrichment in the heavy isotope, respectively, relative to standard. Therefore, the ratios of these stable isotopes are useful in deducing the precipitation source areas of recharge to an aquifer (Mazor, 1991).

These pairs of isotopes are also useful towards unravelling the processes which the water has been subjected to in the course of the hydrological cycle. On a global average, the general meteoric relationship between ^{18}O and ^{2}H was found to be linear for natural water and has been defined by the global meteoric water line (GMWL) with the following equation for freshwater worldwide (Craig, 1961):

$$\delta^{2}H = 8 * \delta^{18}O + 10\ ‰$$

The concept of the deuterium excess (d-excess) is defined as $d = \delta^{2}H - 8*\delta^{18}O$ (Dansgaard 1964). The d-excess characterises the isotope composition of the evaporated moisture. A large d-excess indicates precipitation derived from an air mass with admixed re-evaporated moisture (Dansgaard, 1964). The GMWL represents an average of several regional and local meteoric water lines (LMWL) that differs from the GMWL in slope and/or intercept as a result of variations in climatic and geographic factors (Clark and Fritz, 1997). The IAEA (2000) established the Global Network of Isotopes in Precipitation (GNIP) in order to document the variations of isotopes in precipitation.

The $\delta^{18}O$ values vary from one rainfall event to another as a result of seasonal changes in ocean temperatures and air–sea interaction conditions and short-term events such as a storm. The range of variation could be up to ±10 ‰ in $\delta^{18}O$ values (Gat, 1996).

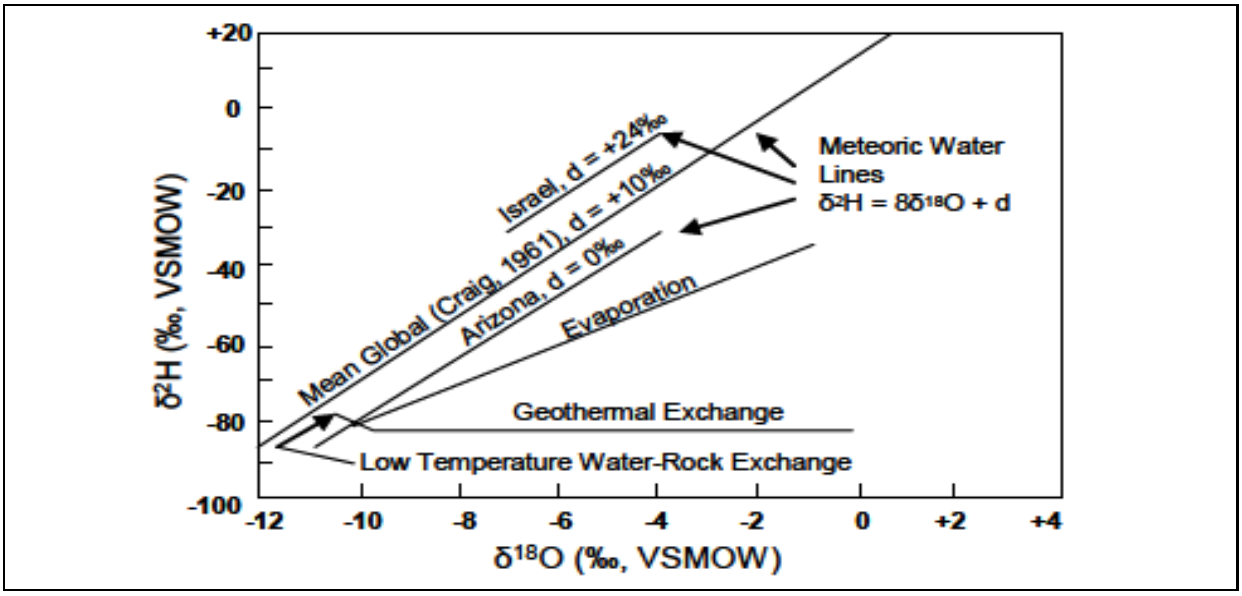

Source: Cook and Herczeg (2000)

Figure 3.3: Examples of the relationship between deuterium and Oxygen-18 in meteoric water, evaporating water and interactions with rock

Fractionation, resulting from the difference between the physical characteristics and different weighted water isotopes, influences the isotope values in the rain and consequently the groundwater composition. Other important notable effects in isotope variations are the following:

- **Temperature effect**: High and rising temperature enriches deuterium and oxygen-18, while vapour gets depleted by these stable isotopes. These isotopic differences are represented by seasonal variations (Mazor, 1991).
- **Continental effect**: It is otherwise known as the distance-from-coast-effect. There is a progressive depletion in isotopic ratio with distance away from the ocean. This exhibits considerable variations from area to area, season to season and even over a low-relief profile. It depends both on topography and climate regime.
- **Altitude effect**: The isotopic composition of precipitation gets more depleted in heavy isotopes at higher elevations. The depletion of the heavy oxygen isotopes varies with elevation ranges between 0.1 and 0.5 ‰ per 100 m and this has enabled the identification of the elevation at which groundwater recharge has occurred.
- **Amount effect**: Intense rainfall has a lower ^{2}H and ^{18}O content. Evaporation increases these contents in little rainfall events more than big rainfall events (Mazor, 1991).

3.3.2 Radio isotopes

Tritium is a radioactive isotope of hydrogen having a half-life of 12.32 years (Fetter, 2001) and was created naturally by cosmic radiation. This enables it to be used as a reliable tool to date relatively young groundwater with <50 years of recharge. The tritium levels denoted by TU (tritium unit), are extremely low in rainwater and represent a $^{3}H/^{1}H$ ratio of 10^{-18}. One TU represents a tritium concentration of $^{3}H/^{1}H=10^{-18}$ and has an activity concentration of 0.119 Bq/kg.

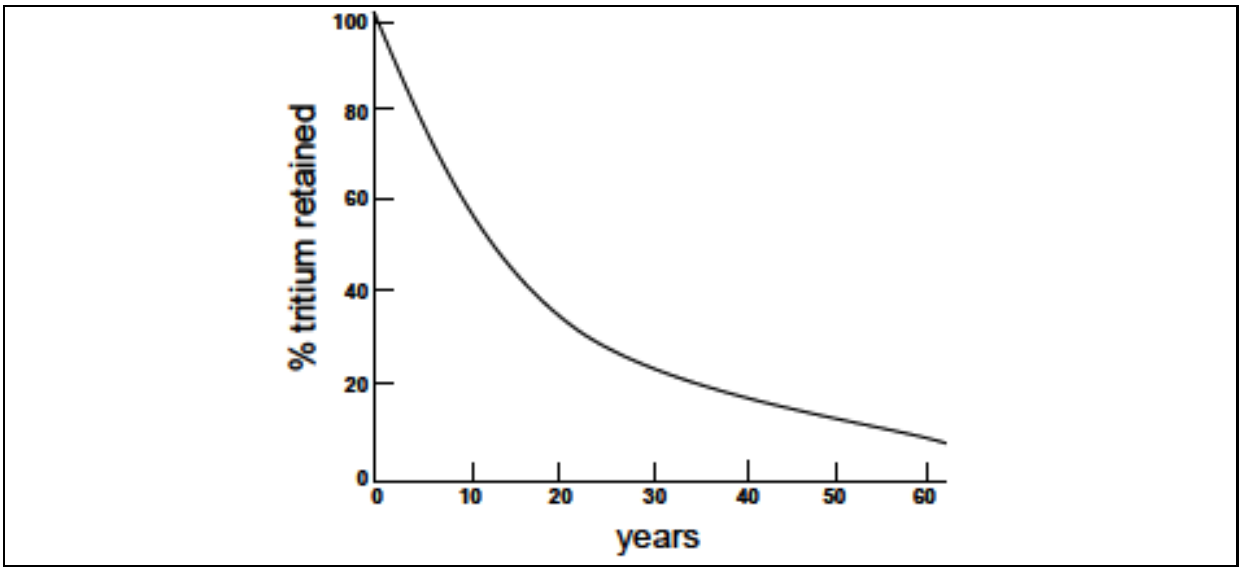

Source: Kendall and McDonnell (1998)

Figure 3.4: Slope of the radioactive decay curve of tritium

Prior to nuclear weapon tests, rainfall tritium contents were in the order of 3 to 5 TU. Sequel to the early 1960s, the thermonuclear test that injected ^{3}H into the atmosphere, the tritium content in precipitation increased to 1 000-fold, especially in the northern hemisphere. Since 1963, the peak tritium concentration has decreased to natural values in winter and about double natural in summer. This event consequently affected the groundwater tritium content as aquifers are being recharged and it is consequently used to differentiate groundwater recharge during the pre-bomb time from younger water (Clark and Fritz, 1997). Its variation provides an insight into local recharge and circulation mechanisms since the tritium level in groundwater is preserved underground and can only be altered by mixing with older water and radioactive decay (Weaver et al., 2007). Therefore, ^{3}H content is often being used to determine dates *ante quem* and *post quem*. For example, water with $^{3}H < 5$ TU must have a residence time of more than 40 years, while water having $^{3}H > 20$ TU must date after 1961 (Clark and Fritz, 1997).

3.3.3 Carbon isotopes

The stable isotopes of carbon in dissolved inorganic carbon were determined to evaluate the geochemical processes such as methanogenesis and sulphate reduction, while ^{14}C of inorganic carbon was measured to deduce groundwater age (Clark and Fritz, 1997). The carbon isotopes of ^{13}C and ^{12}C play an important role in quantifying water–rock interactions in the process of ^{14}C age determination of groundwater. Their ratios also allow us to identify the proportion of biogenic and carbonate CO_2 in water and to determine initial geological settings of groundwater recharge. Carbon-14 is derived from the atmosphere. The original ^{14}C present in groundwater is essentially influenced, either by gradual decay over time, or dissolution of carbonate rocks that contain no carbon-14. Both processes decreased the ^{14}C content in groundwater with increasing residence time underground. The increment in the natural concentrations of both carbon-14 and tritium in water resulted from thermonuclear testing, particularly in the early 1960s. Therefore, elevated concentrations of ^{3}H and ^{14}C in groundwater indicate the presence of recent recharge. The carbon-14 content, however, decreases in old water through radioactive decay. Hence, ^{14}C values can be used as a residence time determination tool, while Carbon-13 values are useful in the identification of the origin of carbon in groundwater (Loehnert, 1988). The longer half-life of carbon-14 (5 730 years) makes it suitable for dating old hydrological systems (Mann et al., 1982).

Chapter 4
METHODS AND MATERIALS

4.1 Desktop Review / Data Acquisition

The existing geophysical, geochemical, hydrological, and hydrochemical data were analysed as part of the desktop review for the study area. This included a collection of relevant meteorological data from the previous work of Oke (2015). Electrical resistivity data and borehole logs were gathered from various sources such as the Ministry of Energy and Mineral Resources, LWC and Groundwater and Geophysical Services Limited to determine the subsurface hydrogeological conditions. Published and unpublished literature related to the study area were also reviewed. Due to the dearth and paucity of data, the research delved in detail with areas situated along the coastline from Apapa in the west to Ibeju-Lekki in the east.

4.2 Field Measurements, Sampling Procedures and Analyses

The methodology employed in this research is presented in the workflow chart shown in Figure 4.1. The research involved essentially two broad techniques that are widely used in probing variations in the subsurface and its fluid content, namely: geophysical and hydrochemical methods. Having done an extensive literature review, the study proceeded to the level of fieldwork during which onsite measurements were taken and recorded for further data processing (geophysical method). Also, physicochemical parameters measurements were also recorded onsite and water samples were collected for various laboratory analyses including major ions, heavy metals, microbial counts and isotopes contents. A quantitative and qualitative interpretation of the analysed data assisted tremendously to evaluate to what extent the aim and objectives of the research have been accomplished.

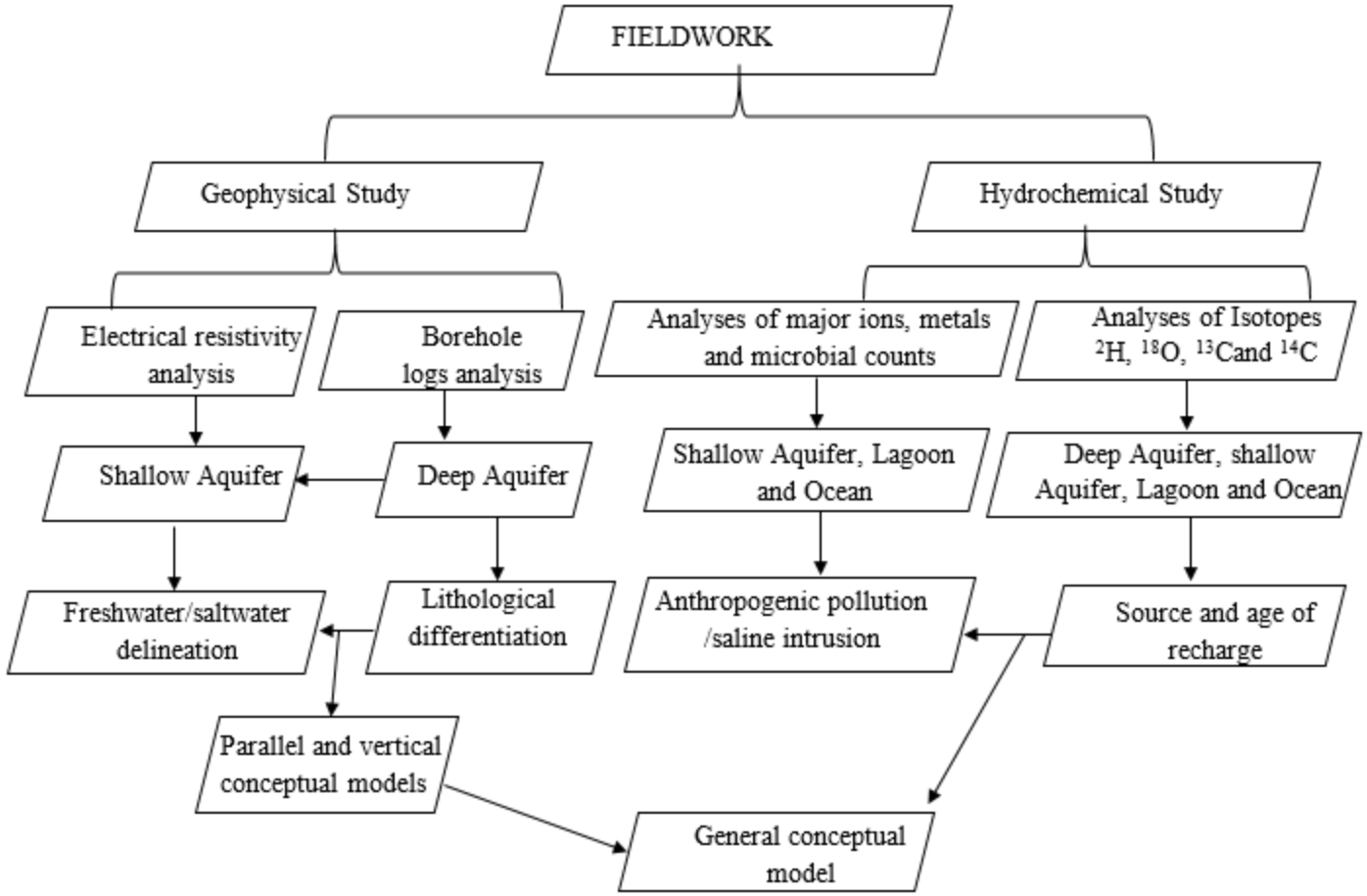

Figure 4.1: Work flow chart showing the summary of methods and analyses adopted in this research

4.2.1 Hydrochemical on-site measurements

The sampling sites comprised shallow wells, mostly hand-dug and surface water located around and across the study area. The choice and number of sampling sites were constrained by accessibility to dug-wells. Sampling was strategically conducted in order to ascertain the variations associated with different seasons. Samples were collected from surface water (Ocean), shallow hand-dug wells, deep boreholes, and rainwater during the September and October 2016, February 2017 and 2018 hydrological years. A total of 171 samples were analysed for major ions, trace metals and microbial counts determination for both dry and wet seasons as well as surface waters (Table 4.1). The samples were collected in different sizes of pre-cleaned airtight plastic containers for various analyses.

Table 4.1: Major ions, metals and microbial count analyses and number of samples analysed for groundwater and surface waters

Season	Water media	Major ions*	Metals**	Microbial count (F. coli)
Wet season	Shallow groundwater	40	40	40
	Surface water (Ocean)	1	1	1
	Surface water (lagoon)	–	3	3
Dry season	Shallow groundwater	42	–	–

* Ca^{2+}, Mg^{2+}, Na^{+}, K^{+}, Cl^{-}, HCO_3^{-}, SO_4^{2-}, CO_3^{2-}, NO_3^{-}
** Zn^{2+}, Cu^{2+}, Pb^{2+}, Mn^{2+}, Fe^{2+}, Ni^{2+}, Cd^{2+}, Ag^{+}, Cr^{2+}

The records of dug-well completion were not available for the study or were non-existent. In most cases, groundwaters were sampled directly from the dug-wells, while we were compelled to take samples via household taps in some places. The surface water samples, however, were taken at least 250 m away from onshore areas and below the surface (>20 cm) to avoid the collection of floating debris, ensure even mixing as well as relatively adequate sample representation. The sampled waters were collected unfiltered and stored in tightly sealed plastic bottles. In other to ensure adequate representation of the groundwater samples at every location, the wells were pumped as the case may be prior to sampling. The onsite measured physico-chemical parameters include water level depth, temperature, and conductivity taken with the aid of a Solinst temperature, level, and conductivity meter, while pH and TDS were also measured in situ using the Hanna HI 98130 multiparameter water quality meter. The coordinates at every location were determined using the GARMIN GPS Map 60CSx Global Positioning System. In addition, it is important to state that water samples

from deep borehole of Lagos State Water Corporation were collected in the year 2018 and analysed strictly for both stable and radiogenic isotopes.

Unfiltered water samples were taken to the laboratory for cation and anion analyses. The cation samples were acidified to below a pH of 2, using nitric acid (30 % HNO_3). Also, a total of 130 water samples were analysed for environmental isotopes for rainwater, both seasons' shallow groundwater and surface water and the deep groundwater (Table 4.2). Samples for ^{18}O and ^{2}H were collected in 10 ml glass bottles with airtight caps. The samples for tritium analysis were collected in sealed one-litre plastic bottles. The samples for the carbon isotope determination were collected by precipitating $BaCO_3$ by adding $BaCl_2$ to 50 L of water that was previously brought to pH ≥12 by the addition of NaOH. The stable Isotope contents in precipitation of the Benin Republic was taken from the GNIP database (IAEA/WMO, 2000) (Appendices A–C show how the samples were collected and the preparation of the samples to be analysed.)

Table 4.2: Environmental isotope analyses and number of samples analysed for groundwater, surface waters and rainwater

Season	Water media	O-H	Tritium (TU)	^{14}C	^{13}C
Wet season	Shallow groundwater	30	21	9	7
	Surface water	3	–	–	–
	Rainwater	1	–	–	–
Dry season	Shallow groundwater	34	–	–	-=–
	surface water	5	–	–	–
	Deep groundwater	5	5	5	5

4.2.2 Laboratory analysis

The major ions and trace metal analyses of water samples for the years 2016 were conducted at the Lagos State Environmental Protection Agency, using an atomic absorption spectrophotometer, while analyses for magnesium, carbonates, and bicarbonates were conducted at the Central Laboratory at the University of Lagos, using the volumetric analysis method. The major constituents' analysis of water samples for the year 2017 was carried out at the Geology Department of the University of Ibadan, using flame photometry for the cations (PFP7 Flame Photometer). Nitrate (NO_3^-), carbonate (CO_3^{2-}) and sulphate (SO_4^{2-}) were determined using a spectrophotometer (model Genesys 20), while Bicarbonate (HCO_3^-) and chloride (Cl^-) were determined by titration in chemistry at the Chemistry Department at the

University of Ibadan. In other to check for the quality of analytical data, error and inconsistency were determined by calculating the Charge Balance Error. The threshold Charge Balance error value of ±10% is the proposed acceptable error (Appelo and Postma, 2005). Only samples that satisfy the proposed acceptable error limit were adopted for data processing and interpretation. In addition, a comparison of measured total dissolved solids (TDS) with the calculated total sum of major constituents showed an agreement and thus increases confidence in the use of the data.

The stable isotopes of ^{18}O and ^{2}H were analysed at the Hydrogeology laboratory at the School of Geosciences, using the Liquid Water Isotope Analyser-model 45-EP at the University of the Witwatersrand, South Africa, while ^{14}C, ^{13}C and ^{3}H analyses were carried out at the i-Themba Environmental Isotope Laboratory in Gauteng, South Africa. All samples were replicated.

The results are represented in the conventional Vienna Standard Mean Ocean Water normalisation (Gonfiatini, 1986). The precision obtained was 0.05 % and 1 % for ^{18}O and ^{2}H, respectively. The results for tritium (^{3}H) were reported in TU with a typical error of ±1 TU (Echinger et al., 1981), while ^{14}C of dissolved inorganic carbon was radiometrically determined by liquid scintillation counting after conversion to benzene (Fontes, 1971). The generated CO_2 by acidification of the field precipitate with phosphoric acid (H_3PO_4) was graphitised and analysed by Accelerator Mass Spectrometry (AMS). The ^{14}C was between 0.7 pMC and 1.0 pMC. The $\delta^{13}C$ was spectrometrically determined and expressed as δ-values related to the Vienna Pee Dee Belemnite. The standard precision for $\delta^{13}C$ is ±0.5.

4.3 Geophysical Field Data Acquisition and Processing

4.3.1 Data acquisition

4.3.1.1 Vertical electrical sounding

The PASI 16GL Earth Resistivity Meter, Serial Number 07073185, complete with peripherals (see www.pasigeophysics.com) was used for resistivity measurement being rugged and reliable measuring equipment. The resistivity meter was applied in the field measurement of apparent resistivity by direct current injection. VES was the survey technique adopted for this study, using the Schlumberger Array, where C1 and C2 are current electrode positions, while P1 and P2 are potential electrode positions. Twelve VES were undertaken (Appendix D II). The choice of electrode configuration adopted was informed by

the availability of space, while current electrode separation (AB) ranges from a minimum of 2 m to a maximum of 30 m. Other pieces of equipment deployed for various purposes were GARMIN GPS Map 60 CSx Global Positioning System, PASI P 100.2 Energiser, cables, steel electrodes, measuring tapes, calculator, and hammers.

4.3.1.2 Electrical resistivity tomography

In order to complement the acquired data made available to us by the Ministry of Energy and Mineral Resources and LWC, a 2D ERT was conducted using an AGI SuperSting R8/IP8 earth resistivity meter, an eight-channel Memory Resistivity and IP Meter with an in-built processor for a 64- and 84 multi-electrodes system (Appendix D I). Three types of electrode arrays were deployed for the investigation for better horizontal and vertical resolution, namely Schlumberger, Dipole-Dipole, and Pole-Dipole. There were variations in the minimum electrode spacing 'a' used (from 1.6 m to 8.0 m) owing to constraints in space since the entire study area was built-up. Notwithstanding, a fairly deeper depth was probed in the traverses, having used expansion factor n=30. The choice of arrays for the survey was based on the desire to have good sensitivity to vertical and horizontal changes in the subsurface resistivity at both shallow and deeper depths, at the same time probing into the deeper depth and to have good vertical and horizontal data coverage under each ERT line. Schlumberger was chosen for a two-dimensional survey array with overlapping data levels because of its good horizontal and vertical resolution. Dipole-dipole was employed because it is good in mapping vertical structures, as well as better horizontal data coverage than Wenner (Loke, 2004). Pole-Dipole is known for deeper depth penetration. In all, nine 2D ERT profiles were measured, covering parts of the study region (Appendix D shows how the geophysical profiling was done). The Earth Imager software was used to invert the apparent resistivity profiles to obtain a 2-D image of the subsurface resistivity distributions. The ERT profiles were inverted using an iterative smoothness constrained least-squares inversion algorithm otherwise known as "OCCAM inversion" after deGroot-Hedlin and Constable (1990) and Loke and Barker (1996). These inversion routines involve a cell based inversion technique otherwise known as finite element method. It subdivides the subsurface into a number of rectangular cells in which resistivities are varied to obtain the best fit with the observed data (Loke, 2004; Ayolabi et al., 2013). In order to achieve an acceptable agreement, the differences between the observed and calculated data were minimized (Loke and Barker, 1996). This difference is given by the root-mean-square error (RMS %).

However, large and unrealistic variations in the output models are disallowed by smoothness constrained models.

The VES was carried out using the Schlumberger array with half current electrode spacing (AB/2) varying from 1 to 200 m. The vertical electrical resistivity field data were interpreted with software known as IPI2WIN. Schlumberger array for 1-D VES was chosen because of its good sensitivity to vertical variations in the subsurface resistivity. At the initial opening of the data file, it displayed a graph without resistivity cross-section. The best fitting two-layered model was chosen based on the recommendation of IPI2WIN software. A best fitting model for the initial interpretation for the input data will be automatically suggested by the software. Editing of the model includes altering the layers quantity by means of joining and splitting (to remove or add layer respectively) and changing the properties of the layers. The degree of uncertainty of the computed model parameters and the accuracy of fit in the curve fitting algorithm are expressed in terms of fitting error (Error=3.62 % to 5.61 %). The resistivity of various layers and the corresponding thickness are generated by a number of inversions until the model parameters of all the VES curves were totally resolved with the fitting error.

4.3.1.3 Borehole geophysical logs

An RG PCL II Logger with PCL IITM software mounted on a vehicle was used. A known voltage was passed through a probe consisting of R8, R16, R32 and R64 units in a water-filled hole, and the resistivity was recorded. The natural gamma radiation of the lithology encountered in the hole was also measured simultaneously with a different probe. The logs obtained included natural gamma rays, short (SH N) and long (LO N). A total of 45 borehole logs, gathered from both government and private drillers, were analysed (Appendix D III). The logs were acquired over the years (as far back as 1995 and as recent as 2015) mainly with the DEI 600 L Logger, and in a few cases, the normal (LO N) resistivity. The natural gamma rays were plotted against depth using Microsoft Office Excel. The type of lithology and the lithological sequence was inferred from the qualitative interpretation of natural gamma ray logs, while the resistivity logs were interpreted both quantitatively and qualitatively to delineate the freshwater aquifer, freshwater–saltwater interface, and saline water horizon thickness.

4.3.2 Data processing

4.3.2.1 Tools used for processing and interpretation

The vertical electrical resistivity field data was curve-matched with the use of a conventional curve-matching technique, and the layer parameters obtained were used as an input model for a computer iteration software known as IPI2win. The true resistivity estimated from the inverse procedure gives the apparent resistivity. The inversion essentially reduces the difference between the modelled and measured apparent resistivity. The commonly-known basic curve types are A, H, K and Q and form the basis of one-dimensional curve interpretation (Figure 4.1). The curve type(s) revealed resistivity variation as the lithology varies with depth.

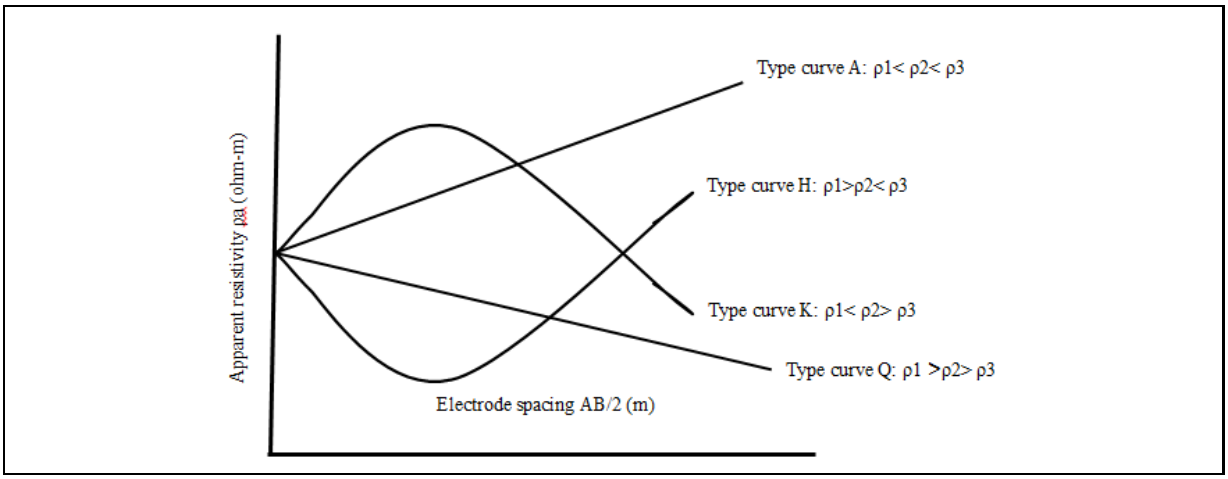

Figure 4.2: Diagram of resistivity curve types in layered structures

The geoelectrical resistivity of sediments being the most variable physical properties, especially in a complex sedimentological environment, may give rise to ambiguity in interpretation; thus, the VES data were calibrated with the available borehole data near the study area. In addition, resistivity ranges for various formations are close and sometimes intermixed. For example, ranges of clay with fresh water and a clayey layer with sand are interfering, while close values exist between ranges for sandstone with freshwater and sandstones with clay, and clay with freshwater and clay with saltwater. These ranges intermix and produce an ambiguity in the interpretation of the VES results. This ambiguity makes it difficult to distinguish depth limits between two types of subsurface lithologies due to the effect of equivalence and suppression. Therefore, the addition of D-Z parameters was necessary to improve the analysis of resistivity data in resolving some ambiguities

encountered in stratigraphic layers. The protective capacities of the upper and near-surface layers were rated based on Oladapo and Akintorinwa's (2007) ratings (Table 4.3).

Table 4.3: Longitudinal conductance/protective capacity rating

Longitudinal conductance (Ω^{-1})	Protective capacity rating
>10	Excellent
5–10	Very good
0.7–4.9	Good
0.2–0.69	Moderate
0.1–0.19	Weak
<0.1	Poor

Source: Oladapo and Akintorinwa (2007)

The computer software SURFER© 13 contouring toolkit was used in producing the aquifer protective capacity model maps. The Radial Basis Function was adopted for interpolation because it gives the best cross-validation results and root mean square errors.

The Earth Imager software was used to invert the apparent resistivity profiles to obtain a 2D image of the subsurface resistivity distributions. The ERT profiles were inverted using an iterative smoothness constrained least-squares inversion algorithm, otherwise known as 'OCCAM inversion', after DeGroot-Hedlin and Constable (1990) as well as Loke and Barker (1996). A measure of this difference is given by the root-mean-square error (%).

In the borehole log studies, the different sand aquifers were identified and classified based on the correlation of natural gamma ray log obtained from different boreholes in Lagos by Coode et al. (2006). The resistivity data presented on the logs resulted from the qualitative interpretation of resistivity values of formation at various zones, while the logs' interpretation was based on the classifications of Zohdy and Martin (1993) and modified by Ibrahim (2008) (Table 4.4).

Table 4.4: Resistivity values for water and sediment rock

Resistivity (Ω m)	Sediment rock	Interpretation
0.5–2.0	Very porous sand, or saturated clay	Seawater, very saline water TDS = 20 000 mg/L
2.0–4.5	Porous sand, or saturated clay	Saline water, TDS = 10 000 mg/L
4.5–10.0	Sandy, saturated, or sandy clay	Salty brackish water, TDS = 10 000–5 000 mg/L
10.0–15.0	Sandy clay, sandy gravel	Brackish water, TDS = 5 000–1 500
15.0–30.0	Sand, gravel, some clay	Poor quality freshwater, TDS = 1 500–700 mg/L
30.0–70.0	Sand, gravel, minor clay	Intermediate quality freshwater, TDS ~100 mg/L
70.0–100.0	Sand, gravel, no clay	Good quality freshwater, TDS small
> 100.0	Coarse sand, gravel, no clay	Very good quality freshwater, TDS very small

Source: Zohdy and Martin (1993), modified by Ibrahim (2008)

The hydrogeochemical processes controlling the chemistry of the groundwater were identified with the aid of PHREEQC inverse geochemical modeling software. RockWare's AqQA software was used for hydrochemical characterisation of the water samples and their visual appreciation through Piper and Schoeller diagrams. Microsoft Excel was used to plot the Gibb's diagram to deduce the mechanisms controlling the water chemistry. Multivariate statistical analysis was performed with the use of the Statistical Package for Social Sciences (SPSS) software, version 21.0, while the principal component analysis was undertaken using Kaiser's Varimax Rotation.

4.4 Field Limitations/Constraints

i. The availability of adequate space for the current electrode spacing was a major challenge in a typical built-up area. Also, the distortion within the topsoil and shallow subsurface, perhaps due to sand-filling, reclamation, and buried cables/utilities, often characterised the acquired data with noise. Furthermore, the host communities in places denied us access to areas that would have been ideal for data acquisition.

ii. Payments had to be made at some places before samples could be taken or research conducted.

iii. Many private hand-dug wells and borehole owners reluctantly granted access, while a few uninformed ones denied us access to their boreholes.

iv. Limited or non-availability of database where information could be pooled for the necessary scientific research is a constraint.

Chapter 5

HYDROGEOLOGICAL UNITS AND HYDRAULIC CHARACTERISATION OF THE COASTAL BASIN

5.1 Introduction

Freshwater occurs on the Earth both as surface water and subsurface water (groundwater). Based on the modes of occurrence, groundwater is more protected and less susceptible to pollution than surface water (Yusuf and Abiye, 2019). Hence, groundwater is a reliable (quality and quantity) natural resource that is accessible to many people as the only source of water supply for their day-to-day activities. However, groundwater resources are unevenly distributed in the world due to differences in the source and amount of recharge, geological setting, especially in the shallow parts of the subsurface – the first few hundred metres – from where often the main groundwater resources are usually being tapped by the inhabitants.

The inevitable saltwater intrusion into the coastal aquifer has long been recognised as a major concern around the world (Ayolabi et al., 2103; Yusuf and Abiye, 2019). Several authors who have worked in a similar terrain concluded that the invasion of a freshwater aquifer by seawater is mostly due to an induced flow of seawater towards a borehole where excessive groundwater is being pumped from aquifers that are in hydraulic connection with the sea (Abdalla et al., 2014; Yusuf and Abiye, 2019).

Therefore, a good understanding of the hydrogeological setting of the study area is a prerequisite to a thorough assessment and characterisation of the subsurface rocks and formation fluid. The field studies, coupled with available geological and hydrogeological information, were synthesised to deduce variations in lithological and fluid content at different depths. In lieu of the above, characterising the aquifer systems of the study area will be discussed under the following subheadings:

5.2 Hydrogeological Units and Hydraulic Properties of the Aquifers

The water table aquifer (first aquifer) is frequently being harnessed by the low-income inhabitants; however, it is of minor importance. The second and third aquifers (upper and lower CPS) are the most exploited, while the lower, most productive aquifer unit is the

Cretaceous Abeokuta Formation, which constitutes a deep aquifer only within the northern parts of Lagos city (Ikeja area) where boreholes are about 750 m deep. A detailed hydrogeological setting of the LCB was discussed in section 2.9 of this thesis.

Regarding the aquifer's hydraulic properties, pumping tests undertaken by Longe et al. (1987) revealed that the second aquifer has an average transmissivity of 3.53×10^{-3} m^2 s^{-1}, storage coefficient of 2.9×10^{-4} and leakage coefficient of 3.2×10^{-9} s^{-1}. The leakage factor indicates the drainage potential from this aquifer horizon to the one below it.

The third aquifer, referred to as lower CPS, underlies the upper CPS and is essentially confined. It is the most productive and most exploited through boreholes. The aquifer showed considerable heterogeneity as indicated by the wide range of hydraulic properties. The transmissivity values varied from 10×10^{-3} m^2 s^{-1} to 25.5×10^{-3} m^2 s^{-1} with an average of 17.4×10^{-3} m^2 s^{-1}, while the storage coefficient varied from 1.3×10^{-4} to 5.3×10^{-4} with an average of 3.29×10^{-4}. An appreciable leakage was deduced from the leakage coefficient which varied from 0.9×10^{-10} s^{-1} to 10.2×10^{-10} s^{-1} (Longe et al., 1987).

The fourth aquifer unit can only be exploited by industrial boreholes; thus, little hydrogeological information exists regarding this formation. However, it is the most protected of all the hydrogeological units in the study area due to its deeper depth of occurrence and associated multilayered confining units from the surface. In summary, considering the hydraulic properties of each hydrogeologic unit, the lower and upper-CPS are highly prolific, relatively protected from surface contaminants and as such are a reliable source of groundwater supply to the inhabitants. However, it is to be noted that the leakage potential which describes the ease of contaminants being transported between these aquifer horizons (lower and upper-CPS) is of great concern, as the pollution occurrence in one threatens the other. The hydraulic characteristics of the main aquifers underlying the study area are summarised in Table 5.1.

Table 5.1: Hydraulic characteristics of the different aquifer units present in the study area (compiled from various sources)

Aquifer name	Thickness (m)	Depth of occurrence (m)	Yield (m^3h^-)	Specific capacity ($m^3h^-m^-$)	Trans-missivity ($ms\times10^{-3}$)	Storage coefficient ($\times10^{-4}$)	Leakage coefficient ($s\times10^{-9}$)
Recent alluvial/ phreatic aquifer	5–22	*From surface	–	–	Tr <1	–	–
Upper coastal plain sand	10–25	<30	100.4	1–14 (mean 7.96)	3.53	2–5	3.2
Lower coastal plain sand	10–35	200–250	54.4–99.3	2.96–17	6.5–35 (mean 17.4)	1.3–5.3 (mean 3.29)	0.9–10.2
Abeokuta formation	–	450–750	–	8	8	–	–

*Present study Source: Longe et al. (1987)

5.3 Geophysical Characterisation of the South Lagos Coastal Basin

Geophysical techniques are known to be useful tools in probing and deducing the subsurface geological and hydrogeological characteristics. Prominent among several geophysical techniques used in the hydrogeological investigation, is the electrical method, particularly the electrical resistivity and electromagnetic methods which rely essentially on resistivity contrasts, and have been successfully applied to investigate seawater intrusion into freshwater aquifers (Goldman et al., 1991; Fitterman and Deszcz-Pan, 2001; Oladapo et al., 2013; Yusuf and Abiye, 2019). Its ability to differentiate between freshwater and saline water, sandy and clayey units with the aid of contrasts in electrical properties, has made it an indispensable method. For example, between freshwater and saline water, and between sand and clay, a contrasting resistivity value exists that is higher in the former than the latter. Hence, the subsurface boundaries between sand and clay layers, freshwater and saline water zones could be delineated. In view of the above submission, electrical resistivity methods, namely VES, was used only to probe the shallow aquifer due to its limited depth of penetration (<50 m), while ERT and borehole logs analyses were complementarily employed to probe deeper depth and also to enhance interpretation. These methods were used to identify aquifer and aquiclude units, determine the freshwater and saltwater horizons and interface, and to project or correlate between the trace patterns of logs from different wells towards establishing the continuity extent of various lithologic layers and its fluid content. In addition, specifically due to the near-surface probe of the VES acquired data, secondary geophysical indices are known as D-Z parameters were equally undertaken to evaluate the protective capacity of the aquifer to pollution and the groundwater potential of the shallow aquifer in the study area. The aforementioned are considered critical in monitoring the inevitable feasible risk of

seawater intrusion, well sites and designs, and determination of geological model of the study area.

5.3.1 Vertical electrical sounding

This method involves the introduction of a time-varying direct current or very low frequency (<1 Hz) electric current into the ground through two current electrodes, while the voltage is measured across another pair of potential electrodes, which may or may not be within the current electrodes, depending on the configuration. The detailed principle, the processes of data acquisition and data processing were presented in Chapter 3 and Chapter 4 (see 3.1.1, 4.3.1.1, and 4.3.2.1). The VES acquired data (primary data) within the investigated depth were processed and interpreted to delineate the subsurface lithologic units and their thicknesses, and to identify aquifers and aquicludes as follows:

Figure 5.1 shows both VES and 2D-ERT points, the base maps showing the projected ERT lines are presented in Figure 5.2**a-c**, while Table 5.2 summarises the quantitative interpretation of all VES in the study area from the geoelectrical, and computer iteration software (IPI2win). The qualitative interpretation of resistivity sounding data from the computer modelled curves is characterised by typical HKH, QH, H, HK, KH, KHK, and K-hybrid model curves (Appendix D II). Figure 5.3 shows typical curve types, resistivity values and layer thicknesses obtained from VES1 to VES4. The inversion results show the interpretation of 50 % soundings curves as a four-layer mode, while the other 50 % are five-layer modes (Figure 5.3 and Table 5.2).

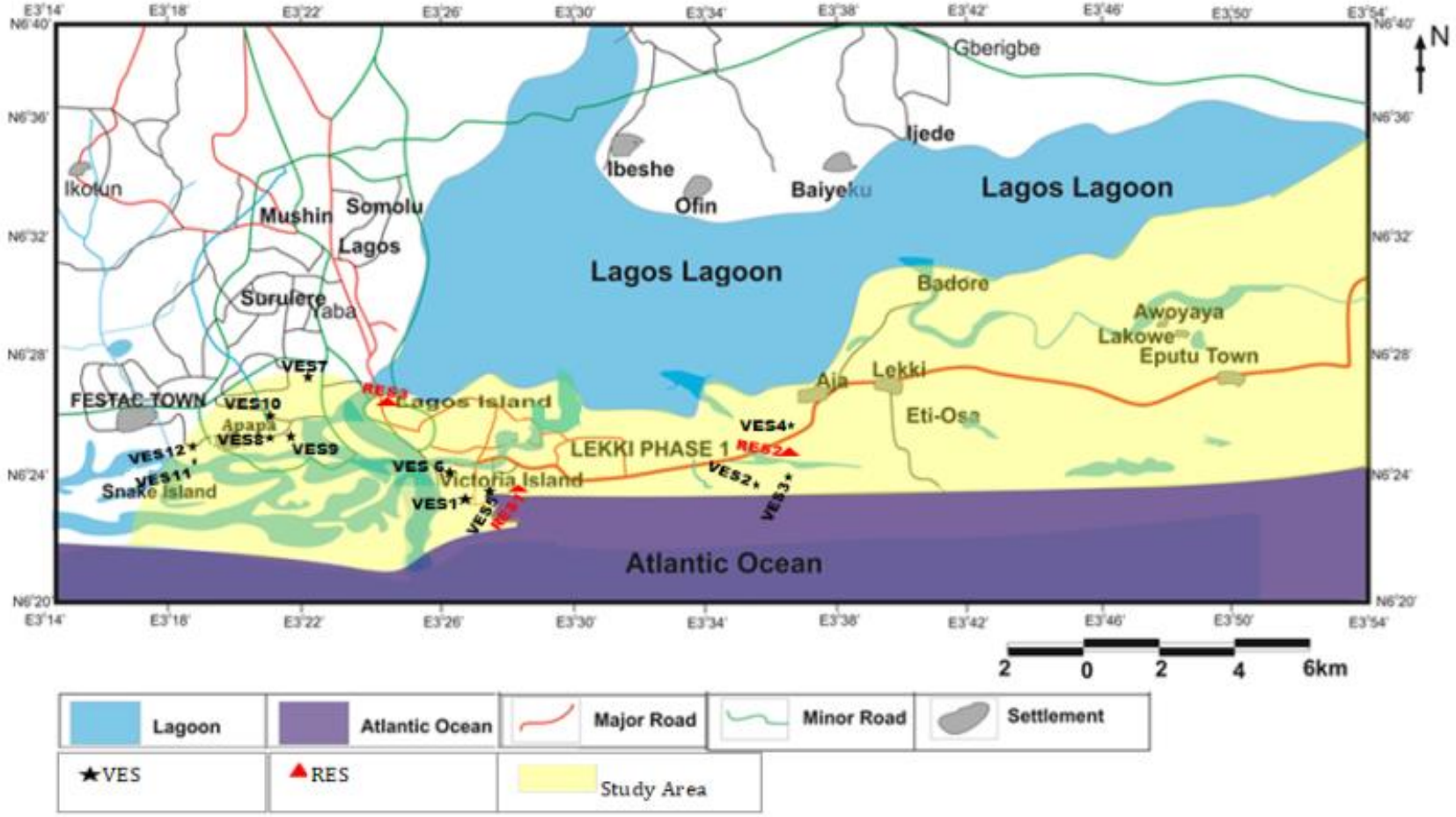

Figure 5.1: Map of the study area showing VES and ERT points

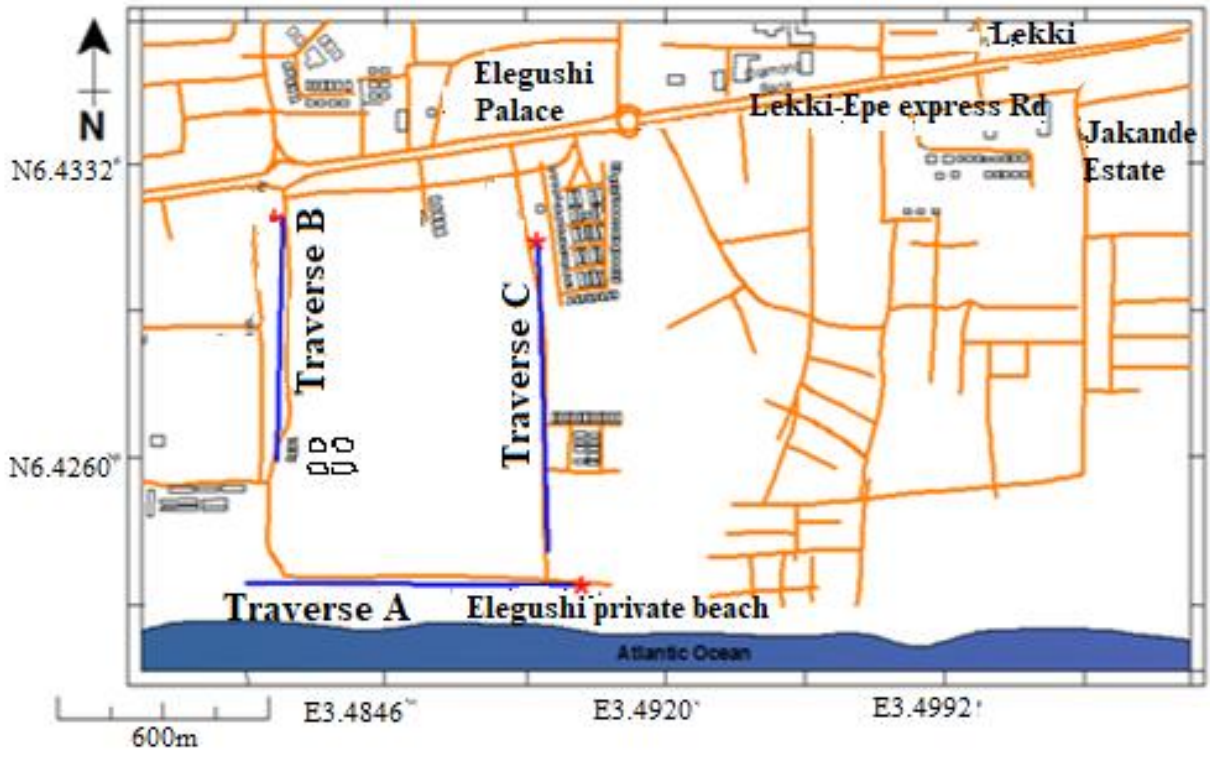

Figure 5.2a: Base map of the study area showing the projected ERT lines at Elegushi

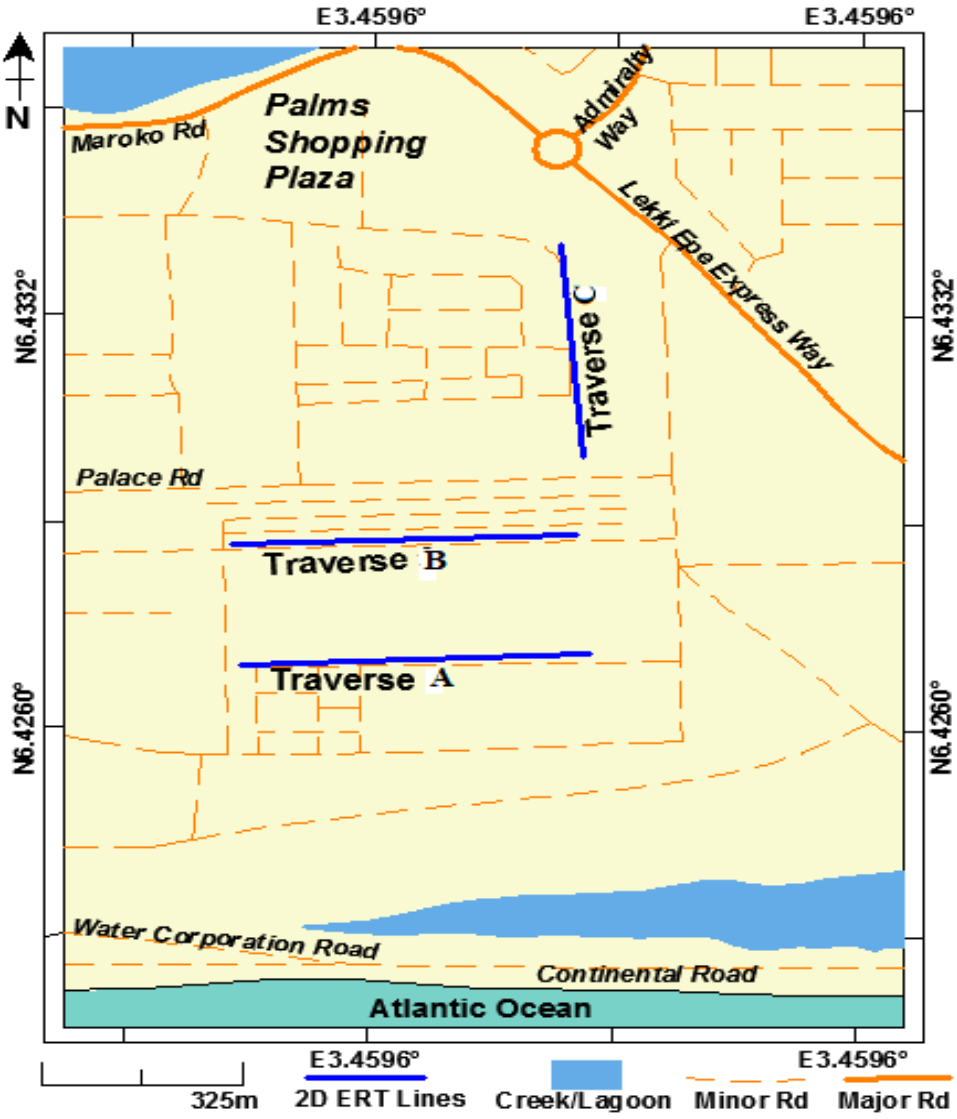

Figure 5.3b: Base map of the study area showing the projected ERT lines at Oniru

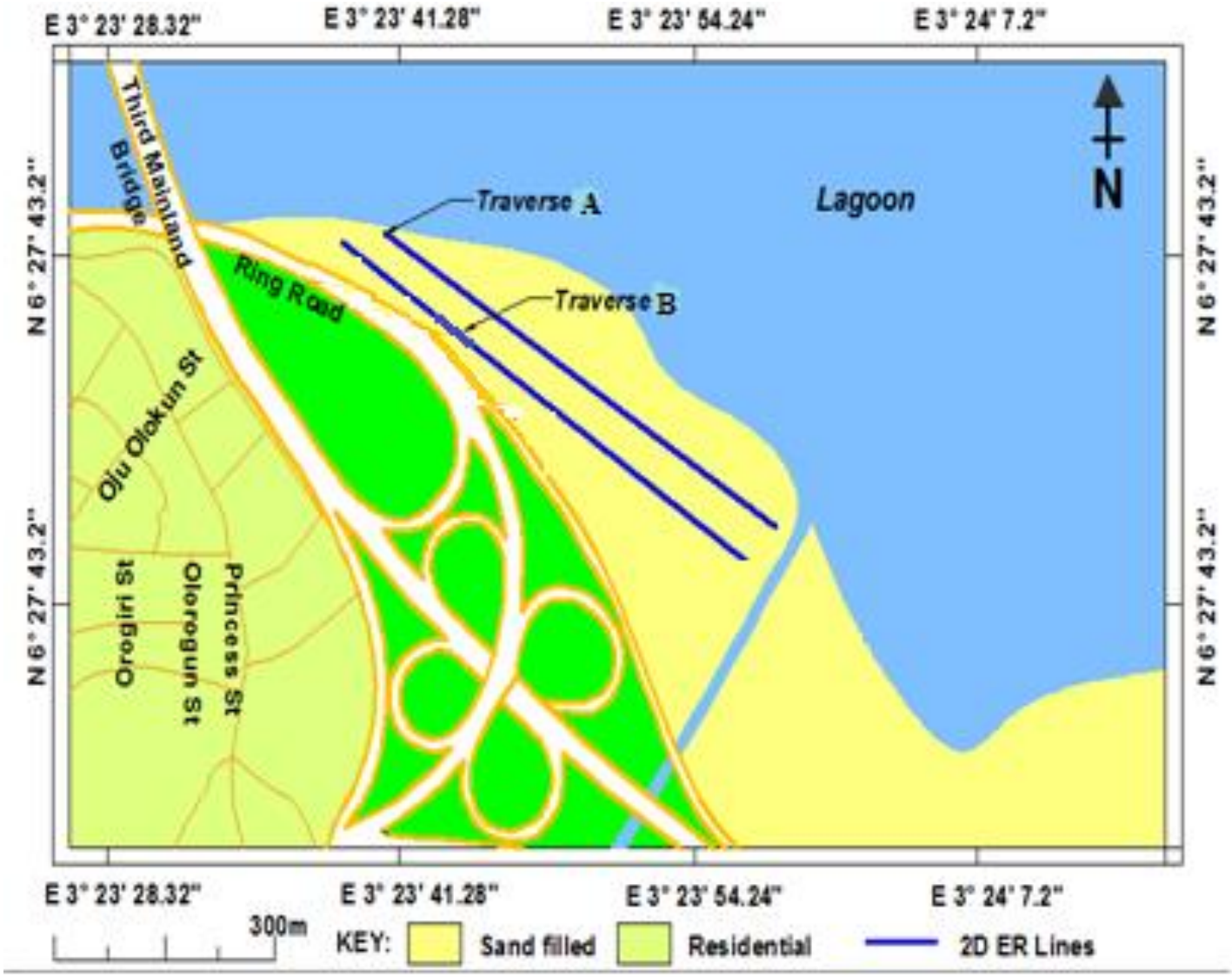

Figure 5.4c: Base map of the study area showing the projected ERT lines at Adeniji Adele

Table 5.2: Summary of vertical electrical sounding results

VES Station	No. of Layers	Curve Type	Apparent resistivity (ρa) (Ω m)	Thickness (h) (m)	Depth probed (m)	Lithology
VES1	5	HKH	7.74	4.55	51.7	Sandy Clay
			3.52	6.7		Clay
			16.9	12.6		Clayey Sand
			2.72	27.8		Clay
			284			Sand
VES2	4	QH	1 915	1.23	19.7	Sand
			41.2	7.66		Sandy Clay
			83.8	10.8		Clayey Sand
			222			Sand
VES3	5	H	76.7	0.5	27.3	Sand
			4	2.96		Clay
			100	5.97		Sand
			38.9	17.9		Clayey Sand
			412			Sand
VES4	4	QH	155	1.61	41.2	Sand
			46.4	5.83		Clayey Sand
			3.56	33.8		Clay
			265			Sand
VES5	5	QH	265	2.29	43.8	Sand
			9.64	2.22		Clay
			156	6.1		Sand
			8.13	33.1		Clay
			605			Sand
VES6	4	HK	70.4	4.32	27.6	Sand
			20	7.32		Clay
			167	15.9		Sand
			16.2			Clay
VES7	5	HKH	36.7	1.84		Sand
			18.6	2.52		Clay
			137	14.8		Sand
			9.42	38.3		Clay
			2 421		57.4	Sand
VES8	4	KH	16.2	0.86		Clay
			61.7	10.4		Sand
			15.1	38.4		Clay
			134		49.7	Sand
VES9	5	HKH	12.5	0.7		Clay
			6.38	1.85		Clay
			78.4	7.08		Sand
			10.4	18.8		Clay
			325		28.5	Sand
VES10	4	KH	84.5	0.5		Clayey Sand

VES Station	No. of Layers	Curve Type	Apparent resistivity (ρa) (Ω m)	Thickness (h) (m)	Depth probed (m)	Lithology
VES1	5	HKH	7.74	4.55	51.7	Sandy Clay
			3.52	6.7		Clay
			16.9	12.6		Clayey Sand
			2.72	27.8		Clay
			284			Sand
VES2	4	QH	1 915	1.23	19.7	Sand
			41.2	7.66		Sandy Clay
			83.8	10.8		Clayey Sand
			222			Sand
VES3	5	H	76.7	0.5	27.3	Sand
			4	2.96		Clay
			100	5.97		Sand
			38.9	17.9		Clayey Sand
			412			Sand
VES4	4	QH	155	1.61	41.2	Sand
			46.4	5.83		Clayey Sand
			3.56	33.8		Clay
			265			Sand
VES5	5	QH	265	2.29	43.8	Sand
			9.64	2.22		Clay
			156	6.1		Sand
			8.13	33.1		Clay
			605			Sand
VES6	4	HK	70.4	4.32	27.6	Sand
			20	7.32		Clay
			167	15.9		Sand
			16.2			Clay
			132	s22.1		Sand
			1.61	43.1		Clay
			246		65.6	Sand
VES11	5	KHK	8.42	0.67		Clay
			96.4	2.24		Sand
			5.61	4.48		Clay
			65.8	45.3		Sand
			3.61		52.7	Clay
VES12	4	K	2.29	0.46		Clay
			56	14.9		Sand
			35.7	32.8		Clayey Sand

The first layer has resistivity and thickness values ranging from 2.29 Ω m to 1 915 Ω m and 0.46 Ω m to 4.55 Ω m, respectively. This is diagnostic of the top admixture of sandy soil. The resistivity values of the second layer varied from 3.52 Ω m to 132 Ω m with thickness ranged

between 1.85 m and 22.1 m. This layer is relatively dominated by clayey soil of approximately 60 % and is identified by low resistivity values and, thus, expected to form the confining and protective layer for the underlying sandy aquifer. The other 40 % entails VES 4 as clayey sand, and VES 8, and VES 10 to VES 12 are sandy units recognised with high values of resistivity, constituting a series of confined and unconfined aquifers.

The third layer is delineated as mostly sandy soil with intercalated clayey sand (75 %). This constitutes the main parts of the first aquifer with clayey sand/sandy clay in some localities. The aquifer is confined where the overlying second lithologic unit is clay, and unconfined where it is sand. The apparent resistivity of this layer varied from 1.61 Ω m to 165 Ω m. Also, the thickness of this layer varied from 4.48 m to 43.1 m. The fourth layer has resistivity values varying from 2.72 Ω m to 265 Ω m, with thickness values ranging from 17.9 m to 45.3 m. This layer is also known to form a confining unit to the underlying aquifer due to the lateral dominance of clay occurrence. The basal fifth layer (which marks the peak penetration of electric current) is mostly sandy for all the sounding surveys, and occurs as confined aquifers with resistivity values ranging from 3.61 Ω m to 2 421 Ω m; however, the thickness of the layer could not be ascertained as the depth of investigation terminated within this unit. The estimation from the geoelectric model for this study revealed that the depth to aquifers varied between 0.46 m and 11.64 m and from 19.7 m to 65.6 m for the first and second aquifers, respectively.

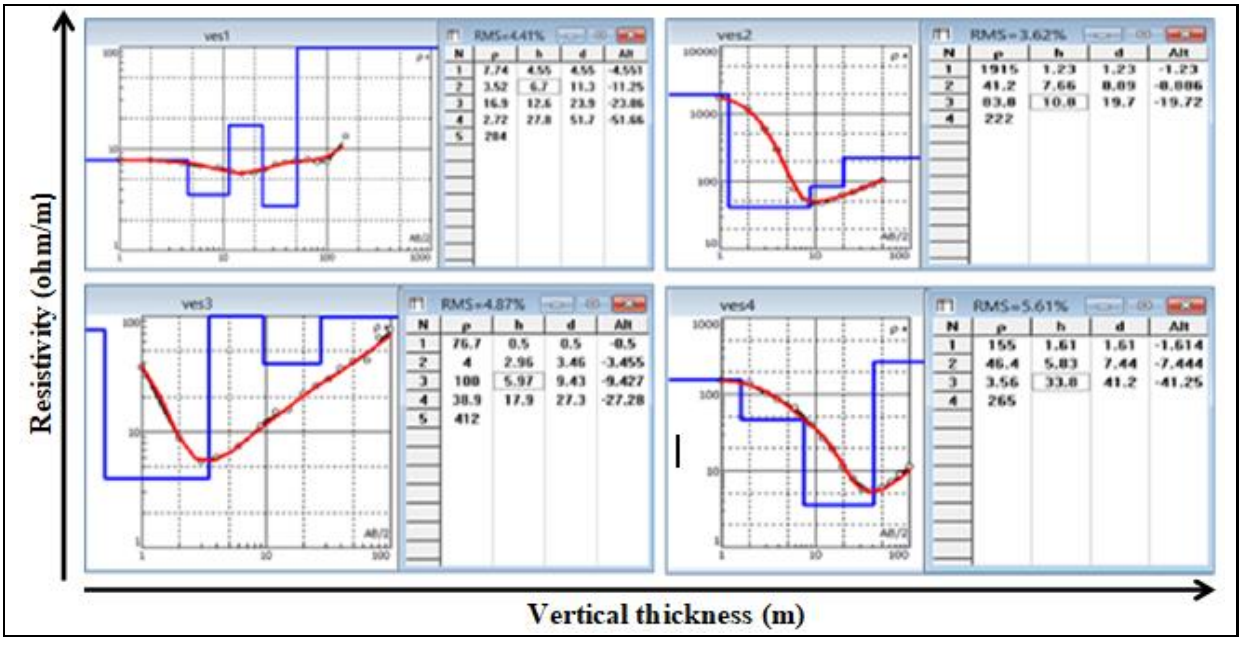

Figure 5.5: Representative resistivity curve from the study area

5.3.2 Estimation of the protective capacity of the shallow aquifers in the study area

This section estimates the overall protective capacity offered by the overlying beds to the underlying aquifer and it was convolved from the acquired VES measurements and thus takes care of aquifer occurrence from the surface to a depth of <50 m. The secondary indices considered for this estimation were longitudinal conductance, transverse resistance, longitudinal resistivity, transverse resistivity, and anisotropy. The principles and inter-pretation of these indices by Maillet (1947) have been detailed in Chapter 3 of this thesis (see section 3.2.3), while the protective capacity rating of Oladapo and Akintorinwa (2007) adopted for this study was presented in Table 4.3.

5.3.2.1 Longitudinal conductance

The D-Z parameters have been calculated for each of the geoelectric units and are presented in Table 5.3 and Table 5.4. The protective capacity of the aquifer has been constructed with the use of SURFER© 13 contouring toolkits, using longitudinal conductance (S) values for both aquifers as shown in Figure 5.4 and Figure 5.5. The Radial Basis Function Method of interpolation using the multiquadric basis Kernel type was chosen for interpolating longitudinal conductance values. Compared to the rest of the interpolation methods, the Radial Basis Function gave the best cross-validation results and root-mean-square errors. The radial basis function is commonly used for interpolating small surfaces and has been found to be appropriate for interpolating EC values (Robinson and Metternich, 2006). For each point, a radial basis function is defined, which depends on the Euclean distance between the prediction location and each sample location. The 'roughness' of the surface is reduced by the action of forming a polynomial function through the data points. Due to the small amount of data, the produced maps have significant errors of 0.804 and 1.8 for the first and second aquifer, respectively. More data could lead to better refinement of the mapped parameters. The maps show a clear picture of the regions in terms of protective capacity evaluation. The dominant blue region of approximately 95 % observed with respect to the first aquifer protective map of <0.7 value, represents a high pollution prone area and vice versa with the second aquifer.

Table 5.3: Estimation of D-Z parameters and its protective capacity: First aquifer

Sample ID	Depth to first aquifer (m)	Longitudinal conductance (mS)	Transverse resistance (Ωm^2)	Longitudinal resistivity (ρt)	Transverse resistivity (ρt)	ρt/(ρt	Anisotropy (ʎ)	Protective capacity
VES1	11.25	2.49	58.8	4.52	5.23	1.16	1.08	Good
VES2	8.89	0.19	2671.04	47.67	300.45	6.30	2.51	weak
VES3	3.46	0.75	50.19	4.63	14.51	3.13	1.77	Good
VES4	1.61	0.01	249.55	154.81	155.00	1.00	1.00	Poor
VES5	4.51	0.24	628.25	18.88	139.30	7.38	2.72	Moderate
VES6	11.64	0.43	450.53	27.11	38.71	1.43	1.19	Moderate
VES7	4.36	0.19	114.4	23.49	26.24	1.12	1.06	Weak
VES8	0.86	0.05	13.93	16.20	16.20	1.00	1.00	Poor
VES9	2.55	0.35	20.55	7.37	8.06	1.09	1.05	Moderate
VES10	0.5	0.01	42.25	84.75	84.50	1.00	1.00	Poor
VES11	0.67	0.08	5.64	8.42	8.42	1.00	1.00	Poor
VES12	0.46	0.20	1.05	2.29	2.28	1.00	1.00	Moderate

Table 5.4: Estimation of D-Z parameters and its protective capacity: Second aquifer

Sample ID	Location	Total longitudinal conductance (mS)	Total transverse resistance ($\Omega m^{2)}$	Longitudinal resistivity (ρL)	Transverse resistivity (ρt)	Anisotropy (ʎ)	Protective capacity
VES1	Island	13.46	347.36	3.84	6.72	1.32	Excellent
VES2	Island	1.26	3576.08	15.63	181.53	3.41	Good
VES3	Island	1.27	1343.53	21.5	49.21	1.51	Good
VES4	Island	9.63	640	4.28	15.54	1.91	Very good
VES5	Island	4.35	1848.95	10.07	42.21	2.04	Good
VES6	Island	0.52	3105.83	53.07	112.53	1.45	Moderate
VES7	Apapa	4.36	2502.79	13.17	43.6	1.81	Good
VES8	Apapa	2.77	1235.45	17.94	24.86	1.17	Good
VES9	Apapa	2.24	771.14	12.72	27.06	1.46	Good
VES10	Apapa	26.77	3029.35	2.45	46.18	4.34	Excellent
VES11	Apapa	1.59	3227.45	33.14	61.24	1.36	Good
VES12	Apapa	1.39	2006.41	34.68	41.63	1.1	Good

The longitudinal conductance values for the first delineated aquifer varied between 0.01 mS to 2.49 mS, while the second underlying aquifer has values ranging from 0.52 mS to 26.77 mS. The first aquifer's longitudinal conductance values were generally <1, the exception being VES 1 with 2.49 mS. The values for the second aquifer were generally >1, with the exception of VES 6 with 0.52 mS. This generally indicated that aquifer protective capacity increases with increasing depth because high longitudinal conductance connotes high protective capacity, while low longitudinal conductance values depict low protective capacity and thus high vulnerability. The longitudinal values obtained from twelve resistivities' sounding interpretation, extending from Apapa to Lagos Island, were used to

estimate the protective capacity and thickness of the overburden shielding the underlying shallow aquifers in the study area. This is because the earth's subsurface acts as a natural filter to infiltrating fluid (Okonkwo and Ugwu, 2015); hence, its tendency to retard and filter percolating contaminated fluid from the ground surface is a measure of its protective capacity (Olorunfemi et al., 1999). In addition, the highly impervious clayed overburden, which is identified by relatively high longitudinal conductance, offers better protection to the underlying layer compared to the low longitudinal conductance lithological units (Abiola et al., 2009).

Similarly, evaluation of the overburden thickness on a regional scale considered the first aquifer to be prone to contamination relative to the underlying aquifer. According to Oteri (1981), the increase in longitudinal conductance (S) may correspond to an average increase in the clay content and a consequent decrease in the transmissivity, and vice versa. It is also common knowledge that a decrease in resistivity or an increase in conductivity values are considered an indication of either high clay content or salinity or both (both factors lead to poor water quality) (Oteri, 1981). The longitudinal conductance values enable the protective capacity rating to be zoned according to Oladapo and Akintorinwa (2007) into excellent, good, moderate, weak, and poor. Based on this classification, Table 5.3 and Figure 5.4 of the first aquifer suggest that about 50 % of the area falls within "poor/weak" protective capacity, while about 36 % constitutes a "moderate" protective capacity rating. About 8 % exhibit "good" protective capacity and the remaining 8 % is having a "very good" protective capacity rating. This implies that the entire study area with respect to the first aquifer, which is characterised by relatively poor to moderate longitudinal conductance, indicates poor to moderate protective capacity. The low value of protective capacity observed connotes the absence of significant clay content as an overburden impermeable material in the first aquifer and thus leading to the rapid percolation of contaminants, whereas in the second aquifer (Table 5.4 and Figure 5.5), 16 % of the area falls under "excellent" protective capacity rating, and 8 % has a "very good" protective rating capacity. About 68 % constitutes a "good" protective capacity zone, while the remaining 8 % falls in the category of "moderate" protective capacity. The relatively high longitudinal conductance of overburden estimation with respect to the second aquifer in the study area envisaged excellent to good aquifer protective capacity rating and therefore, minimising or inhibiting the infiltration of pollutants from the surface.

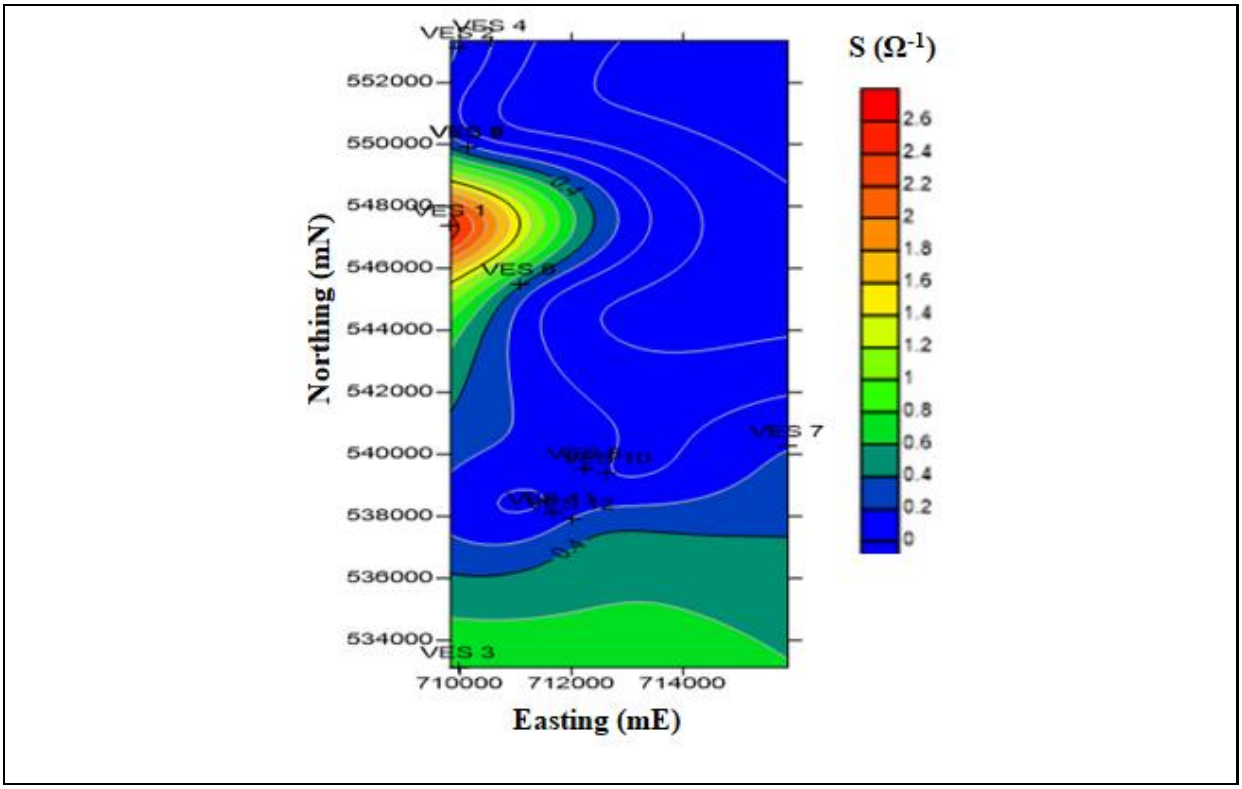

Figure 5.6: First aquifer protective capacity map

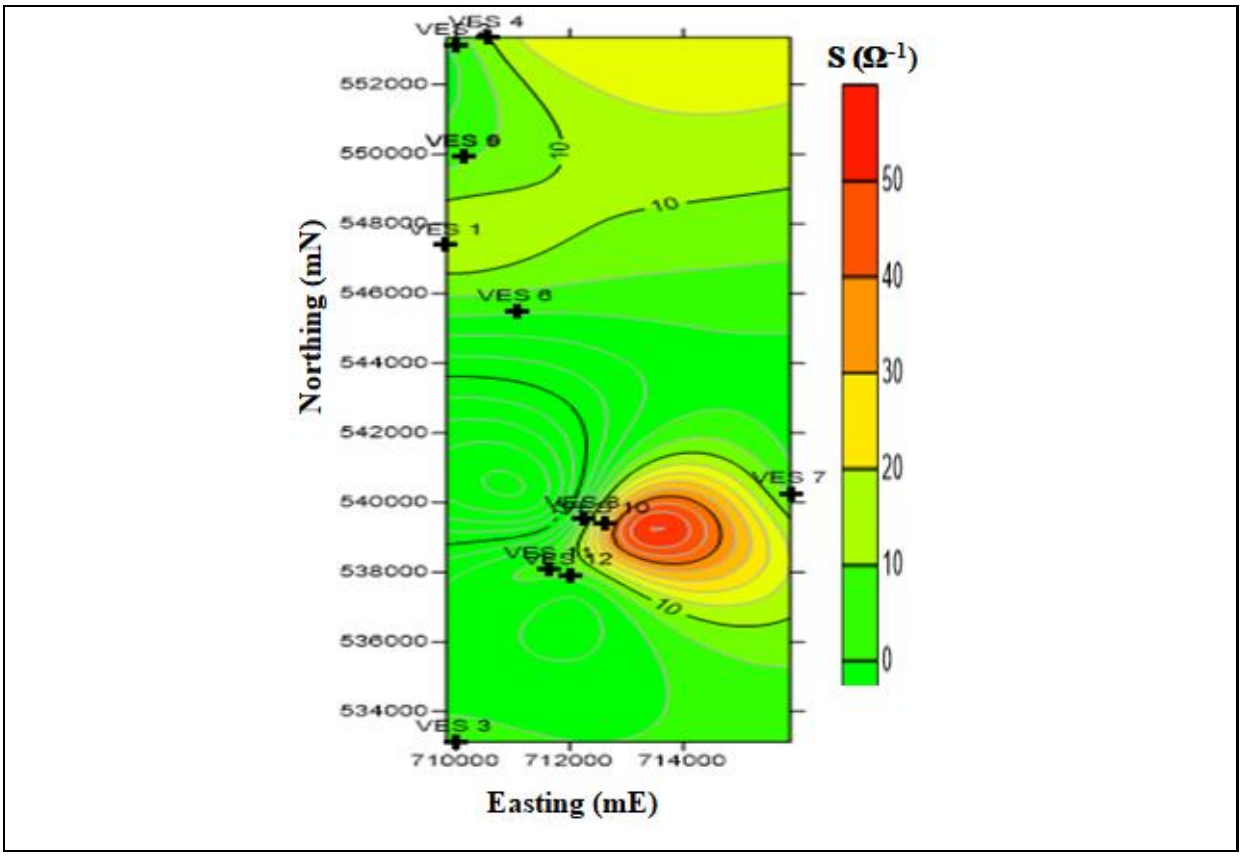

Figure 5.7: Second aquifer protective capacity map

5.3.2.2 Transverse resistance

The T-values vary from a minimum of 1.05 to 2 671.04 Ω m^2 and 347.36 to 3 576.08 Ω m^2 for the first and second aquifer, respectively. An increase in T-values were associated with regions of high transmissivity; hence, highly permeable to fluid movement. The first aquifer is characterised by low T-values relative to the second aquifer, thus the second aquifer should be accorded priority in terms of a target for groundwater potential.

5.3.2.3 Coefficient of anisotropy

The anisotropy of the resistivity in rocks is caused by a number of factors, including orientation of elongated grains, or layering with different resistivity values. It may also be due to rock fracturing, metamorphism, and disseminated ore grains in the rocks (Habbeijam, 1972; Watson and Barker, 1999). The coefficient of anisotropy is usually 1.0 but seldom exceeds 2.0. The first and second aquifer essentially have values within the recommended range, the exception being VES 1 (2.52) and VES 5 (2.72) for the first aquifer, and VES 2 (3.41) and VES 4 (4.34) for the second aquifer. The observed elevated coefficient of anisotropy values above 2.0 for the shallow aquifer (first and second aquifers) indicate an increase in hardness due to compaction of rocks (Keller and Frieschknecht, 1966) and/or may suggest the presence of an extraneous or intrusive body with resistivity higher than the host rocks, resulting in an anomaly coefficient of anisotropy value (Isife and Obasi 2012).

5.3.3 Estimation of the shallow aquifer potential in the study area

This aspect assessed the aquifer potential of the second aquifer using the secondary hydrogeophysical indices derived from VES12 data which includes: aquifer resistivity (ρa), aquifer thickness (h), aquifer conductivity (σ), longitudinal conductance (S), transverse resistance (T), hydraulic conductivity (K), and transmissivity (Tr). The results and figures for all the parameters are presented in Table 5.5 and from Figure 5.6 to Figure 5.12. The VES stations comprised Apapa in the west (VES 7 to VES 12) and Lagos Island and Lekki in the east (VES 1 to VES 6). The major aquifer units within the investigated depths are the third and fourth geoelectric layers that fall within the second aquifer.

Table 5.5: Dar Zarrouk estimated hydraulic parameters for shallow aquifers

LOC ID	Longitude	Latitude	Aquifer resistivity (ρa) (Ω m)	Aquifer thickness (h) (m)	Aquifer conductivity σ = 1/ρa	Longitudinal conductance S= h/ρa(Ω^{-1})	Transverse resistance T = h/ρa (Ω m^2)	K (m/day)	Tr (m^2/day) K × S
VES1	709833	547384	16.9	12.6	0.0592	0.7456	212.94	0.2599	3.2749
VES2	709977	553128	83.8	10.8	0.0119	0.1289	905.04	1.7611	19.02
VES3	709977	533128	38.9	17.9	0.0257	0.4602	696.31	0.7039	12.5995
VES4	710554	553349	46.4	5.83	0.0216	0.1256	270.512	0.869	5.066
VES5	710142	549922	156	6.1	0.0064	0.0391	951.6	3.7008	22.5747
VES6	711064	545486	167	15.9	0.006	0.0952	2655.3	4.0147	63.8341
VES7	715880	540262	137	14.8	0.0073	0.108	2027.6	3.1688	46.8977
VES8	712249	539552	61.2	10.4	0.0163	0.1699	636.48	1.2097	12.5809
VES9	710142	549922	78.4	7.08	0.0128	0.0903	555.072	1.6264	11.5146
VES10	712636	539395	132	22.1	0.0076	0.1674	2917.2	3.0311	66.9865
VES11	711660	538095	65.8	45.3	0.0152	0.6884	2980.74	1.3191	59.7568
VES12	711996	537920	91.7	47.7	0.0109	0.5202	4374.09	1.9613	93.5532

Aquifer transverse resistance, aquifer transmissivity, aquifer resistivity, aquifer thickness and aquifer hydraulic conductivity

The transverse resistance value varied between 212.94 ($\Omega\ m^2$) at VES 1 and 4 374.09 ($\Omega\ m^2$) at VES 12, while aquifer transmissivity ranged from 3.2749 m^2/day to 93.5532 m^2/day at VES 1 and VES 12, respectively, within the area of study. The entire area is characterised by a high transmissivity potential for groundwater, the exception being VES 1 and VES 4 (Table 5.5, Figure 5.6 and Figure 5.7).

The aquifer resistivity, aquifer thickness and hydraulic conductivity presented in Table 5.5 and Figure 5.8, Figure 5.9 and Figure 5.10 revealed the variability in aquifer resistivity, aquifer thickness and hydraulic conductivity across the length of the study, ranging from 6.1 m to 47.7 m for thickness; 16.9 Ω m to 167 Ω m for resistivity; and 0.2599 m/day to 4.0147 m/day for hydraulic conductivity. Generally, it can be deduced that areas underlain by relatively thick aquifer material have higher Tr values than thin substratum aquifer material. The predominant occurrence of high transverse resistance in a geological formation implies high resistivity or higher thickness with favourable aquifer conditions (Teikeu et al., 2012). Therefore, based on the progressive increase from west to east and north to south in transverse resistance, aquifer resistivity, aquifer thickness and transmissivity, the aquifer prolific zones is comparatively higher in the eastern and southern parts than the western and northern parts of the study. This assertion is evidently clear from the perfect agreement in profiles drawn for transverse resistance (Figure 5.6**b**), transmissivity (Figure 5.7**b** and **c**), aquifer resistivity (Figure 5.8**b**), aquifer thickness (Figure 5.9**b** and **c**) and hydraulic conductivity (Figure 5.10**b**). The variations in the aquifer potential across the study area may be attributed to variation in lithology, water quality and/or degree of saturation. However, on the basis of high transverse resistance, VES1 and VES4 had the worst aquifer yield potential in the study area. The most appropriate locations for well drilling across the area for high yield are suggested in the soundings of VES 2, VES 6, VES 7, VES 11, and VES 12 due to high values of aquifer thickness, transverse resistance, transmissivity, and porosity (Table 5.5).

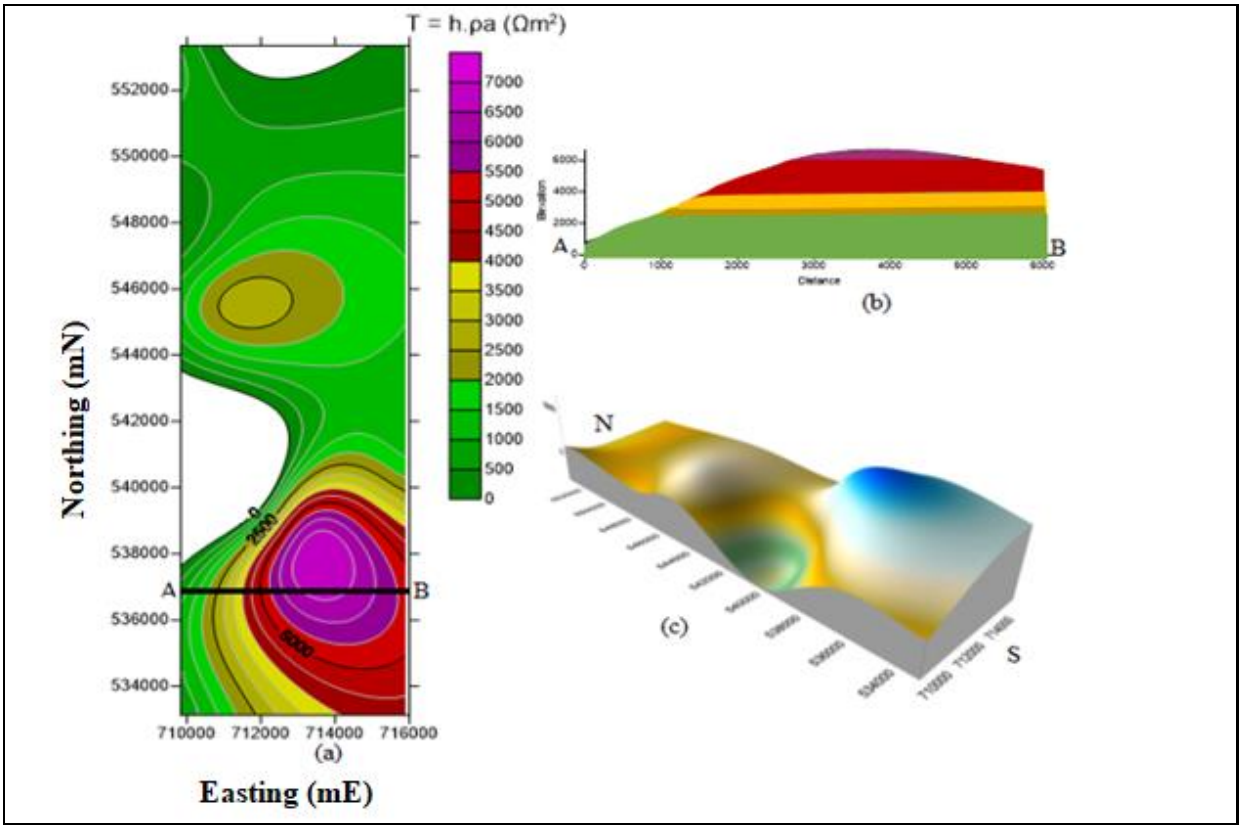

Figure 5.8: (a) Aquifer transverse resistance – T=h.ρa (Ω m) contour map; (b) Aquifer transverse resistance profile; (c) Three-dimensional surface view of aquifer transverse resistance

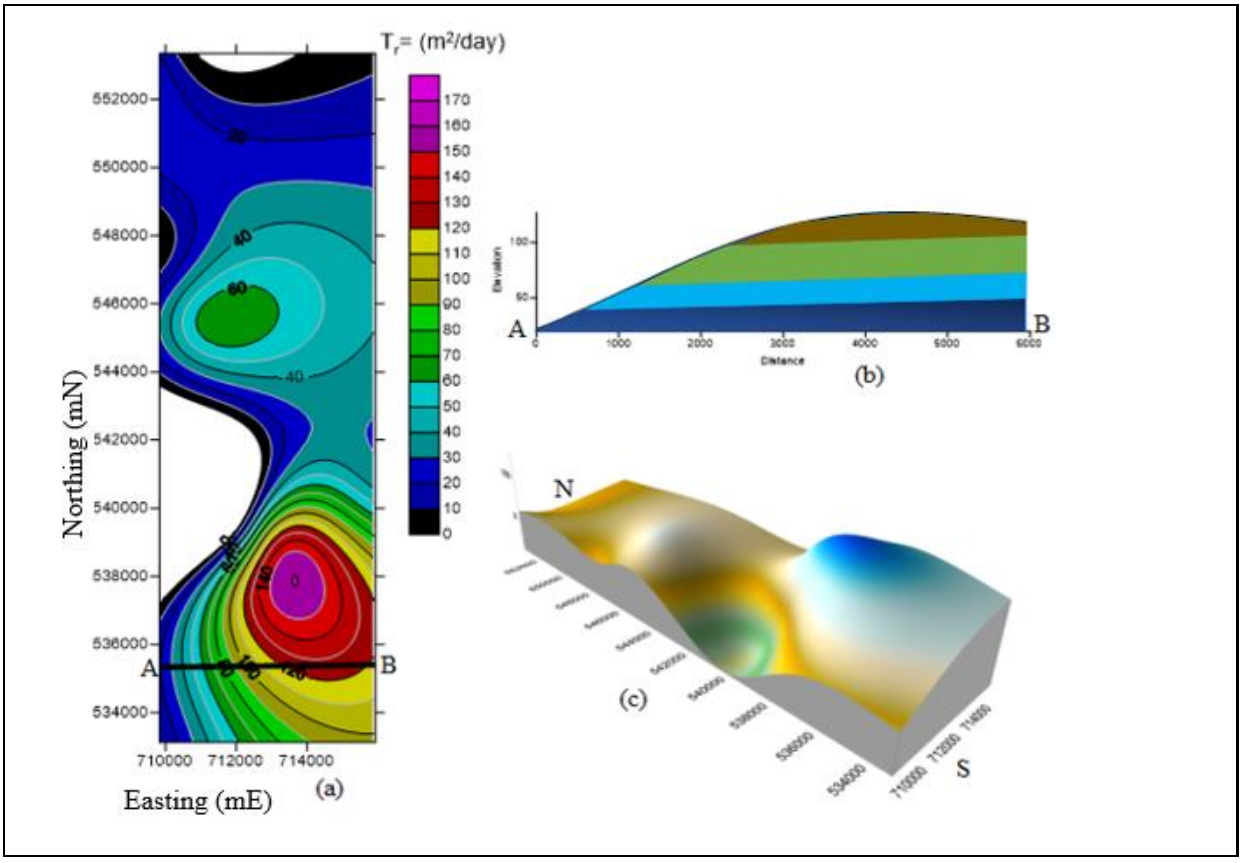

Figure 5.9: (a) Aquifer transmissivity – Tr=K×S (m^2/day) contour map; (b) Aquifer transmissivity profile; (c) Three-dimensional surface view of aquifer transmissivity

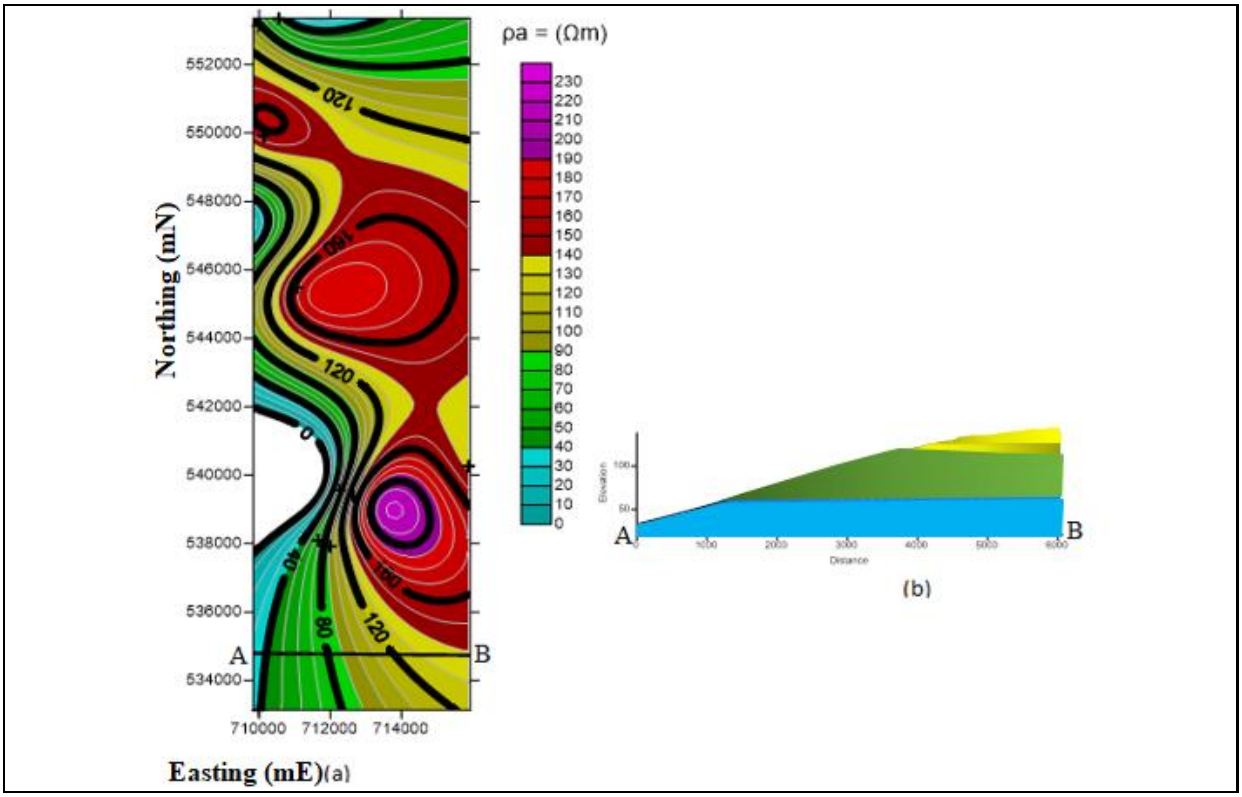

Figure 5.10: (a) Aquifer resistivity–ρa (Ω m) contour map; (b) Aquifer resistivity profile

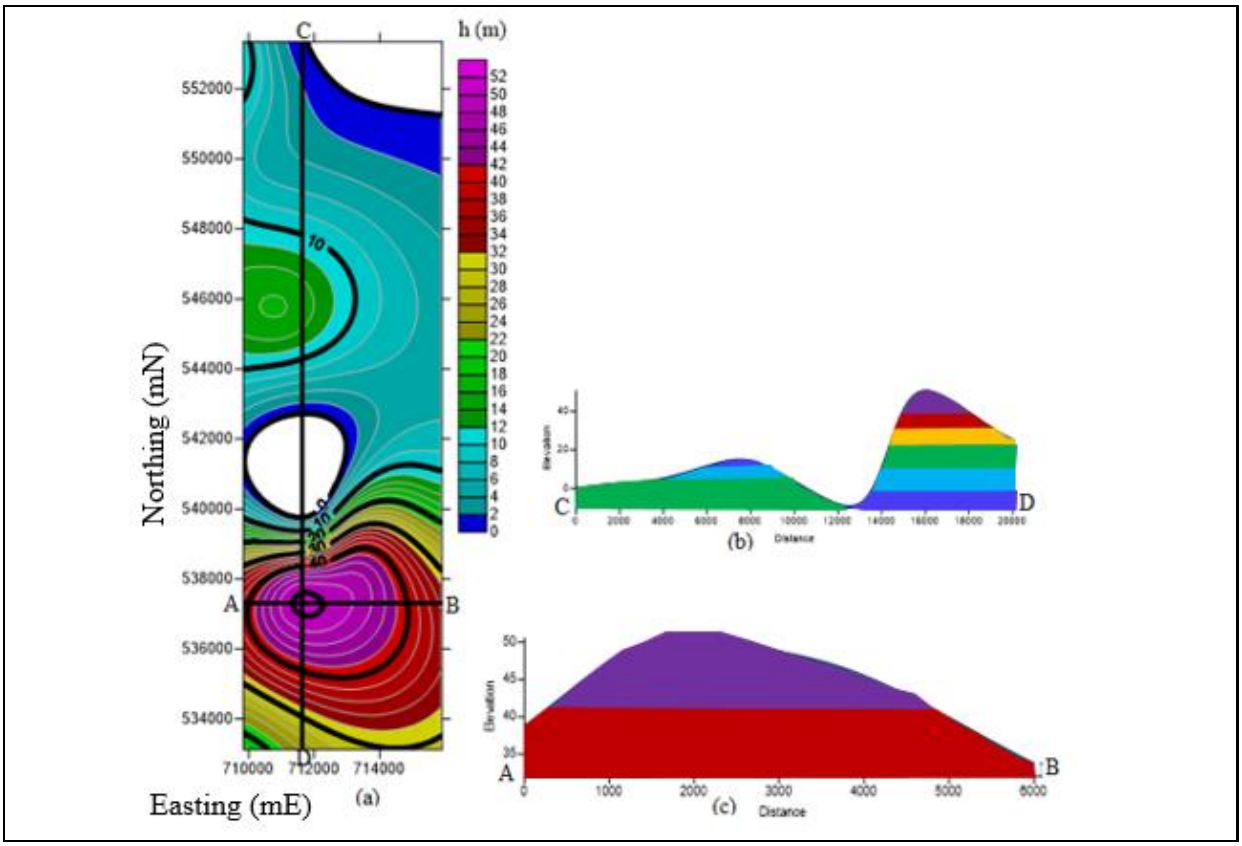

Figure 5.11: (a) Aquifer thickness (h=m) contour map; (b and c) Aquifer thickness in profiles in north–south and west–east directions

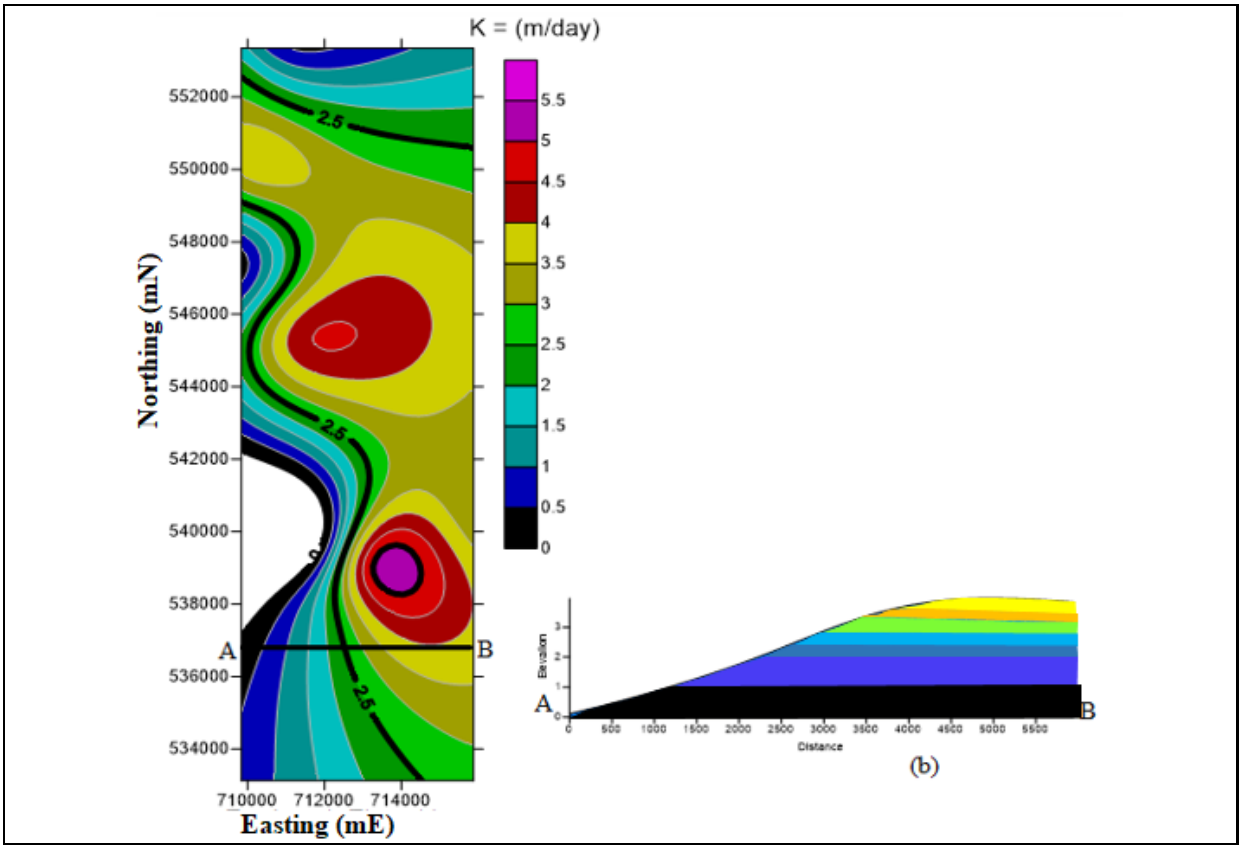

Figure 5.12: (a) Aquifer hydraulic conductivity–K (m/day) contour map; (b) Aquifer hydraulic profile

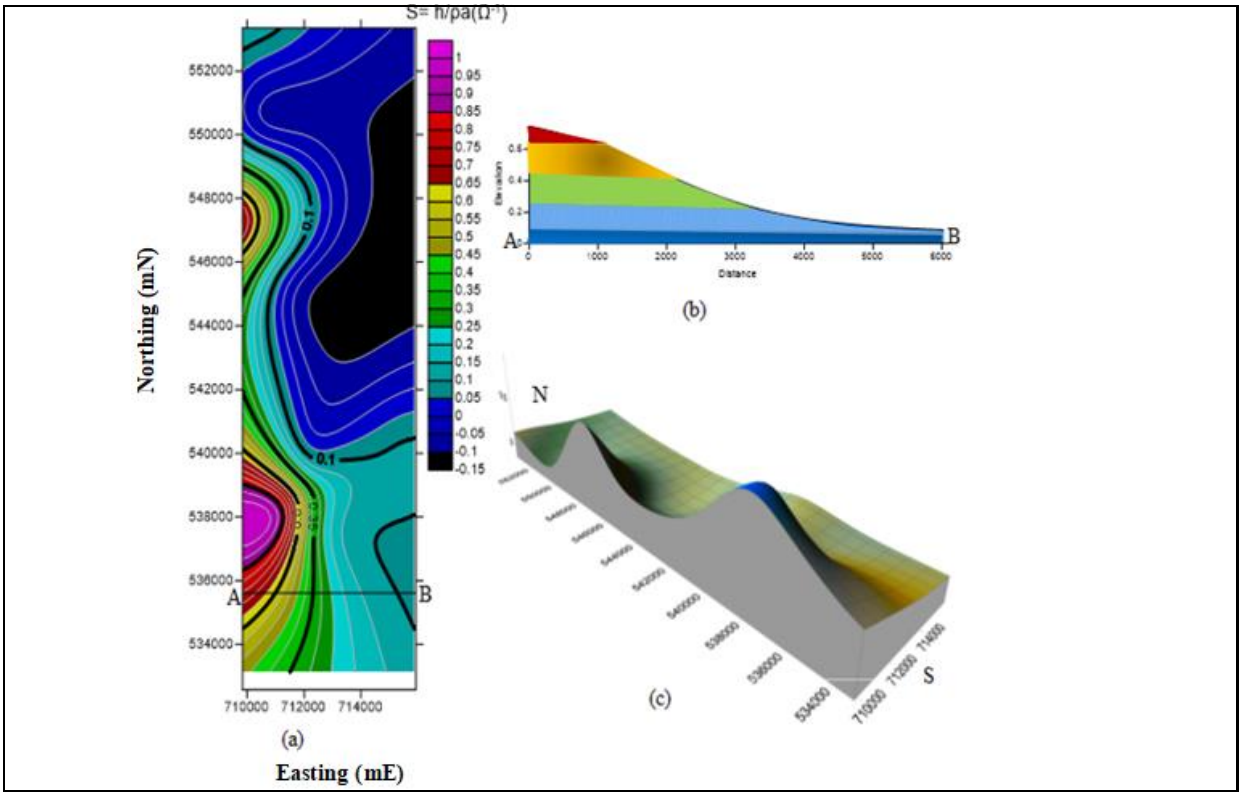

Figure 5.13: (a) Aquifer longitudinal conductance – S=h/ρa (Ω^{-1}) contour map; (b) Aquifer longitudinal conductance profile; (c) Three-dimensional surface view of aquifer longitudinal profile

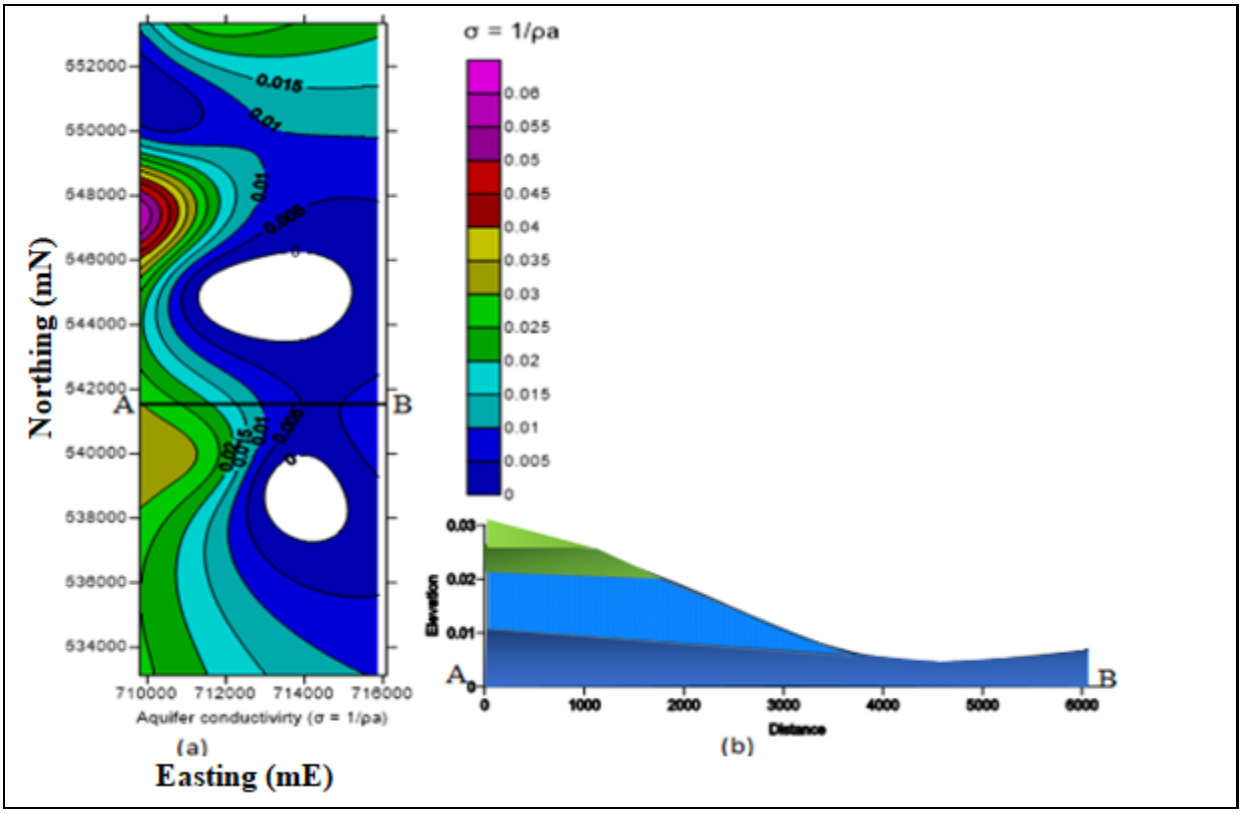

Figure 5.14: (a) Aquifer conductivity – σ=1/ρa; (b) Aquifer conductivity profile

5.3.4 Aquifer longitudinal conductance and aquifer conductivity

The longitudinal conductance value varied between 0.0391 (Ω^{-1}) at VES5 and 0.6884 (Ω^{-1}) at VES 1, while the conductivity value ranged from 0.006 at VES 6 to 0.0592 at VES 1 (Table 5.5). The aquifer longitudinal conductance and aquifer conductivity contour maps as well as their profiles are presented in Figure 5.11 and Figure 5.12. Profiles A–B from both parameters showed a striking similarity with a gradual decrease in conductivities from the west with distance away from the saline sources to the east. Similarly, the three-dimensional surface view also revealed a north-south increase in longitudinal conductance values. The longitudinal conductance (S) may be related to the variation in the resistivity of substrata with depth. However, it may be noted that the layer's resistivity depends more on the saturation content of the aquifer and not necessarily aquifer thickness (Shilaja et al., 2016); hence, a thicker aquifer may not necessarily correlate with higher resistivity as in the case of VES 1 and VES 3 in the present study. The high S-values corroborated by high conductivity values obtained at VES 1, VES 3, VES 11, and VES 12 and may likely be due to high salinity of the groundwater or high clay, or both (Ugada et al., 2013).

This may be substantiated by the geophysical analysis of electrical resistivity and borehole logs, which showed the presence of both saltwater intrusion and the intercalated clay layers in the subsurface of the study area (Yusuf and Abiye, 2019). Furthermore, an appreciable increase in 'S' value may correspond to an average increase in the clay content and consequent decrease in transmissivity of the aquifer (Oteri, 1981). In the present case, despite a high porosity value and high longitudinal conductance value at VES 1 and VES 4, the corresponding low transmissivity value suggests appreciable clay content. It can thus be concluded that high longitudinal conductance values were due to the presence of both clay and brackish/saline intrusion into the fresh aquifer in the study area.

5.3.5 Electrical resistivity tomography

The ERT surveys involve the measurement of potential gradient developed between two pairs of electrodes arising from the introduction of direct current into the subsurface using a separate electrode pair. Mostly, in the subsurface porous media, the transport of electrical current occurs predominantly through the movement of ions in the pore fluid, so that a medium's electrical resistivity depends predominantly on fluid saturation, porosity, and fluid electrical conductivity. Therefore, ERT surveys are capable of detecting and delineating spatial and temporal variation in lithological and hydrological properties of the coastal sediments (Kulessa, 2007). The application and theories of the ERT to hydrological problems of the subsurface are well established (Rubin and Hubbard, 2005; Vereecken et al., 2006; Ayolabi et al., 2013). In this study, the process of data acquisition was detailed in Chapter 4 (see 4.3.1.2).

The obtained data along the three grouped 2D ERT profiles covers only the central parts of the study area, namely Elegushi beach, Oniru beach, and Adeniji Adele (Ilubinrin) (Figure 5.2**a-c**). The data was processed using RES 2D and the results are presented in Figure 5.13, Figure 5.14, and Figure 5.15. The arrays employed are dipole-dipole and pole-dipole for better horizontal and higher depth probing. The 2D ERT sections revealed variations in the subsurface resistivity, the geoelectric property that delineates different lithologies as well as its fluid content. The interpretation from the ERT revealed that the subsurface lithologic units comprised different layers with varying resistivity values, ranging from topsoil, clay, sandy clay/clayey sand, and sand. Deductions from the available borehole logs showed that the aquifer is constituted by the sandy clay/clayey sand and sand layers with various degrees of aquifer yields due to the differences in porosity and permeability of the aquifer materials. In

this study, parts of the aquifer units, especially the second aquifer, have been impacted by saline water due to an incursion by saline water from the nearby Ocean or lagoon, and where it occurs, it is characterised by a low resistivity value. Other sources of contamination observed from the study included the infiltration of saltwater from the creeks, accumulation, and percolation of wastewater through unlined drainage from the canal, wastewater from the adjoining canal and infiltration from polluted streams.

The intrusion experienced in the coastal domain was suspected to be as a result of an increase in groundwater abstraction or withdrawal for both domestic and industrial use leading to a drop in the freshwater table, and consequently inducing incursion of denser saltwater to flow further inland (Oteri and Atolagbe, 2003; Adepelumi et al., 2008; Adeoti et al., 2010; Harikrishna et al., 2012). In a similar study, Ayolabi et al. (2013) also deduced that excessive groundwater extraction is responsible for saline water intrusion into the coastline aquifer. This problem is particularly imminent within the study area that many prolific boreholes that were initially producing freshwater after drilling suddenly became salty a few months later and were, therefore, abandoned. The observed patterns of the saline water incursion from the geoelectrical resistivity results in most cases were lateral and generally identified with resistivity value (<10 Ω m) (Figure 5.13 and Figure 5.14). It further revealed that the groundwater was affected by both brackish and ocean water situated north and south of the study area, respectively.

At Elegushi, Figure 5.2**a** on the base map, three traverses were undertaken (**a–c**) in this domain, and Figure 5.13 presents the processed ERT map. Traverse-**a** was carried out parallel, probing a higher vertical depth using pole-dipole while **b** and **c** separated 500 m apart, were surveyed perpendicular to the ocean and the lagoon, to reveal the progressive seawater incursion (marked in blue) into the neighbouring coastal aquifers employing dipole-dipole array. The vertical depths of penetration were 219 m, 174 m, and 122 m for traverses **a**, **b** and **c**, respectively. The parallel a-traverse was 200 m from the ocean and the subsurface is essentially characterised by low resistivity, reflective of saline incursion into the aquifer as revealed from the 2D ERT model. It is obvious that between the lateral distances (117–152 m; 200–250 m) the aquifer has been impacted by the seawater intrusion to a depth of 30–90 m beneath the surface, with a resistivity value of <10 Ω m. This indicates that the second aquifer has been impacted by saline water. Similarly, traverses **b** and **c** were both probed from a 300 m distance to over a kilometre away from the Ocean to ascertain the progressive saltwater incursion inland. Traverse **b** revealed incursion of saline water into the subsurface

aquifer to a depth of between 15 m and 45 m. This is an indication of saline incursion deducible from its exhibited low resistivity value. This definitely, reflects an influence from the brackish water due to the contaminant flow in a south-eastern and eastern direction. The observed low resistivity at traverse **c** at a depth range of between 30 m and 90 m is a clear indication of a change in lithology and fluid content. This portion has been highly impacted by saltwater and has greatly affected the second aquifer. The contaminant spread becomes imminent at a lateral distance of 320 m, indicating the presence of saline intrusion.

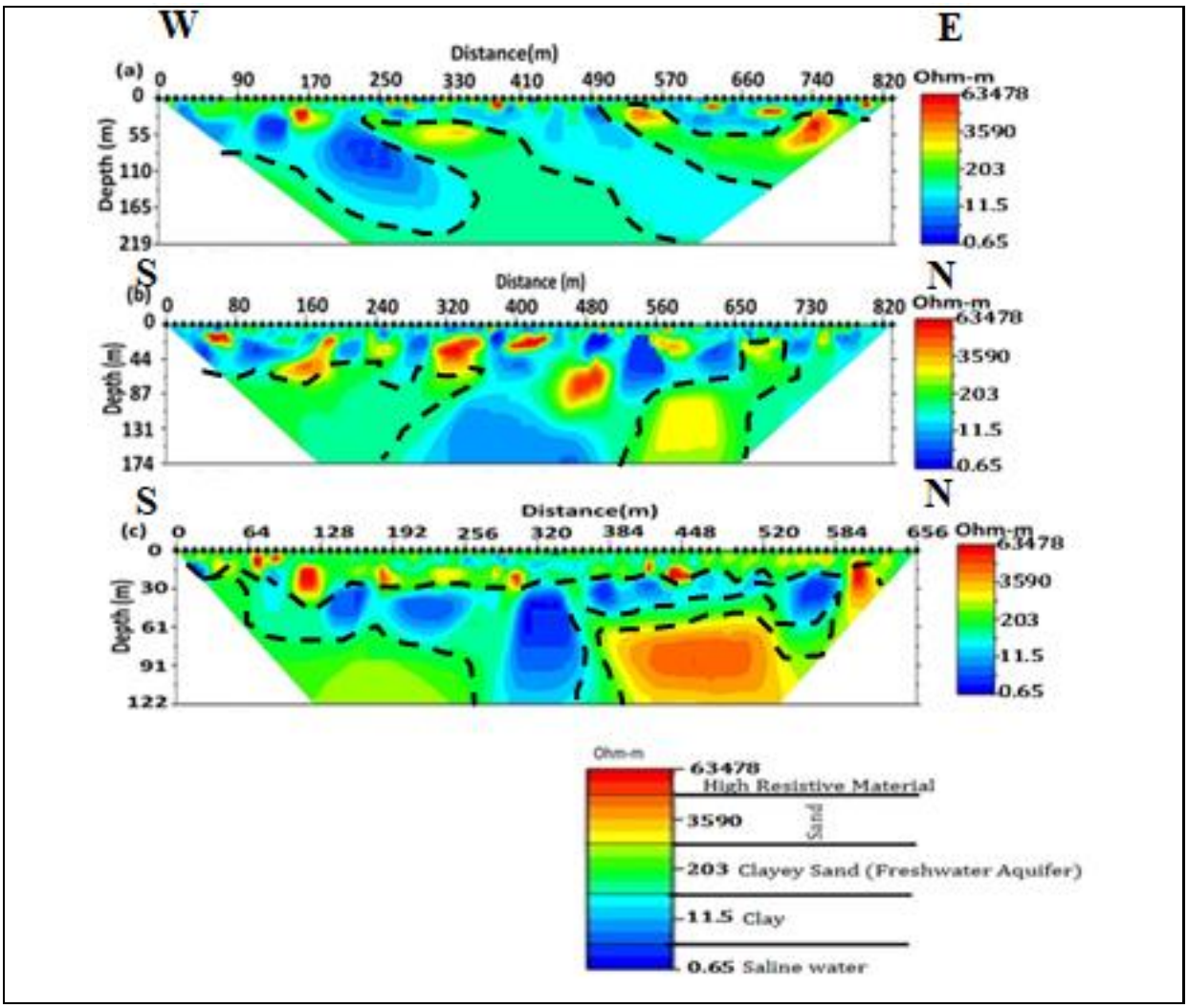

Figure 5.15: Earth Imager Inverted Resistivity – Depth models for the ERT lines for Elegushi traverses a, b and c

At Oniru, Figure 5.2**b** on the base map, a resistivity survey was conducted along three traverses (**a–c**) and presented in Figure 5.14. Traverses **a** and **b** were taken parallel to the lagoon, while traverse **c** was carried out perpendicular at distances of 650 m, 400 m, and 800 m away from the lagoon. The area coverage of investigation for traverses **a**, **b** and **c** were

118 m and 480 m, 122 m and 567 m, and 141 m and 405 m for both depths and lateral distances, respectively. At traverse **a**, resistivity distributions of extremely low value are restricted to the near-surface aquifer within the depth ranging from 0–10 m, as revealed by the 2D ERT inverted.

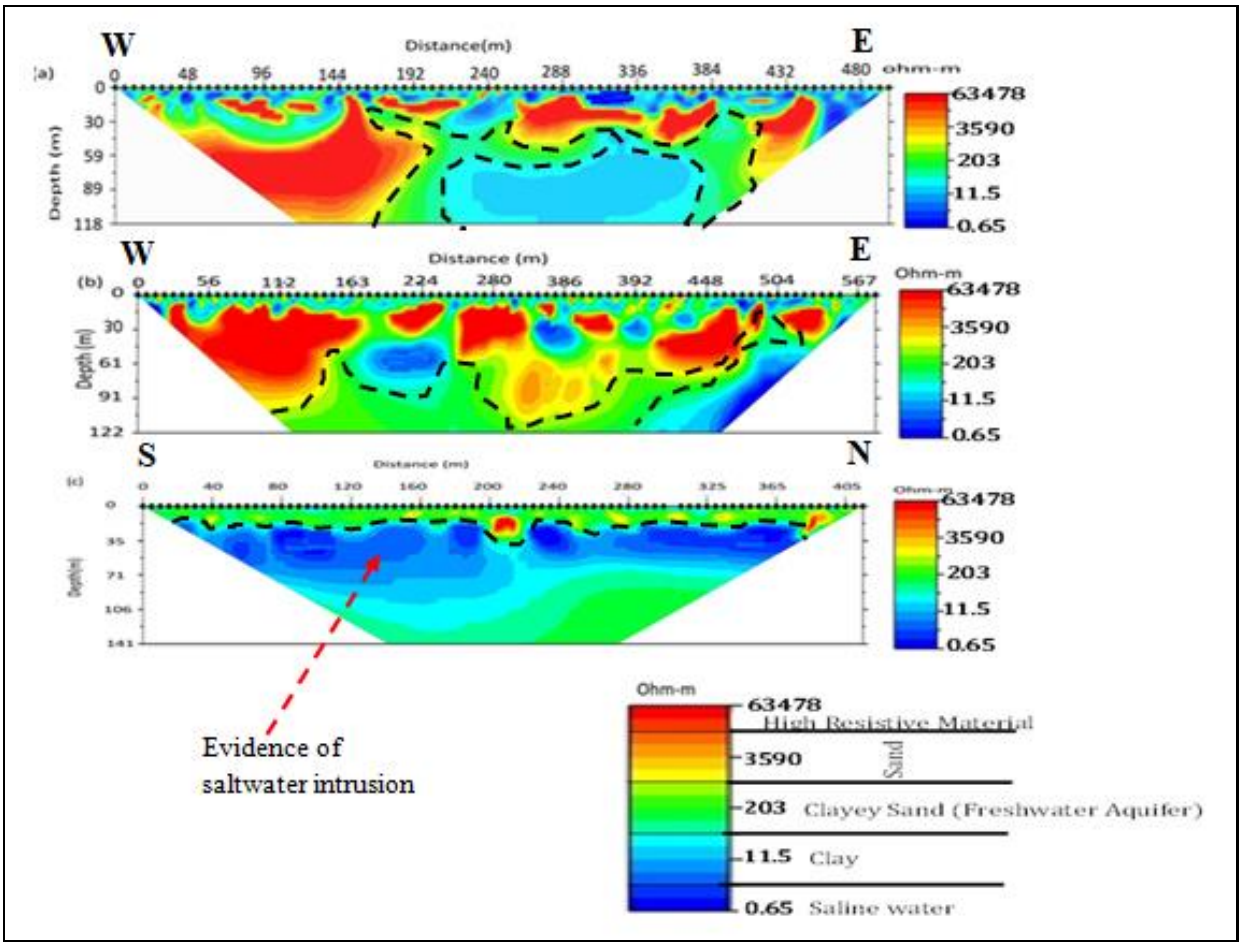

Figure 5.16: Earth Imager Inverted Resistivity Depth models for the ERT lines for Oniru traverses a, b and c

This is connected with the combination of clay, on the one hand, and the infiltration of wastewater or leachate generated from both (domestic and industrial) into the subsurface via unlined drainage and the wastewater channel. At traverse **b** the low resistivity value diagnostic of contaminant plume was observed between a depth of 30 m and 60 m and at lateral distances of 224 m and 286 m; this apparently indicates a saltwater intrusion. However, traverse **c** was conducted to monitor the gradual encroachment into inland by the saline water. This shows dominantly low resistivity values within a depth of 20 m to 50 m and also exhibits lateral occurrence. This may be a lateral invasion of the freshwater aquifer by seawater. There is also a gradual decrease in the degree of intrusion with distances further

inland that is evident from wider contaminant plume spread at a lateral distance between 0 m and 240 m. This may be as a result of high pressure near the source of the intrusion, which decreases with distance and thus leads to volume reduction of saltwater being transgressed and/or the presence of a competent underlying bed serving as seal retarding its percolation. It can thus be deduced that the second aquifer was greatly impacted.

Adeniji Adele, otherwise known as Ilubunrin, Figure 5.2**c** on the base map, is a land-fill reclaimed portion on the lagoon and the processed map was presented in Figure 5.15. Two traverses were taken parallel to the Lagoon at 100 m and 200 m away from the lagoon for both **a** and **b**, respectively. The 2D model revealed the status of the probed subsurface within the vertical depth of 138 m and 139 m for traverse **a** and **b**. The traverses characterised predominantly by low resistivity at the surface up to a depth of 10 m, maybe suggesting the presence of clay or wastewater infiltration from the adjacent canals and streams. However, traverse **b** was suspected to have been impacted by brackish water at depths between 30 m to 70 m below the surface. The southern spread pattern exhibited by the plume could be confirming the general north-south groundwater flow direction. Generally, deducible from the depth of intrusion occurrence, ERT has revealed that the second aquifer was greatly impacted and mostly affected by the saline intrusion in the study area.

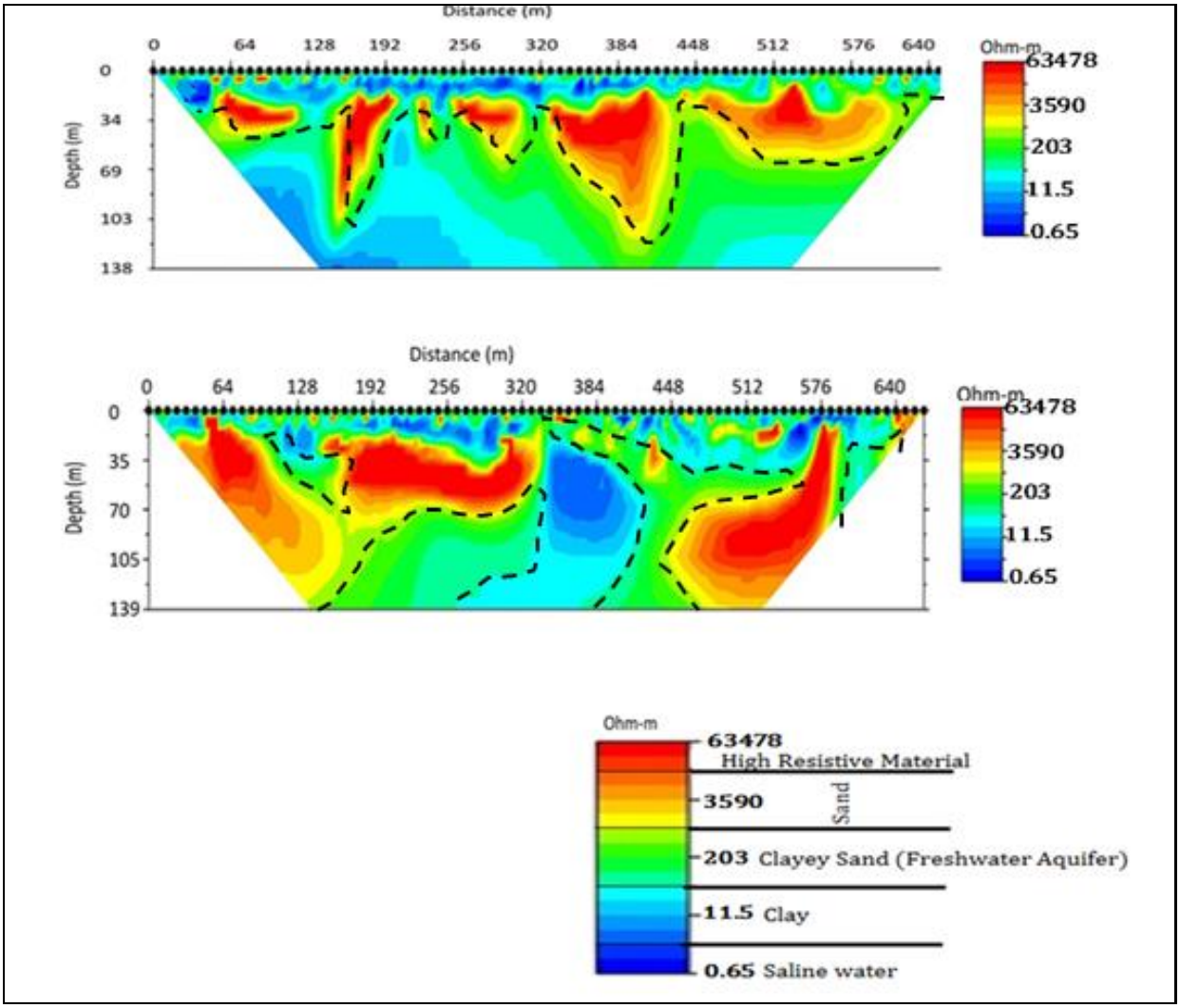

Figure 5.17: Earth Imager Inverted Resistivity Depth models for the ERT lines for Adeniji Adele (Ilubinrin) traverses a and b

5.3.6 Geophysical borehole logs

Geophysical logging methods provide an additional toolbox to identify rock formations that are permeable and thus productive, and the clayey formation so that it may be eliminated from the search for potential aquifers. It is a tool comprising several measurement devices (e.g. resistivity and gamma rays) that were lowered into the subsurface, and continuous readings of physical values were taken and sent via the cable to the surface unit. The method allows better identification of the subsurface layers and their fluid contents and also removes the ambiguity of suppressed thin layers by surface geophysical methods. The natural gamma logs are used primarily for lithologic identification and stratigraphic correlation.

The geophysical borehole data acquisition process for this study was described in Chapter 4 (see 4.3.1.3). The log interpretation involved superimposing the resistivity log of the

boreholes in the study area on the natural gamma ray log which discriminated between sand and clay or shale. This superimposition enabled the tracing of the relatively low resistivity zones within sand units across the boreholes. The occurrence of relatively low resistivity zones within the sand, compared to clay or shale, indicated the presence of more dissolved solute in the saturating fluid characteristics of saltwater intrusion.

Representative logs for each area were chosen from the available geophysical logs and grouped into two axes (A and B) (Figure 5.16 and Figure 5.17) for ease of examination and correlation. The correlation of some selected well logs into axes A and B from west to east was guided by the availability of borehole logs, its location and the desire to develop a cross-section model to enhance understanding of the subsurface hydrogeological processes. Specifically, representative borehole logs with the highest level of penetration close to the ocean in the south, and boreholes close to the lagoon in the north were chosen and correlated to gain an insight into the extent of saline intrusion for every locality across the stretch of the study. The saltwater–freshwater interface and horizons deduced from geophysical borehole logs are presented in Table 5.6, while Figure 5.16 and Figure 5.17 show the diagrammatic representation.

Seventeen out of the 45 borehole logs interpreted were not affected by saline intrusions, which implies 62 % of the examined holes were intruded by seawater (Table 5.6). The A-axis constitutes logs at the southern parts of the coastal belt relative to the B-axis, while the B-axis comprises the northern parts of the coastline next to the lagoon. The A-axis comprises Apapa–Victoria Island–Lekki–Ajah–Sangotedo and Awoyaya, while the B-axis is made up of Ikoyi–Lakowe–Akodo both from west to east, respectively. Information from available borehole logs, combined with a qualitative interpretation of the natural gamma ray, shows that the study area is underlain by the alternation of sand and clay with the admixture of varying proportions indicated by changes in the values of gamma rays as related to different layers. The logs revealed three to four aquiferous zones of varying thicknesses and extents, the majority of which are regional and traceable along with distances, while others exhibit local occurrences. These aquifers are separated by confining units made up of clay or sandy clay. The shallowest depth of 14 m for the freshwater-saline water interface was recorded at the western and central parts of the study area at Apapa (BH16) and Ikoyi (BH42), while the deepest freshwater-saltwater interface depth of 157 m was intercepted at Ajah (BH20) (Table 5.6).

A-AXIS: Victoria Island–Lekki–Ajah–Sangotedo–Awoyaya

Five representative borehole logs stretching from Victoria Island (BH26) to Lekki (BH25) to Ajah (BH20) to Sangotedo (BH2) to Awoyaya (BH35), were selected to generate the geo-section for the A-axis (Figure 5.16). The A-axis traversed within the land tract from the central parts eastwards. A detailed interpretation is presented in Table 5.6 and Figure 5.16 reveals the regional occurrence of a clay column along the traverse, which increases in thickness in an easterly direction, varying from 80 m at Sangotedo (BH2) and extends to >150 m at Awoyaya (BH35) within the depth of investigation. The extensive occurrence of the clay unit truncates the CPS aquifer at the south-eastern parts of the study area and probably accounted for the difficulty experienced in the availability and exploitation of fresh groundwater.

B-AXIS: Apapa–Ikoyi–Badore–Lakowe

The geo-section for the B-axis (Figure 5.17) encompassing Apapa (BH44) to Ikoyi (BH4) to Badore (BH5) and Lakowe (BH38) was generated utilising only four well logs. A summary of the interpretation is also presented in Table 5.6. The B-axis revealed a clay column occurrence that thickens towards the east. The clay serves as a seal, preventing the upconing of saline intrusion. Furthermore, the resistivity logs were equally interpreted to delineate the saline intrusion horizons and freshwater–saline water interfaces. The resistivity values along A-axis (west to east) ranged from 44 Ω m to 51 Ω m, 26 Ω m to 40 Ω m, 64 Ω m to 68 Ω m, 64 Ω m to 30 Ω m with the corresponding freshwater-saltwater interface thicknesses ranging between 66 m and 126 m, 49 m and 134 m, and 25 m and 157 m for Victoria Island, Lekki and Ajah, while Sangotedo and Awoyaya were unaffected. Concerning the B-axis, the resistivity values ranging between 18 Ω m and 20 Ω m, and 9 Ω m and 15 Ω m, with freshwater-saline water interface occurrence at depth ranges from 38 m to 105 m, and 51 m to 112 m for Apapa and Ikoyi, respectively, while Badore and Lakowe devoid of saline intrusion are exception within the depth of investigation (Figure 5.16 and Figure 5.17). The observed increase in resistivity values as shown in the resistivity logs can be explained with an increase in sand content and the occurrence of more freshwater or water with a lower TDS value than the layers above and below (Zohdy et al., 1990). It is, however, expected that resistivity gradually grades through intermediate water to good quality water as it increases with depth.

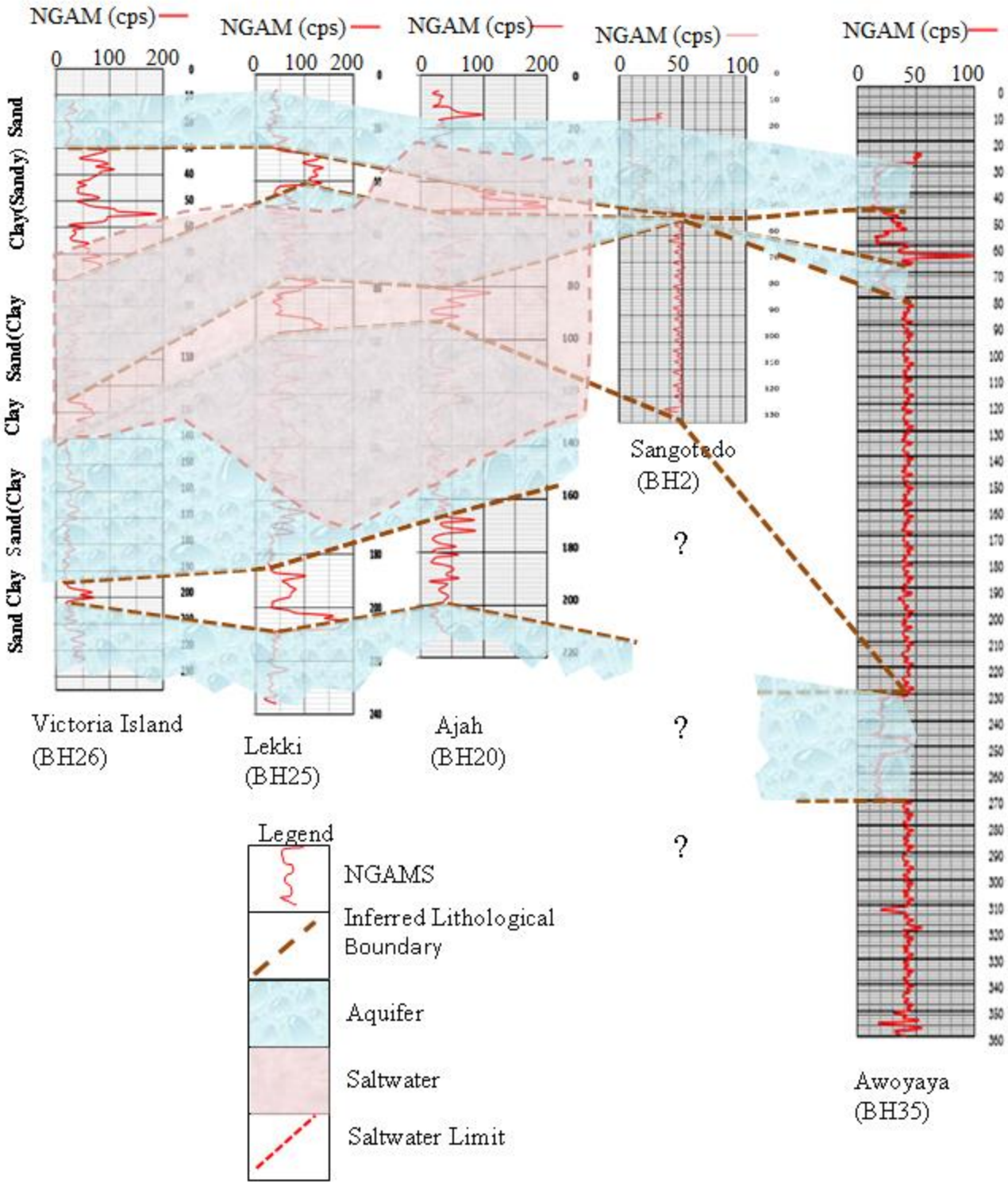

Figure 5.18: Typical fresh/saline water interfaces along the A-axis using natural gamma ray logs

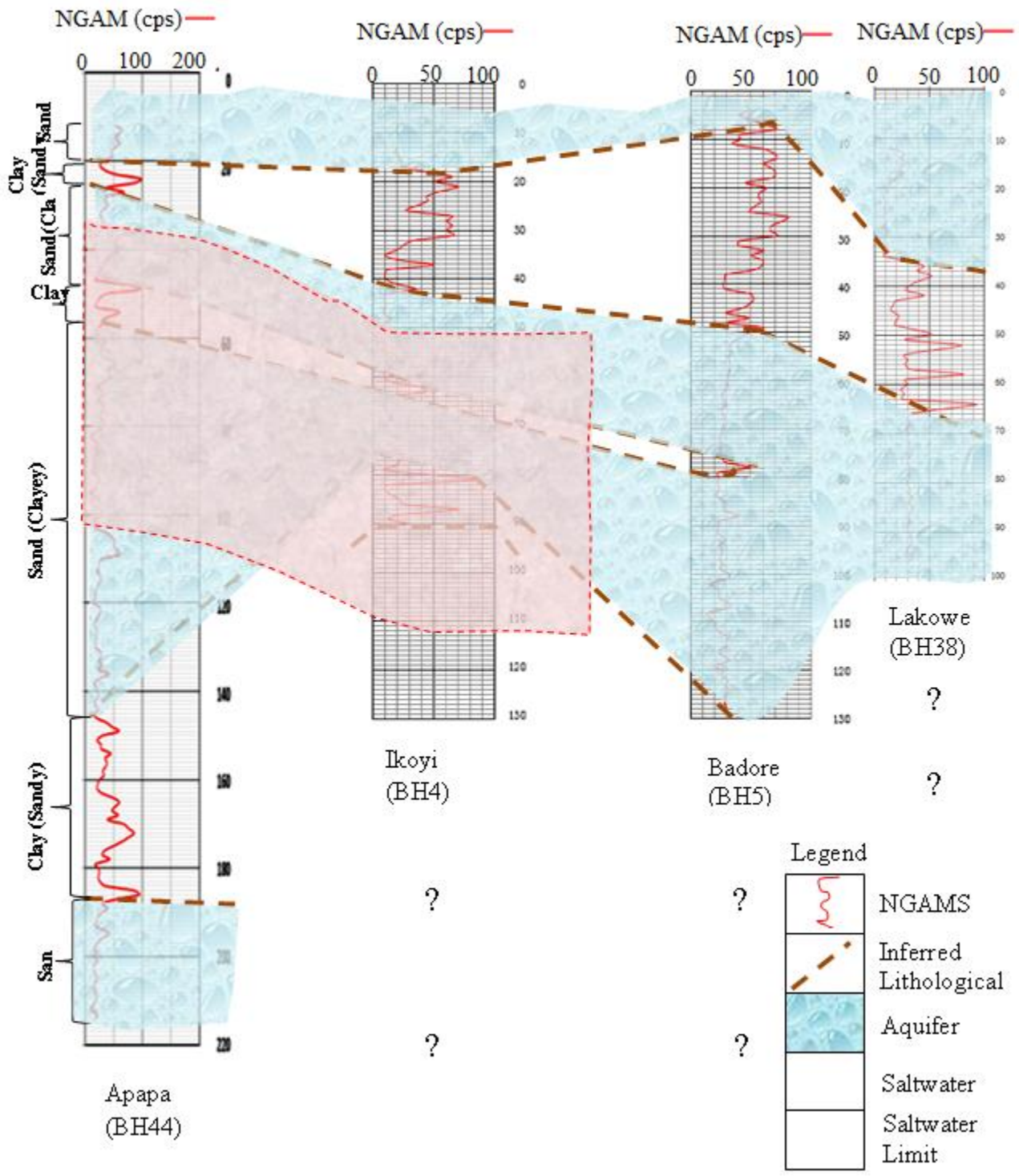

Figure 5.19: Typical fresh/saline water interfaces along the B-axis using natural gamma ray logs

Table 5.6: Ranges of freshwater–saltwater interface thicknesses and corresponding resistivities and freshwater zones

BH* S/N	Address	Coordinates		Freshwater–saltwater interface (m)		Resistivity at freshwater–saltwater interface (Ωm)		Freshwater zones (m)	Remarks
				Top	Bottom	Top	Bottom		
BH1	1st Avenue Ikoyi	N 06 26. 781'	E003 27. 106'	75	108	18	21	0-27, 37-45, 47-55, >130	Affected
BH2	Ajayi Apa/Sangotedo	N 06 26.010'	E003 44.216'	-	-	-	-	14-53	Unaffected
BH3	Ajegunle water works	N 06 25'44.34''	E003 19'10.61''	30	70	4	18	0-21, 76-130	Affected
BH4	Osborne Estate Ikoyi	N 06 24.781'	E003 28.205'	51	112	9	15	10-13, >113	Affected
BH5	Badore	N 06 29.781	E003 42.205'	-	-	-	-	5-10, 53-76, 80-130	Unaffected
BH6	MRS Apapa	N 06 25.499'	E003 20.138'	-	-	-	-	10-18, 30-36, 37-50, 52-70	Unaffected
BH7	Etim nyang CRT. VI	N 06 24'00.20"	E003 26'02.60"	-	-	-	-	16-34, 66-93,106-127, 148-277	Unaffected
BH8	APMT YARD, APAPA	N 06 26'31.53"	E003 22'47.98"	-	-	-	-	13-25, 30-37,51-116, 124-190	Unaffected
BH9	Azare cr.Apapa	N 06 26 .109'	E003 21.964'	-	-	-	-	5-35,47-54, 58-120,135-228	Unaffected
BH10	Oniru Estate	N 06 25'48.90"	E003 29'55.00"	71	128	20	28	16-27, 167-202	Affected
BH11	Cappa VI	N 06 26'27.50"	E003 26'01.20"	77	117	28	31	15-30, 137-180, 183-198, 206-220	Affected
BH12	Ijora Olopa	N 06 27'58.20"	E003 22'43.00"	17	66	46	50	12-15, 106-145, 157-158,169-217, 225-229	Affected
BH13	Ijora CFAO	N 06 27'13.50"	E003 22'08.30"	-	-	-	-	28-35, 38-42, 46-91, 104-123, 128-132	Unaffected
BH14	Clover,Lekki	N 06 25'30.34"	E003 30'47.44"	39	114	42	33	14-18, 170-189,199-207	Affected
BH15	Apapa Wharf	N 06 25'32.80"	E003 22'34.29"	39	115	21	31	33-38, 124-170	Affected
BH16	Apapa DSTV	N 06 26.386'	E003 19.614'	14	58	57	56	11-13, 78-116, 131-160, 168-174, 177-179	Affected
BH17	Ajah/Eastline prject	N 06 26.572'	E003 35.156'	-	-	-	-	24-43, 52-58, 64-70, 74-147	Unaffected
BH18	Victoria Island	N 06 25'38.90"	E003 25'59.40"	63	129	39	35	155-208, 217-222, 234-272	Affected
BH19	Lagos Island/FIRS.	N 06 26.922'	E003 23.775'	-	-	-	-	14-19, 33-56, 70-112, 132-178	Unaffected
BH20	Ajah/ITB Construction	N 06 26.819'	E003 32.985'	25	157	64	68	18-24, 158-165, >200	Affected
BH21	Lekki/JP EST. PHS III	N 06 27'48.10"	E003 34'40.10"	78	130	68	68	28-36, 47-74, 131-143,158-165, 174-183,190-230	Affected
BH22	V/I Joseph N. Close.	N 06 25'33.00"	E003 25'32.40"	66	135	35	37	155-190, 196-212, 217-236	Affected

BH* S/N	Address	Coordinates		Freshwater–saltwater interface (m)		Resistivity at freshwater–saltwater interface (Ωm)		Freshwater zones (m)	Remarks
BH23	MTN Call Centre Lekki	N 06 27.966'	E 003 34.120'	-	-	-	-	5-13, 25-31, 38-43, 60-116	Unaffected
BH24	NNS Beecroft Naval Base, Apapa	N 06 27'32.8"	E 003 22'16.7"	-	-	-	-	12-21, 26-35, 42-48, 53-162, 192-214	Unaffected
BH25	OMORIRE JOHNSON Street, Lekki	N 06 26' 11 .90"	E 003 31' 32.40"	49	128	48	54	6-26, 173-187, >209	Affected
BH26	OZUMBA NBADIWE, VI	N 06 24' 22 .10"	E 003 25' 04.06"	66	126	44	51	12-30, 139-194, > 202	Affected
BH27	Tin-Can, APAPA	N 06 26' 07 .72"	E 003 20' 09.88"	-	-	-	-	6-23, 31-36, 87-199, >208	Unaffected
BH28	PRODECO Guest House , VI	N 06 24' 20.796"	E 003 24' 49.620"	45	134	26	40	15-21,148-153,160-170,173-215	Affected
BH29	IKATE ELEGUSHI, Lekki	N 06 26' 36 .60"	E 003 29' 35.20"	-	-	-	-	20-30, 98-118, 128-194, >208	Unaffected
BH30	Femi Okunnu, Lekki	N 06 26' 33 .30"	E 003 30' 26.90"	82	115	46	49	12-14, 182-220	Affected
BH31	WILLOW GREENS Estate, Lekki	N 06 26' 55 .70"	E 003 30' 38.60"	88	115	47	49	12-13,166-189,200-236,243-247	Affected
BH32	Zenith Bank Head Office , VI	N 06 25' 48 .20"	E 003 26' 04.60"	66	129	40	38	153-205,217-240	Affected
BH33	Civil Centre Nigeria	N 06 25.781'	E003 27.106'	-	-	-	-	20-106	Unaffected
BH34	Oniru Royal Estate	N 06 25.781'	E003 27.106'	22	90	10	24	-	Affected
BH35	Eko Akete, Awoyaya	N 06 28.213’	E 003 46.970’	-	-	-	-	26-47, 230-270	Unaffected
BH36	Federal Palace Hotel	N 06 25.796’	E 003 24.431’	21	130	17	30	-	Affected
BH37	Victoria Island	N 06 25.451	E 003 25.705	38	97	20	20	18-31,107-238	Affected
BH38	HFP Cemetery, Lakowe	N 060 28.241	E 0030 47.900	-	-	-	-	13-36, 70-95	Unaffected
BH39	NIGERDOCK,SNAKE ISLD	N06 25.528	E003 19.422	28	58	12	17	109-129	Affected
BH40	LSWC, Ikoyi	N 06 25.781'	E003 25.754'	18	66	3	5	110-130	Affected
BH41	Niger Biscuit, Apapa	N 06 25. 781'	E003 19 106'	53	117	22	28	123-130	Affected
BH42	Osborne Est, Ikoyi	N 06 25.781'	E003 26 106'	14	136	12	52	137-142, 150-220	Affected
BH43	Police Headquarters, Obalende	N 06 26.913	E 03 24.448	26	47	36	18	51-112	Affected
BH44	Takwa Bay Island, Apapa	N 06 25.789	E 0030 23.304	38	105	18	20	10-21, 26- 35, 106-143, >188	Affected
BH45	L/I, Apongbon wwks.	N 06 27.634	E 003 22.899	-	-	-	-	50-57,74-104,110-217,221-246	Unaffected

*BH=Borehole

Chapter 6

ISOTOPE CHARACTERISATION OF THE BASIN

6.1 Introduction

In order to identify the source(s), movement, or interaction between surface water and groundwater and to estimate the residence time within the aquifer, water samples were analysed for environmental isotopes ($\delta^{18}O$, $\delta^{2}H$, Tritium, Carbon-13 and Carbon-14) signatures. Table 6.1 and Table 6.2 represent the stable isotopic data sets, while the carbon and tritium data are presented in Table 6.3. The sample location map and the resulting stable isotope plots of $\delta^{2}H$ vs $\delta^{18}O$ along the LMWL for the Benin Republic are presented in Figure 6.1, Figure 6.2a and Figure 6.2b. It is important to note that the field campaigns were undertaken three times due to logistic and accessibility constraints.

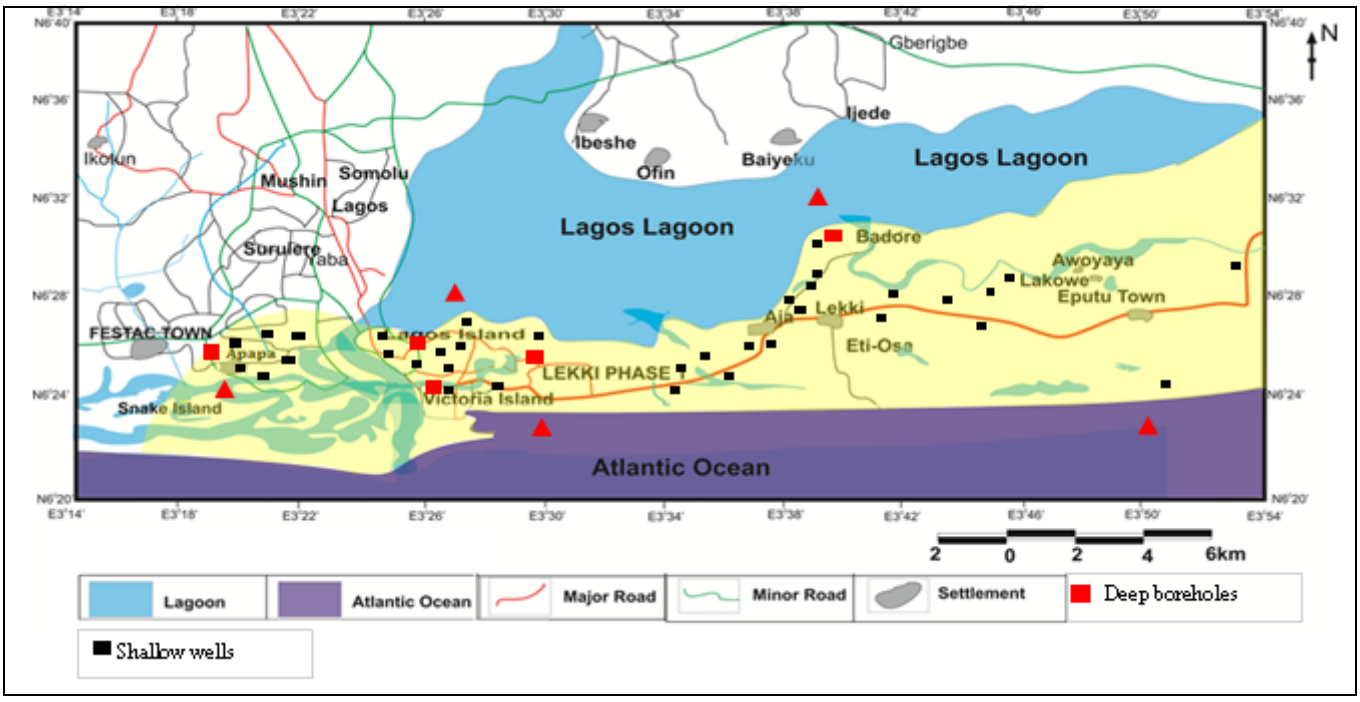

Figure 6.1: Location of sampled wells, boreholes, and surface water

Table 6.1: Isotope results and calculated temperature for rainy season water samples in the Lagos Coastal Basin

Sample ID	Longitude (E)	Latitude (N)	Well-depth (m)	δ^2H (‰)	$\delta^{18}O$ (‰)	Deuterium excess (‰)	T (°C) calculated
Shallow groundwater (GW)							
GW1	06°26.520'	003°19.876'	4.5	-0.9 ±0.4	-0.08 ±0.08	-0.32	17.4
GW2	06°26.631'	003°19.775'	7.0	-18.2 ±0.1	-2.58 ±0.04	0.12	12.4
GW4	06°28.163'	003°21.560'	7.2	-8.5 ±0.1	-0.88 ±0.04	-2.29	15.8
GW5	06°27.899'	003°21.561'	3.87	-24.8 ±0.6	-4.26 ±0.08	5.49	9.1
GW6	06°26.555'	003°22.017'	6,0	-5.6 ±0.3	-1.19 ±0.09	2.85	15.2
GW7	06°26.899'	003°19.837'	11.2	-8.3 ±0.2	-3.11 ±0.09	13.80	11.4
GW8	06°27.196'	003°23.052'	6.5	-6.5 ±0.2	-2.39 ±0.04	10.51	12.8
GW9	06°26.908'	003°24.627'	7.12	-7.9 ±0.4	-2.41 ±0.04	9.26	12.8
GW10	06°27.483'	003°23.925'	4.25	-6.7 ±0.1	-2.34 ±0.05	9.89	12.9
GW12	06°27.815'	003°23.259'	9.1	-3.0 ±0.1	-0.63 ±0.05	1.51	16.3
GW13	06°27.464'	003°22.938'	12.0	-8.1 ±0.2	-2.77 ±0.05	11.62	12.1
GW14	06°25.891'	003°24.590'	3.75	-14.4 ±0.2	-3.89 ±0.10	13.18	9.8
GW15	06°26.629'	003°25.243'	5.6	-11.4 ±0.3	-3.13 ±0.05	10.86	11.3
GW16	06°26.648'	003°24.640'	5.0	-14.9 ±0.9	-3.30 ±0.11	8.50	11
GW17	06°26.213'	003°24.317'	4.8	-20.2 ±0.4	-4.81 ±0.09	13.94	8.8
GW18	06°26.341'	003°28.077'	4.2	-11.6 ±0.2	-3.49 ±0.04	13.13	10.6
GW20	06°26.268'	003°31.209'	3.45	-16.8 ±2.8	-2.10 ±0.27	-2.13	13.5
GW21	06°25.884'	003°32.618'	9.5	-7.9 ±0.4	-0.83 ±0.08	-2.00	15.9
GW23	06°29.328'	003°34.864'	9.0	-8.2 ±0.4	-1.99 ±0.05	5.99	13.6
GW25	06°30.124'	003°36.007'	7.2	-7.9 ±0.4	-3.10 ±0.07	13.79	11.5
GW27	06°27.820'	003°40.300'	6.3	-13.5 ±0.2	-2.13 ±0.06	1.65	13.3
GW28	06°28.139'	003°42.195'	6.12	-13.4 ±0.2	-2.83 ±0.08	6.66	11.9
GW29	06°28.427'	003°48.325'	7.4	-19.8 ±0.2	-2.64 ±0.11	-1.10	12.3
GW30	06°29.103'	003°53.303'	5.85	-17.4 ±0.1	-2.52 ±0.05	0.50	12.6
GW32	06°28.415'	003°38.133'	7.6	-8.6 ±0.3	-2.81 ±0.07	11.32	12
GW33	06°28.466'	003°34.616'	13.2	-10.3 ±0.1	-1.71 ±0.07	1.83	14.2
GW36	06°28.121'	003°33.873'	7.45	-18.1 ±0.4	-3.97 ±0.02	10.11	9.7
GW37	06°26.380'	003°31.305'	8.2	-9.4 ±0.1	-1.79 ±0.14	3.25	14
GW40	06°26.959'	003°32.928'	4.35	-14.2 ±0.4	-3.70 ±0.06	12.13	10.2
Deep groundwater (DWG)							
DGW1	6 26.576	3 21.872	190	-21.3 ±1.2	-4.06 ±0.13	11.19	9.5
DGW2	6 27.133	3 25.741	235	-19.7 ±1.1	-3.89 ±0.17	11.44	9.8
DGW3	6 25.646	3 25.646	230	-16.5 ±0.7	-3.43 ±0.10	11.01	10.7
DGW4	6 26.411	3 25.500	355	-18.7 ±0.3	-3.78 ±0.05	11.51	10
DGW5	6 30.511	3 36.684	185	-24.7 ±1.7	-4.65 ±0.17	12.51	8.3
Rainwater (RW)							
RW1				3.3 ±0.1	-1.65 ±0.02	15.05	14.3
LMWL				-12.2	-2.9		
Surface water (SW)							
SW1	06°29.673'	003°25.666'		-11.4 ±0.2	-3.17 ±0.08	11.05	11.3
SW3	06°31.541'	003°34.756'		-13.7 ±0.1	-3.47 ±0.07	10.93	10.7
SW2	06°23.349'	003°26.525'		2.7 ±0	0.11 ±0.02	1.89	17.8

Table 6.2: Isotopes results for dry season water samples in the Lagos Coastal Basin

Sample No.	Location name	Longitude (E)	Latitude (N)	Well-depth (m)	δ^2H (‰)	$\delta^{18}O$ (‰)	d= excess (‰)
Shallow groundwater (GW)							
GW1	Coconut 1	06˚26.520'	003˚19.876'	4.5	-9.8 ±1.1	-2.90 ±0.2	10.76
GW2	Coconut 2	06˚26.631'	003˚19.775'	7.0	-12.9 ±2.0	-3.33 ±0.5	10.75
GW4	Ijora	06˚28.163'	003˚21.560'	7.2	-12.5 ±0.4	-3.33 ±0.2	10.89
GW5	Badia	06˚27.899'	003˚21.561'	3.87	-10.3 ±0.9	-2.89 ±0.3	10.22
GW6	Wharf	06˚26.555'	003˚22.017'	6.0	-7.6 ±0.5	-2.29 ±0.3	8.72
GW7	Kirikiri Rd	06˚26.899'	003˚19.837'	11.2	-3.7 ±0.7	-0.73 ±0.3	1.54
GW8	Marina park	06˚27.196'	003˚23.052'	6.5	-11.6 ±3.1	-2.72 ±0.3	7.73
GW9	Obalende	06˚26.908'	003˚24.627'	7.12	-11.8 ±0.4	-3.29 ±0.1	11.59
GW10	Adeniji	06˚27.483'	003˚23.925'	4.25	-10.8 ±0.4	-2.79 ±0.1	9.03
GW12	Isale Eko	06˚27.815'	003˚23.259'	9.1	-9.9 ±0.5	-2.70 ±0.1	9.18
GW13	Island	06˚27.464'	003˚22.938'	12.0	-9.4 ±0.2	-3.20 ±0.2	13.29
GW14	VI	06˚25.891'	003˚24.590'	3.75	-8.9 ±4.1	-3.13 ±0.4	13.38
GW15	Ikoyi	06˚26.629'	003˚25.243'	5.6	-11.2 ±0.3	-3.36 ±0.2	12.62
GW17	VI	06˚26.213'	003˚24.317'	4.8	-13.6 ±0.5	-3.38 ±0.2	10.35
GW18	LekkiPhase1	06˚26.341'	003˚28.077'	4.2	-11.6 ±0.6	-3.22 ±0.1	11.28
GW20	Igboefon	06˚26.268'	003˚31.209'	3.45	-15.3 ±0.3	-3.71 ±0.3	11.08
GW21	Lafiaji	06˚25.884'	003˚32.618'	9.5	-13.0 ±0.4	-3.13 ±0.3	9.17
GW22	Ajiwe	06˚28.161'	003˚34.789'	–	-15.5 ±0.4	-3.35 ±0.1	8.31
GW23	Oke iranla	06˚29.328'	003˚34.864'	9.0	-12.9 ±0.4	-3.06 ±0.2	8.88
GW24	Ado	06˚29.861'	003˚35.154'	7.2	-15.4 ±0.5	-3.37 ±0.2	8.52
GW25	Badore	06˚30.124'	003˚36.007'	6.3	-12.0 ±0.2	-2.93 ±0.2	8.74
GW27	Abijo	06˚27.820'	003˚40.300'	6.12	-16.8 ±1.0	-3.77 ±0.1	9.94
GW28	Awoyaya	06˚28.139'	003˚42.195'	7.4	-19.7 ±0.4	-3.98 ±0.3	8.59
GW29	Igando	06˚28.427'	003˚48.325'	5.85	-8.6 ±0.6	-1.71 ±0.1	3.51
GW32	Sangotedo	06˚28.415'	003˚38.133'	7.6	-13.1 ±0.6	-2.74 ±0.3	6.29
GW33	Ajah	06˚28.466'	003˚34.616'	13.2	-13.0 ±0.4	-2.52 ±0.1	4.86
GW36	Ajah	06˚28.121'	003˚33.873'	7.45	-16.4 ±2.1	-3.26 ±0.4	6.70
GW37	Idado	06˚26.380'	003˚31.305'	8.2	-11.1 ±0.6	-2.60 ±0.3	7.34
GW40	Ikota	06˚26.959'	003˚32.928'	4.35	-15.7 ±0.3	-3.45 ±0.2	8.87
GW41	Ogombo	06˚ 26.977′	003˚ 36.753′	2.41	-12.5 ±0.3	-2.48 ±0.2	5.04
GW42	Ibeju Lekki	06˚ 29.352′	003˚ 53.770′	5.2	-11.5 ±0.4	-2.54 ±0.1	6.54
GW43	Eleko	06˚ 26.433′	003˚ 51.360′	6.38	-16.9 ±2.9	-3.04 ±0.4	4.70
GW44	Lakowe	06˚28.455′	003˚ 43.820′	3.48	-11.2 ±0.8	-2.39 ±0.2	5.71
GW45	Awoyaya	06˚ 28.678′	003˚ 42.682′	4.2	-13.2 ±0.3	-2.78 ±0.2	6.50
Surface water (SW)							
SW1	Lagos Lagoon	06˚29.673'	003˚25.666'	–	2.5 ±0.6	0.36 ±0.1	-0.02
SW2	Oniru beach	06˚23.349'	003˚26.525'	–	2.3 ±0.5	0.79 ±0.1	-3.26
SW3	Ajah Lagoon	06˚31.541'	003˚34.756'	–	-1.9 ±4.6	-0.26 ±0.4	-0.06
SW4	Okun Ajah	06˚ 24.137′	003˚ 35.343′	–	1.9 ±0.2	0.82 ±0.0	-3.97
SW5	Apapa Creek	06˚ 24.902′	003˚ 21.935′	–	2.1 ±0.2	0.55 ±0.0	-1.85

6.2 Deuterium (^2H) and Oxygen-18

The ^2H and ^{18}O values of precipitation and infiltrating water are controlled by factors such as temperature, latitude and altitude effects, evaporation, intensity and duration of rainfall, and

condensation in recharge and drainage areas (Clark and Fritz, 1997; Dansgaard, 1964). The general meteoric relationship between ^{2}H and ^{18}O defined by GMWL and the concepts of the d-excess are detailed in Chapter 3 (see 3.3.1).

The location of the data on the GMWL, however, indicates the source of air moisture. The LMWL established by Loehnert (1988) for Ore Agbabu, southwest Nigeria, was defined by equation 6.1:

$$\delta^{2}H = 7.2 * \delta^{18}O + 9.4 \text{ ‰} \ldots\ldots\ldots\ldots\ldots\ldots\ldots 6.1$$

Whereas, the LMWL for the Cotonou GNIP–IAEA station, an extension of the LCB and her immediate neighbouring country, between the years 2005 to 2015 is defined by:

$$\delta^{2}H = 7.1 * \delta^{18}O + 9.1 \text{ ‰} \ldots\ldots\ldots\ldots\ldots\ldots\ldots 6.2$$

This study, however, adopted the Cotonou LMWL for this research due to the common features shared by both basins and the closeness of the local GNIP–IAEA station. The LMWL showed low vapour humidity relative to the GMWL resulting from its lower slope value.

A slope is a function of humidity and temperature (Gat, 1981; Rozanski et al., 1997) of a particular groundwater territory. The plots in Figure 6.2 show that the groundwater samples were plotted around and along the LMWL, indicating that the groundwater in the coastal aquifer is generally of meteoric origin. Furthermore, while samples that plot above the LMWL indicate rapid infiltration, samples that plot below and away from the LMWL, connote evaporation prior to recharge (Gat, 1981; Yusuf et al., 2018). Therefore, the plot of shallow groundwater samples above and below the LMWL indicated rapid infiltration to the shallow aquifer in one part and the effect of evaporation on the other.

The observed slight seasonal variations may be attributed to the intensity and amount effect of rainfall as noted by Dansgaard (1964), that at any given location, the heavier rainfall is more isotopically depleted than the light intensity rainfall during the dry season as the air moisture is subjected to a lesser Rayleigh condensation process. These results remain in perfect agreement with several observations for low latitude marine sites of the IAEA monitoring stations (IAEA, 1992). The variations resulting from recharge events and evaporation from unsaturated zones indicated that seasonal fluctuations were preserved in the shallow groundwater aquifer. In the groundwater samples, the median $\delta^{2}H$ and $\delta^{18}O$ of -10.3

and -2.58 ‰; and -12.3 and -3.05 ‰ were observed for the wet and dry seasons, respectively, reflecting the peculiar feature of shallow groundwater. This observation corresponds with many well-known phenomena documented in most stable isotopes of O and H. The diagrams of δ^2H and $\delta^{18}O$ (Figure 6.2) also reveal that most of the samples fall on the evaporation line or mixing line represented by a regression line defined by Equations 6.2 and 6.4 for both wet and dry seasons.

$$\delta^2H = 3.48^* \delta^{18}O - 2.8 \text{ ‰} \ldots\ldots\ldots R^2 = 0.49 \text{ (Wet season)} \ldots\ldots\ldots\ldots\ldots 6.3$$

$$\delta^2H = 3.89^* \delta^{18}O - 0.87 \text{ ‰} \ldots\ldots\ldots R^2 = 0.59 \text{ (Dry season)} \ldots\ldots\ldots\ldots\ldots 6.4$$

(a)

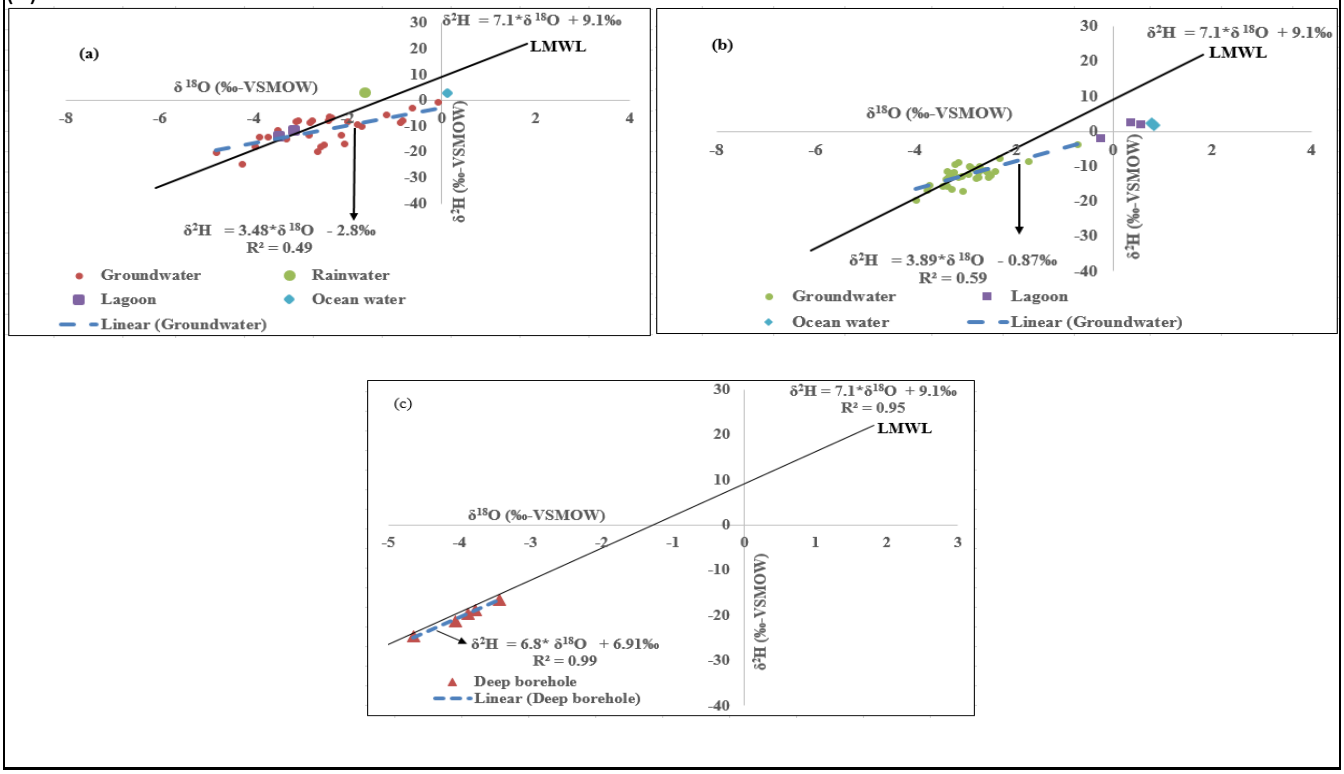

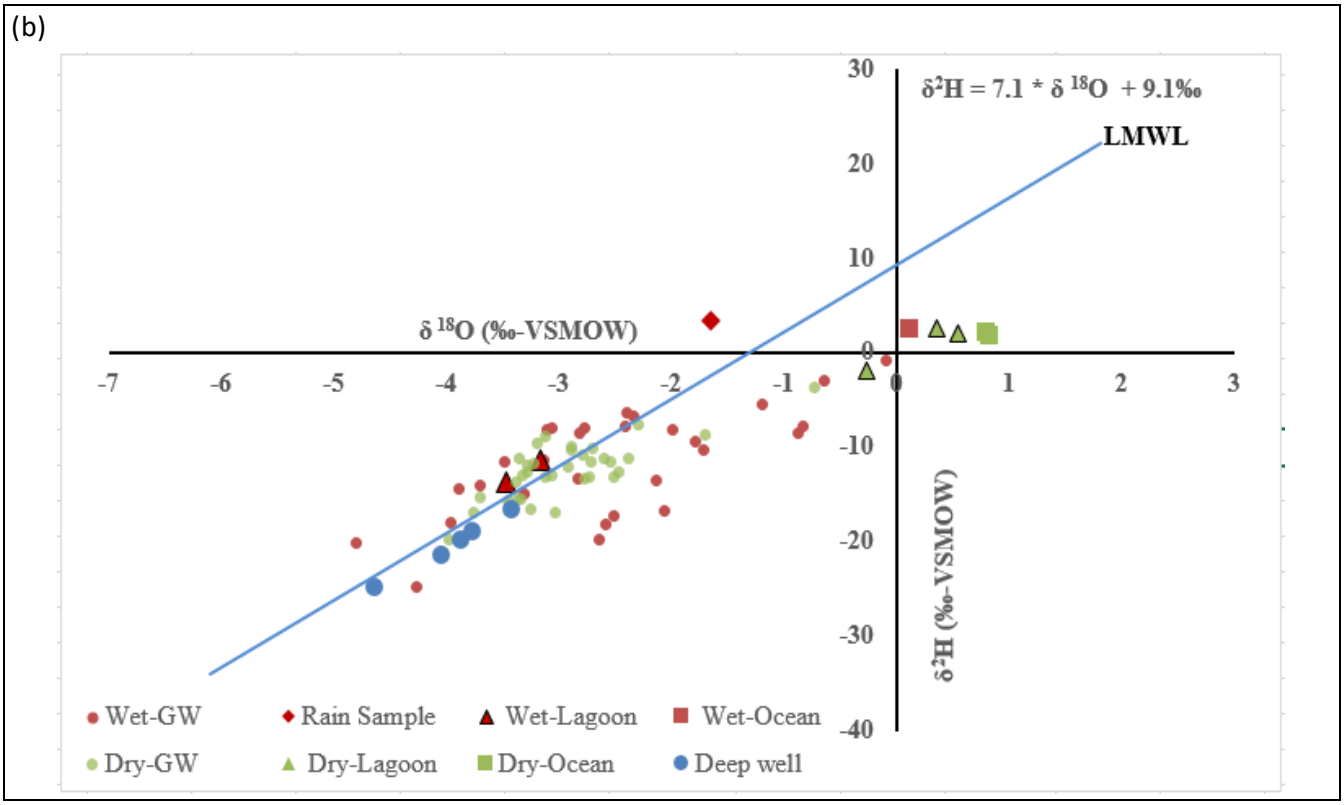

Figure 6.2: Plot of δ^2H vs $\delta^{18}O$ (‰) for shallow groundwater in wet and dry seasons, deep wells, surface water and rainwater in the Lagos Coastal Basin

The low slopes of 3.48 and 3.89 exhibited by both wet and dry seasons are also suggestive of the evaporation process. According to Gat and Gonfiantini (1981) and Sheppard (1986), evaporation from a freshwater surface commonly results in an evaporation line with a lower slope of 3.5–6.0 in a normal range of relative atmospheric humidity of 75 % to 10 %. The position of rainwater above the LMWL could be related to the condensation effect which is controlled by regional air circulation from the South Atlantic Ocean; however, its enrichment in ^2H implies domination by a local moisture source. According to Clark and Fritz (1997) and Abiye (2013), this occurrence could be due to low humidity in the vapour. In addition, groundwater samples collected at the central parts of the study area between the lagoon and the ocean (GW 13, GW 14, GW 15, GW 16, GW 17 and GW 18) (Table 6.1) exhibited a mixture between lagoon water and groundwater. The observed mixed isotopic signatures may suggest either or both of the following:

i. Movement of the lagoon water through and below the coastal aquifer to the sea, supported by the striking similarity in isotopic signatures between the groundwater sample GW15 and that of the Lagos lagoon sample (SW1) maybe confirming the fact that the lagoon is recharging the aquifer to the south.

ii. The depletion in stable isotopes for the lagoon and groundwater in the wet season may be related to the interaction with rainfall, while enrichment of the duo in the dry season may be due to an evaporation effect. Specifically, the lagoon water exhibits a prominent dilution in the wet season and more saline in the dry season, evident from their relative locations in Figure 6.2.

Concerning the deep groundwater, the environmental isotope plot in Figure 6.2 portrays that the samples fell slightly below and along the GMWL, indicating that the groundwater samples were of meteoric origin with little evaporation significance deducible from its slope. The mixing line is represented by a regression line defined by Equation 6.5:

$$\delta^2H = 6.8^* \delta^{18}O + 6.9 \text{ ‰} \ldots\ldots\ldots R^2 = 0.99 \text{ (Deep wells)} \ldots\ldots\ldots\ldots\ldots 6.5$$

From Table 6.3, the observed relative depletion in $\delta^{18}O$ and δ^2H suggests the presence of deep circulating groundwater in the basin. Although the deep aquifer recorded a relatively more depleted stable isotope value, the isotopic values fell in the same range with about 15 % of the shallow groundwater (Tables 6.1 and Figure 6.2). These intermixing isotopic signatures could suggest a probable mixture of preserved old water in the less permeable layers (clay layer or matrix) recently recharged water for the shallow aquifer.

Generally, surface waters are highly enriched with respect to ^{18}O and ^2H, with higher values recorded in the seawater relative to the Lagoon water (Figure 6.2, Table 6.1 and Table 6.2). Specifically, the seawater samples collected in both seasons (wet and dry) close to the seashore south of the study area have an isotopic composition value that is higher than 0 ‰ for both isotopes as reported for modern oceanic seawater. In the dry season, however, surface water samples collected close to the sea, at the Apapa creek (SW 5) and the Lagos lagoon (SW 1) exhibit both marine and evaporation influence on the isotopic composition with positive stable isotopes values. Contrarily, the Ajah lagoon (SW 3) at a greater distance from the sea has isotopic compositions that are only reflective of strong evaporation due to spatial isolation (Table 6.2 and Figure 6.2). Whereas, in the wet season, both the Lagos and Ajah lagoons (SW 1 and SW 3) have similar depleted values as groundwaters with respect to ^2H and ^{18}O and were plotted above the LMWL, but in the same region with parts of the groundwater on LMWL (Figure 6.1, Table 6.1). According to Clark and Fritz (1997), it was rare to find surface water and groundwater plotted above the GMWL but in low humidity regions, re-evaporation of precipitation from local surface waters created vapour masses with isotopic content that plot above the LMWL. The shift above the LMWL indicates the impact

of rainwater on the surface water bodies and may also suggest that the vapour evaporated from the hydrologically closed basin.

Furthermore, interpretation of d-excess was undertaken in order to ascertain the possible source of precipitation in the area which gives rise to recharge to the aquifers. The $\delta^{18}O$ values were plotted against d-excess (Figure 6.3) and the distribution has a range of variations from -2.29 ‰ to 13.94 ‰ for the wet season, 1.45 ‰ to 13.38 ‰ for the dry season and 11.01 ‰ to 12.51 ‰ for the deep groundwater samples. The high d-excess with depleted ^{18}O could be due to the mixing of regional air mass (depleted ^{18}O) and local moisture (enriched ^{2}H). These ranges of values reflect the influence of both local and regional moisture circulation, indicating highly enriched humidity in the area. Therefore, the similarity in the distribution pattern of d-excess and ^{18}O for both shallow and deep aquifers could indicate a recharge from mixed moisture sources. On a global scale, the average d-excess value is known to be about 10 ‰ (Craig, 1961) but it differs with variations in humidity, wind speed, and sea surface temperature during evaporation; accordingly, the low d-excess values reflect high humidity during the formation of vapour mass (Clark and Fritz, 1997; Abiye, 2013).

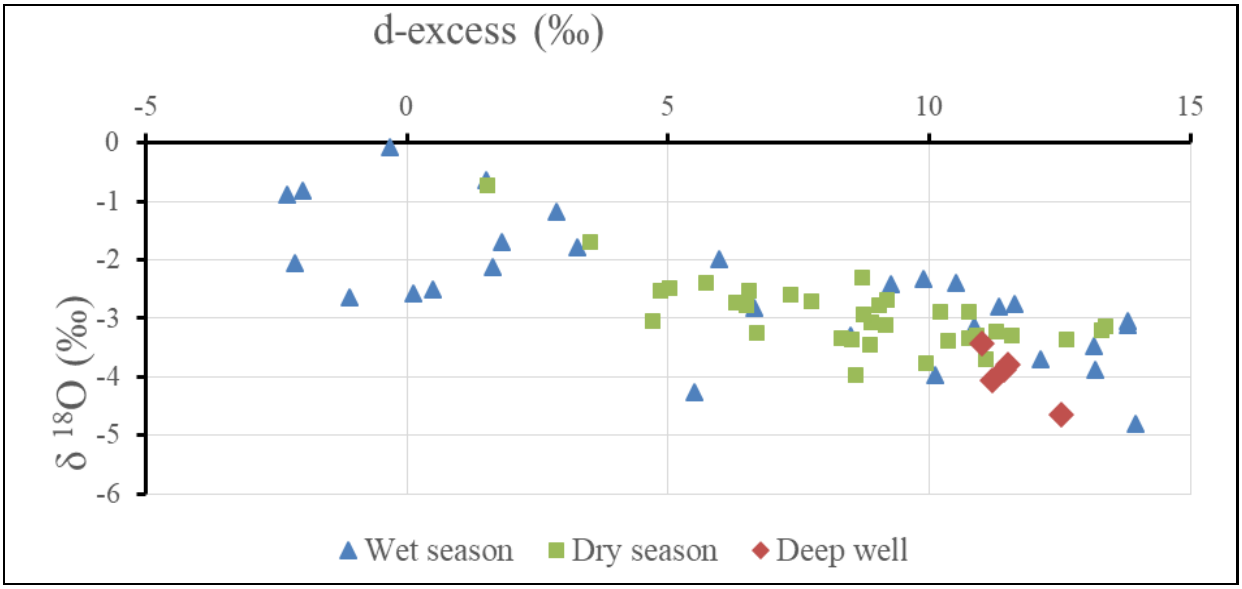

Figure 6.3: Plot for d-excess vs ^{18}O values in groundwater samples

The groundwater isotope contents of the LCB in the south are isotopically enriched relative to the isotope compositions of groundwater studied in the northern parts of Nigeria (Kehinde, 1993; Goni and Edmunds, 2001; Adelana et al., 2003), but are similar in isotopic compositions to groundwater from the basement and sedimentary basin of South West

Nigeria (Loehnert, 1988) and those reported from other countries in West Africa, for example, Ghana (Acheampong and Hess, 2000; Jorgensen and Banoeng-Yakubo, 2001). The observed depletion of stable isotope compositions from south to north in groundwater may be attributed to both the altitude and continental effect of incident rains. Generally, the stable isotope of oxygen (^{18}O) and hydrogen (^{2}H) are valued as natural tracers because they neither decay with time nor get removed from water during the exchange process of water and rock. The LCB groundwater has not been defined through any form of long-term isotope monitoring. Consistent, regular, and long-term sampling is, however, required in order to quantify the seasonal recharge in the basin without which no detailed interpretation of these fluctuations can be undertaken. However, the groundwater samples in the study area clustered around and along the LMWL on the $\delta^{2}H$–$\delta^{18}O$ plot (Figure 6.2) revealed that the observed relatively enriched mean values of $\delta^{2}H$ >-11.6 ‰, $\delta^{18}O$ >-2.53 ‰; $\delta^{2}H$ >-12.3 ‰, ^{18}O >-2.90 ‰; $\delta^{2}H$ > -20.2 ‰, ^{18}O > -3.96 ‰, exhibited by the groundwater's wet season, dry season and deep boreholes indicate a low altitude nature of the basin. In addition, due to the less variability in the stable isotopic composition typifying the basin, it is considered that monsoonal rainfall derived from the south (Atlantic Ocean) was most likely the source of precipitation recharging the LCB. The groundwater samples are subjected to various degree of evaporation and as such exhibited some variation in stable isotopic composition and distribution along the LMWL. Considering the size and altitude of the study area, the major process that may yield any significant note in the isotopic composition of the rainfall depends on its amount and intensity.

Therefore, the mean annual rainfall of about 1 800 mm in the study area could have produced the relatively depleted isotopic signature preserved in the shallow groundwater. From Figure 6.2, it can be deduced that the groundwater originated essentially from local rainfall, and variation in its isotopic composition may be related to the prevailing climatic conditions. Furthermore, in the wet season, the spatial distribution of isotopes in some of the groundwater (Figure 6.2 and Table 6.1) reflects isotopic signatures similar to those found in the lagoon water samples. This similarity, besides the similar d-excess values, suggests a common recharge source (precipitation) for both the lagoon and groundwater and may also indicate that the lagoon acts as a notable source of recharge to the groundwater in parts of the basin. In comparison, the expected relative depletion in $\delta^{2}H$ and $\delta^{18}O$ values characterising the deep confined aquifers and its plot along the LMWL indicates precipitation from a mixed moisture source as the main source of recharge but under conditions different from the

modern climatic conditions. Moreover, the intermixing in values of δ^2H and $\delta^{18}O$ between the deep aquifer and a few samples from the shallow aquifer (Figure 6.2) may suggest either that the concerned shallow groundwater (relatively isotopically depleted) is a mixture of young and old water (low tritium) preserved in relatively impermeable sediments; or upconing due to over-exploitation, which allows older water to move upgradient; or aquifer recharged by younger but poorly tritiated rainwater.

Table 6.3: Analytical results for tritium and carbon in water samples of the study area

Sample ID*	Tritium (TU)	^{14}C (Percentage modern carbon)	Mean residence time ^{14}C (year)	^{13}C (‰)
Shallow groundwater (GW)				
GW2	1.7 ±0.3	78.8 ±2.4	1 950 ±10	-17.86
GW5	2.8 ±0.3	-	-	-
GW6	1.7 ±0.3	-	-	-
GW7	1.1 ±0.3	78.9 ±2.4	1 950 ±10	-12.79
GW8	1.3 ±0.3	66.9 ±2.2	3 350 ±10	-22.95
GW9	1.8 ±0.3	-	-	-
GW10	2.2 ±0.3	-	-	-
GW13	0.2 ±0.2	59.1 ±2.2	4 350 ±10	-15.32
GW17	1.7 ±0.3	72.7 ±3.1	2 650 ±10	-12.99
GW18	1.5 ±0.3	74.5 ±2.3	2 450 ±10	-12.56
GW25	0.9 ±0.3	81.6 ±2.4	1 700 ±10	-20.51
GW27	1.4 ±0.3	-	-	-
GW28	1.2 ±0.3	-	-	-
GW30	1.8 ±0.3	83.4 ±2.4	1 500 ±10	-
GW32	1.2 ±0.3	-	-	-
GW33	1.1 ±0.3	88.0 ±2.4	1 050 ±10	-
GW37	0.1 ±0.2	-	-	-
GW40	1.7 ±0.3	-	-	-
Deep groundwater (DGW)				
DGW1	0.3 ±0.2	26.3 ±0.23	10 720 ±70	-19.34
DGW2	0	22.7 ±0.23	11 900 ±81	-19.55
DGW3	0.0 ±1.2	28.2 ±0.21	10 180 ±60	-18.19
DGW4	0.2 ±0.2	22.4 ±0.19	12 030 ±69	-21.26
DGW5	0.3 ±0.2	39.8 ±0.25	74 00 ±50	-21.38
Rainwater (RW)				
RW1	2.2 ±0.3	-	-	-
Surface water (SW)				
SW1	1.7 ±0.3	-	-	-
SW3	2 ±0.3	-	-	-
SW2	1 ±0.3	-	-	-

6.3 Tritium content

Tritium (^{3}H) has been reliably employed to distinguish groundwater recharge during the pre-bomb time from younger water (Clark and Fritz, 1997). Its variation provides an insight into local recharge and circulation mechanisms. Sequel to the thermonuclear test of the early sixties that injects ^{3}H into the atmosphere, the tritium content in precipitation increased a thousand-fold, especially in the northern hemisphere. Since 1963, the peak tritium concentration has decreased to natural values in winter and about double the natural value in summer. This event consequently affected the groundwater tritium content as aquifers are being recharged. Therefore, ^{3}H content can often be used to determine dates *ante quem* and *post quem*. However, this research study adopted the tritium values documented at the Cotonou GNIP–IAEA stations (O1–NATITINGOU/6539100, O1–COTONU/6534403 and O1–KANDI/6530600) over a period of 13 years (2005–2018) as the basis for its interpretation. In these years, tritium values were partially captured in 2012, 2014 and 2016 hydrological years. For all the stations, the minimum value of 1.08 TU was recorded in 2012, while 3.5 TU was the maximum value documented in 2016. The general mean tritium values for the years ranged from 1.8 to 3.15 TU. Similarly, Loehnert (1988) reported a tritium value of 2 TU for rainwater during the August break in parts of Southwestern Nigeria, which was in good agreement with the GNIP–IAEA Cotonou stations. Based on the above, it may be proposed for the area under study, and the entire Dahomey Basin at large, that waters having a $^{3}H>1$ TU, are considered a mixture of recent waters with a low ^{14}C, while water with $^{3}H<1$ TU are relatively older waters or a mixture of old and recent recharged water. The analytical result of tritium and carbon content in the shallow unconfined aquifer, deep aquifer, surface water as well as rainwater is presented in Table 6.3, while Figure 6.4 reveals possible interaction in the hydrological system of the basin.

The tritium values ranged from 0.1 TU to 2.8 TU for the unconfined shallow groundwater; 0.0 TU to 0.3 TU for the confined deep groundwater; 1.7 TU to 2.0 TU for surface water and 2.2 TU for a single rainwater sample (Table 6.3). Therefore, rainwater and surface water with a tritium composition value of >1 TU recorded for this study, may be considered as modern water. The shallow groundwater data, however, apparently reveals clustering into two distinct groups, consisting of a group of relatively young immature shallow groundwater having a tritium value of >1 TU, and an older group of more mature or admixture of old and recent recharge groundwater with a value of <1 TU (Figure 6.4). The young shallow groundwater includes all the samples, the exception being GW13 and GW37, with extremely low tritium

values. The anomalous occurrence of low tritium shallow groundwater, GW 13 and GW 37 (Table 6.3), represents mixture of more mature old recharge shallow groundwater. This scenario may be explained by either a probable mixture of recent water with low tritium content water or due to the presence of relatively impermeable sediments, which increases the residence time and enables the decay of the tritium. An additional possibility to the above is that the aquifer was recharged by younger low tritium containing rainwater (Kehinde, 1993; Yusuf et al., 2018).

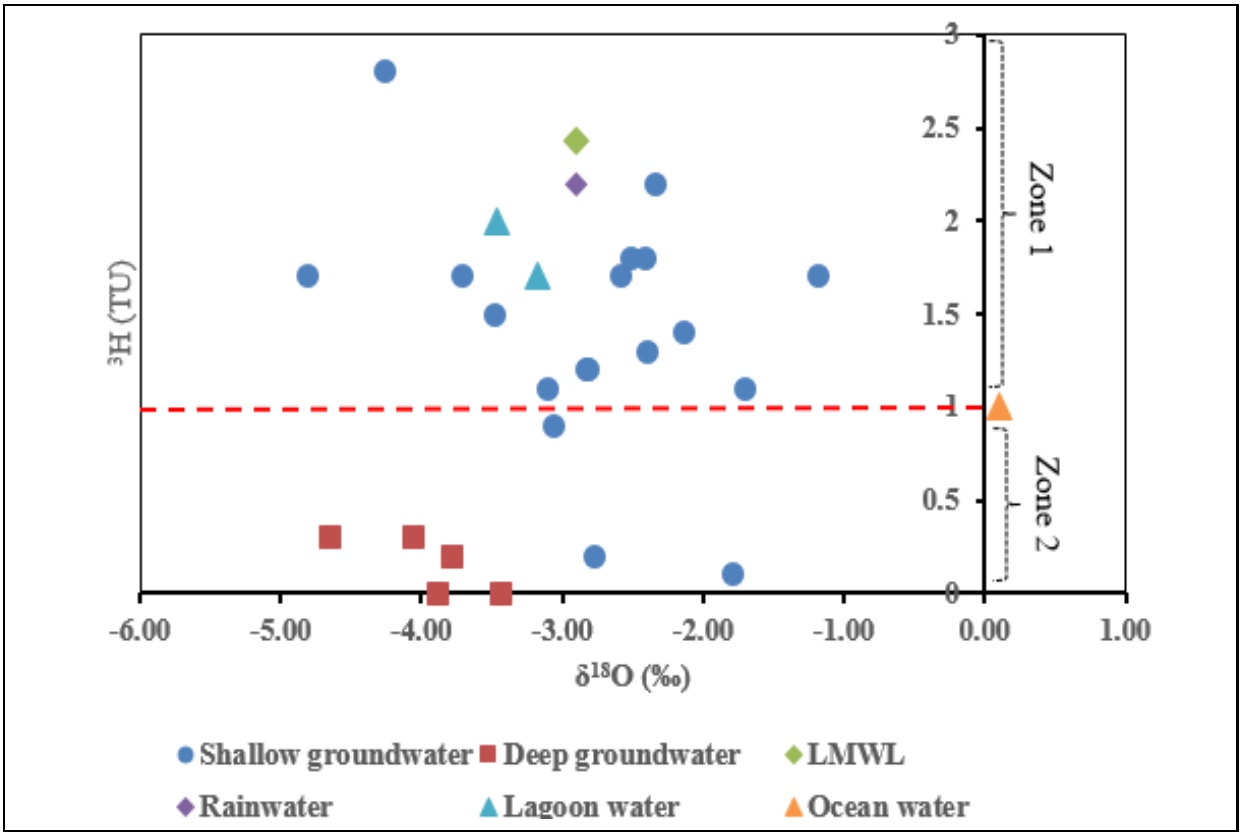

Figure 6.4: Plot of ^{3}H vs $\delta^{18}O$ (‰), differentiating groundwater into old water and young water

In addition, shallow groundwater and surface water appear to be a proper mixture of infiltrated rainwater with tritium contents close to the mean precipitation. This is evidenced by the occurrence of rainwater, surface water and the shallow groundwater in Zone 1 as observed in Figure 6.4, which suggested possible interactions between the water bodies. However, the deep groundwater occurrence at Zone 2 revealed a total disconnection from the surface water and rainwater. The few shallow groundwater occurrences in Zone 2 suggested possible but limited interaction between old water and young recharge water (Figure 6.4). The varying tritium concentrations may either depict variable residence times or infiltration with variable tritium content into the aquifer (Kehinde, 1993; Yusuf et al., 2018).

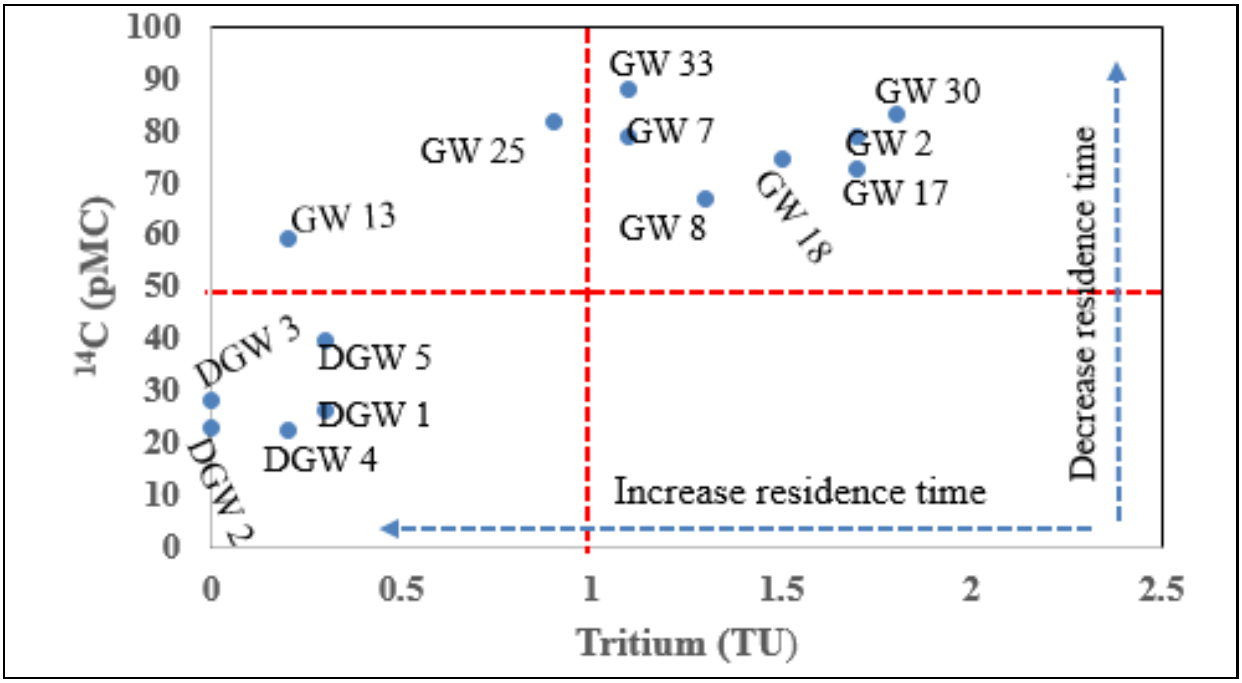

Figure 6.5: Plot of ^{14}C vs ^{3}H for groundwater in the study area

Generally, the concentration of ^{3}H in the aquifer systems decreases with depth and eventually becomes non-detectable in parts of the deeper aquifers (>180 m) (Table 6.4; Figure 6.5). This may be indicating an increase in the residence time in the deeper aquifer. According to Abiye (2013), groundwater samples with a near-zero tritium value have been in circulation for a long time (>50 years) and are not derived from present-day rainfall in Southern Africa. This assertion is similar and agrees well with the observed scenario in the deep aquifer of the study area and, thus, recharge could be derived from rainfall different from the present-day climatic conditions.

6.4 Carbon-14 and ^{13}C

Dating of groundwater with radiocarbon cannot be carried out directly on the water molecules but is dependent on the dissolved inorganic carbon and dissolved organic carbon in water. These dissolved carbon constituents get into the groundwater from atmospheric CO_2 through the soil zone. The carbon isotopes of ^{13}C and ^{12}C are essential and vital tools to quantify the interactions between water and rock in the case of ^{14}C age determination of groundwater. The carbon isotopes were carried out in the study area to establish an input function for dating groundwater and unravelling the source of carbon in the basin (Table 6.3). The increment in the natural concentrations of both carbon-14 and tritium in waters resulted from the thermonuclear testing in the early 1960s and, therefore, elevated concentrations of

^{3}H and ^{14}C in groundwater indicate recent recharge. The carbon-14 content, however, decreases in old water through radioactive decay and, hence, making it a useful residence time determination tool, while Carbon-13 determination is useful in the identification of the origin of carbon in groundwater (Loehnert 1988). The measured ^{13}C values vary between -22.99 ‰ and -12.56 ‰ for the shallow aquifer. The observed depletion in ^{13}C concentration in both the shallow unconfined groundwater and the deep confined groundwater may probably be due to secondary CO_2 producing reactions (Vogel and Ehhalt, 1963; Mook, 1976; Kehinde, 1993) such as carbonate weathering and cation exchange processes as the major factors of carbonate geochemistry within the coastal aquifer. The carbonate weathering is suggested as a result of calcite dissolution from the Cretaceous Ewekoro limestone. Carbon-13 values, however, become less variable with depth and vary from -21.38 ‰ to -18.19 ‰, suggesting that the effects of interactions between carbonates and organic matter on $\delta^{13}C$ have become stable or balanced at a deeper depth (Table 6.3). In addition, the depletion of ^{13}C values connotes little or no marine carbonate rock, with enriched ^{13}C values available for dissolution in the subsurface (Mazor, 1991).

Concerning carbon-14 activity, it was found to vary from 59.1 to 88.0 pMC for groundwater from the shallow interstitial aquifer. In the recently recharged water, the ^{14}C content is expected to be close to or above 100 % because ^{14}C is derived from the soil CO_2 and is likely to contain bomb ^{14}C. The moderately ranged activity of ^{14}C observed in the basin's shallow groundwater is indicative of young and locally recharged sources of water that is not very high in ^{14}C content. According to Dorr et al. (1987), the ^{14}C content of shallow groundwater ranges from 90 pMC to about 50 pMC, depending on the local condition of carbonate dissolution. Murray et al. (2015) identified two groups of water for the study area: The first group is shallow and recently recharged groundwater with ^{14}C values between 74 pMC and 94 pMC, comprising GW 2, GW 7, GW 17, GW 18, GW 25, GW 30, and GW 33. The second is a mixed group identified with intermediate ^{14}C values varying from 50 pMC to 70 pMC, entailing GW 8 and GW 13 samples. However, in the confined deep groundwater, the ^{14}C values ranged between 22.4 pMC and 39.8 pMC (Table 6.3). The highest ^{14}C concentration value of 39.8 pMC corresponds with the shallowest borehole depth of 185 m at DGW 5, while the DGW 4 with a depth of 355 m recorded the least value of 22.36 pMC for ^{14}C activity, indicating a decrease in ^{14}C content with an increasing groundwater depth. In summary, a decrease in ^{14}C activities connotes an increase in mean groundwater ages with depth.

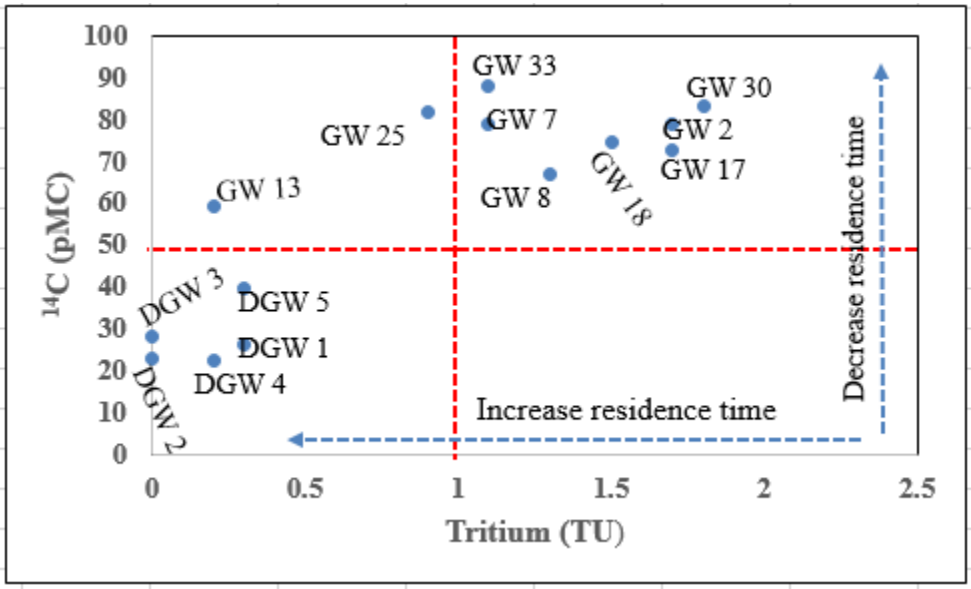

Figure 6.6: ^{3}H–^{14}C relation of selected deep and shallow groundwater samples in the Lagos Coastal Basin

Also, based on carbon-14 and carbon-13 contents, most of the samples lacked evidence of mixing; indicating that variation in the activity of carbon-14 is essentially due to radioactive decay and represents the true residence time of groundwater. Furthermore, diffusion of CO_2 gas from the unsaturated zone to the groundwater could also affect the measured carbon activity in water (Fontes and Edmunds, 1989; Le Gal La Salle et al., 2001). When diffusion occurs, modern CO_2 increases carbon-14 activity of groundwater and consequently reduces the estimated groundwater residence time (Le Gal La Salle et al., 2001). Diffusion is known to occur in modern groundwater with high pH, where the dissolution of CO_2 gas is enhanced (Stumm and Morgan, 1981; Fontes and Edmunds, 1989). Thus, the low pH characterising the study area suggests that the diffusion process does not affect the estimated carbon-14 activity. Similarly, the relative correlations agreement between tritium and carbon-14, namely high ^{3}H occurrence, led to high ^{14}C occurrence and vice versa (Figure 6.6). This further suggests that a carbon-14 signature remains unmodified and still reflects the groundwater renewal rate. In comparison, the ^{14}C values are relatively higher in shallow groundwater samples within a range of 59.1±2.2 pMC to 88± 2.4 pMC, compared to the deep aquifer within a range of 22.4±0.19 pMC to 39.8±0.25 pMC, resulting in a MRT ranging from 4350±10 to 1050±10 years for shallow groundwater and 12030±10 to 7400±10 years for deep groundwater.

Furthermore, in an attempt to gain an insight into the climatic conditions under which the deep aquifer recharge occurred, this research study proposed the use of temperature correlation method as stated below:

i. Retrieval of the available air temperature and stable isotope of ^{18}O data between 2005 and 2012 from the Cotonou GNIP–IAEA station (GNIP/M/BJ/O1–COTONU/6534403).

ii. Oxygen-18 values plotted against the corresponding air temperature of the present-day climatic conditions (Figure 6.7).

iii. From the graph, the relationship between temperature and the stable isotope of ^{18}O was established by the equation Y = Xt–C; where Y represents ^{18}O', where X means relationship gradient, t means unknown temperature and C means the intercept.

From the above relationship, the recharge temperature of the deep aquifer could be deduced by substituting the relevant deep groundwater data as defined by Equation 6.6:

$$t = \frac{Y + C}{X} \quad \ldots\ldots\ldots\ldots\ldots\ldots\ldots\ldots \quad 6.6$$

Based on the above temperature correlation for precipitation in Cotonou, the recharge temperature of the deep confined aquifer was calculated using Equation 6.7.

$$\delta^{18}O = 0.54 * t – 17.6 \text{ ‰} \quad \ldots\ldots\ldots\ldots\ldots..6.7$$

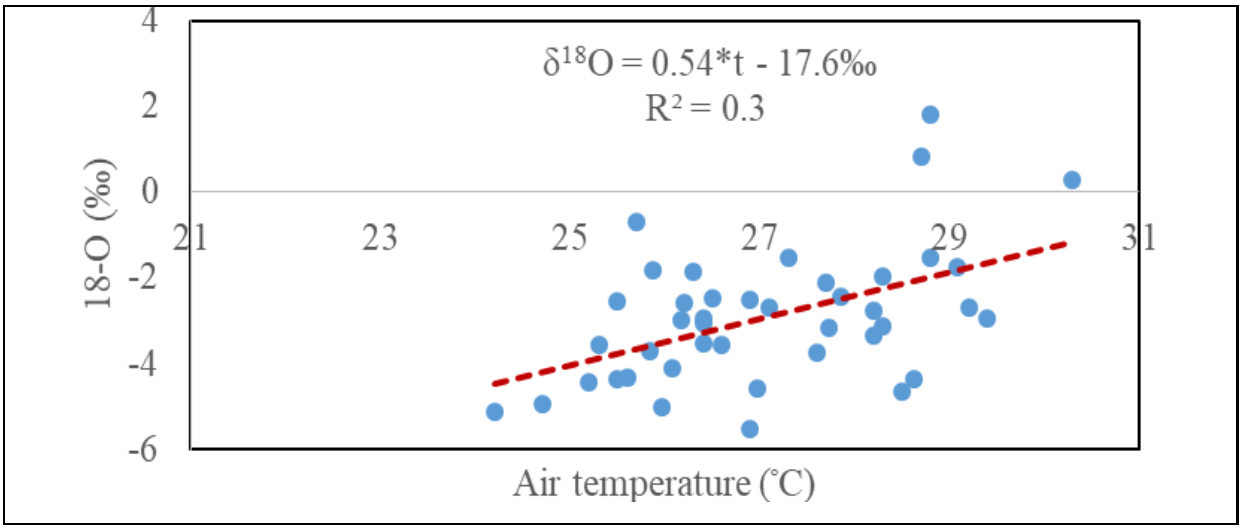

Figure 6.7: The ^{18}O relationship with air temperature

The calculated ambient temperature during rainfall that generated recharge, reveals a variation in the shallow aquifer (Table 6.1), where high temperatures ranging between 11 °C and 17.4 °C (average 13.41 °C) were recorded, with the exception of a few samples: GW 5 (9.1 °C); GW 14 (9.8 °C); GW 17 (8.8 °C); GW 36 (9.7 °C); and GW 40 (10.2 °C). The exceptional low-temperature occurrence in parts of the shallow aquifer may be related to mixing of the deep-seated old water with young water through excessive abstraction, whereas

lower recharge temperatures that vary from 8.3 °C to 10.7 °C (average 9.7 °C) documented for the deep aquifers could be indicating recharge occurrence under more humid climatic conditions. The above assumption is further substantiated by Figure 6.8 and Figure 6.9 differentiating the recharge period based on ^{18}O and ^{14}C content; annual temperature (T °C) and the ^{14}C age of deep aquifers and selected samples from the shallow aquifer.

Based on the globally adopted geological time scale, the boundary between the Holocene and Pleistocene is set at 12500 years from the present, which is equivalent to the ^{14}C values of 22±1.7 pMC. Based on the ^{14}C data, groundwater recharge into the shallow groundwater took place in the Holocene, with relatively warm climatic conditions. In contrast, the deep aquifer recharge occurred partly between Late Pleistocene and early Holocene. The depletion of $\delta^{18}O$ in the deep groundwater samples may be explained by a significant contribution of Late Pleistocene recharge from cold climatic conditions (Figure 6.9). On the other hand, warm temperature was linked to isotope enrichment in recharging water in the Holocene (Figure 6.8). This signifies loss of rainwater through evaporation and less availability of water for recharge due to an increase in ambient temperature. In general, the shallow groundwater experienced recharge under present climatic conditions and thus remains renewable. In contrast, the deep aquifers were recharged under the last humid period and, by implication, recharge nowadays rarely reaches the deep aquifers. Therefore, the deep aquifer is subjected to gradual depletion with continued groundwater abstraction without replenishment.

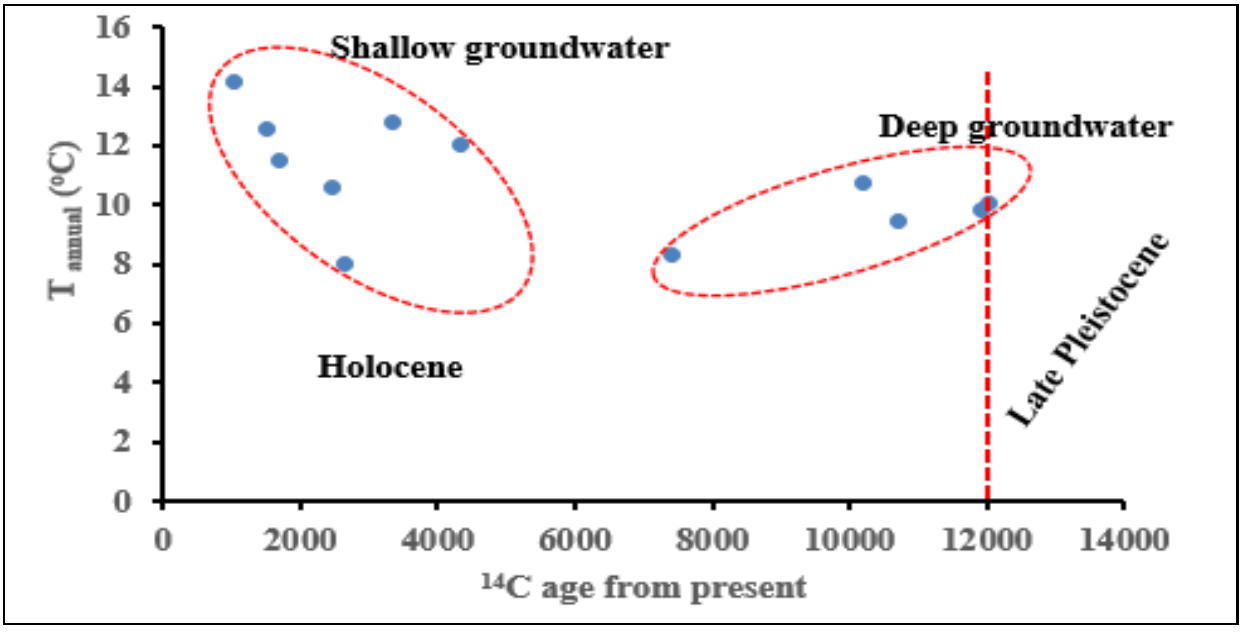

Figure 6.8: Plot of annual temperature variation vs ^{14}C ages during Holocene and Pleistocene for groundwater in the study area

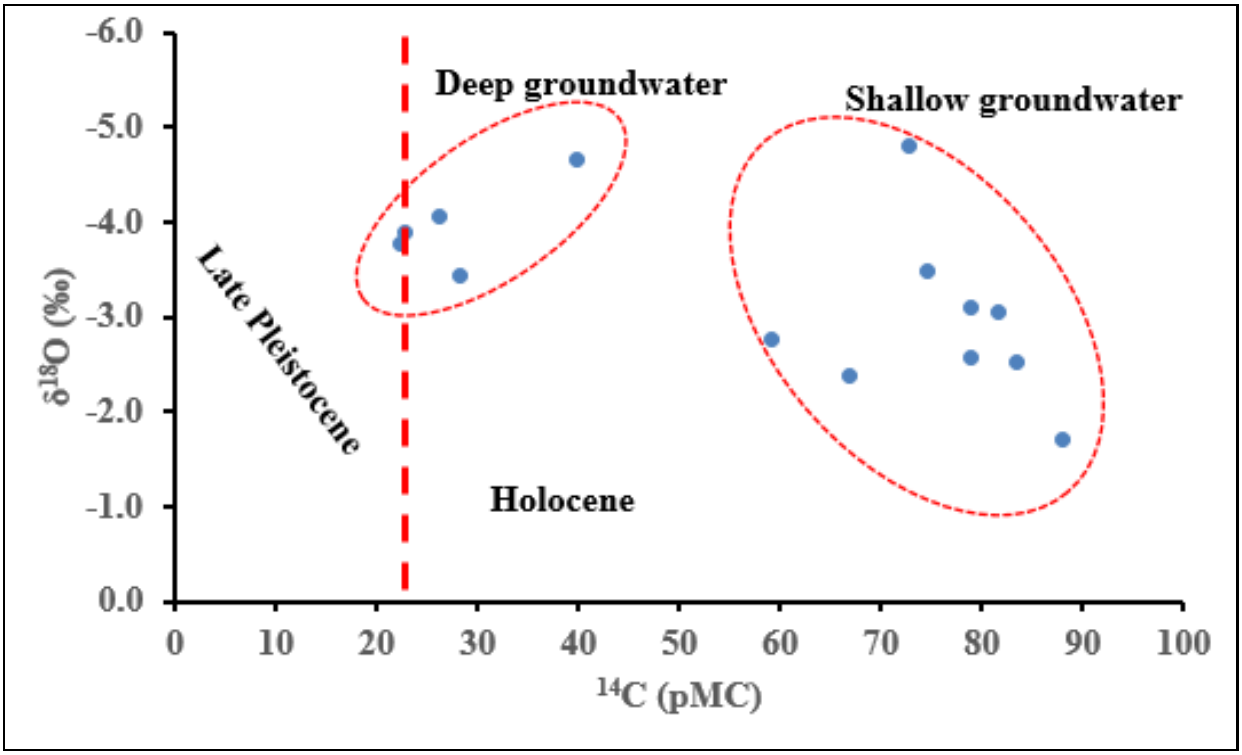

Figure 6.9: Plot $\delta^{18}O$ (‰) vs ^{14}C activity (22 ± 1.7 pMC) as Holocene and Late Pleistocene boundary for groundwater in the study area

Chapter 7

HYDROCHEMISTRY OF THE SHALLOW GROUNDWATER AQUIFER IN LAGOS COASTAL BASIN

7.1 Introduction

The hydrochemical signatures of groundwater resources, both in time and space, are essentially influenced by the characteristics of their catchment area, hydrochemical processes and aquifer composition (Oke, 2015). The key factors that drive variations in hydrogeochemistry involve both geogenic and anthropogenic factors. The natural (geogenic) process includes but is not limited to, redox transformation, complexation, ion exchange, dissolution and precipitation, rock–water interaction, intermixing of water bodies (saline water and freshwater) and many others which are site-specific (Drever, 1997; Schwartz and Zhang, 2003). On the other hand, the artificially induced (anthropogenic) factors are mainly related to industrial activities, urbanisation, landfills, and aquifer over-exploitation (Appelo and Postma, 2005). Physicochemical and hydrochemical analyses are excellent tools to decipher the source of mixing in groundwater and surface water systems (Clark and Fritz, 1997; Appelo and Postma, 2005). Coastal aquifer salinisation is mostly due to seawater intrusion; however, other factors could influence the quality of groundwater that are related to geochemical processes and anthropogenic impacts, and hence, the importance to differentiate the sources of salinisation and behaviour of the aquifer to minimise the vulnerability of an aquifer to pollution (Han et al. 2014).

Owing to the fact that the LCB is characterised by high population density, coupled with increasing industrial development and the peculiar hydrogeochemical nature, necessitated detailed hydrochemical investigation, and establish its state of pollution besides its protection potential. More importantly, the vast majority of the low-class populace in and around the basin obtain water from the coastal aquifer. Thus, the physicochemical parameters of shallow groundwater along the coastal strip of the LCB were measured to understand the pollution status and possible interactions between these resources. It is worthy to mention that additional data for brackish surface water (P-SW 1, P-SW 2 and P-SW 3) was obtained from a study by Yusuf et al. (2014), only for its physical parameters and major ions content towards deducing the relationship between groundwater and the surrounding surface water.

In this research, the study area was divided into three segments for ease of identification and clarification (Figure 7.1).

Starting from the western segment – jointly known as Apapa and denoted by 'App' – the study area included samples GW 1 to GW 7 (the Apapa, Ajegunle, Ajeromi, Wharf, Ijora, and Badia areas) and terminated by the Lagos lagoon to the east and bordered by the creek to the south. The central parts – collectively referred to as Island and denoted by 'Isl' – constituted samples GW 8 to GW 19, GW 21, GW 37, GW 38, GW 39 and GW 40 (the Island, Ikoyi, Obalende, Lekki and Ajah areas). The eastern parts – generally described as Etiosa and represented by 'Eti' – made up the remaining samples from GW 20 to GW 45, except for the occurrence of GW 21, GW 37 to GW 40 in the series (the Igbo efon, Awoyaya, Badore, Awoyaya, and Sangotedo up to Ibeju Lekki areas). It is to be noted that the central and eastern parts of the study area are a land tract located between the ocean and the Lagos lagoon; it is encompassed by the lagoon in the north and west and the ocean in the south. It is also worthy to mention that the water samples under investigation are essentially water from the surficial aquifer collected mostly through large-diameter hand-dug wells, essentially <10 m deep, with the exception of a few borehole samples such as GW 7 (BH 1), GW 13 (BH 2), GW 23 (BH 3), GW 28 (BH 4), and GW 33 (BH 5), with an estimated depth range of ≤15 m. The shallow dug wells were more focused on this research being the most vulnerable to contamination and their relative function (most exploited) to the dominant low-income inhabitants. A summary of the physicochemical, major ions and bacteriological data from the groundwater and surface water is presented in Table 7.1 and Table 7.2, while the detailed analytical results for the wet and dry seasons are presented in Appendices E and F. The summary tables (Table 7.1 and Table 7.2) contain statistical results for the minimum, maximum and mean concentrations.

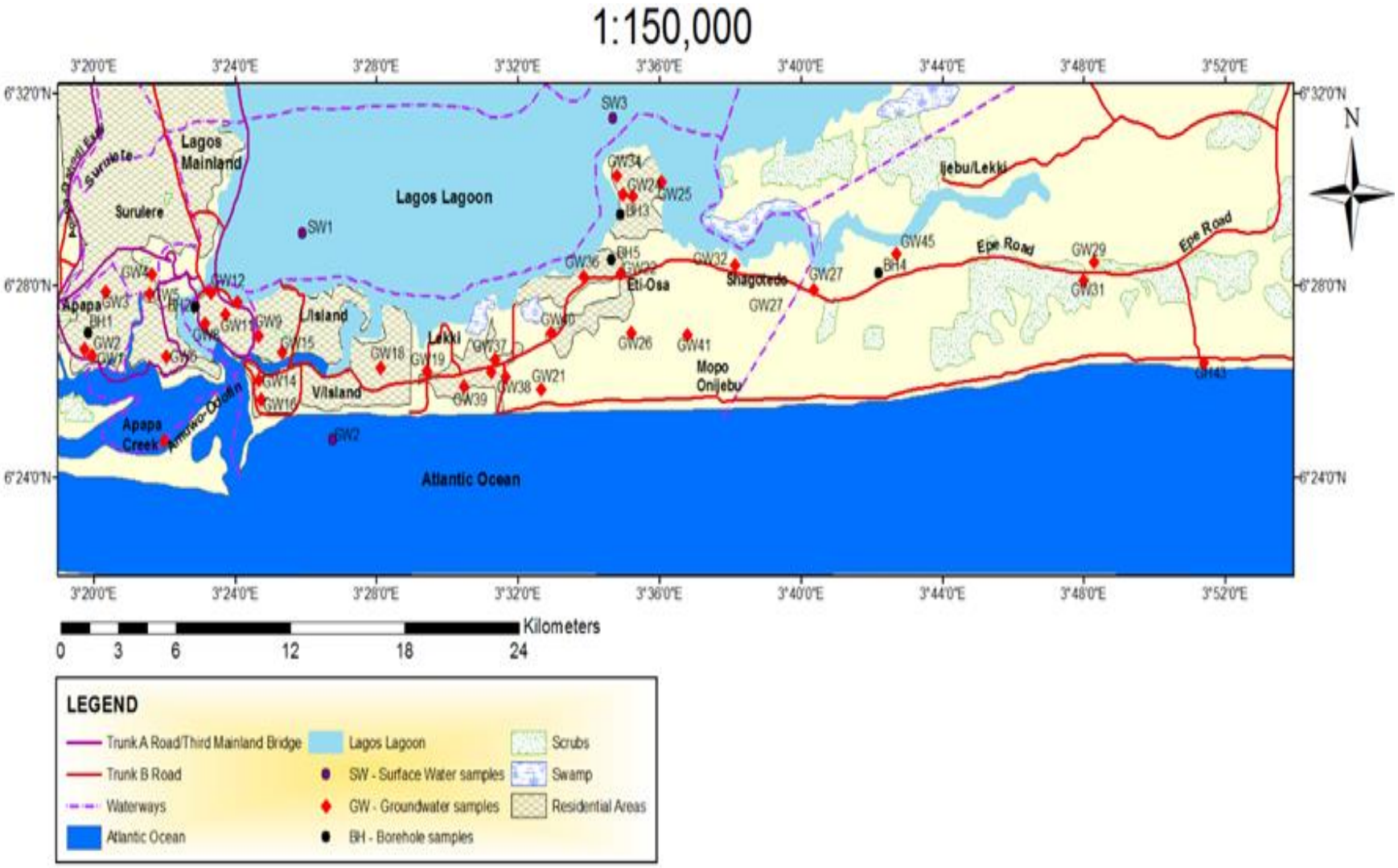

Figure 7.1: Location map of the study area showing the sampling points for hydrochemical analysis

Table 7.1: Summary of physicochemical, major ions, microbial population in groundwater obtained for the wet and dry seasons in the study area

Parameters	Wet season			Dry season			WHO(2018), SON* (2007)
	Minimum	Maximum	Mean	Minimum	Maximum	Mean	
pH	5.40	8.60	7.26	5.10	8.70	7.40	7.5–8.5
TDS (mg/L)	69.00	1 642.00	458.85	114.00	1 916.00	361.43	500*
EC (µS/cm)	111.00	3 284.00	885.35	142.00	3 832.00	638.93.62	1 000*
Total Hardness as $CaCO_3$	48.00	668.00	199.45	–	–	–	100
Temperature (°C)	26.00	29.50	27.8	27.60	30.70	28.8	
Turbidity (NTU)	0.10	99.80	11.06	–	–	–	5 NTU
Ca^{2+} (mg/L)	0.05	97.13	11.11	8.20	12.80	11.1452	75*
Mg^{2+} (mg/L)	1.29	16.77	5.91	2.44	6.23	3.6995	30
Na^{+} (mg/L)	0.15	14.77	2.42	4.10	9.10	5.4756	200
K^{+} (mg/L)	0.14	23.77	3.04	3.89	9.01	5.7005	50
Cl^{-} (mg/L)	1.00	720.00	110.65	2.50	9.73	4.755	250
HCO_3^{-} (mg/L)	6.10	335.51	101.68	17.00	97.00	67.39	–
CO_3^{2-} (mg/L)	3.00	210.00	51.54	0.80	6.00	3.70	–
NO_3^{-} (mg/L)	<0.001	108.70	22.353	<0.001	0.06	0.025	10
SO_4^{2-} (mg/L)	<0.001	88.00	36.234	0.01	0.21	0.089	200
Faecal coliform/100 ml	2.00	201.00	170.00	–	–	–	Nil

* SON = Standards Organization of Nigeria.

Table 7.2: Summary of physical, bacteriological and macro-element contents of surface water (lagoon and ** ocean) obtained in the study area

Parameters	Minimum	Maximum	Mean	WHO (2018), SON (2007)
pH	7.83	8.25	7.98	7.5-8.5
TDS (mg/L)	2 000	35 040	10 260	500*
EC (µS/cm)	3 999	48 000	24 100.25	1 000*
Temperature (°C)	29.8	32	31.3	
Ca^{2+} (mg/L)	321.28	1 750	1 031.57	75*
Mg^{2+} (mg/L)	1313	5 036	3 868.56	30
Na^{+} (mg/L)	1750	8 675	5 981.13	200
K^{+} (mg/L)	44	294.67	169.17	50
Cl^{-} (mg/L)	2 327	15 582	8965	250
HCO_3^{-} (mg/L)	40	365.94	133.49	
CO_3^{2-} (mg/L)	30	180	76.5	
NO_3^{-} (mg/L)	9.6	245	175.65	10
SO_4^{2-} (mg/L)	102	1862	1 039.25	200
Faecal coliforms/100 ml**	34	1 733	646	Nil

**From present study, *SON (2007) Source: Yusuf et al. (2014)

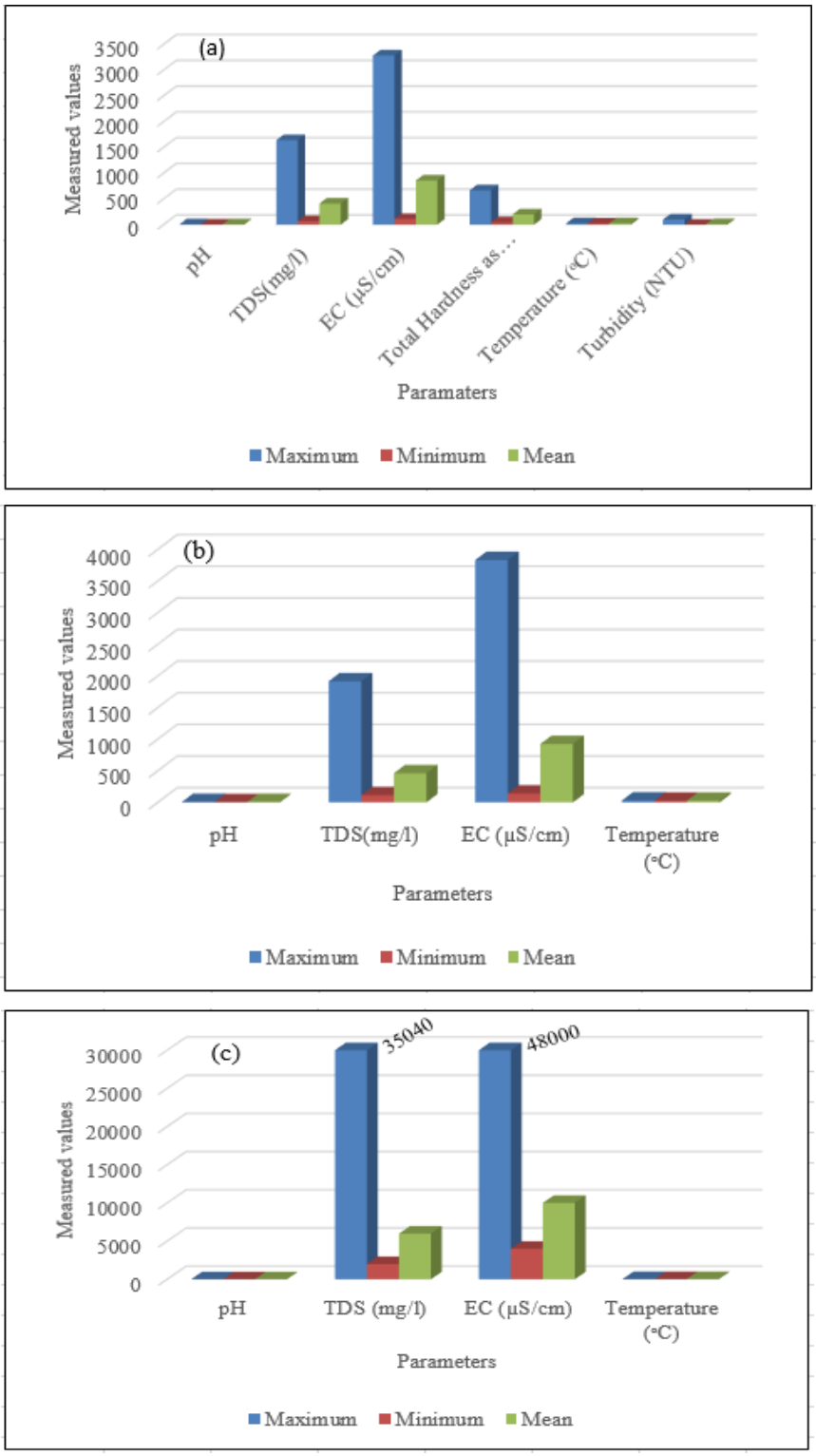

Figure 7.2: Graphical representation of a statistical summary of physical parameters in groundwater: (a) wet season (b) dry season (c) surface waters

7.2 Physicochemical Parameter Evaluation

7.2.1 pH and temperature

The pH values recorded in the analysed groundwater samples ranged from 5.40 to 8.60, with a mean of 7.26; and 5.1 to 8.7, with a mean of 7.22, for wet and dry seasons, respectively. This suggests that the groundwater in the area ranged between a slightly acidic–neutral pH and slightly alkaline. In the surface water, the pH ranged between 7.83 and 8.25, with an average value of 7.98, reflecting near alkaline characteristics of the surface water. A comparison of the pH values for both surface water and groundwater revealed a striking similarity, particularly in the wet season, though the surface water average demonstrated to be slightly alkaline (Table 7.1, Table 7.2 and Figure 7.2a-c). This may be an indication of mixing between the groundwater and surface water (brackish water) or the dissolution of carbonate rocks. The temperatures of the water at the time of the sample collection ranged from 26 °C to 29.5 °C with an average of 27.8 °C and 27.6–30.7 °C, with a mean value of 28.8 °C, in the wet and dry seasons, respectively (Table 7.1; Figure 7.2a and b). This temperature range is low in comparison with the temperature of 70 °C recorded by Onwuka and Amadi (1989) for a borehole at a depth of 750 m in parts of Lagos. Therefore, it may be deduced that the temperature of the present study indicated a shallow aquifer and that the groundwater temperature increases with increasing depth, with an estimated temperature gradient of 0.06 °C/m.

7.2.2 Electrical conductivity

In the groundwater samples, the EC values varied between 111 µS/cm and 3284 µS/cm (average 885.35 µS/cm) for the wet season, and between 114 µS/cm and 3832µS/cm (average 638.93 µS/cm) for the dry season (Table 7.1). The highest values of EC were recorded in the west (App) and central parts of the study area (Isl) in proximity to the lagoon and creek in the north, while the lowest value was documented in the eastern segment (Eti) and towards the south (Figure 7.3 and Figure 7.4). This may be indicating the influence of surface water with the fresh groundwater through bank infiltration, flash floods or surface run-off as it flows towards the Ocean. In surface waters, the expected highest occurrence value of 48000 µS/cm was recorded for the seawater, while a steady value of 3999 µS/cm was documented in the lagoon at P-SW 1, P-SW 2 and P-SW 3 which might be due to the upper specification limit of the equipment used during the field campaign (Table 7.2).

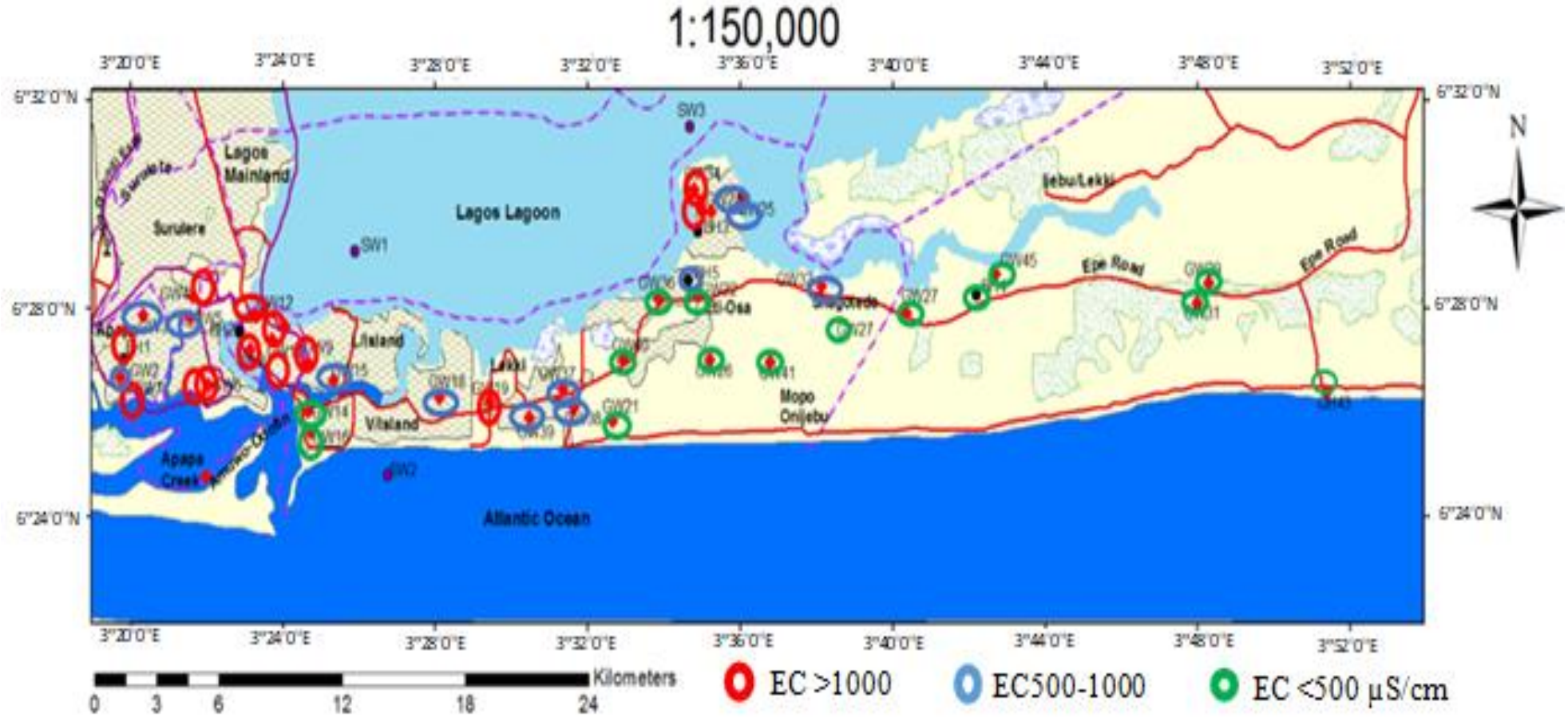

Figure 7.3: Spatial distribution map of electrical conductivity in groundwater

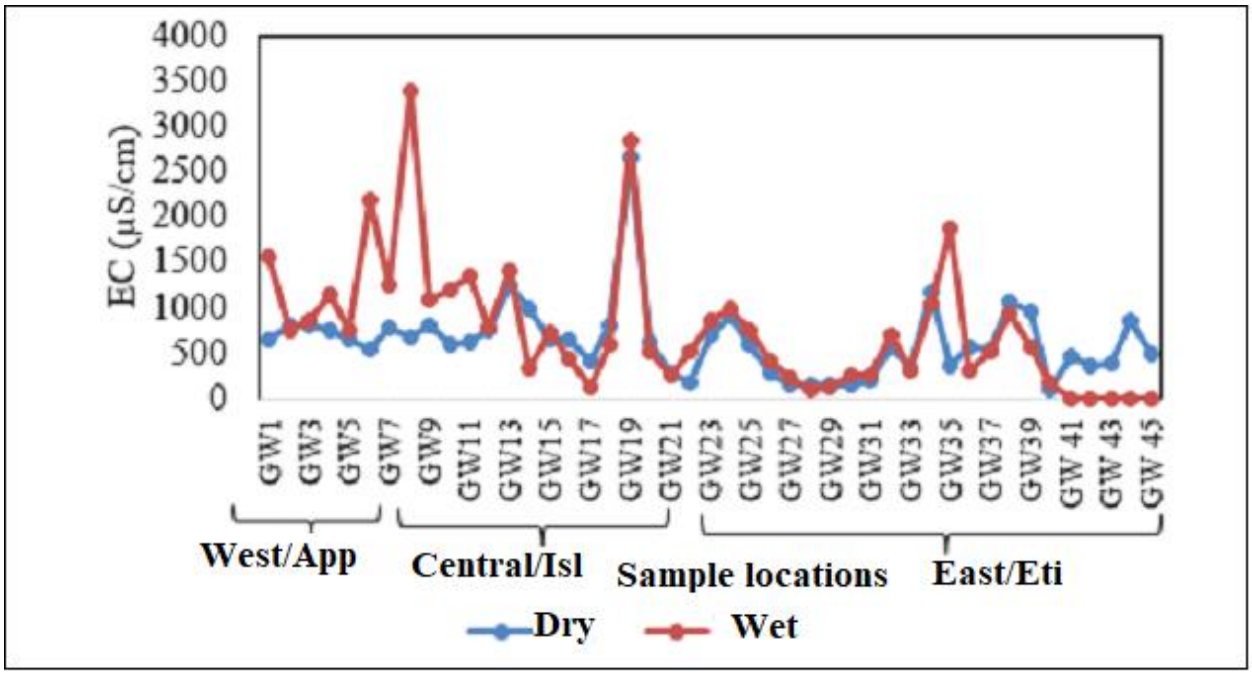

Figure 7.4: Graphical representation of electrical conductivity trend from west to east in groundwater

7.2.3 Total dissolved solids

In the study area, the TDS value varied from a minimum of 69 mg/L to a maximum of 1642 mg/L (average 458.85 mg/L) in the wet season, while during the dry season it varied from 114 mg/L to 1324 mg/L (average 361.45 mg/L) (Table 7.1). The high concentration of TDS in the groundwater samples reflects that the water was not entirely fresh and may be related to water–rock interaction, rainwater chemistry, ion exchange (clays and sandy clay lenses) and probably anthropogenic sources that will be discussed in detail at a later stage. The TDS exhibited a similar pattern of higher occurrence in the west and central parts of the study area (Figure 7.5).

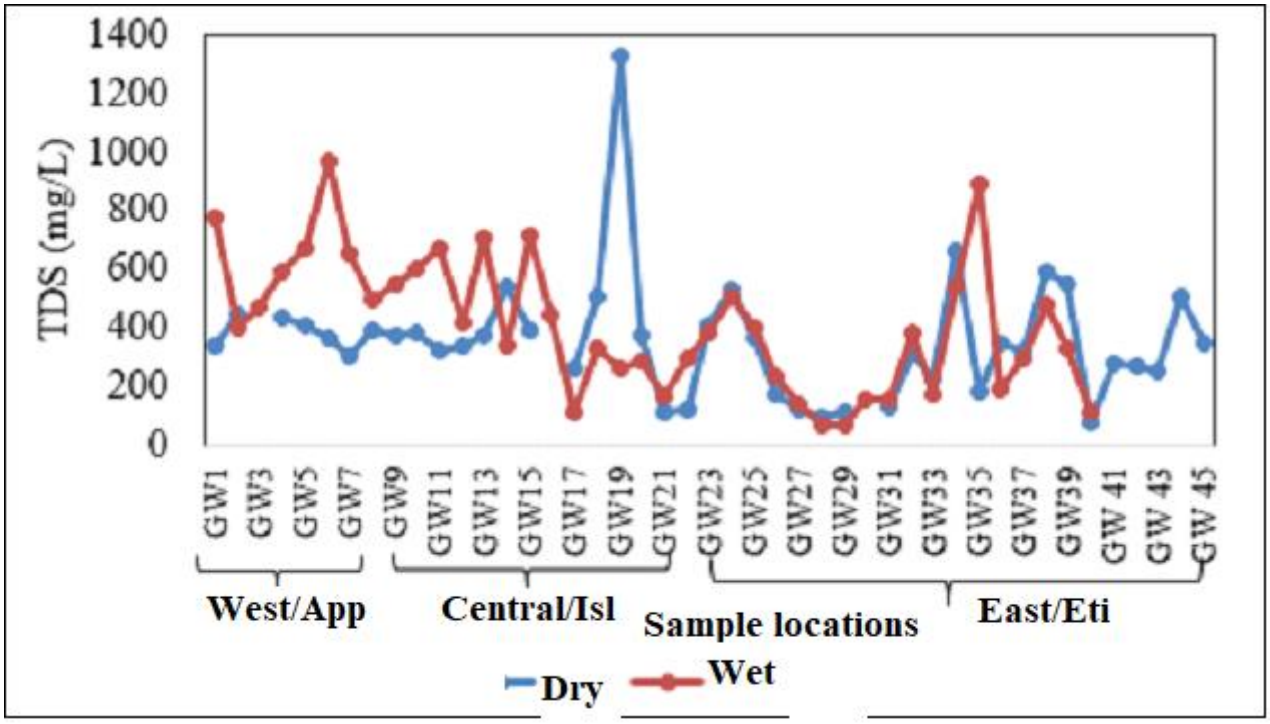

Figure 7.5: Total dissolved solid distribution (west to east) in groundwater across the study area

7.2.4 Microbial counts

Table 7.1 and Table 7.2 also contain the total viable plate counts obtained for both groundwater and surface water samples in the wet season. The microbial content is higher in the shallow large diameter wells than in the protected boreholes. According to Ocheri et al. (2014) high faecal coliform is often associated with the sanitary condition of the environment of the wells. Thus, the sources of pollution could be traced to pit latrines, indiscriminate waste disposal, poor urban planning, and groundwater interaction with contaminated surface waters. Although both surface water and groundwater were considered polluted based on the microbial counts, the surface water is more polluted than the groundwater as demonstrated by the higher average microbial count occurrence. The ratio of the microbial count in surface water relative to the groundwater was four times higher. This implies that the surface waters are more prone to pollution and deterioration than the groundwater.

7.3 Major Ion Chemistry

Calcium is the predominant cation found in the groundwater of the study area. The Ca^{2+} values varied between 0.05 mg/L and 97.13 mg/L (average 11.11 mg/L) for the rainy season and from 8.2 mg/L to 12.8 mg/L (average 11.15 mg/L) in the dry season (Table 7.1; Figure

7.5). Though the average values are almost equal for both seasons, higher individual values were noted for the dry season. Furthermore, the variation in the Ca^{2+} concentration recorded for both seasons could be indicating the differential dissolution of carbonate rocks and ion exchange processes. The Mg^{2+} concentration varied from 1.29 mg/L to 16.77 mg/L (average 5.91 mg/L) for the wet season, and from 2.44 mg/L to 6.23 mg/L (average 3.7 mg/L) for the dry season. The observed higher magnesium value (Mg^{2+} >Ca^{2+}) exhibited in the wet season with a Ca^{2+}/Mg^{2+} ratio of <1 in 75 % of the groundwater samples, with the exception of GW1–5, 14, 16–18, 30 and 38) may be due to marine influence (Appendix H). The Na^{+} concentration in the wet season varied between 0.15 mg/L and 14.77 mg/L (average 2.42 mg/L), and in the dry season from 4.10 mg/L to 9.10 mg/L (average 5.47 mg/L). The higher values recorded in the dry season may be attributed to the evaporation effect, leaching of salt or ion exchange between the aquifer material (clayey sand) and the solution. The K^{+} values varied from 0.14 mg/L to 23.77 mg/L (average 3.04 mg/L) in the wet season, and from 3.89 mg/L to 9.01 mg/L (average 5.7 mg/L) in the dry seasons. The potassium concentrations demonstrated a similar pattern with sodium exhibiting a higher average value in the dry season relative to the wet season (Table 7.1; Figure 7.5). The order of cationic abundance for both seasons is as follows: Ca^{2+} > K^{+} > Na^{+} > Mg^{2+} and Ca^{2+}> Mg^{2+} > K^{+} > Na^{+} for the respective dry and wet seasons. The unusual high average concentration of K^{+} than Na^{+} in groundwater may be related to leaching of the clay minerals, since the aquifers are hosted in the sand and clayey sand deposits essentially characterised by clay matrixes (Yusuf and Abiye, 2019), or it may also be related to parts of different transported materials brought from the upstream to sand-fill the study area during land reclamation (an ongoing process in parts of the study area) and subsequently washed into the aquifer.

The dominance of anions in the study area for the seasons was as follows: Cl^{-} > HCO_3^{-} > SO_4^{2-} for the wet season and HCO_3^{-} > Cl^{-} > SO_4^{2-} for the dry season. Bicarbonate was the dominant anion with concentrations varying from 6.1 mg/L to 335.51 mg/L (average 101.68 mg/L) for the wet season, and 17 mg/L to 97 mg/L (average 67.39 mg/L) for the dry season. Similarly, the CO_3^{2-} dissolution varied from 3 mg/L to 210 mg/L (average 51.54 mg/L) for the wet season, and from 0.8 mg/L to 6.0 mg/L (average 3.7 mg/L) the dry season (Table 7.1; Figure 7.6). While bicarbonate was the abundant anion in all sampled groundwater, it was, however, in some locations equalled by chloride in the wet season, a good pointer to the mixture of water from various sources. The dominance of HCO_3^{-} is an indicator of carbonate dissolution and decomposition of organic matter (Avtar et al., 2013). It

was suggested that the groundwater is in contact with rapidly dissolving carbonate rock which increases the relative concentration of these ions in solution during recharge processes. The hardness of the groundwater, which is a function of calcium carbonate, is reflected in its value ranging between 48 mg/L and 668 mg/L (average 199.45 mg/L) as $CaCO_3$ for the wet season samples.

Chloride was the principal anion and varied between 1 mg/L and 720 mg/L (average 110.65 mg/L) and between 2.5 mg/L and 9.73 mg/L (average 4.76 mg/L) for wet and dry seasons, respectively. The higher chloride concentrations observed in the wet season could indicate marine impact, besides the influence of rainwater, leaching and evaporation processes. Nitrate was also dominant in the wet season relative to the dry season with respective mean concentrations of 22.35 mg/L and 0.0251 mg/L, indicating a higher anthropogenic contribution to the aquifer in the wet season than in the dry season. This is also a reflection of the interaction between the groundwater and highly contaminated surface water which serves as a conveyor belt for all the generated industrial and domestic wastes from the upstream to the Ocean in the downstream direction. A comprehensive study of groundwater quality of the southeastern parts of Lagos between 1999 and 2000 on the impact of urbanization, it was found that in all the sampled wells sulphate, nitrate and chloride were noted at objectionable proportion (Adelana et al., 2003; 2004; 2005). Therefore, the presence of high nitrate concentration particularly during the wet season may be linked to anthropogenic activities. Similarly, the concentration of sulphate was also higher in the rainy season than in the dry season (Table 7.1; Figure 7.6a and b), probably related to marine impact due to high-intensity rainfall that enhances flash floods and surface water movement to hand-dug wells or breakdown of organic matter. In addition, an increase in sulphate from fossil fuel combustion has been observed in precipitation over the LCB (Aderogba, 2012). Therefore, atmospheric deposition of sulphate through rainfall in such an urbanised and industrial area of study may have caused the aquifer signatures in the wet season.

In surface water, it is important to state that SW 1, SW 2 and SW 3 are lagoon waters with a significant salinity difference, while SW 4 is the sample from the Ocean and represented only the rainy season samples. Magnesium is the dominant cation in the brackish water, while sodium remains the dominant cation in the ocean. Chloride, as expected, was the predominant anion in both media (Table 7.2; Figure 7.6c).

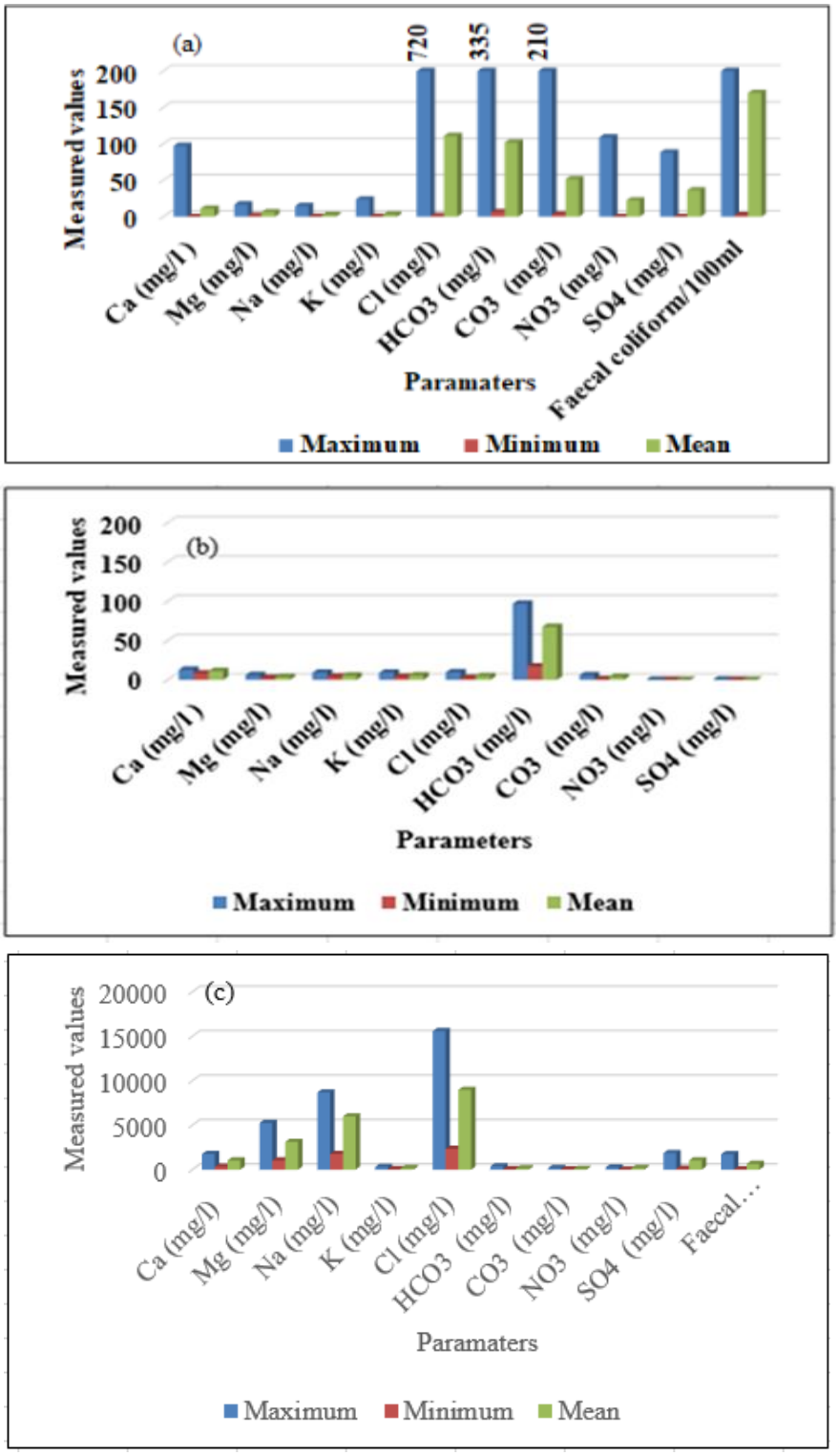

Figure 7.6: Statistical summary of groundwater major ions in (a) the wet season, (b) dry season and (c) surface water

7.4 Metals

Not until recently, attention on the quality of groundwater was focused essentially on dissolved mineral salts. Among the pollutants, organics, and metals have been the subject of

concern because of their long-standing toxicity when exceeding specific thresholds. Trace elements generally exist in small amounts in a natural water system. The source of metals to groundwater may be from different natural and anthropogenic sources. Once liberated into the groundwater, the element distribution repeatedly undergoes modification by complex geochemical and biological processes (Klovan, 1975). The study of metal concentration in groundwater may be used to deduce their possible sources. The trace elements of interest in this study were $Fe^{2+/3+}$, Pb^{2+}, Cu^{2+}, Cr^{2+}, Cd^{2+}, Ag^{+}, Mn^{2+}, Ni^{2+} and Zn^{2+} due to their constituted harmful effects, not only on human health but also on environmental degradation at large. Table 7.3 presents the statistical summary of metal occurrence in both groundwater and surface water in the wet season. For visual appreciation, the elemental variation in groundwater is presented as a graph in Figure 7.6.

Table 7.3: Summary of metal concentrations

Heavy metals	Groundwater range	Mean	Standard deviation	Surface water range	Mean	Standard deviation
Zn^{2+}(µg/l)	<0.1-240	8.4	37.9	<0.1-19.9	6.7	11.4
Cu^{2+}(µg/l)	<0.1-1,330	49.3	214	<0.1	<0.1	<0.1
Mn^{2+}(µg/l)	<0.1- 14900	382.4	2,354.4	4-10	244.9	347.7
$Fe^{2+/3+}$(µg/l)	<0.1-1,580	118	266.9	104.5-240	173.5	68.2
Ni^{2+}(µg/l)	179-567	50.1	142.1	<0.1-10	8	1.4
Cd^{2+}(µg/l)	<0.1-10	0.2	0.6	21.6-190	70.1	10.3
Ag^{+}(µg/l)	<0.1-40	2.7	7	24,974.8-24,980	16,651.5	14,420.6
Pb^{2+}(µg/l)	<0.1-30	2.1	4.3	<0.1-450	151.2	261.8
Cr^{2+}(µg/l)	3.9-5	14.3	14.3	<0.1-120	65.2	63.3

The metal occurrence in groundwater and surface water showed the following trends: $Mn^{2+} > Fe^{2+/3+} > Ni^{2+} > Cu^{2+} > Cr^{2+} > Zn^{2+} > Pb^{2+} > Ag^{+} > Cd^{2+}$ and $Ag^{+} > Pb^{2+} > Fe^{2+/3+} > Cd^{2+} > Cr^{2+} > Zn^{2+} > Mn^{2+} > Ni^{2+} > Cu^{2+}$. Pollution of the surface water was not surprising; it is the main recipient of various forms of anthropogenic wastes generated within the state from inland to the coast. The most striking of this result is that, except for iron that occurred across the whole area, all other metals that had elevated concentrations in groundwater such as Mn^{2+}, Ni^{2+} and Cu^{2+} occurred between GW 1 (App) and GW 6 (App), an industrial zone situated at the western domain of the study area (Figure 7.7). Thus, the anomalous occurrences of these metals in the western part strongly indicated local anthropogenic input arising from industrial activities such as untreated effluents and wastes from numerous tank

farms, pharmaceutical companies, and metallurgical plants, coupled with municipal and domestic wastes.

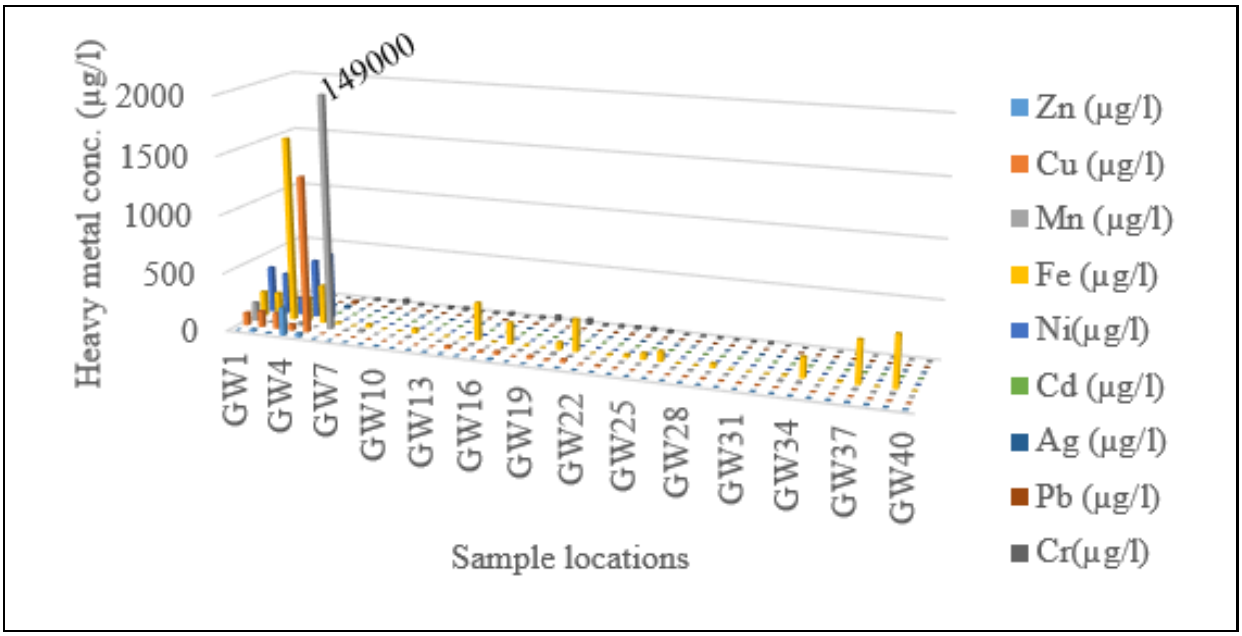

Figure 7.7: High concentration of metals in groundwater at the western axis of the study between GWI and GW7 (Industrial zone)

7.4.1 The heavy metal pollution index

The degree of contamination resulting from metals in water was evaluated using the Heavy Metal Pollution Index (HPI) method (Kim et al., 1998; National Institute of Environmental Research, 2007; Odukoya and Abimbola 2010, Ayolabi et al., 2013). The tolerable level is the elemental concentration in the water considered safe for human consumption (Lee et al., 1998; Ayolabi et al., 2013). The WHO (2018) and SON (2007) standards were adopted as tolerable levels for water. The HPI was calculated by the following equation by Mohan et al. (1996):

$$HPI = \frac{M_c/T_L}{N_m} \quad \text{..... 7.1}$$

Where:

M_c represents the heavy metal concentration in water;

T_L = a tolerable level; and

N_m = number of heavy metals under consideration.

When the HPI is >1, the water is regarded as being contaminated. More than 50 % of groundwater in the area is polluted, having an HPI between 1.0 and 2.86. Mn^{2+} contributed the highest percentage (62 %) to the HPI, followed by $Fe^{2+/3+}$ (19 %), and closely followed by Ni^{2+} (8 %), Cu^{2+} (8 %), Cr^{2+} (2 %) and Zn^{2+} (1 %) (Figure 7.8).

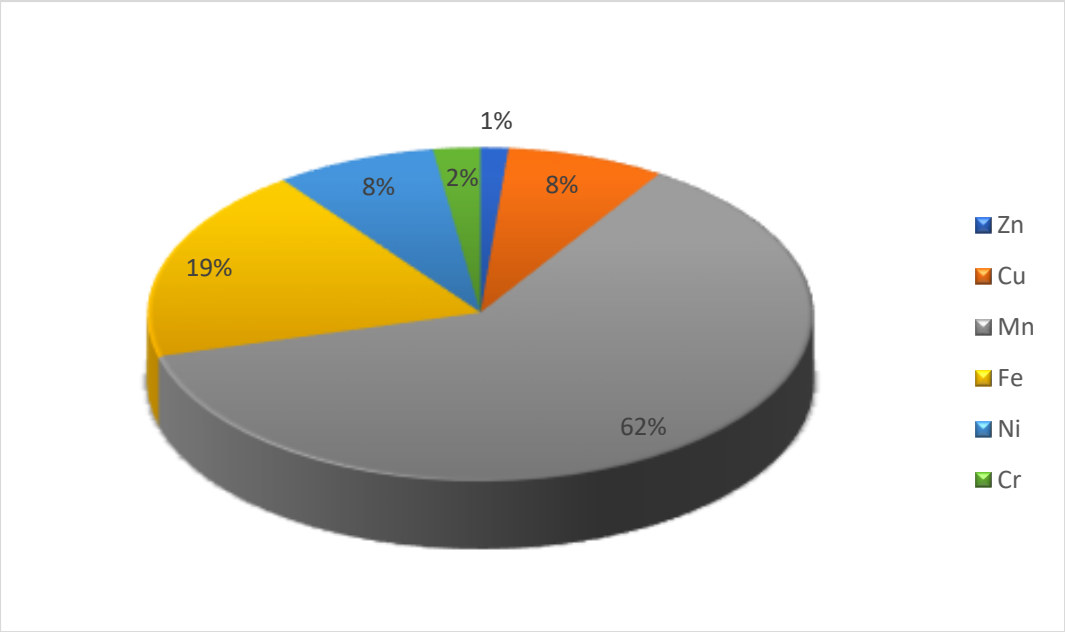

Figure 7.8: Percentage contributed by significant metals to HPI in groundwater

Furthermore, in addition to the metals plot (Figure 7.8), the spatial distribution of EC and NO_3 were plotted to further demonstrate the impact of urbanization, land use pattern and anthropogenic activities across the entire study area (Figure 7.9 and Figure 7.10). The EC values were found to be highest in the western and central parts of the study while the eastern part has the least values, thus connoting the influence of the surface brackish waters on the nearby shallow groundwater (Figure 7.8). However, with respect to NO_3, the occurrence of elevated concentration of nitrate across the study area is a reflection of an urbanisation impact due to anthropogenic input that emanated from human wastes.

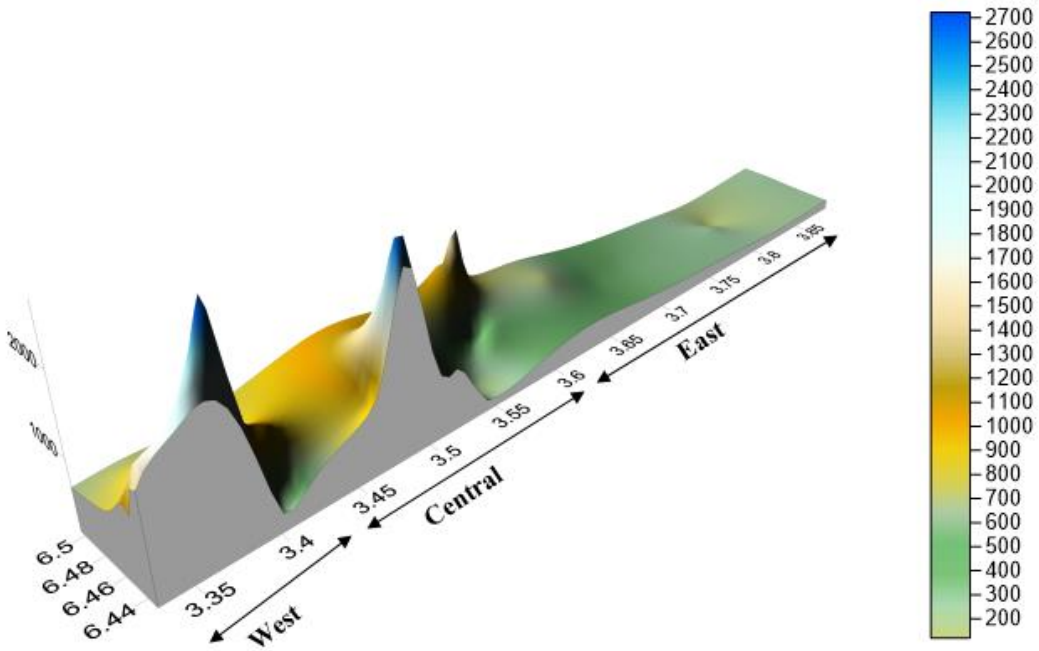

Figure 7.9: ***3D view of spatial distribution of EC across the study area.***

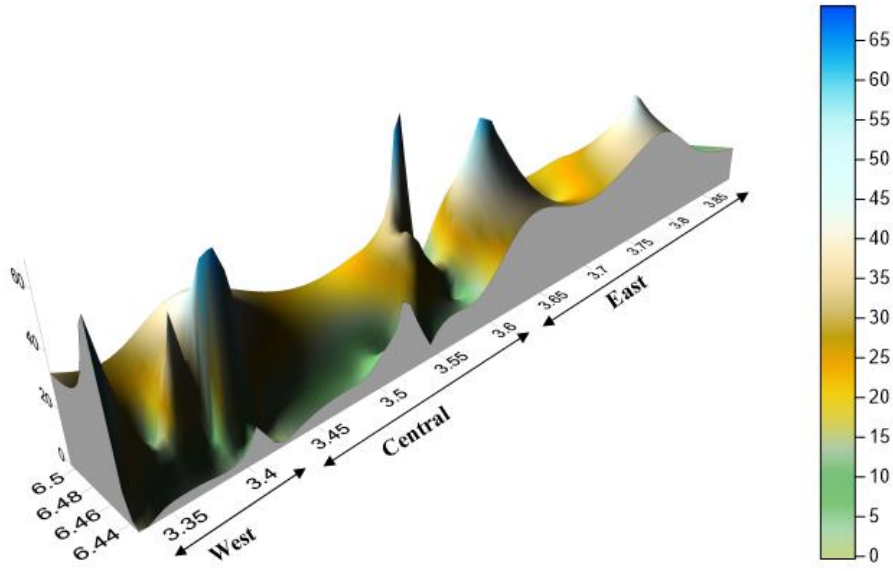

Figure 7.10: ***3D view of spatial distribution of NO_3 across the study area.***

7.5 Hydrogeochemical Evaluation

7.5.1 Hydrogeochemical facies

The Piper Trilinear diagram is a very useful tool in bringing out the groundwater chemical relationship in more concise terms (Walton, 1970). In the present study, hydrochemical data were plotted on the Piper Trilinear diagram (Piper, 1944), and Schoeller diagram (Schoeller, 1967) to evaluate the groundwater composition in wet and dry seasons. Furthermore, according to Hem (1985), the water in which no cations or anion constitute as much as 50 % of the total, should be recognised as a 'mixed type' and identified by dominant cations and anions. In this study, a 50 % minimum benchmark for individual cation or anionic concentrations (meq/L) in their respective totals has been considered in formulating the water type.

The hydrochemical facies of the individual wells sampled is presented in Appendices H and I, while Appendix J shows the summary of facies' distribution for both seasons across the study area. The piper plot for the wet season groundwater revealed essentially four distinct hydrochemical types: Ca-Mg-HCO_3, Ca-Mg-Cl-SO_4, mixed Ca-Mg-Cl, and Ca-Cl, and the predominant types were the Ca-Mg-HCO_3, Ca-Mg-Cl-SO_4, constituting about 37.5 % and 32.5 %, respectively, while the dry season was composed of Ca-HCO_3, Ca-Mg-HCO_3, Ca-Na-HCO_3 and Ca-Na-Mg-HCO (Figure 7.9). The Ca-HCO_3 and Ca-Mg-HCO_3 water types with 39.5 % and 37.5 % were the dominant water types. The dominant occurrence of these water types gives credence to the recent recharge of the unconfined surficial aquifer. The hydrochemical facies for surface water was Mg-Cl for the lagoon samples (P-SW 1, P-SW 2, and P-SW 3) and Na-Cl for the ocean water (SW 4). Detailed discussion regarding facies changes in groundwater with seasons is discussed in the next sub-section.

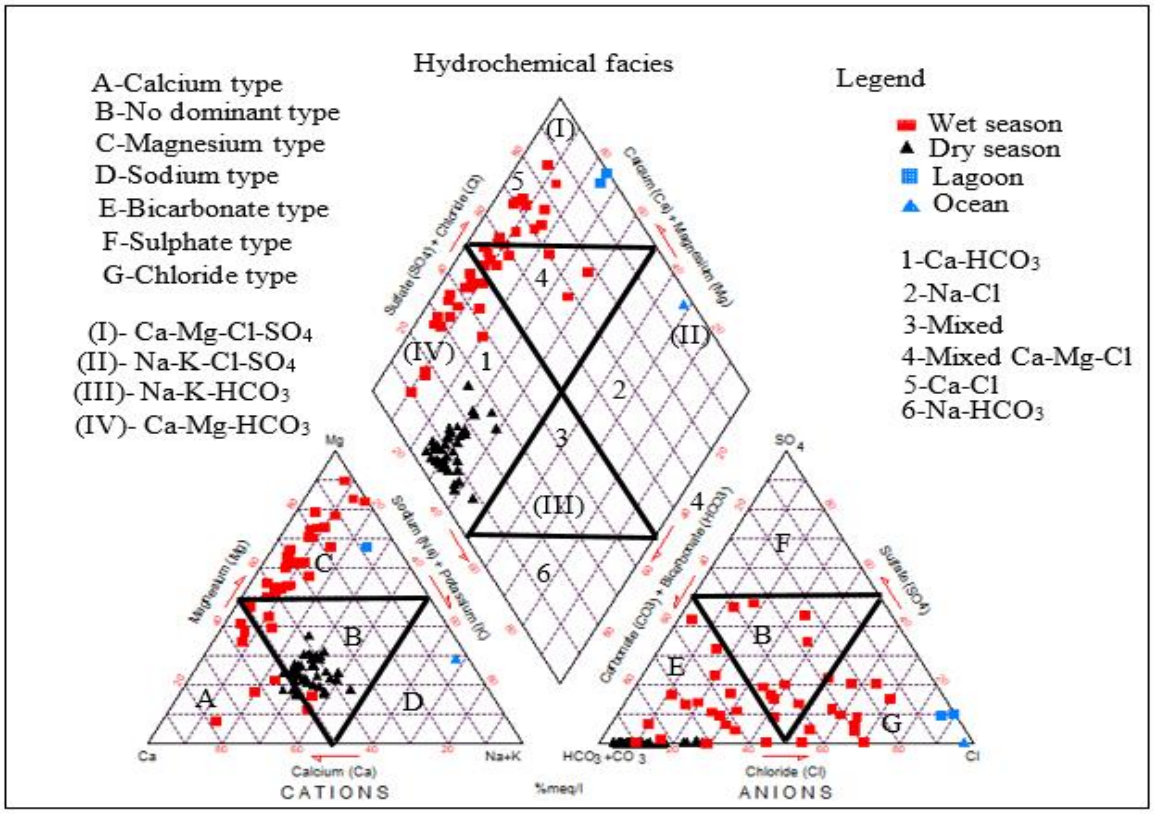

Figure 7.11: Piper plot showing the types of water of the Lagos Coastal Basin in the wet and dry seasons

The chloride type water, especially Mg-Cl observed in about 25 % of groundwater in the wet season, are compositionally similar to the brackish water facies (Mg-Cl) of the lagoon water P-SW 1, P-SW 2 and P-SW 3 (Appendix H; Figure 7.11). This also indicates possible interaction between the surface water and groundwater, and brackish water may be suspected as the major source of Mg^{2+} in the groundwater and thus the marine influence on the surficial aquifer is further at play in parts of the phreatic aquifer.

7.5.2 Hydrochemical evolution

The rock–water interaction and various hydrogeochemical processes such as precipitation, dissolution, and cation exchange in an aquifer with increasing residence time, are responsible for variation in groundwater composition as it evolves into different water facies from the recharge area through transition to the discharge zone.

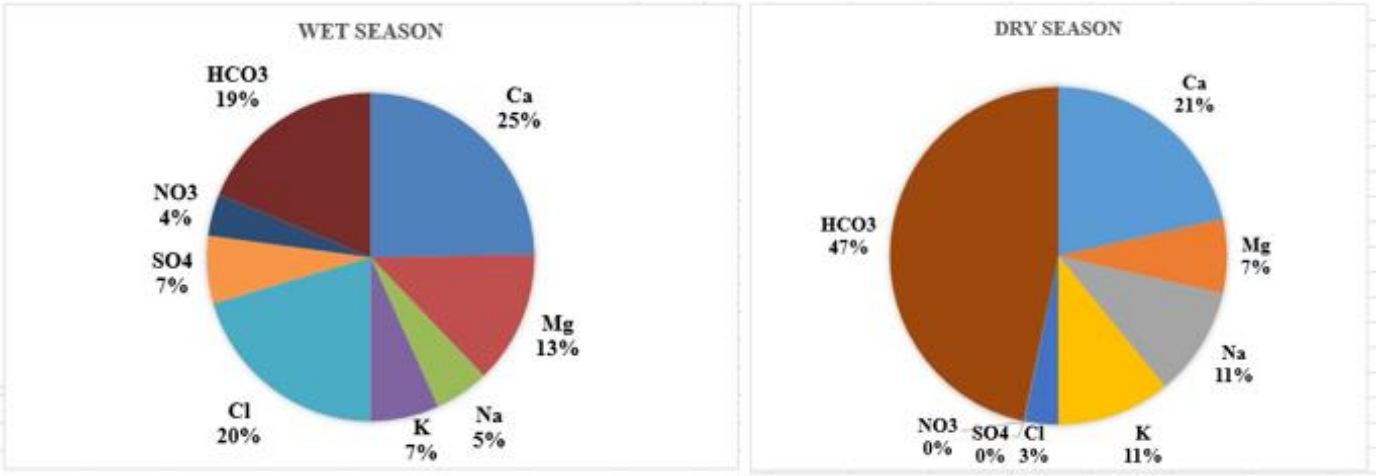

Figure 7.12: Percentage composition of mean occurrence of major ions in groundwater

7.5.2.1 Dry season water types

The dry season water samples are essentially characterised by calcium bicarbonate (Ca-HCO_3) type of water (Figure 7.12). The high concentration of HCO_3^- is an indicator of carbonate dissolution or decomposition of organic matter. The Ca-HCO_3 water type is generally derived from the carbonate dissolution such as calcite, which contributes Ca^{2+} and HCO_3^- to the groundwater. During the process of water–rock interaction, an increase in the concentration of Ca^{2+} and HCO_3^- with a consequent reduction in the concentration of Mg^{2+} and Cl^-, might have resulted in a Ca-HCO_3 water type. Calcium carbonate is the major component of the Tertiary Ewekoro limestone, which occurred in the northern parts of the regional Dahomey basin, the southern end at which the current study area is situated. It may also occur as cementing material in sedimentary rocks. As depicted in Figure 7.10, the Ca-HCO_3 and Ca-Mg-HCO_3 types are normally dominated by the earth's alkaline water and weak acids (Karanth, 1987). The excess of Na^++K^+/Cl^- ratio in the dry season may suggest leaching of soil salts or cation exchange and also reflects the higher concentration of alkalis from sources other than precipitation (Appendix I and Figure 7.10). Furthermore, the high K^+ concentration could be washed-in from the hinterland materials used to sand-fill the study area, especially considering the very shallow depth occurrence of the surficial aquifer. In summary, it may be inferred that as Ca^{2+} and Mg^{2+} are removed from the water, Na^+ and K^+ from rock are added to the groundwater, indicating the process of cation exchange.

7.5.2.2 Wet season water types

In the wet season, groundwater occurs in different facies (Appendix H). The percentage composition of the mean for the major ions in the wet season is also presented in Figure 7.10. The series of water types recorded in the wet season is a true reflection of the discharge area and it ranged from Ca^{2+}, Mg^{2+}, HCO_3^-, Cl^- and SO_4^{2-} dominated water types. The different facies types could be explained by:

i. Leaching and dissolution of salts: The high concentration of chloride ion as observed in the wet season is associated with decreasing bicarbonate concentration and enriching of sulphate concentrations (Figure 7.12). This process clearly defines leaching and dissolution of soluble salts through precipitation and surface run-off during groundwater movement to the ocean and, consequently resulted in various forms of HCO_3-Cl-SO_4 water types, depending on the dominant cation.

ii. Simple mixing between brackish water and fresh groundwater through flash floods indicated by the relative enrichment of magnesium and impoverishment of calcium with increasing chloride (Figure 7.12): When carbonate sediments first emerge from the marine environment, they undergo flushing of seawater by freshwater during which time the salinity decreases and the hydrochemical facies becomes dominated by Ca-HCO_3, and thus the coastal freshwater is dominated by Ca^{2+} and HCO_3^- from the dissolution of calcite, such that cation exchanger has essentially Ca^{2+} adsorbed to their surfaces. When seawater charged with Na^+ and Cl^- as the dominant ions, intrudes in to or mixes with the fresh coastal water, then the following cation exchange reaction according to Martinez and Bocanegra (2002) may occur:

$$Na^+ + ½\ Ca\text{-}X \rightarrow Na\text{-}X + ½\ Ca^{2+} \ldots\ldots\ldots 7.1$$

As the exchanger site picks up Na^+, then Ca^{2+} or Mg^{2+} are released and the hydrochemical water types evolve from Na-Cl water to Ca-Cl or Mg-Cl. The general Mg^{2+}/ Cl^- ratio of <1 (Appendix H), characterising the wet season, may also be a good pointer to the mild impact of marine on the water table aquifer. Simply put, an increase in the concentrations of Mg^{2+}, Cl^- and SO_4^{2-} and the consequent reduction in the concentration of Ca^{2+} and HCO_3^- as observed in the wet season. This process might have resulted the groundwater to evolve to various water types depending on the dominant cation or anion (Appendix H; Figure 7.12). Another possible explanation for the decrease in calcium concentration could be when

calcium from carbonate rocks is removed and replaced with magnesium from groundwater throughout an ion exchange reaction (dolomitisation process).

In addition, classification based on Schoeller (1967) pointed out ions enrichment in groundwater as follows:

$rHCO_3 > rSO_4$ …… Type I

With longer residence time the relationship stated above changes to:

$rCl > rHCO_3$ …… Type II

With further increase in the residence time, the below ionic phase evolves:

$rCl > SO_4 > rHCO_3$ …… Type III

At the final and advanced stage of ionic transformation, the concentration reaches:

$rCl > rSO_4 > rHCO_3$ coupled with $rNa > rMg > rCa$ ……Type IV

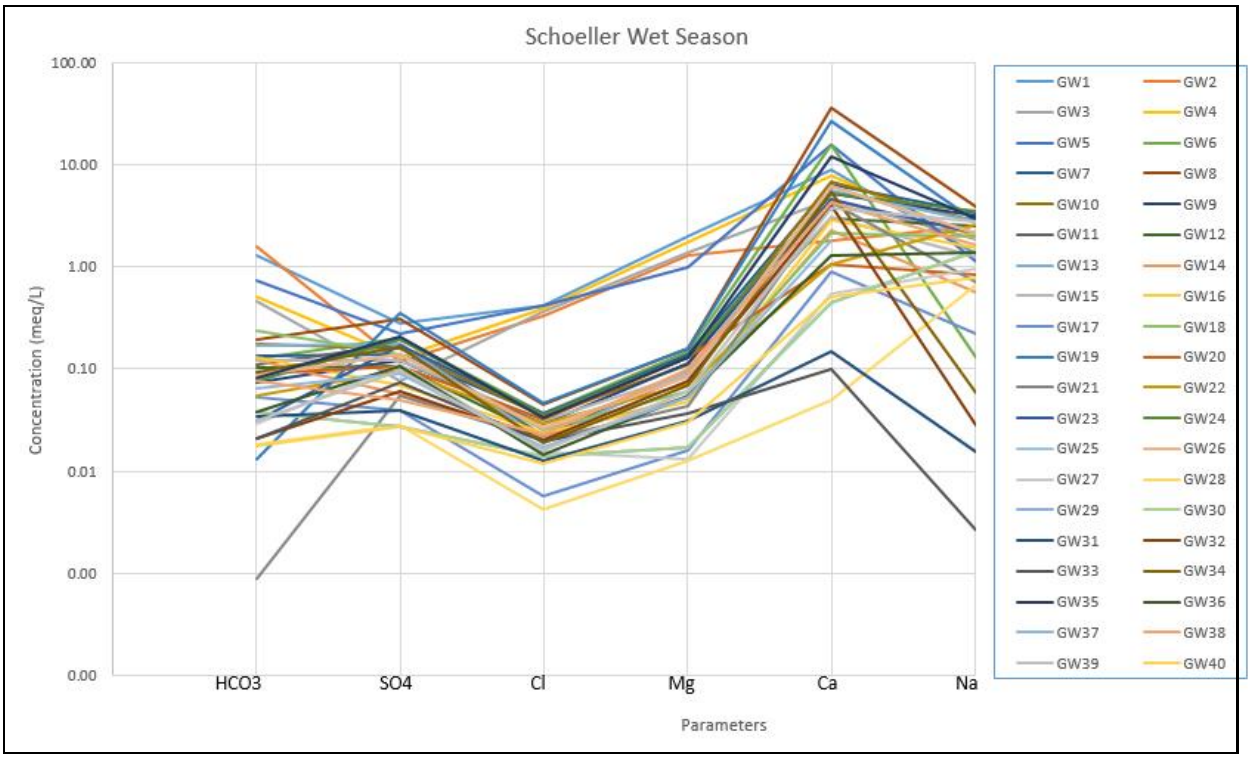

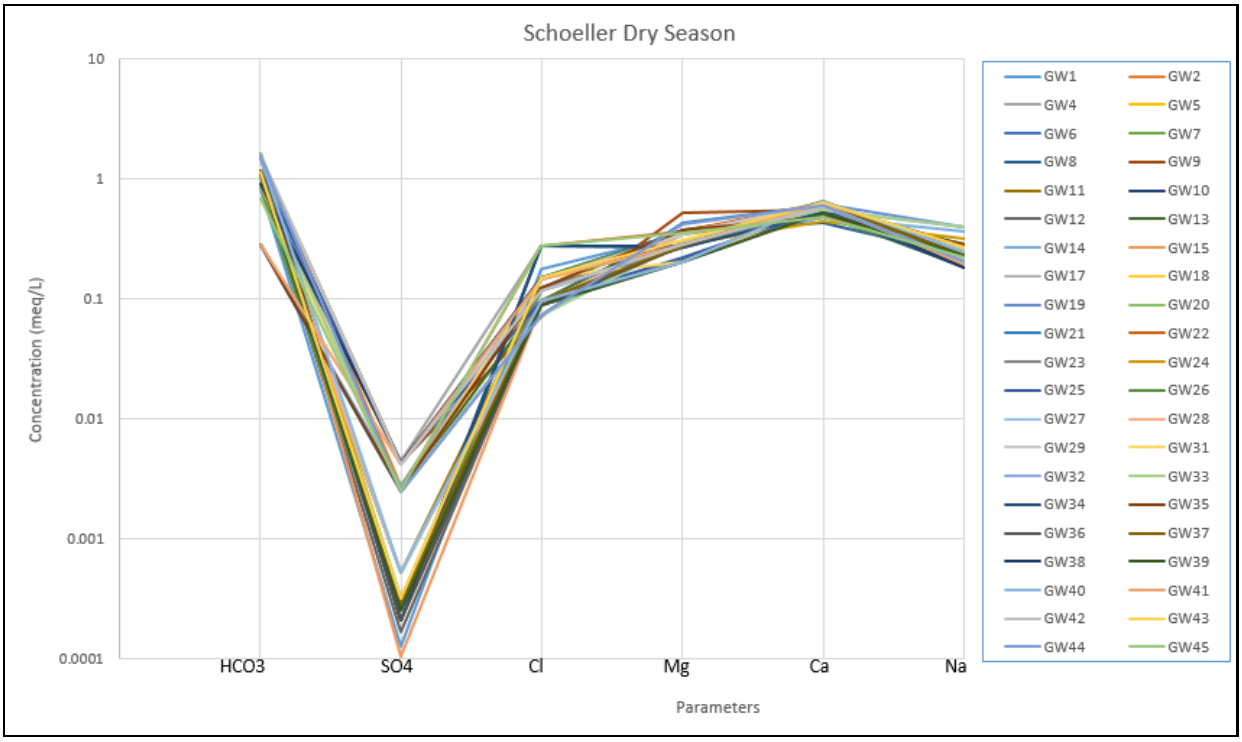

Figure 7.13: Schoeller plot showing water types of the Lagos Coastal Basin in wet and dry seasons

The evolution in ionic type from Type I to Type IV depends on the residence time of water in the subsurface and the degree of water–rock interaction. The samples collected from the present groundwater investigation ranged from Type I to Type III in the wet season, indicating water with different residence times resulting from heterogeneous sources. However, the dry season can be classified as Type I water and it is essentially homogenous freshwater (Figure 7.13). The distinct dissimilarities exhibited by both seasons further buttress the fact that there is little or no interaction between surface water and the shallow surficial groundwater during the dry season in the study area, as clearly established by the stable isotope study (Yusuf et al., 2018), a situation which may be conceived to be resulting from a drastic drop in the volume of the surface water during the dry season. In general, it may be deduced that the strata sediment characterisation and interactions are responsible for the present ionic concentration in the groundwater.

7.5.3 Hydrogeochemical processes

In the study area, the analysed groundwater samples revealed calcium and bicarbonate as the dominant ions in groundwater, especially during the dry season (Appendices E and G), suggesting carbonate dissolution. The dissolved CO_3^{2-} within the soil and unsaturated zone

produce weak carbonic acid (H_2CO_3) which dissociates and enhances the dissolution of calcium carbonate.

The reactions between carbonic acid (atmospheric CO_2 and water) and calcium carbonate in the soil give bicarbonate and calcium ions and this can be denoted as written below in Equation 7.2 and 7.3 (Garrels, 1976).

$$CO_2 + H_2O \rightarrow H_2CO_3 \text{ ..... } 7.2$$

(Carbonic acid formation)

$$CaCO_3 + H_2CO_3 \rightarrow Ca^{2+} + 2HCO_3^- \text{ ..... } 7.3$$

(Calcite/Limestone dissolution)→ Calcium + Bicarbonate

Considering the location of the study area, which is in contact with the ocean and brackish water, the marine influence through flash floods and surface run-off acts as a contributory factor to the high magnesium occurrence in the groundwater during the wet season, giving credence to Mg-calcite [Ca Mg (CO_3)] (Appello and Postma, 2005). The Mg-calcite may be divided into low and high Mg-calcites; the low Mg-calcites have <5 mol % Mg, while the 5–30 mol % Mg is regarded as the high Mg-calcites (Morse and Mackenzie, 1990). Based on the above submission, all the groundwater samples in the dry season and 14 samples (35 %) from the wet season, may be classified as low Mg-calcites with <5 mol % Mg. The remaining 65% from the wet season is under high Mg-calcites with magnesium values between 5 mol % Mg and 12 mol % Mg. The magnesium abundance in the rainy season may be from the marine source through flash floods triggered by high intensity rainfall which led to an increase in the volume of the connecting surface water of the lagoon and creeks, and subsequent occurrence of riverbank overflow. It is also worthy to mention that 50 mol % Mg is not the same thing as dolomite (Appello and Postma, 2005).

7.5.3.1 Chemical weathering

The rapid dissolution of soluble rocks (carbonates, gypsum, halite) and gradual dissociation of relatively soluble rock (silicates) resulting from rock–water interaction, are part of the chemical weathering that plays a role in mineral enrichment and depletion. The measurement in groundwater of these rock components informed the dominant weathering process that characterises a particular aquifer. To gain an insight into the chemical processes that govern water quality, the present study proposed a new formula or methods for identification and differentiation between carbonate and silicate weathering in groundwater.

The proposed methods are cationic contribution evaluation [Ca^{2+}+Mg^{2+} vs total cation (TZ^{+})], and ionic ratio plots of HCO_3^{-}/Ca^{2+}vs Ca^{2+}/Mg^{2+} and HCO_3^{-}/Ca^{2+} vs Ca^{2+}/Na^{+}. All measurements are in meq/L. Cationic contribution in groundwater derived from carbonate or silicate weathering can be established from the analysed water samples as follows:

1. Cationic evaluation:

i. Calculate the total cations [Ca^{2+}+Mg^{2+}+Na^{+}+K^{+} (TZ^{+})] in solution in meq/L.

ii. Calculate the sum of calcium and magnesium in solution (Ca^{2+}+Mg^{2+}) in meq/L.

iii. The estimated Ca^{2+}+Mg^{2+} is related to the total cations (TZ^{+}) in meq/L.

The assumptions below were proposed for interpretation purposes:

i. If the sum of Ca^{2+}+Mg^{2+} ≥0.5 TZ^{+} is 50 % and above (TZ^{+}), then carbonate weathering is the dominant process.

ii. If the sum of Ca^{2+}+Mg^{2+} <0.5 TZ^{+} is less than 50 % (TZ^{+}), then silicate weathering dominates.

In the present study, the concentration of Ca^{2+}+Mg^{2+}, relative to the total cations, was 85 % in the wet season and 70 % in the dry season, both of which are far and above the <50 % TZ^{+} for silicate weathering (Figures 7.14**a** and 7.14**b**). Therefore, carbonate weathering is the dominant process that controls the groundwater quality in the study area. The R^2 values of approximately 0.98 and 0.88 for both seasons further supported the validity of carbonate dissolution as the dominant process.

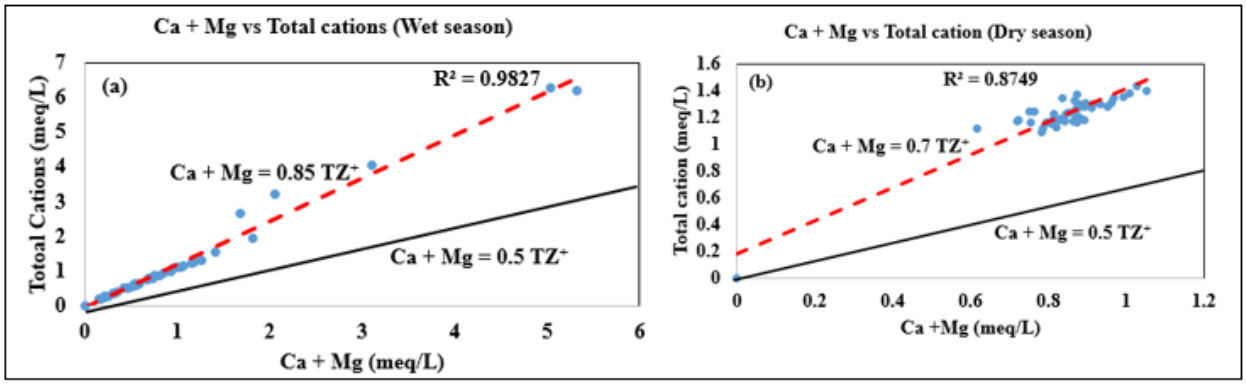

Figure 7.14: Ca^{2+}+Mg^{2+} vs total cations showing carbonate dissolution

2. Ionic ratio plots proposition (HCO_3^{-}/Ca^{2+} vs Ca^{2+}/Mg^{2+} and HCO_3^{-}/Ca^{2+} vs Ca^{2+}/Na^{+} (Appendices H and I):

i. The ratios of the related elements to the objective were calculated.

ii. The ionic ratios were plottted on the logarithmic graph.

iii. From the graph, boundaries were created for various weathering types based on the relative natural abundance of respective ions in groundwater. The considered weathering or dissolution processes are evaporates, silicates and carbonates.

The assumptions below (boundary range) were made for interpretation purposes:

i. 0.01–0.1 marks the zone of occurrence for evaporates.

ii. 0.1–1.0 is the silicate zone.

iii. >1 is the carbonate zone.

iv. Based on the bivariate plots of ionic ratios presented in Figure 7.15, it may be concluded that carbonate dissolution is the predominant weathering process characterising the shallow groundwater system in the study area. However, the few samples that fell within the silicate zone may be attributed to contribution as the groundwater crosses heterogeneous aquifers.

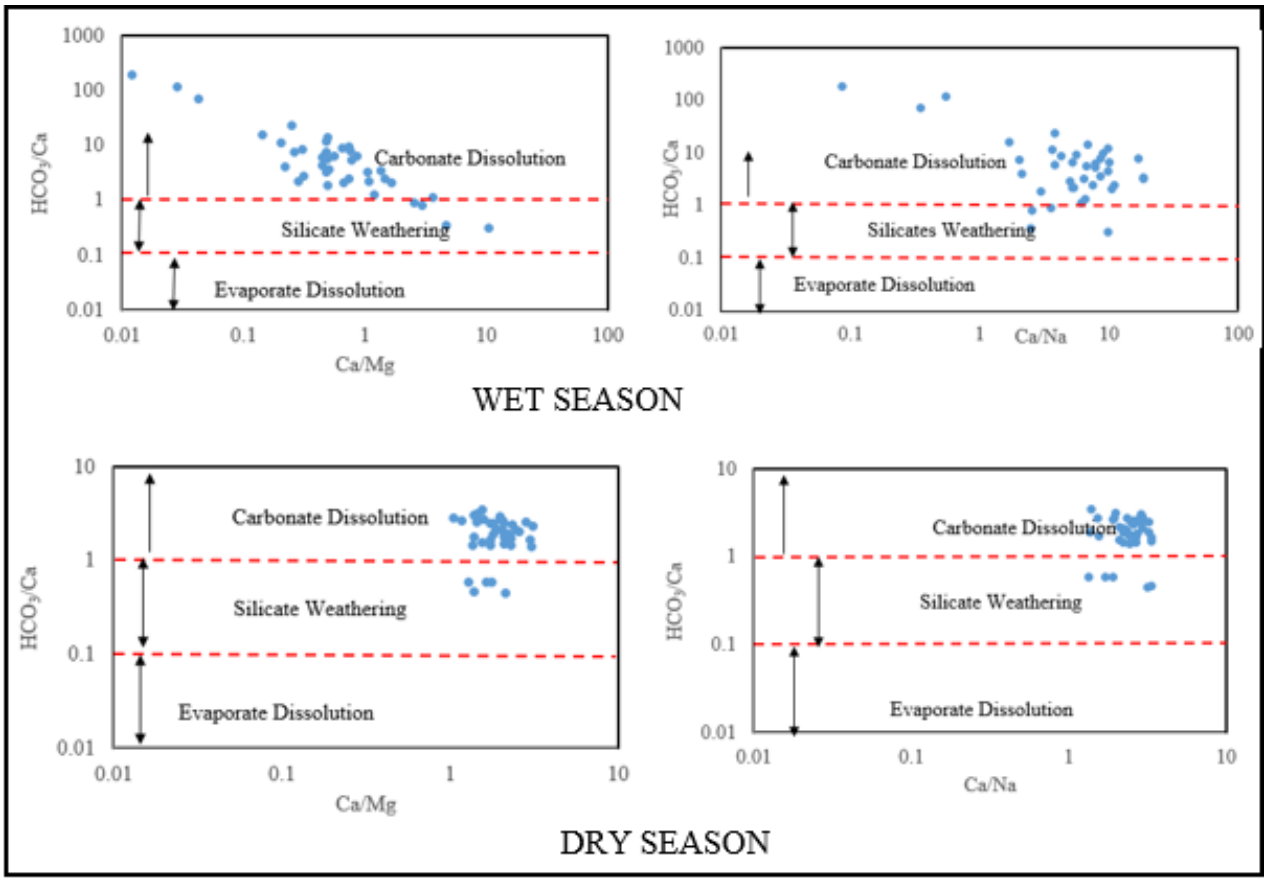

Figure 7.15: Bivariate plot Ca^{2+}/Na^{+} vs HCO_3^{-}/Ca^{2+} and Ca^{2+}/Na^{+} vs HCO_3^{-}/Ca^{2+} to identify the dominant chemical weathering in the groundwater of study area

7.5.3.2 Ion exchange processes

Although there are many proposed methods by different authors to assess ion exchange that controls the groundwater chemistry, this study adopts the $Ca^{2+}+Mg^{2+}/ HCO_3^{-} + SO_4^{2-}$ ratio by (Cerling et al., 1989) reported in meq/L for this purpose. The reverse ion exchange is identified by an excess of ($Ca^{2+}+Mg^{2+}$) over ($HCO_3^{-} + SO_4^{2-}$), while ion exchange is marked by a higher occurrence of ($HCO_3^{-} + SO_4^{2-}$) over ($Ca^{2+}+Mg^{2+}$) (Cerling et al., 1989; Fisher and Mulican, 1997; Edet et al., 2011). This may be represented by Equation 7.4. Here, the aquifer matrix picks up the Na^{+} in solution in exchange for its adsorbed/attached Ca^{2+}. The hydrochemical composition thus evolves from Na-Cl to Ca-Cl or Mg-Cl. In the case of an opposite reaction, the following equation 7.4 occurs (Martinez and Bocanegra, 2002):

$$1/2Ca^{2+} + Na\text{-}X \rightarrow 1/2Ca\text{-}X + Na^{+} \text{ (reverse reaction)} \quad \ldots\ldots 7.4$$

The Ca^{2+} ion in solution is taken up by the exchange site in return for Na^{+} on its surface. The former sodium-rich water turns into calcium-rich water and thus the Na-HCO_3 water type evolves to that of a Ca-HCO_3 water type, indicating the freshening process.

In the study area, the calculated ionic ratio of $Ca^{2+}+Mg^{2+} / HCO_3^{-} + SO_4^{2-}$ <1 in 90 % of the samples was in the wet season. Similarly, 85 % of the samples had a ratio of $Ca^{2+}+Mg^{2+} / HCO_3^{-} + SO_4^{2-}$ <1 in the dry season. This suggests the dominance of ion exchange or secondary leaching as the source for dissolved salts in the basin. However, a few groundwater samples, 10% and 15% for both wet and dry seasons exhibited $Ca^{2+}+Mg^{2+} / HCO_3^{-} + SO_4^{2-}$ >1 as the groundwater tends to flush out brackish water to restore its freshness. It is important to point out here that the $Ca^{2+}+Mg^{2+} / HCO_3^{-} + SO_4^{2-}$ >1, as observed in the wet season, may be attributed to reverse ion exchange or a mixture of various waters. However, in the dry season, it does not necessarily imply reverse ion exchange; the higher ionic ratio than unity may be due to leaching as a source of dissolved salts or evaporation effects which tend to enrich the soil salinity.

Complementarily, the Durov diagram (1948) (Figure 7.16) was employed to substantiate the assertion observed about the ionic process governing the groundwater in the basin. The fact that the mixed water type prevails in the wet season was supported by data plotted in Figure 7.14; where 67.5 % of the samples plotted in Field 5 of the plot along the dissolution or

mixing line. Based on the classification of Lloyd and Heathcoat (1985), this trend can be attributed to fresh recently recharged water exhibiting simple dissolution or mixing with no dominant major anion or cation. In addition, a few samples (15 %) in Field 4, showing Cl^- as a dominant anion, indicating that the groundwater is related to a mixture through flash floods resulting from bank overflow by brackish water. The remaining 17.5 % in Field 3 and Field 6 exhibited ion exchange processes, whereas in the dry season, samples plotted in Field 6 of the plot along the ion exchange line, showed that the groundwater is related to ion exchange with Ca-HCO_3 water. The remaining 15 % belongs to Field 5 of the plot along the simple dissolution of the rock or mixing line with no dominant anion or cation. In general, it is clear from the above that ion exchange and dissolution of rocks or mixing with other water types essentially contribute to the groundwater chemistry, while rock dissolution and ion exchange were the dominant exchange processes characterising the wet and dry seasons, respectively. This may be reflecting the complexity of the basin as the main recipient of all water types from the upstream side of the area.

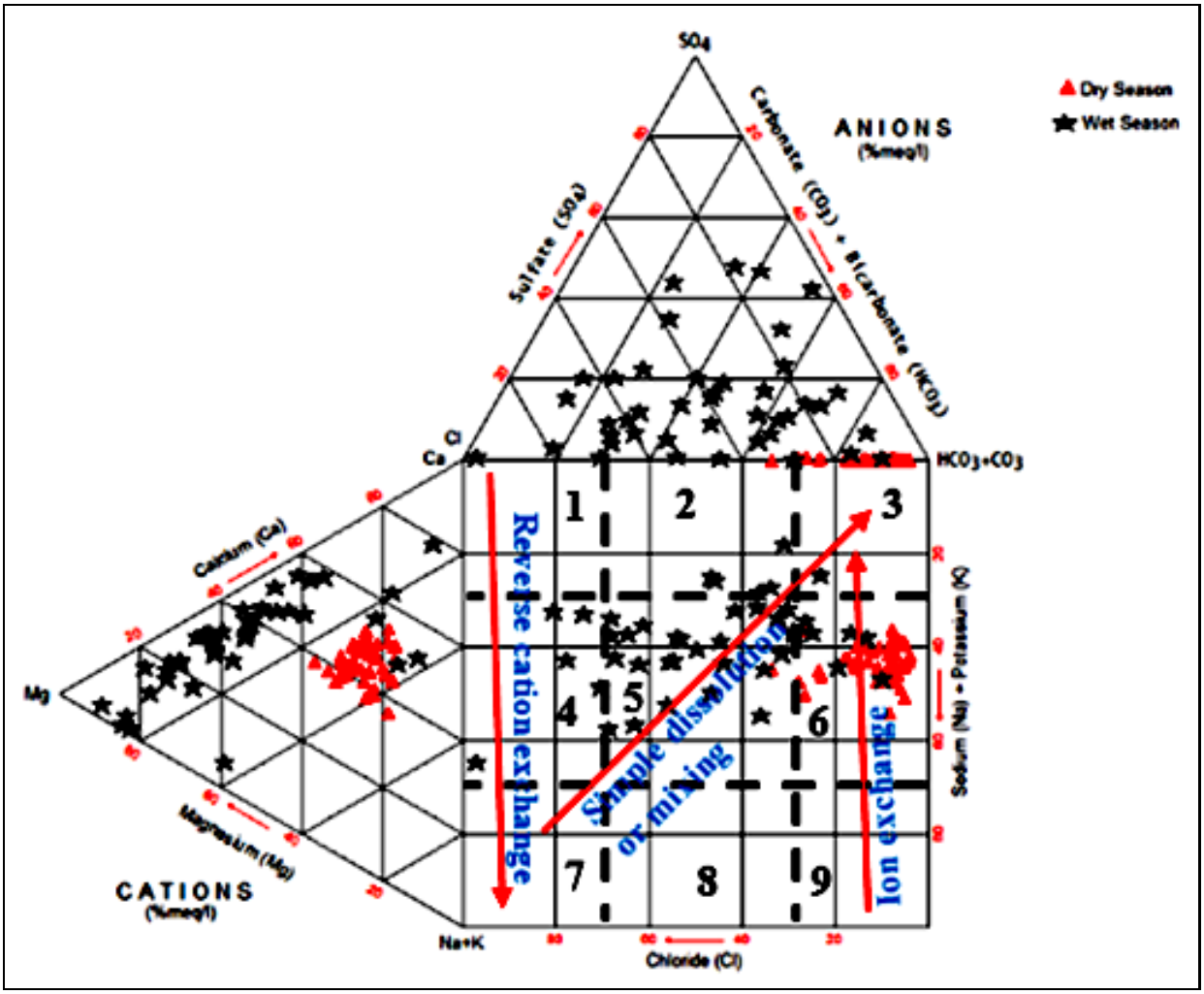

Figure 7.16: Durov plot depicting hydrochemical processes involved

7.5.3.3 Evaporation effect

The evaporation effect was further elucidated with the use of the correlation between Oxygen-18 and Cl^- and between Na^+/Cl^- and EC to examine the degree and trend of evaporation in the study area. In general, both methods demonstrated that chloride enrichment of the wet and dry season in the basin was slightly different. The slight variation may be due to the humid nature of the coastal basin throughout the year with mean atmospheric temperature difference of ±3 °C between the wet and dry season. In the wet season, the relative concentration and evaporation in the basin are reflected by an increase in chloride with oxygen-18 enrichment, and a constant sodium chloride ratio with increasing EC (Figure 7.17**a** and **b**). In an evaporation environment, the chloride concentration is expected to remain constant with an increasing EC value (Appello and Postma, 2005). In the study area, it was proposed that the evaporation observed in the wet season may be a result of a mixture of the surrounding highly evaporated surface water with the shallow groundwater

through flash flooding, bank infiltration and surface run-off. The evaporation was further enhanced by the flat nature of the study area, which tends to hold water at the surface for a longer period prior to infiltration. Several authors have reported that a decrease in Na^+ compared to Cl^- indicate the influence of other sources such as leaching of salt from the surface or recharge due to evaporated water (Chidambaram et al., 2009; Prasanna et al., 2010), where both of them were the possible cause for the present study.

In the dry season, however, the ^{18}O vs Cl^- showed a horizontal trend line indicating that, despite oxygen enrichment, the chloride content remains constant, while the Na^+/Cl^- ratio vs EC scatter diagram showed a trend line that slightly increases in the Na^+/Cl^- ratio with an increasing EC (Figure 7.17**a** and **b**). This may be suggesting an insignificant effect of evaporation on the shallow groundwater quality in the dry season. In general, although a relatively higher regression coefficient factor was recorded for the wet season, the low R^2 value observed for both seasons is a good pointer to the fact that evaporation may not be the dominant geochemical process controlling the groundwater quality in the basin.

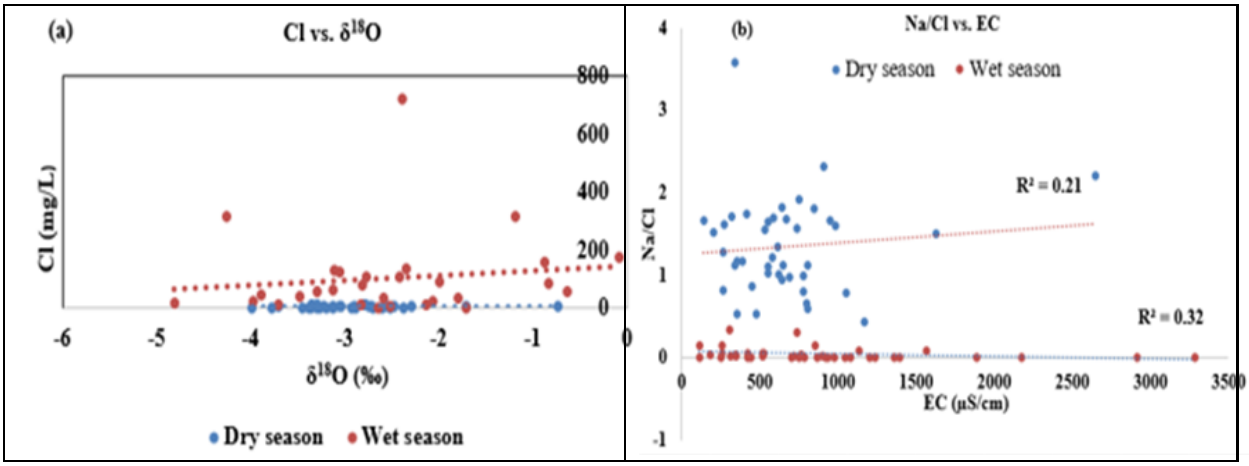

Figure 7.17: Shows scatter diagram indicating evaporation influence

Furthermore, the Gibbs diagram (1970) was used to deduce the main mechanisms controlling the groundwater chemistry, namely the sources of dissolved chemical constituents, such as precipitation dominance, rock dominance and evaporation dominance. The Gibbs diagram is, however, subject to modification to accommodate the peculiarity of a particular region. The modification was carried out in the present study using the following as guidelines:

i. Based on the deduction of the stable isotope study for the basin (Yusuf et al., 2018), rainfall is the main source of recharge to the aquifer in LCB, but mixes with older water and surface water.

ii. The recharge water is subjected to evaporation prior to infiltration due to the flat nature of the study area that holds water longer at the surface before infiltration. The area is subjected to evaporation prior to infiltration as observed by the isotope study (Yusuf et al., 2018) and thus were given adequate consideration in the modification attempt.

iii. The analysis of hydrochemical composition revealed that water–rock interaction also played a notable role in the chemistry of the shallow groundwater; hence, the need to propose a modified Gibbs diagram that will be suitable for the basin under consideration as presented in Figure 7.18.

iv. Although the TDS for pure rainwater (precipitation) is expected to be less than 100 mg/L, this might be altered due to various factors such as a mixture of groundwater with highly charged surface water and rainwater of marine origin that is equally known to be strongly diluted rainwater (Appelo and Postma, 2005).

v. The TDS boundary to demarcate a suitable evaporation line for the area under study was achieved by averaging the TDS values for both seasons, from where the lower boundary for the evaporation line was generated.

The present study revealed that most of the groundwater samples from the two seasons (wet and dry) plotted essentially in the rock-dominance and partly in the evaporation fields. The correlation of the higher TDS value with the corresponding $Na^+ / (Na^+ + Ca^{2+})$ in Figure 7.18 indicates that cation exchange reactions involving Na^+ and Ca^{2+} may account for the variability in groundwater chemistry (Li et al., 2013, 2016; Sunkari et al., 2019). Besides, the meteoric origin of the groundwater might have been lost due to water–rock interaction, mixture with high charged surface waters and ion exchange reactions.

Therefore, the modified diagram as presented in this study represents the real field situation and it can thus be concluded that the main mechanisms controlling the surficial groundwater in ascending order, are evaporation besides carbonate rock dissolution as presented in Figure 7.18.

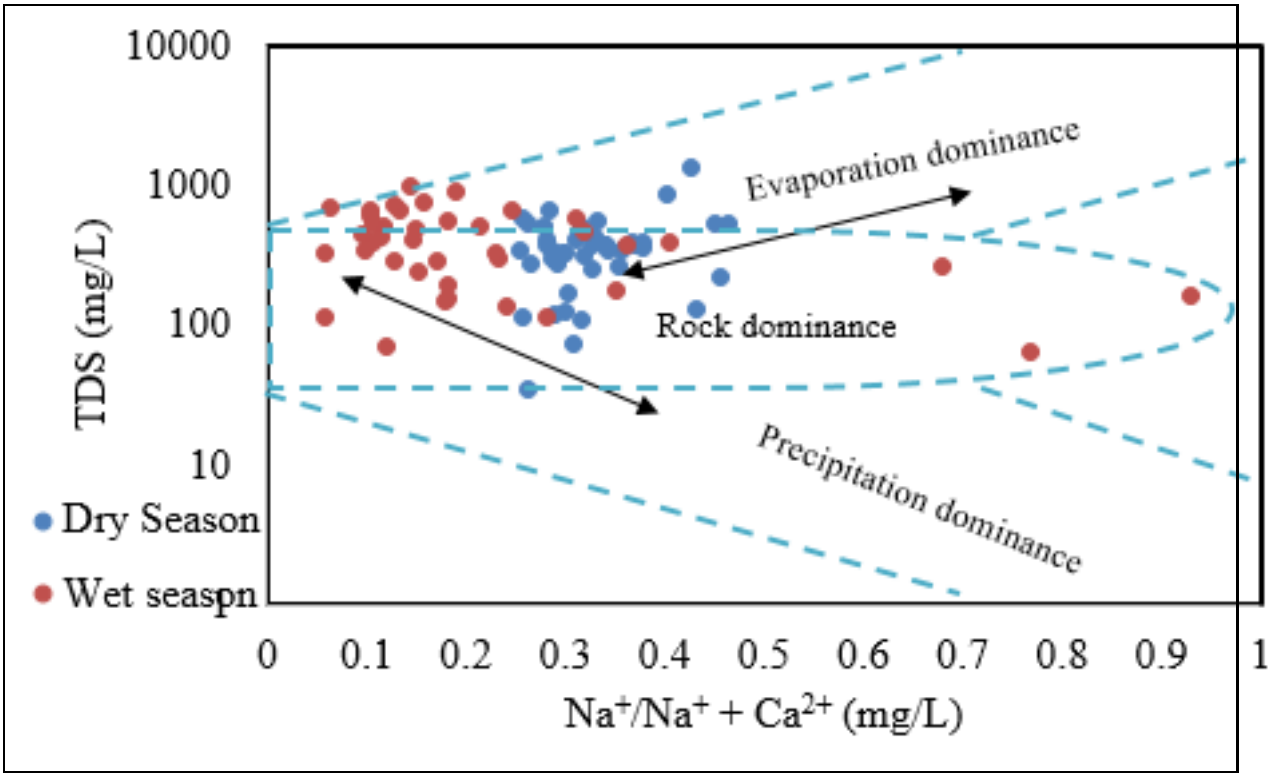

Figure 7.18: Proposed modified Gibbs diagram showing groundwater evolution in the basin

In furtherance to justify the modern recharge of the shallow aquifer in the study area, an attempt to classify the groundwater into modern water (water recharged under present climatic conditions) and old water (water recharged under humid climatic conditions) was proposed using an ionic ratio. This research work is proposing a plot of $Ca^{2}+ / (Ca^{2+} + HCO_3^-)$ vs TDS to deduce the classification. In achieving this objective, the following assumptions were made:

i. That mineral is in contact with the solution and solubility occurs.

ii. That carbonates (calcites) dissolution dominate the system.

iii. That the longer the recharge of water into the aquifer, the more charged/saturated the groundwater; hence, the water class is broadly subdivided into two classes, namely: modern recharge water and old recharge water based on the degree of aquifer saturation.

iv. The recharge rating assumption values (Rr) ranged between 0 and 1.

If Rr >0 ≤0.5 = Modern water (youngest water tends towards 0); if Rr >0.5 <1 = Humid water (oldest water tends towards 1).

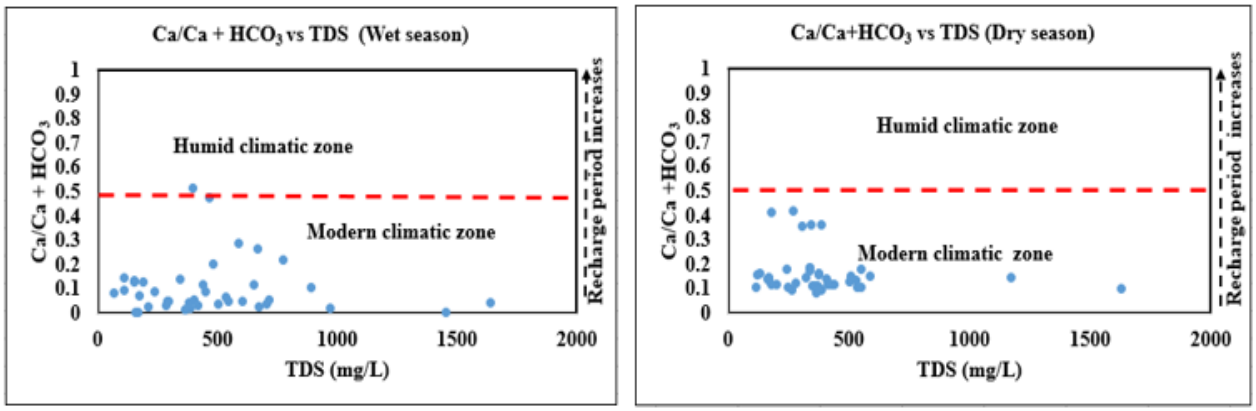

Figure 7.19: Showing the prevalent climatic condition that recharged the shallow groundwater in the study area

The plot of $Ca^{2+}/Ca^{2+} + HCO_3^-$ vs TDS (Figure 7.19) revealed samples from both seasons and fell below 0.5, indicating water recharged under modern climatic condition based on the aforesaid assumptions. However, there were two samples with values greater than 0.5 from the wet season, connoting recharge under a humid climate condition. This may be due to the mixing of the modern recharged water with deeper humid recharged groundwater. This deduction is in agreement with the isotope study of Yusuf et al. (2018) that groundwater of old/intermediate age for some of the samples in the LCB resulted from the mixture of old and recently recharged groundwater. In summary, this proposed method has been able to identify and classify the surficial coastal aquifer of Lagos as essentially recently recharged groundwater.

7.5.4 Ionic ratio to evaluate marine impacts

Ionic ratios are widely employed worldwide to understand the seawater ingress along the coastal aquifer domain (Sanchez et al., 1998; Barbecot et al., 2000; Kim et al., 2003; Moujabber et al., 2006; Batayneh et al., 2014; Sridharan and Nathan, 2017). Apart from groundwater chemistry, mineralogy of rocks may also be utilised significantly (Nwankwoala and Udom, 2011, Masindi and Abiye, 2018). It is well known that no single variable definitively identifies seawater intrusion; however, by considering various analyses we can ascertain when fresh groundwater mixes with seawater (Werner and Gallagher, 2012). This research made use of ionic plots such as SO_4^{2-}/Cl^-, Mg^{2+}/Cl^-, Na^+/Cl^-, and HCO_3^-/Cl^- to investigate the possible marine influence on the surficial aquifer of the study area. In addition to the existing ratios, this research proposes the use of $Ca^{2+} + Mg^{2+}$ vs Cl^- and Ca^{2+}/Mg^{2+} ratios against Cl^- for the same purpose. The use of chloride is imperative because it is known

to be highly conservative in nature. Chloride enters groundwater through wet and dry depositions during precipitation and a rainout effect (Hainsworth et al., 1994; Guan et al., 2010; Oke, 2015). Based on Starinsky et al. (1983), the Na^+/Cl^- ratio is used to indicate saltwater intrusion where the ratio values are less than unity, and when the ratio is greater than or equal to unity, it connotes fresh meteoric water. In the present study, all the groundwater samples in the wet season exhibited values less than one for all water samples (Appendix H), while the dry season samples have Na^+/Cl^- ratio values generally above unity (for 92% of the samples), the exception being the samples GW4, GW22, GW31 and GW45 (Appendix I). This may indicate simple mixing of groundwater with the brackish water through flash floods or surface run-off as a major process in the wet season, whereas the dry season indicates fresh meteoric water that probably originates from water–rock interaction where the average value of Na^+/Cl^- is greater than unity (Appendix I). The few samples that demonstrated salinity in the dry season may be related to leaching from the soil surface and evaporation. In general, most ions (Na^+, Mg^{2+}, SO_4^{2-}, and HCO_3^-) correlated positively with the Cl^- in the wet season (Figure 7.20**a**, **c**, **e** and **g**), indicating that such ions were derivatives of mixing water. The low to moderate regression coefficient (R^2) indicated slight mixing or highly diluted brackish water. A slight positive correlation observed for the wet season reflects a signature of slightly saline groundwater. In contrast, in the dry season, the ions plot does not show any significant correlation, but almost horizontal with Cl^- (Figure 7.20**b**, **d**, **f** and **h**), reflecting equilibration in the enrichment of the ions which is due to leaching of salts. Lack of intermixing between the brackish surface water and the unconfined groundwater during the dry season was further supported by the insignificant R^2 values recorded for the period.

In addition, according to Sridharan and Nathan (2017), the HCO_3^-/Cl^- ratio of 0.0069 suggests saltwater intrusion. This implies that values higher than this ratio could connote fresh water. The high HCO_3^-/Cl^- ratio varying from 1.93 to 21.82 in the dry season are indicative of freshwater recharge in 100 % of the water samples. However, this ratio gradually decreases below unity, indicating mixing influence with surface water in 62.5 % of the water in the wet season (Appendix H). The HCO_3^-/Cl^- ratio for all samples in both seasons was greater than that of the seawater ratio of 0.0069, connoting the absence of seawater intrusion. However, the low value documented for the wet season was gradually tending towards the ratio (0.0069), indicating that such water is derived from simple mixing by highly diluted brackish

water through flash floods or surface run-off or leaching of salt by precipitation from the surface that washed into the aquifer through rainfall.

The low value of the SO_4^{2-}/Cl^- ratio varied between 0.01 and 0.06 in 57 %, and from 0.1 to 11.06 in 87.5 % for the dry and wet seasons' groundwater samples, respectively (Appendices H and I). The low SO_4^{2-}/Cl^- ratio for the dry season indicate a low content of sulphate salts in the leached sediments that have been reduced substantially by rock dissolution (Appendix I), while a high SO_4^{2-}/Cl^- ratio reflects enrichment of sulphate salts in the leached sediments probably due to an additional source from atmospheric deposition through rainfall.

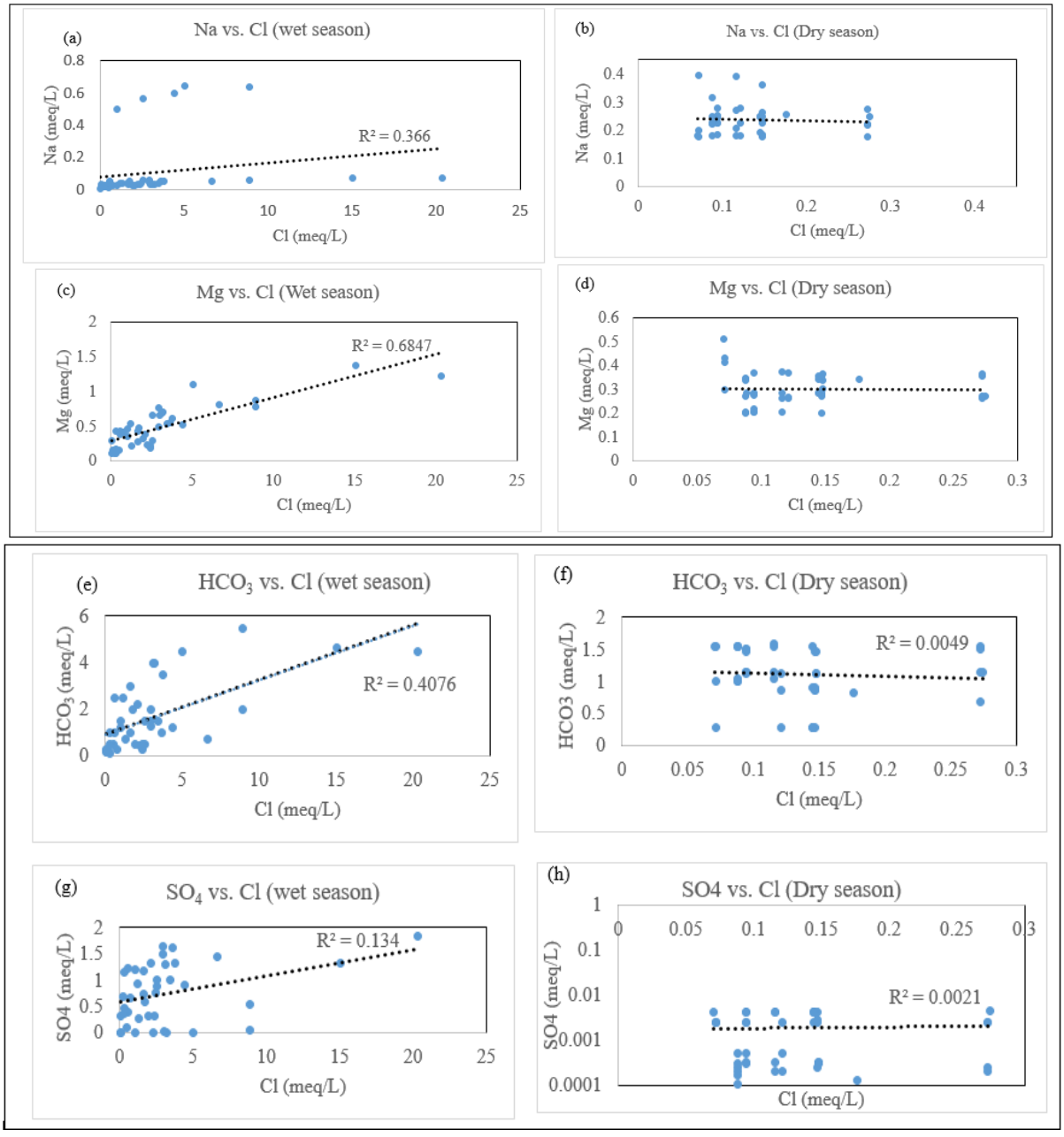

Figure 7.20: Ionic plots showing marine impact evaluation

Furthermore, the evaluation of the marine impact based on the proposed ions and interpretation is therefore as follows: The Ca^{2+}+Mg^{2+} vs Cl^- diagram reveals a slight correlation in the wet season, whereas in the dry season it does not show any relationship (Figure 7.21**a** and Figure 7.21**b**). This is indicative of slight mixing between flash floods and freshwater in the wet season and lack of interaction between aquifer and surface water in the dry season. This occurs in the wet season when the volume of water in both the lagoon and creeks increases and consequently leads to flash floods and surface run-off as the brackish water flows to the ocean. Similarly, in the wet season, the ratio of Ca^{2+}/Mg^{2+} vs Cl^- revealed a pattern different from other ionic ratios exhibiting a negative correlation (Figure 7.21**c**). This is possibly reflecting enrichment of Mg^{2+} with increasing Cl^- in the wet season, resulting from intermixing between surface water and groundwater. In addition, it may also be deduced that salinity increases with a more negative correlation, although the R^2 value might not be significant depicting minimal marine influence; however, the negative intercept value (-0.0233) exhibited by Ca^{2+}/Mg^{2+} vs Cl^- in the wet season suggests simple mixing between the phreatic aquifer and the flash floods or surface run-off. The Ca^{2+}/Mg^{2+} vs Cl^- ratio in the dry season follows a similar pattern of the preceding ions connoting freshwater devoid of saline/brackish water interaction (Figure 7.21**d**). This provides additional evidence to the assertion that there is no interaction between the phreatic aquifer and surface water during the dry season. Therefore, the proposed ions proved useful in distinguishing between the mixed water of brackish and fresh aquifer origin.

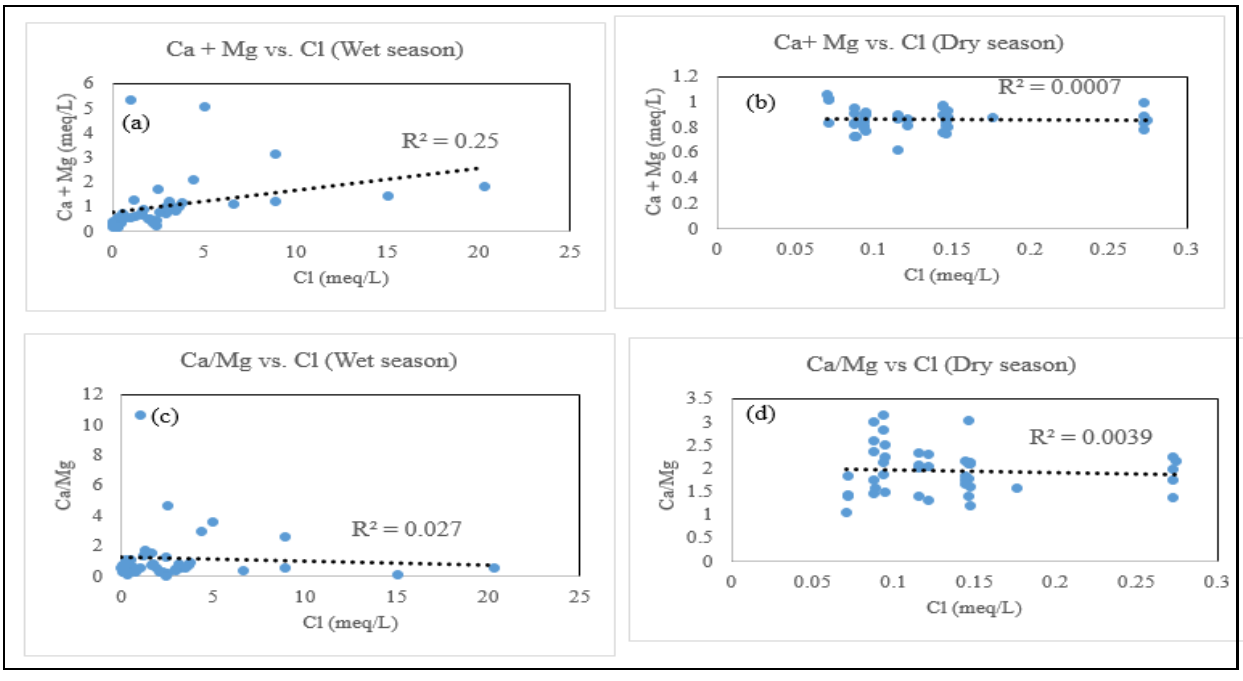

Figure 7.21: Ionic plots indicating the mixing of seawater with fresh water

Moreover, with the estimation of the mixing rate and quantification of the extent of seawater intrusion into the aquifer, the seawater fractions (freshwater) in the groundwater samples were undertaken using the popularly known conservative tracer 'chloride concentration' (Appello and Postma 2005) with the aid of the formula below:

$$f_{Seawater} = \frac{C_{Cl-sample} - C_{Cl-fresh}}{C_{Cl-sea} - C_{Cl-fresh}} \quad \text{.....7.4}$$

Where:

^{C}Cl-sample is the Cl^- concentration of the sample

^{C}Cl-sea is the Cl^- concentration of the ocean (15 582 mg/L)

^{C}Cl-fresh is the Cl^- concentration of freshwater (11 mg/L, sample no. 28). This sample had the lowest EC value (Appendix E).

It was revealed from equation 7.4 that the contribution of seawater to the groundwater (seawater/ brackish water fraction) varied from 0 % (GW27) at the eastern segment away from the saline source to 17.70 % (GW8) at the central parts in proximity to the brackish surface waters areas. This connotes freshness of the phreatic aquifer in the eastern domain, while western and central parts indicated mixing between the brackish water and the shallow groundwater. Interestingly, the highest value of $f_{seawater}/f_{brackishwater}$ corresponds with the highest measured values of Cl^- and EC (720 mg/l and 3284 µS/cm, respectively) in the central parts of the study in proximity to the lagoon (GW 8). Generally, the higher saline water ingress indicator values were recorded for groundwater samples in the proximity of the lagoon and creeks (GW 1, GW 5, GW 6, GW 8, GW 13, GW 19, and GW 35). This confirms that interaction occurs between brackish surface waters and the congruent water-table aquifer. In addition, the maximum percentage of the mixing ratio of 17.70 % recorded at (GW 8)

further supported that salinity of the phreatic aquifer is of brackish water source especially from the lagoon and the creeks.

7.6 Geostatistical Analysis of the Results

To facilitate further understanding of the different water types, statistical analysis (factor analysis) was used to evaluate the hydrochemical results. This is because the geostatistical method simplifies and organises large geochemical data sets to enhance the quality of interpretation (Amadi, 2010). The statistical analysis was performed using SPSS package (version 16.0) for Windows. The use of factor analysis is to sort out hydrochemical processes and relationships of the analysed groundwater data and it has been successfully employed over the past couple of years (Lawrence and Upchurch, 1982; Saad and Turgeon, 1988; Amadi, 2011). The original data matrix is then reduced from an 'n' variable necessary to describe the N samples to a matrix factor (m<n) for every N sample. It was also required to transform the variables so that the axes become orthogonal, which then accommodates the definition of new independent variables. By doing so, the first factor (highest factor loading) explains as much as possible of the total variance of the observations and the subsequent factors to explain as much as possible of the residual variances. The factor analysis involves three main essential steps: extraction of initial factors, rotation of factors and calculation of scores for each factor. In the present study, principal components were used for factor extraction, whereas varimax rotation with Kaiser Normalization was used for orthogonal rotation and results in uncorrelated factors (Usunoff and Guzman, 1989, Amadi et al., 2012). The computed factor scores for each observation expressed the importance of each factor at that observation site (Dalton and Upchurch, 1978; Amadi et al., 2012).

Table 7.4: Statistical summary of dry season analysis of physicochemical parameters

Parameters*	Minimum	Maximum	Mean	Standard deviation	Variance	Skewness	Kurtosis
pH	5.10	8.70	7.40	0.7495	0.562	-.807	1.868
TDS (mg/L)	114.00	1 324.00	361.42	203.2377	41 305.568	2.628	11.549
EC (µS/cm)	142.00	2 648.00	638.93	400.0473	60 037.824	3.157	15.117
Ca^{2+} (mg/L)	8.20	12.80	11.1452	1.23193	1.518	-0.650	-0.517
Mg^{2+} (mg/L)	2.44	6.23	3.6710	0.82596	0.682	0.689	0.945
Na^{+} (mg/L)	4.10	9.10	5.4695	1.22257	1.495	1.415	2.393
K^{+} (mg/L)	3.89	9.01	5.6598	1.61099	2.595	1.016	0.206
Cl^{-} (mg/L)	2.50	9.73	4.7207	2.07865	4.321	1.492	1.539
HCO_3 mg/L)	17.00	97.00	67.9762	24.60764	605.536	-0.779	-0.082

CO_3^{2-} (mg/L)	0.80	6.00	3.7071	1.46710	2.152	-0.405	-0.179
NO_3^- (mg/L)	0.00	0.06	0.0246	0.01853	0.000	0.420	-1.085
SO_4^{2-} (mg/L)	0.01	0.21	0.0893	0.07909	0.006	0.322	-1.531

Table 7.5: Summary of the rainy season physicochemical (macro and micro) variables statistical analysis in the study area

Parameters (mg/L)	Minimum	Maximum	Mean	Standard deviation	Variance	Skewness	Kurtosis
PH	5.40	8.60	7.26	0.62252	0.388	-0.564	1.259
TDS (mg/L)	69.00	1642.00	458.85	337.9012	114 177.208	1.788	4.058
EC (µS/cm)	111.00	3284.00	885.35	700.0847	490 111.695	1.781	3.722
Ca^{2+} (mg/L)	0.05	97.13	11.1194	20.00919	400.368	3.300	11.173
Mg^{2+} (mg/L)	1.29	16.77	5.9100	3.66580	13.438	1.107	1.267
Na^+ (mg/L)	0.15	14.77	2.4235	4.29013	18.405	2.374	3.978
K^+ (mg/L)	0.14	23.77	3.0422	5.88561	34.640	2.615	5.751
Cl^- (mg/L)	1.00	720.00	110.6500	143.05684	20 465.259	2.842	9.227
HCO_3^- (mg/L)	6.10	335.51	101.6807	89.87256	8 077.077	1.102	0.211
CO_3^{2-} (mg/L)	3.00	210.00	51.5465	48.85313	2 386.628	1.490	1.950
NO_3^- (mg/L)	0.00	108.70	22.3525	25.31828	641.015	1.684	2.535
SO_4^{2-} (mg/L)	0.00	88.00	36.2355	26.09299	680.844	0.148	-1.136
Zn^{2+} (mg/L)	<0.0001	.2390	0.008435	0.0378692	0.001	6.091	37.860
Cu^{2+} (mg/L)	<0.0001	1.3343	0.049310	0.2140334	0.046	5.998	36.793
Mn^{2+} (mg/L)	<0.0001	149.0000	3.734872	23.5573806	554.950	6.325	40.000
Fe^{2+} (mg/L)	<0.0001	1.5821	0.118042	0.2668982	0.071	4.507	23.970
Ni^{2+} (mg/L)	<0.0001	0.5660	0.050105	0.1420884	0.020	2.799	6.747
Cd^{2+} (mg/L)	<0.0001	0.0038	0.000223	0.0006327	0.000	4.924	27.417
Ag^+ (mg/L)	<0.0001	0.0349	0.002657	0.0069829	0.000	3.650	13.411
Pb^{2+} (mg/L)	<0.0001	0.0266	0.002072	0.0042939	0.000	5.014	28.652
Cr^{2+} (mg/L)	<0.0001	0.0469	0.014347	0.0142693	0.000	0.724	-0.340

It can be easily recognised from the data presented in Table 7.4 and Table 7.5 that the central tendency was estimated with the mean and that the data distribution was all positively skewed for both seasons, the exception being pH in the wet season and bicarbonate, carbonate and calcium in the dry season. This implies an essential even distribution of data around the central tendency devoid of domination by outliers (Amadi et al., 2012). The wide standard deviations and variances observed in TDS, EC, bicarbonates (HCO_3^-) in both seasons, and chloride (Cl^-), calcium (Ca^{2+}), carbonate (CO_3^{2-}), nitrate (NO_3^-), sulphate (SO_4^{2-}) and manganese (Mg^{2+}) in the wet season showed their randomly fluctuating concentration levels in the groundwater and/or suggested that the chemical composition of the groundwater was being regulated by multiple sources in the study area. In other words, the groundwater has a mixed origin that was possibly an infiltration of pure meteoric water affected by brackish water through flash floods or surface run-off. In each case, a normality test was carried out based on the combined effects of skewness and kurtosis. The observed significant difference

in the symmetrical parameters concerning iron, manganese, nickel, cadmium, silver, lead, and chromium in the wet season (Table 7.5) indicated a non-normal distribution; hence, giving credence to a possibility of their enrichment through anthropogenic sources (Amadi et al., 2012). Furthermore, factor analysis, being a useful tool for better understanding of the relationship among variables and revealing clusters that are mutually correlated with the data, was conducted to reveal an overall impression about assembling the samples in a multidimensional space defined by the analysed variables. This procedure reduces the overall dimensionality of the linearly correlated data by using a smaller number of new independent variables called varifactor, each of which is a linear combination of originally correlated variables (Table 7.6 and Table 7.7). Based on the Liu et al. (2003) factor, loadings may be classified into three, namely strong, medium, and weak, corresponding to >0.75, 0.75–0.50, <0.50 values, respectively. The main principal component loadings were also presented in simple statistical diagrams relative to PCA 1 for ease of assessment.

Table 7.6: Factor loading and communalities Factor for groundwater chemistry in the wet season

Parameters (mg/L)	F1	F2	F3	F4	F5	F6	F7	Com-munality
pH	0.556	-0.044	0.138	0.175	-0.355	-0.148	0.518	0.777
TDS (mg/L)	0.575	0.276	0.151	0.030	0.426	0.368	0.216	0.794
EC (µS/cm)	0.927	0.075	-0.075	-0.009	0.216	0.043	0.041	0.920
Ca^{2+} (mg/L)	0.160	0.790	0.106	0.145	-0.049	-0.044	0.215	0.733
Mg^{2+} (mg/L)	0.908	0.199	0.152	-0.070	0.077	-0.051	-0.032	0.901
Na^{+} (mg/L)	0.112	0.891	0.243	0.338	-0.017	-0.023	0.071	0.986
K^{+} (mg/L)	0.134	0.934	0.018	0.294	-0.011	-0.012	0.083	0.984
Cl^{-} (mg/L)	0.855	0.069	0.170	-0.024	0.065	-0.053	-0.053	0.775
HCO_3^{-} (mg/L)	0.903	0.097	0.013	-0.070	-0.126	0.249	0.004	0.908
CO_3^{2-} (mg/L)	0.923	0.067	-0.003	-0.062	-0.158	0.178	-0.061	0.921
NO_3^{-} (mg/L)	-0.008	-0.171	-0.040	-0.019	0.909	-0.079	-0.070	0.868
SO_4^{2-} (mg/L)	0.478	0.051	-0.079	0.062	0.481	-0.552	-0.060	0.781
Zn^{2+} (mg/L)	-0.065	0.713	-0.136	-0.157	0.009	-0.017	-0.098	0.556
Cu^{2+} (mg/L)	0.023	0.363	0.913	0.076	-0.0050	-0.011	0.013	0.974
Mn^{2+} (mg/L)	0.302	-0.079	-0.033	-0.011	-0.010	0.858	0.028	0.837
$Fe^{2+/3+}$ (mg/L)	-0.071	0.255	0.067	0.909	-0.083	0.016	0.028	0.909
Ni^{2+} (mg/L)	0.048	0.917	0.368	0.058	-0.051	-0.023	0.039	0.986
Cd^{2+} (mg/L)	-0.094	0.015	-0.051	0.941	0.073	-0.040	-0.025	0.904
Ag^{+} (mg/L)	0.215	0.810	0.279	-0.128	-0.054	0.028	0.003	0.801
Pb^{2+} (mg/L)	0.140	0.124	0.955	-0.046	0.001	0.016	0.055	0.952
Cr^{3+} (mg/L)	0.503	-0.432	-0.072	-0.136	-0.336	-0.215	-0.035	0.623
Faecal coliform	-0.127	0.160	0.023	-0.043	0.135	0.089	0.889	0.860
Eigenvalues	5.452	4.901	2.168	2.056	1.617	1.367	1.198	

% of variance	24.783	22.275	9.856	9.348	7.349	6.215	5.447	
Cumulative %	24.783	47.059	56.915	66.262	73.611	79.826	85.273	

Table 7.7: Factor loading and communalities for groundwater chemistry in the dry season

Parameters (mg/L)	F1	F2	F3	F4	F5	F6	Com-munality
TDS (mg/L)	0.828	0.093	-0.183	-0.094	-0.026	0.083	0.744
EC (µS/cm)	0.884	-0.050	0.113	0.096	-0.060	-0.129	0.825
Ca^{2+} (mg/L)	-0.297	0.024	0.588	-0.010	0.551	-0.176	0.769
Mg^{2+} (mg/L)	-0.028	0.150	0.091	0.033	-0.076	0.855	0.873
Na^{+} (mg/L)	0.015	0.233	0.091	0.178	-0.663	-0.530	0.817
K^{+} (mg/L)	-0.125	-0.521	-0.540	0.289	0.027	0.246	0.533
Cl^{-} (mg/L)	0.121	0.637	-0.055	-0.311	0.066	0.097	0.724
HCO_3^{-} (mg/L)	-0.016	0.155	-0.123	0.261	0.702	-0.135	0.866
CO_3^{2-} (mg/L)	-0.125	0.833	0.038	0.381	0.002	0.102	0.815
NO_3^{-} (mg/L)	-0.031	0.032	-0.025	-0.924	-0.127	-0.004	0.619
SO_4^{2-} (mg/L)	-0.023	-0.048	0.848	0.105	-0.186	0.220	0.770
Eigenvalue	1.586	1.690	1.354	1.256	1.123	1.077	
% Variance	14.574	13.508	13.096	11.911	11.838	11.039	
% Cumulative	14.574	28.082	41.179	53.090	64.928	75.968	

For this study, a factor loading of >0.5 was chosen as the parameters that influenced the factor. Seven-factor and six-factor components (Eigenvalue >1) emerged, accounting for in the wet and dry season, respectively (Tables 7.6 and 7.7).

In the wet season the first factor (F1) loading with 24.78 % of the total variance, showed higher loadings for TDS, EC, Mg^{2+}, Cl^{-}, HCO_3^{-}, CO_3^{2-}, pH and Cr^{3+}, depicting a large influence of natural and anthropogenic processes. The high concentration of Cl^{-}, Mg^{2+}, TDS, and EC is an indication that the groundwater was in contact with water of marine origin and, thus, a high possibility of intermixing between surface water run-off, flash floods and surficial groundwater of the study area is suggested. The high TDS value with a dominance of Mg^{2+}, Cl^{-}, HCO_3^{-} and CO_3^{2-} is mainly due to the impact of carbonate dissolution and leaching of salts into a permeable zone of the formation. Also, the pH of the water is suspected to have been influenced by calcite dissolution, organic matter, atmospheric precipitation, and anthropogenic activities.

The second factor (F2), which accounts for 22.28 % of the total variance, showed a high positive loading for Na^{+}, K^{+}, Ca^{2+}, Zn^{2+}, Ni^{2+} and Ag^{+}, and may indicate leaching of salts, while the enrichment of Na^{+} and K^{+} relative to Ca^{2+} may be due to the ion exchange process or derivatives from leaching of clay minerals since the aquifer are essentially hosted within the clay matrix of sand and clayey sand. The association of zinc, nickel and silver in this

factor reflects the mixing of domestic and industrial effluent with the groundwater in the wet season.

The third factor (F3) included a very strong loading from copper and lead and constituted 9.85 % of the total variance. This further indicated an anthropogenic input due to leachate from domestic waste discharge and decay of abandoned electronics, vehicle, and machine scraps.

The fourth factor (F4) was represented by iron and cadmium with 9.35 % of the total variance. The strong factor loading of >0.9 associated with both elements suggested common anthropogenic sources. The study area, being an industrial area, is characterised by industrial effluents disposal, sewage and land fill leachate, galvanised pipes, welding, battery and electroplating, all of which are the possible sources of these elements in the groundwater.

The fifth factor (F5) that accounts for 7.35 % of the total variance, showed a higher loading of nitrate. Nitrate enrichment in groundwater indicates anthropogenic sources (domestic, industrial, or agricultural) in the coastal aquifer because nitrate has no known lithological source.

The sixth factor (F6) associated with manganese, constituted 6.22 % of the total variance. This suggested anthropogenic sources which may be linked to leachate from domestic waste discharge and deterioration of abandoned electronics, vehicles, and machine scraps.

The seventh factor (F7), with a higher loading for faecal coliforms, accounted for 5.45 % of the total variance. The presence of faecal coliforms in groundwater indicates contamination by animal and human faeces (wastes).

In the dry season, the F1 factor showed a higher loading for TDS and EC, constituting 14.57 % of the total variance. The linear relationship between these parameters indicates high mineralisation due to weathering. As the TDS increases with more dissolution of minerals, the salinity equally increases and consequently increases the EC of the groundwater.

The F2 factor, enriched with CO_3^{2-} and Cl^-, constituted 13.51 % of the total variance, with a low loading of HCO_3^-, Na^+ and Mg^{2+}. This type of association might indicate gradual leaching of salts from the surface. However, it has a moderate but negative loading with respect to K^+. This may indicate a different source for the potassium which is likely to be derived from the sand-filled materials brought from the hinterland.

Factor F3 is represented by SO_4^{2-}, Ca^{2+} and K^+ with a total data variability of 13.10 %. The positive loading of SO_4^{2-} and Ca^{2+}, with a negative loading of K^+, denote their antithetic covariance. The positive loading of Ca^{2+} and SO_4^{2-} may not necessarily indicate dissolution or weathering of sulphate-bearing minerals such as gypsum and anhydrite, since the source of these rocks has not yet been known or reported in the study area. Possible sources of sulphate could be seawater. Besides anaerobic decomposition of organic wastes, municipality dumps, and dead plants could also release H_2S, which joins the oxic zone, and interacts with H_2O and dissolved oxygen to generate SO_4^{2-}. In the study area, we suggested atmospheric deposition, decomposition of organic wastes besides anthropogenic contribution from domestic aerosols and industrial wastes as the likely sources.

Factor F4, constituting 11.91 % of the total variance, was represented by a highly negative loading for NO_3^-, indicating an anthropogenic impact from a unique source and substantial reduction in NO_3^- contribution to the shallow groundwater in the dry season.

Factor F5 showed a higher loading for Ca^{2+} and HCO_3^-, constituting 11.84 % of the total variance. This may be indicating the dissolution of carbonate minerals in the presence of soil CO_2. It may also indicate the leaching of salt and further demonstrate the freshness of the aquifer. In addition, the significant negative loading between Ca^{2+} and Na^+ may be suggesting an ion exchange process.

Factor F6, constituting 11.04 % of the total variance, was enriched in Mg^{2+} with a negative loading for Na^+, Ca^{2+} and HCO_3^-, indicating ion exchange processes, leading to enhancement of Mg^{2+}.

In the present study, the extracted seven factors and six factors for the wet and dry seasons, respectively (eigenvalues >1) accounted for 82.27 % and 75.97 % of the total variance, revealing their significant contribution to the variance of groundwater hydrochemistry in the area. The remaining 15 and 5 factors with eigenvalues <1 for both the wet and dry seasons accounted for only 17.83 % and 24.13 % of the total variance that have a negligible influence on the groundwater. Similarly, the high communalities ranging between 0.556 and 0.984; 0.533 and 0.876 recorded for both wet and dry seasons, indicated that most of the variance of each variable is explained by the extracted factors.

The plot of dominant factors was undertaken in other to appreciate and identify the dominant chemical processes and common hydrogeochemical variables based on principal components

(Figure 7.22**a-e**). Figure 7.22**a** and 7.22**b** represent the wet season, while the dry season is represented by Figure 7.22**c-e**. Although, geogenic contribution plays a major in both seasons, however, the anthropogenic influence was equally prominent in the wet season.

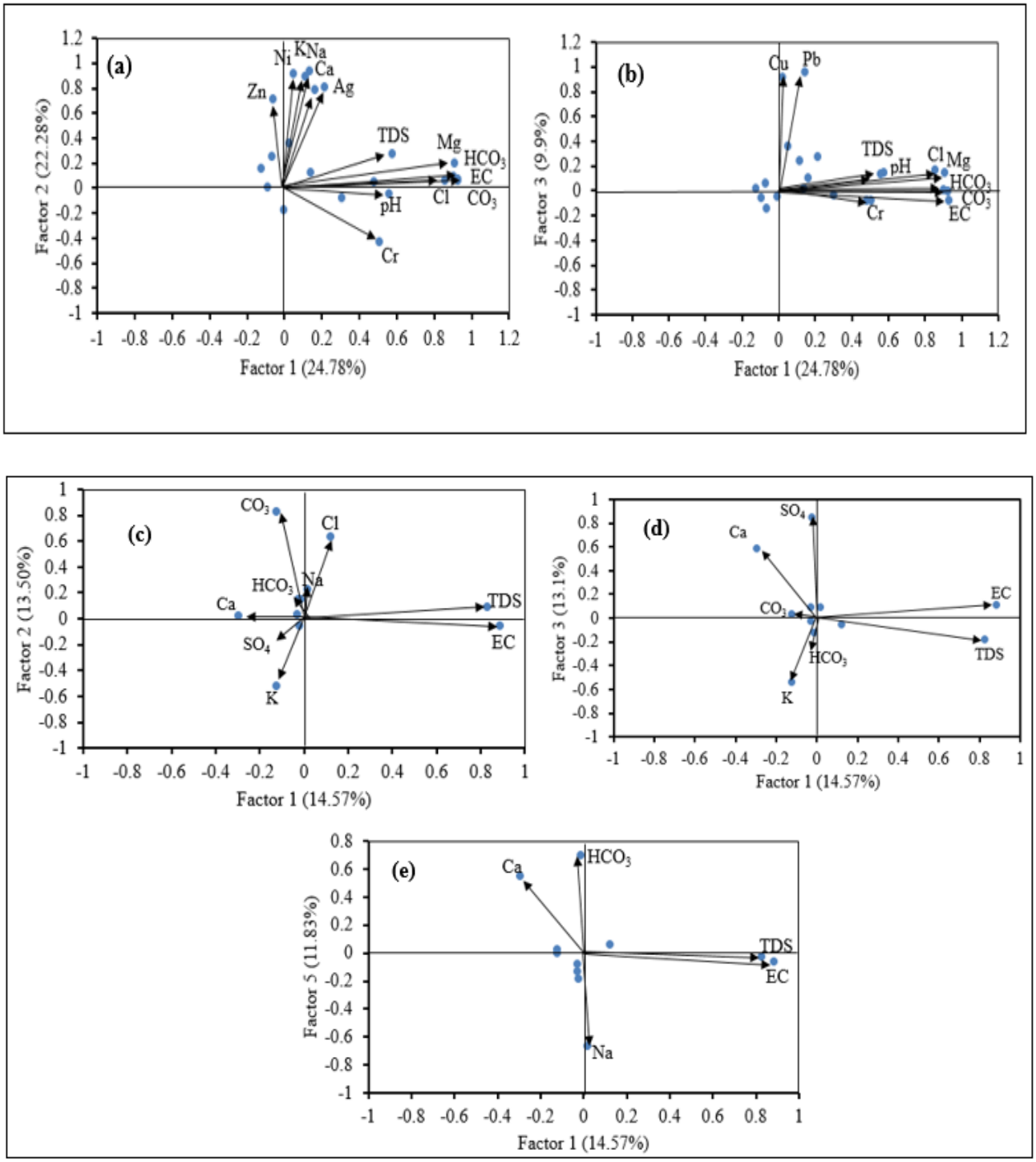

Figure 7.22: Loading plot of F2, F3 and F5 on F1 showing essentially geogenic contributions during the wet and dry seasons

7.7 Geochemical Modelling

The saturation indices (SI) is useful in predicting the possible chemical reactions and evolution of groundwater in a particular terrain. The SI result may be used as an indicator of rock types that were responsible for the dominance of chemical constituents in water chemistry (Belkhiri et al., 2012; Oke, 2015). The state of mineral saturation was calculated from the analytical data. The SI of a mineral indicates the degree of saturation of a particular mineral phase in an aqueous solution from where the trend of precipitation or dissociation of the mineral phases may be deduced. Calculation of equilibrium for carbonate minerals is dependent upon the accuracy of the chemical analysis and pH measurement (Sacks and Tihansky, 1996).

To assess the dissolution/precipitation of these minerals, their saturation indices were simulated using the thermodynamic software PHREEQC (Parkhurst and Appelo, 1999) and plotted on a graph in Figure 7.23**a** and **b**. The PHREEQC results show that water samples from the study area were undersaturated and supersaturated variably for all the rock minerals as presented in Table 7.8. It was observed that gypsum and halite (evaporate) were dominated by negative saturation indices (Table 7.8; Figures 7.23**a** and **b**) implying that the groundwater was essentially undersaturated with respect to these minerals for both seasons. This gives further credence to the anaerobic decomposition of organic matter as the possible source of sulphate to the groundwater. In the wet season, the groundwater appeared to be in transition from an under-saturation to super-saturation state with respect to calcite (Figure 7.23**a**).

The positive saturation index for calcite in the dry season and the majority of the samples in the wet season (Figure 7.23**b**) suggested that those samples are saturated with respect to calcite under present conditions. The supersaturation exhibited by calcite for both seasons in most samples under the present condition suggested longer residence times of the minerals relative to the undersaturated mineral constituents such as halite and gypsum in groundwater (Ako et al., 2012; Sunkari et al., 2019) and also indicated the dominance of carbonate weathering. Samples with negative saturation indices as observed for both seasons connoted shorter residence time for these minerals in the groundwater and may have been suddenly precipitated into the water (Sunkari et al., 2019).

In addition, the most negative SI values in groundwater exhibited by halite and gypsum may also imply an insignificant contribution of these minerals to the groundwater chemistry; however, they may exercise an important control over the dissolution of calcites and

bicarbonates in the study area. Furthermore, it was observed that the source of the chloride concentrations are not limited by mineral equilibrium and thus could not originate from brine water, therefore, Na^+ and Cl^- loading may be attributed to ion exchange resulting from mixed water (Jankowski et al., 1998). In summary, the modelling result agrees with deductions from various hydrochemical plots (Trilinear, Gibbs and Durov) and scatter diagrams that carbonate weathering and ion exchange are the major processes controlling the groundwater quality in the study area.

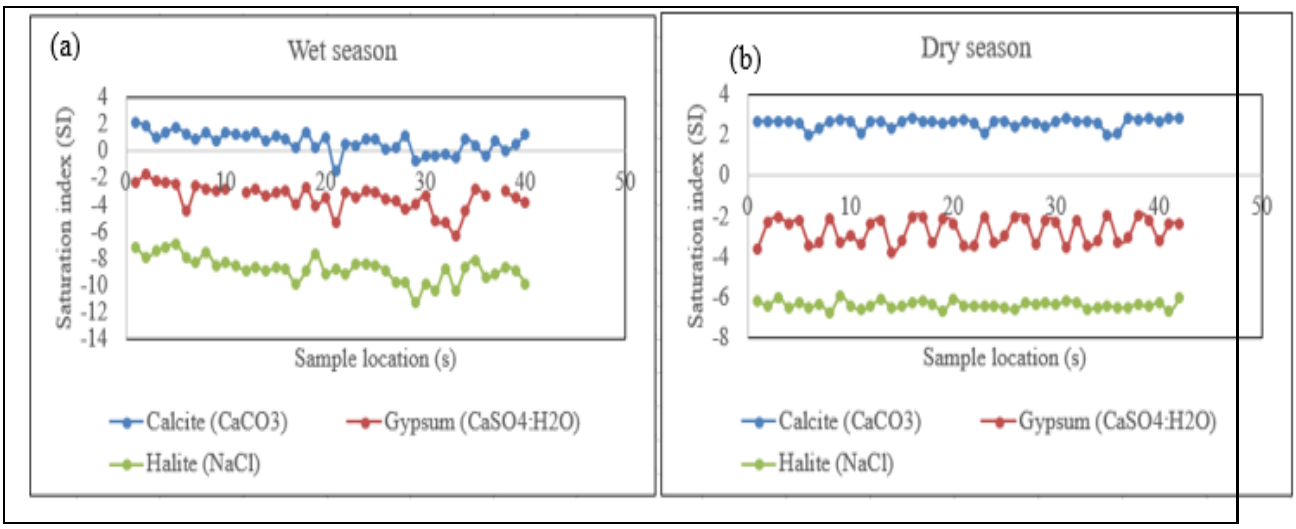

Figure 7.23: The saturation index of minerals in wet and dry seasons

Table 7.8: Saturation indices of aquifer rock minerals in both wet and dry seasons

Sample ID*	Wet season			Dry season		
	Calcite ($CaCO_3$)	Gypsum ($CaSO_4$:H_2O)	Halite (NaCl)	Calcite ($CaCO_3$)	Gypsum ($CaSO_4$:H_2O)	Halite (NaCl)
GW1	2.19	-2.28	-7.16	2.69	-3.6	-6.18
GW2	1.83	-1.73	-7.95	2.68	-2.32	-6.43
GW3	0.98	-2.26	-7.48	D	D	D
GW4	1.43	-2.31	-7.22	2.69	-2.08	-6.02
GW5	1.72	-2.46	-6.91	2.67	-2.36	-6.53
GW6	1.32	-4.44	-7.98	2.57	-2.23	-6.26
GW7	0.84	-2.61	-8.35	2.03	-3.44	-6.54
GW8	1.41	-2.78	-7.55	2.36	-3.31	-6.32
GW9	0.78	-2.94	-8.53	2.66	-2.17	-6.75
GW10	1.38	-2.82	-8.35	2.78	-3.33	-5.98
GW11	1.23	-	-8.61	2.71	-2.93	-6.4
GW12	1.11	-3.04	-8.89	2.12	-3.39	-6.64
GW13	1.39	-2.88	-8.68	2.66	-2.4	-6.44
GW14	0.77	-3.3	-8.96	2.69	-2.21	-6.09
GW15	1.11	-3.14	-8.71	2.36	-3.78	-6.52
GW16	0.9	-2.9	-8.85	D	D	D
GW17	0.3	-3.99	-9.9	2.68	-3.24	-6.47
GW18	1.44	-2.72	-8.97	2.87	-2.07	-6.28
GW19	0.26	-4.08	-7.66	2.69	-2.06	-6.19
GW20	1.06	-3.51	-9.17	2.66	-3.31	-6.33

Sample ID*	Wet season			Dry season		
	Calcite ($CaCO_3$)	Gypsum ($CaSO_4$:H_2O)	Halite (NaCl)	Calcite ($CaCO_3$)	Gypsum ($CaSO_4$:H_2O)	Halite (NaCl)
GW21	-1.52	-5.32	-8.74	2.59	-2.17	-6.71
GW22	0.53	-3.06	-9.2	2.68	-2.35	-6.08
GW23	0.41	-3.49	-8.48	2.77	-3.43	-6.41
GW24	0.87	-2.96	-8.44	2.61	-3.43	-6.41
GW25	0.85	-3.04	-8.5	2.1	-2.05	-6.48
GW26	0.19	-3.59	-8.95	2.68	-3.33	-6.4
GW27	0.28	-3.73	-9.74	2.7	-2.95	-6.54
GW28	1.14	-4.38	-9.82	2.41	-2.03	-6.61
GW29	-0.71	-3.92	-11.34	2.68	-2.14	-6.31
GW30	-0.3	-3.31	-9.87	D	D	D
GW31	-0.36	-5.25	-10.37	2.63	-3.36	-6.35
GW32	-0.2	-5.32	-8.77	2.42	-2.22	-6.28
GW33	-0.49	-6.26	-10.37	2.68	-2.32	-6.39
GW34	0.85	-4.49	-8.68	2.81	-3.54	-6.17
GW35	0.45	-2.86	-8.12	2.68	-2.25	-6.28
GW36	-0.3	-3.35	-9.4	2.68	-3.42	-6.57
GW37	0.73	-	-9.2	2.58	-3.2	-6.52
GW38	0.06	-3.02	-8.69	2.02	-1.98	-6.43
GW39	0.54	-3.45	-8.93	2.1	-3.28	-6.54
GW40	1.21	-3.85	-9.89	2.85	-3.08	-6.49
GW41	-	-	-	2.72	-1.93	-6.37
GW42	-	-	-	2.83	-2.19	-6.48
GW43	-	-	-	2.7	-3.18	-6.26
GW44	-	-	-	2.83	-2.41	-6.71
GW45	-	-	-	2.83	-2.36	-6.06

D = Dry hole

Chapter 8

HYDROGEOLOGICAL CONCEPTUAL MODELLING OF PARTS OF THE LAGOS COASTAL BASIN SYSTEM

8.1 General Statement

A conceptual model is a graphical representation of a groundwater flow system (Anderson et al., 2002) and it is an essential aspect in the characterisation of groundwater systems. A typical conceptual hydrogeological model represents a simplification of hydrogeological conditions and may be used to determine the hydrostratigraphic unit and their hydraulic properties and define the groundwater flow system (Anderson et al., 2002). This includes but is not limited to the identification of model boundaries, aquifer property variations and the relationship between groundwater and surface water. The success of any conceptual model depends on its ability to represent the actual field conditions. Despite the lack of data in the study area, an attempt was made to develop specific cross-sectional and generalised models for the area based on the available geological and hydrogeological data, as well as field observations. The combined knowledge gained from the preceding chapters and understanding of the hydrogeological settings of the area from literature played an important role in the model conceptualisation. The models were constrained and conceived in a stepwise manner as follows:

i. The lithological delineation into sands and clays was carried out by geophysical methods (VES, ERT and borehole logs) as presented in Chapter 5.

ii. The combination of the aforesaid methods was equally used to establish freshwater–saltwater interface, depth, and thickness, and lateral extent of saltwater intrusion.

iii. The average value of upper and lower saltwater interfaces from geophysical boreholes for every discerned locality was used to conceive the parallel model (Table 8.1), while the choice of boreholes adopted for vertical model prediction was based on the location of some selected boreholes fitting into the desire to enable vertical borehole correlation between the lagoon and the ocean from north to south (Table 8.2).

iv. Water level measurements were undertaken to ascertain the local groundwater flow directions and its influencing factors.

v. Complementarily, the hydrochemical and environmental isotopes result classified the lens of water with depth ranges conservatively from the surface to ≤10 m above the saline zone of intrusion, as essentially freshwater.

vi. Sequel to the guide enumerated above, three distinct models were proposed for the basin, namely the specific models constructed parallel and perpendicular to the ocean in a west–east and north–south directions, respectively (Figure 8.2 and Figure 8.3) and the generalised model (Figure 8.4). The conceptual models project the possible extent in kilometre of saline water intrusion in the study area.

8.2 Local Groundwater Flow Direction

Groundwater generally moves from higher regions to lower regions (elevations) and from higher pressure zones to lower pressure zones. The water table elevation and water pressure surface are known as the hydraulic head in groundwater hydraulics. Groundwater movement always occurs along the downward direction of the hydraulic head gradient. The hydraulic gradient is often, but not always, similar to that of the land surface (Harter, 2015).

The water level measurements enabled the determination of the local groundwater flow direction, location of recharges and discharge areas and the relationship between groundwater and surface water systems. The measurement of the water table depth in the unconfined aquifer obtained during this research was used to construct the water table (local groundwater flow direction) maps for the study area (Figure 8.1 and Figure 8.2). The dry season water level map was used in this study because groundwater would be relatively in a hydrodynamic equilibrium at the time. The maps established striking similarities in the flow pattern of groundwater for both dry and wet seasons. Contrary to the general north–south regional flow of groundwater characterising the coastal city of Lagos, the flow of groundwater within the study area exhibits a complex pattern resulting from different surface waters that encircle the terrain and the subsurface topographical features. The main drainage systems are the ocean, lagoon, and creeks, while others are canals, rivers, and streams. Generally, the groundwater direction is principally influenced towards the surface water with a dominant influence draining a particular area (gaining stream). The notable zones of influence could essentially be divided into two zones, namely lagoons, creeks and canals zone, and the ocean zone. The influence of the lagoon, creeks, and canals predominates from the west to the east of the study. These water bodies interact with the groundwater by receiving and transmitting water

to the neighbouring aquifers. Towards the eastern end of the study area at 3°45'00" E to 3°54'00" E the groundwater flows towards the river adjoining the lagoon in a south–north direction.

Furthermore, local groundwater mounds, from where groundwater flows in all directions, essentially in north-western to north-eastern and south-western to south-eastern directions, were observed across the study area (Figure 8.1 and Figure 8.2) and this further explains the complexity of the flow pattern characterising the study area. The variations are due to the directional changes of groundwater flow dictated by topographical features such as mounds and depressions and the occurrence of alternating clay layers. The observed depression zones is well in agreement with the deductions from previous authors in the study area, who suggested that the subsurface features were part of miogeoclinal depressions formed at the edge of the rifting Atlantic Ocean in the Quaternary (Kingston et al., 1983). Finally, the nature of recent alluvial sediments constituting the aquifer, enhances percolation and infiltration of rainfall to recharge the aquifer.

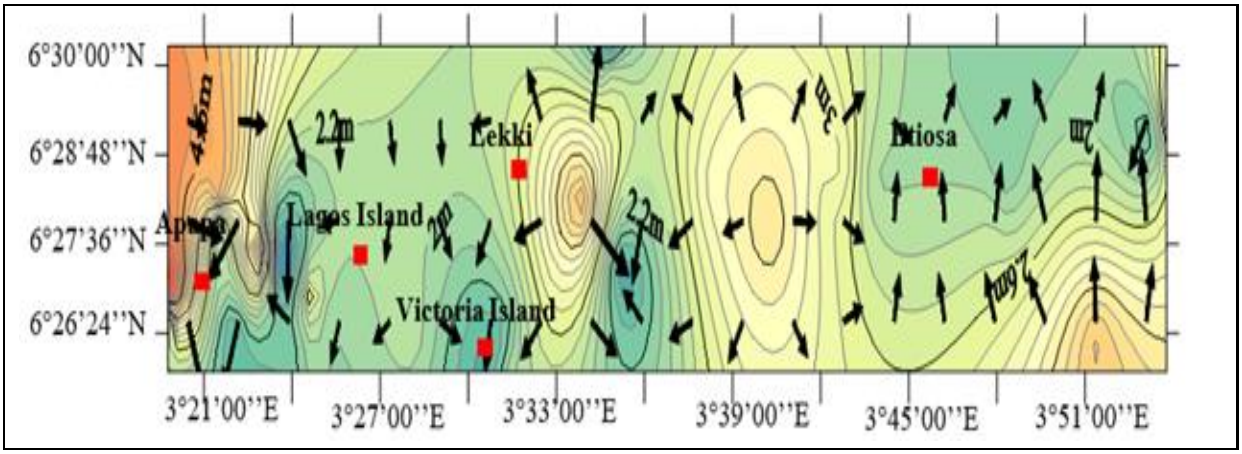

Figure 8.1: Groundwater level map showing groundwater flow direction in the study area: Dry season

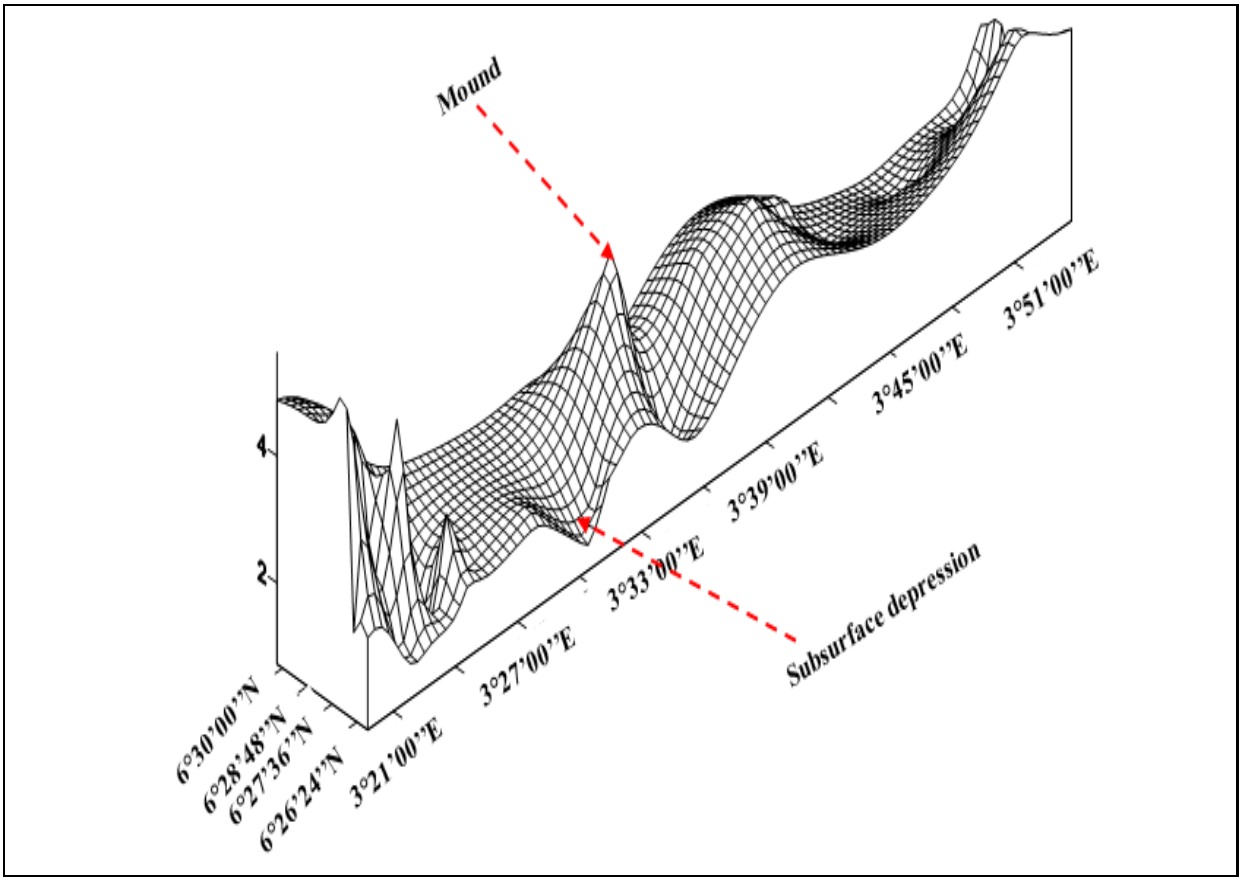

Figure 8.2: Three-dimensional view of the subsurface topographical features controlling groundwater flow direction in the study area: Dry season

8.3 Geological Conceptual Model for the Lagos Coastal Basin System

A hydrostratigraphic model of an area could be formulated by combining several geologic formations into a single hydrostratigraphic unit or a geologic formation may be subdivided into aquifers and aquicludes depending on the hydraulic characteristics of the study area (Anderson et al., 2002). A well-informed knowledge about the relationship between the different hydrostratigraphic units, lateral and vertical extent is indispensable for accurate conceptual model construction.

The extent and spatial distribution of the various hydrostratigraphic units for the LCB systems have been derived from various geophysical investigations and were similar to the previous geological and hydrogeological investigations carried out by some authors in the study area (Adelana et al., 2008; Oladapo et al., 2013).

Table 8.1: Model parameters for the parallel conceptual model

Location	Upper intrusion zone			Lower intrusion zone		
	Average upper interface depth (m)	Average lower interface depth (m)	Intrusion thickness (m)	Average upper interface depth (m)	Average lower interface Intrusion depth (m)	Intrusion thickness (m)
Apapa	28	108	80	-	-	-
Victoria Island A	30	110	80	133	168	35
Victoria Island B	68	120	52	128	157	29
Lekki	40	70	30	92	170	78
Ajah	15	65	40	82	120	38
Sangotedo	Unaffected	Unaffected	Unaffected	Unaffected	Unaffected	Unaffected
Awoyaya	Unaffected	Unaffected	Unaffected	Unaffected	Unaffected	Unaffected

The first predictive model (Fig8.3) was conceived parallel to the Ocean and along the coast and highlighted the lateral and vertical extent of seawater intrusion. From the model, it is apparent that two distinct major saltwater zones with varying thicknesses, separated by clay layer, existed beneath the study area between 15 m and 120 m; and 82 m and 170 m. Generally, the depth to the top of the first saline intrusion layer varied between 15 m and 68 m, while the upper interface of the second layer ranged between 82 m and 133 m. The thickness of the first and second intrusion layers from west to east varied between 80 m and 30 m; and 78 m and 29 m, respectively (Table 8.1). This is in agreement with the two zones of saltwater intrusion delineated by Adepelumi et al. (2008) at a depth ranging between 10 m and 30 m; and 60 m and 100 m in parts of the study area. However, the present study revealed wide spread incursion of saline water into the groundwater of Lagos coastal basin connoting possible advancement of saline invasion and further deterioration of the fresh coastal aquifer. Besides aquifer geometry and configuration, the greater impact of the intrusion observed at the western and central parts of the study area may be due to the location (proximity to saline/brackish water source) and human-induced activities. This may be supported by the reduction in the magnitude of the intrusion and it eventual pinch out at some points near the surface at a distance away from saline sources in the eastern limit of the study area.

The observed local saltwater intrusion of the phreatic aquifer above the main zone of intrusion wedge at Ajah (Fig8.3) was probably due to over-exploitation through excessive pumping of the limited fresh groundwater resources and thus perturbed the hydrodynamic

equilibrium in the aquifer and/or reduction in groundwater gradients, thus leading to the displacement of freshwater by saltwater (Adepelumi et al. 2008; Lee and Song 2007; Oyedele and Momoh 2009). In general, the depth to saline water is shallower in proximity to the saline source except where it is constrained by geological features. Therefore, groundwater users around the study area, targeting high quality and reliable fresh groundwater accessibility, may have to drill conservatively to various depths ranging between 150 m and 200 m.

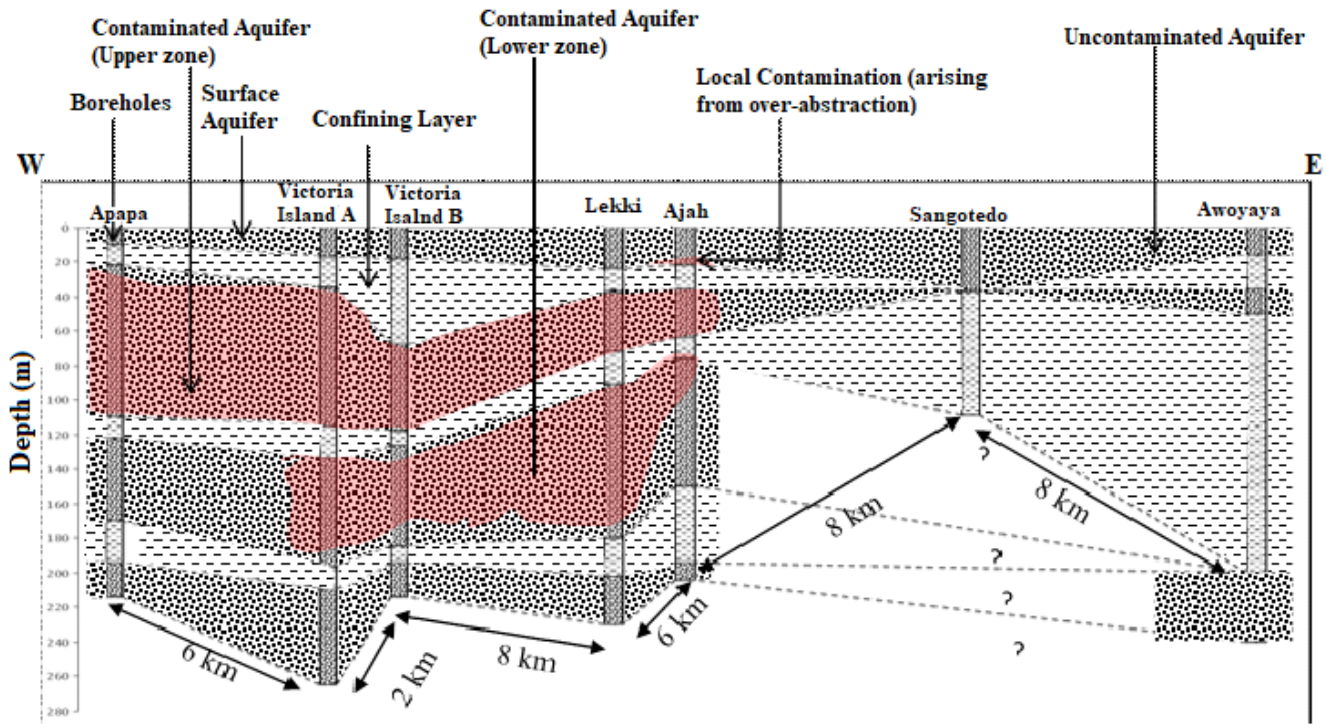

Figure 8.3: Conceptual cross-section model parallel to the ocean and lagoon

Table 8.2: Model parameters for a vertical conceptual model

Location	Upper interface depth (m)	Lower interface depth (m)	Intrusion thickness (m)
Ikoyi A	18	66	48
Ikoyi B	56	124	68
Victoria Island A	45	134	89
Victoria Island B	66	135	69

The vertical model (Fig 8.4) was conceived perpendicular to the Ocean in the south and the lagoon in the north to show the variations in the extent of saline intrusion. The interface depths from the north (lagoon) to the south (Ocean) ranged between 18 m and 66 m for the upper interface while the lower interface varies between 66 m and 135 m (Table 8.2). It is obvious that the saline incursion into the coastal aquifer in the central parts of the study area is bi-polar in nature, i.e. saline incursion from the brackish lagoon water in the north as well as the Atlantic Ocean in the south. The depth to the saline water zone was found to be relatively shallow, except where it was constrained by a confining bed. Greater thickness of the saline water zones between 69 m and 89 m was observed towards the ocean in Victoria Island, while less thick beds ranging between 48 m and 68 m separated by local clay units were found towards the lagoon coastline at Island and Ikoyi.

Local saltwater contaminations were observed at the phreatic aquifer suspected to be arising from over-abstraction of the groundwater (Fig 8.4). Unless proactive measures are taken, over-exploitation of groundwater in the study area may enhance the possible occurrence of regional/local land subsidence. Over-pumping of groundwater can lead to land subsidence as reported in many groundwater aquifers around the world (Galloway et al. 1999; Galloway and Burbey 2011). The saline invasion of fresh coastal aquifer as deduced from the geophysical logs is consistent with the hydrogeochemical study of the shallow groundwater in parts of the area under investigation by Oyeyemi et al. (2015) who attributed high TDS and Cl concentration ranges between 10405 mg/l and 12005 mg/l and 432 mg/l and 724 mg/l, respectively to interaction between saline/brackish water and freshwater.

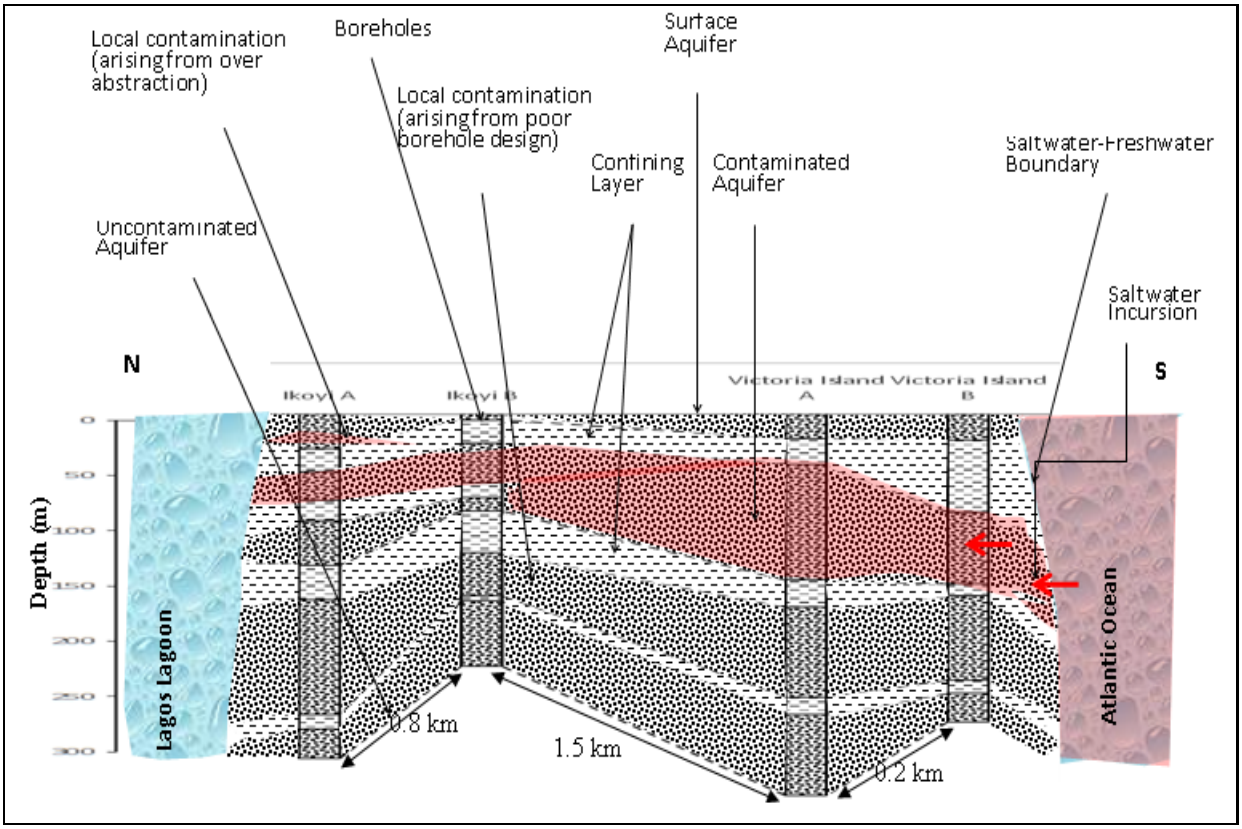

Figure 8.4: Conceptual cross-section model perpendicular to the ocean and lagoon

The generalised conceptual model (Figure 8.5) for the study area explains the possible interaction between groundwater and surface water bodies. The model was developed based on the understanding of the hydrogeology of the area harnessed from previous work and deductions from geophysical investigations, hydrogeochemical studies, groundwater flow direction, and environmental isotope data from the present study. Based on the model concepts, the basin was subjected to intrusion from the lagoon in the northwest, and creeks and canals connected to the lagoon in the south-west and the ocean in the south. This showed that saltwater interacted with a freshwater aquifer through several pathways, including lateral invasion, upward coning, and infiltration/percolation from coastal water. The model also revealed, as expected, that the aquifer close to the saline lagoon and creek waters suffers from acute saltwater intrusion. This suggested an interaction between the surface water bodies and the coastal fresh groundwater. The severity of the intrusion is thus prominent at the western limit and central parts of the area where all the tributaries are connected to the saline parts of the lagoon, linking the Atlantic Ocean via a commodore channel. The salinity of the surface water bodies depends on the amplitude and direction of the Ocean tides (Oyedele and Momoh, 2009). The effect of tidal fluctuations is most pronounced at the shoreline and

decreases with increased distance inland from the coast evident from the gradual decrease in EC values of both surface water and groundwater away from the Ocean.

Also, another salinity contributory factor worthy of note is the occasional coastal flooding resulting from climatic change which led to a rise in the sea level and its consequent transgression in a landward direction. When the sea level rises, the freshwater–saltwater interface is pushed landward, and freshwater zones of the aquifer are displaced by saltwater. When this occurs, the ocean surge will inundate the coastal lowlands, erode beaches, exacerbate coastal flooding and infiltrate into the subsurface. This, as well as excessive drafting of groundwater (combined), makes the problem worse. In general, the predicted models were found to be in tandem with the complementary results from geophysical investigations, and chemical and environmental isotope studies undertaken in this research.

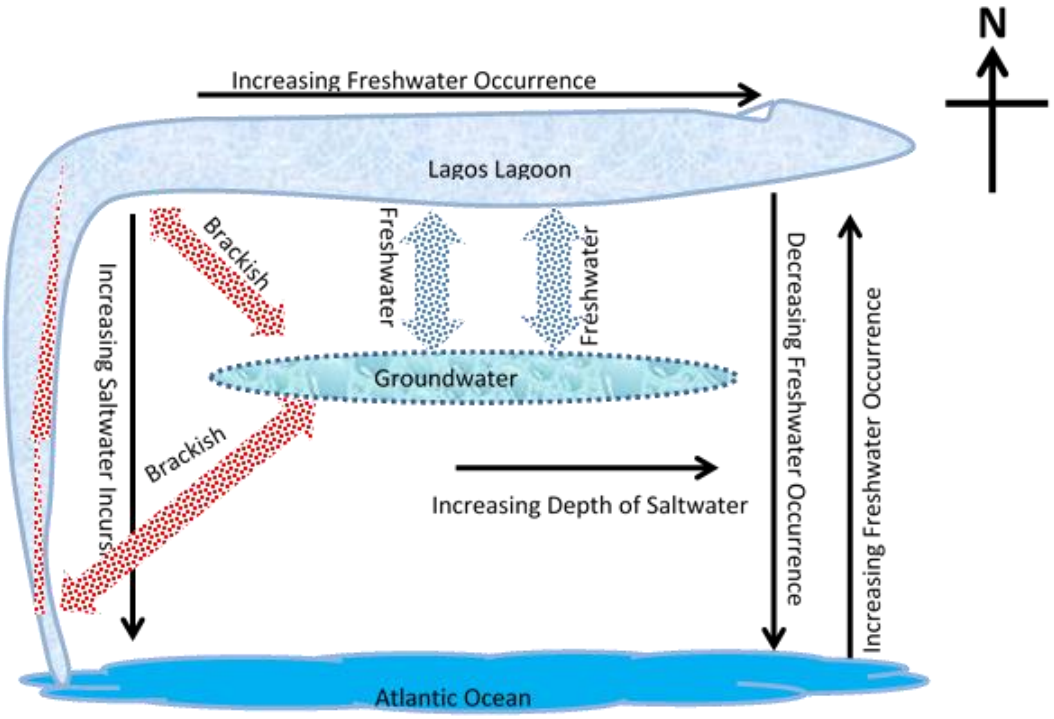

Source: Adapted from Yusuf et al. (2018)

Figure 8.5: General conceptual model for surface water and groundwater interaction in the study area

8.4 Model Limitations

The conceptual models connote the simplified versions of the physical system; therefore, it will inherently contain some degree of uncertainty. In an attempt to represent the real world

conditions or fixing boundary conditions in the conceptual models, uncertainties may be introduced to the system through the input parameters. The main challenge in the development of the groundwater model in the LCB has been the scarcity of reliable data for the study area. The poorly dated borehole logs prevented the ability to predict the systematic saline invasion of the fresh groundwater.

Chapter 9
SYNTHESIS AND CONTRIBUTIONS TO KNOWLEDGE

9.1 Synthesis

The geophysical, hydrogeochemical and environmental isotopes were interpreted and synthesised to characterise the hydrogeology of the LCB and understand interactions between surface water and groundwater systems. Geophysical studies which include VES, ERT and borehole logs were employed to reveal and delineate the hydrogeological characteristics of the subsurface and it was complemented by hydrochemical and environmental isotope analyses of both the subsurface and surface water. Due to the high vertical resolution but limited depth of penetration characterising the VES, it was constrained to the shallow aquifer, while the ERT with a higher and better horizontal resolution and borehole logs covered both the shallow aquifer and the deep groundwater. The major ions and trace metal analyses were carried out for the shallow groundwater and surface water, while environmental isotope studies were undertaken for the surface water, the shallow groundwater, and the deep groundwater systems.

Concerning the shallow aquifer, the qualitative interpretation of VES within the limited depth of penetration at <50 m in the study area revealed a four-layer and five-layer mode, and each distinct geoelectric layer represents alternation of sand, clayey sand, sandy clay, and clay soils. From the VES, the first layer has resistivity and thickness values ranging from 2.29 Ω m to 1 915 Ω m and 0.46 Ω m to 4.55 Ω m, respectively, which is typical of the top admixture of sandy and clayey soil. The admixture of the topsoil was confirmed by the ERT sections which also revealed the presence of both very low and very high resistive materials. The presence of very high resistive materials in places above the sand resistivity value was suggested to be alluvial or transported materials purposely brought from the hinterland for sand filling during land reclamation. The observation from the VES conforms to the lithological units delineated by the ERT, exhibiting an alternation between sand and clay from the surface to a maximum depth of 219 m penetrated by the equipment. In order to verify the alternation of lithological layers of the LCB aquifer systems observed on the VES and ERT sections, a geophysical borehole log analysis was undertaken. The borehole logs equally displayed alternation between sand, clayey sand and clay through deeper depth,

corroborating the existence of alternation in the subsurface lithological layers, and the importance of integrating several methods is further displayed. In addition, all the geophysical methods agreed that the distinct layers of sand and clayey sand are hosting the aquifers, while the clay and sandy clay are the confining units. Also, the shallow aquifers are essentially unconfined near the surface and semi-confined or confined with increasing depth and clay occurrence.

Regarding protective capacity and groundwater potential of the shallow aquifer evaluation, the higher values of longitudinal conductance (S) and transmissivity (Tr) recorded for the second aquifer relative to the first aquifer, indicated that the second aquifer is more protected, less vulnerable, and more prolific than the first aquifer. This may be justified by the increase in the thickness of clay layers to confine the underlying aquifer, and also an increase in the sand or clayey sand thickness with increasing depth that enhances transmissivity of the aquifer as reflected in the ERT and borehole log sections. The vulnerability of the phreatic aquifer was supported by high concentrations of some trace metals and faecal coliforms in the shallow groundwater.

Furthermore, the occurrence of a phreatic aquifer almost at the surface level with a depth as shallow as <0.5 m in places particularly in the rainy season, was confirmed by VES, ERT and the water table measurements. Based on the VES and ERT sections, the topmost parts of the shallow aquifer from the surface to a depth of 10–13 m are suggested to be freshwater devoid of saline intrusion, whereas the observed surficial low resistivity was suspected to be contributed by the clay layers/matrix or wastewater. In order to better understand the salinity nature of the phreatic aquifer, major ion analysis within the depth range from the surface to a depth of 10 m was carried out. The outcome agreed with the above submission, revealing essentially freshwater that is dominated by Ca-HCO_3 and Ca-Mg-HCO_3 water types, particularly in the dry season. This part of the shallow aquifer connotes the lens of a freshwater aquifer overlying the main saline zone of intrusion identified by Oteri and Atolagbe (2003) and Adelana et al. (2008). However, in the rainy season, the high rise in sea level and tidal influence, high-intensity rainfall, occasional flooding of the saline lagoon and creeks occurs leading to temporary salinity in the phreatic aquifer in proximity to the ocean. The occurrence of Ca-Mg-HCO_3, Ca-Mg-Cl-SO_4, mixed Ca-Mg-Cl, and Ca-Cl, water types indicated the mixing of water from various sources. Contrary to the observation of Oladapo et al. (2013) that the occurrence of saline intrusion begins from the surface around the study area, the present study surmised that the high salinity of the phreatic aquifer in the study area

particularly in the rainy season resulted from simple mixing of brackish water with the shallow groundwater through flash floods or surface run-off during heavy downpours or a rise in sea level during the wet season.

The interaction between the surface water and groundwater was further supported by the water level map, which shows the local groundwater flow in multiple directions against the general north–south flow movement of the surface water. The complex flow patterns exhibited by the groundwater were attributed to the subsurface topographical features. In addition, the elevated concentrations of NO_3^-, microbial counts, and some trace metals such as Mn^{2+} and Fe^{2+} recorded in the wet season for both surface water and groundwater in parts of the study area, are also a good pointer to mutual contact between the waters. Multivariate statistical analysis also revealed that mineral dissolution and anthropogenic input are the main sources of physicochemical indices and trace elements in the groundwater. In order to substantiate the interaction between surface water and groundwater in the wet season, an environmental isotope analysis was employed. The occurrence of shallow groundwater and the lagoon water in the same zone, particularly in the wet season, suggests rainfall as a common source of recharge and may also indicate possible interactions between the two water bodies. In addition to the existing ionic ratios, the use of Ca^{2+}+Mg^{2+} versus Cl^- and Ca^{2+}/Mg^{2+} ratios against Cl^- proposed in this study for marine impact evaluation, were equally employed for further deductions of marine influence on the surficial aquifer. In general, the dry season demonstrated a lack of intermixing between the brackish water and the phreatic groundwater, while the wet season samples revealed simple mixing between the phreatic aquifer and flash floods or surface run-off emanated from high-intensity rainfall and surface waters. Although geophysical studies revealed localised intrusion occurrence at the base of the first aquifer indicating stress on groundwater, this was not detected, neither by hydrochemical nor by environmental isotopes analyses. This may be due to the difference and variation between the location as well as the depth at which the water was sampled (<10 m) and the depth of localised saline intrusion at around 15 m below sea level.

Furthermore, the residence time of the water types characterising the shallow groundwater of the study area revealed recently recharged groundwater with mixing characteristics in places. The proposed ionic plot of Ca^{2+}/Ca^{2+}+HCO_3^- vs TDS further supported recharge to the groundwater under modern climatic condition. Although the recharge fell mainly in the modern climatic zone, only a few of the samples for both seasons were closer to the upper limit of the modern climatic zone (0.5), indicating their relative maturity in age. The plots of

^{3}H and ^{18}O were well in tandem with the ionic ratio, with most of the shallow groundwater samples plotted in the zone of the short residence time suggesting recently recharge water, while some samples exhibited and provided credence to mixing characteristics of the shallow groundwater with high residence time (relatively old water) indicated by plots near and below the inferred boundary. In addition, as presented in the relationship between ^{3}H and ^{14}C, it can be stated that water with a tritium concentration above 1 TU constitutes a shallow aquifer, with the exception of sample GW 13 and GW 25. The occurrence of a tritium value above 1 TU associated with low ^{14}C water, could be indicating a mixture of recent recharge with relatively old water preserved within the clay layers and/or probably resulted from over-exploitation of groundwater. The pressure indication on the groundwater was revealed by the conceptual cross models as localised saline upconing. This assertion agrees with the saline upconing phenomenon documented for the study area by previous authors (Oyedele, 2001; Oteri and Atolagbe, 2003; Adepelumi et al., 2008; Yusuf and Abiye, 2019). The ^{14}C values are relatively higher in shallow groundwater samples with a range from 59.1±2.2 pMC to 88± 2.4 pMC, resulting in an MRT ranging from 4350±10 to 1050±10 years, giving additional evidence to mixing of young water with relatively old water. Based on the ^{14}C data and temperature of recharge estimation, groundwater recharge into the shallow groundwater took place in the Holocene, with relatively warm climatic conditions.

Generally, groundwater in the LCB is isotopically enriched relative to the isotope compositions of groundwater studied in the northern parts of Nigeria (Kehinde, 1993; Goni and Edmunds, 2001; Adelana et al., 2003), but similar in isotopic compositions of groundwaters from the basement and sedimentary basin of southwestern Nigeria (Loehnert, 1988) and surprisingly similar to those reported from other west African countries such as Ghana (Acheampong and Hess, 2000; Jorgensen and Banoeng-Yakubo, 2001); Cotonou (Kpegli et al., 2018) and Togo (Akouvi et al., 2014). The observed south-north depletion of stable isotope compositions in groundwaters may be attributed to the altitude and continental effect of the incident rain.

Regarding the hydrogeochemical processes controlling the shallow aquifer, ionic evaluations revealed that the source of ions in groundwater is from weathering of carbonate rock, which belongs to the shallow marine Ewekoro limestone and that this formation contributed overwhelmingly to the solute hydrogeochemistry. In addition to the rock dominance and ion exchange processes revealed by the Gibbs diagram and Durov diagram, the above submission was verified using the two proposed methods by this study for the evaluation of the chemical

processes, namely: $Ca^{2+} + Mg^{2+}$ / total cation (TZ^{+}) and ionic plots of HCO_3^{-}/Ca^{2+} vs Ca^{2+}/Mg^{2+} and HCO_3^{-}/Ca^{2+} vs Ca^{2+}/Na^{+}. The observed 0.7 TZ^{+} and 0.8 TZ^{+} values in the first method for both seasons, and the occurrence of ionic plots essentially in the carbonate weathering zone as observed in the second method, supported the dominance of carbonate dissolution. In addition, geostatistical analysis of the water samples is an attestation to carbonate dissolution, ion exchange processes, surficial water interaction with groundwater and anthropogenic contribution as identified by various factors in the dry and wet seasons. The geochemical model results reflecting supersaturation of calcite for both seasons further indicated that carbonate weathering and ion exchange processes are the main processes that control groundwater chemistry, thereby supporting the aforementioned methods.

Concerning the source of carbon, the depleted $\delta^{13}C$ values which varied between -22.95 ‰ and -12.56 ‰ in the shallow unconfined groundwater, may probably be due to secondary CO_2 producing reactions such as carbonate weathering and cation exchange processes as the major factors of carbonate geochemistry within the coastal aquifer (Vogel and Ehhalt, 1963; Mook, 1976; Kehinde, 1993). Therefore, the depleted $\delta^{13}C$ values characterising the shallow groundwater give credence to the calcite dissolution and cation exchange process from carbonate rock. Although the effect of evaporation was revealed by the isotope study for both seasons, its impact on the geochemical process was minimal.

With respect to the deep groundwater, the source of recharge was associated with precipitation with little or no evaporation effect. From the plot of ^{3}H vs $\delta^{18}O$, the occurrence of the deep groundwater samples (DGW1 to DGW5) in Zone 2, explained the non-association of the rainwater and surface water with the deep aquifers in recent times. The non-association with modern climatic conditions may be further substantiated with the recharge temperature and ^{14}C activities, which suggested humid (Late Pleistocene–Holocene) as the recharge temperature and 12030±10 to 7400±10 years as the MRT for the deep aquifers.

As previously pointed out from the ERT sections, traverses taken parallel and perpendicular to the ocean and lagoon revealed that the zone of saline intrusion domiciled within the second aquifer and not from the surface. The complex spread pattern of intrusion in north–south, south–north, south–east and eastern directions, affirmed the complex groundwater flow pattern dictated by the subsurface topography. The saline intrusion occurrence within the depth range from 15 m to 90 m, 20 m to 60 m and 20 m to 70 m in the central parts of the

study area as observed in the ERT sections, indicated that the second aquifer is highly impacted. This is similar to the geophysical borehole logs, which identified an intrusion zone between 15 m and 152 m; and 14 m and 137 m freshwater–saline water interface along the A and B axes, respectively. The thickness of the intrusion increases from the western axis of the study, reaching a maximum at the central parts and eventually pinches out towards the eastern end of this study. However, saline intrusion expression at a shallower depth of 15 m may be suggesting an upward leakage from the underlying aquifer. The above suggestion may be giving credence from the isotope study where a low tritium value and low ^{14}C activities recorded by some of the shallow groundwater samples, indicate a mixture of underlying upconing older water with a younger overlying aquifer due to excessive abstraction of the groundwater (GW 13, GW 25 and GW 37).

Besides, regarding the deep aquifer, which in this context consists of both second and third aquifer systems with depths of ≥180 m, constitutes the five boreholes being used by the Lagos State Water Corporation to serve both the domestic and industrial water needs of the inhabitants around the study area. Aquifers at these depths are devoid of saline intrusion, a submission that is justified by the geophysical investigations such as the ERT section and borehole logs. Furthermore, the non-interaction status between the deep groundwater systems (DGW 1 to DGW 5), and both the brackish water and the seawater was reflected in the occurrence of the water bodies at different zones. This may be an attestation to the freshness and high yield quality of the deep groundwater systems which make it suitable for domestic and public consumption.

Finally, in order to represent the real field situation in a simplified pictorial format, the results described in the preceding chapters were put together to conceive the conceptual models towards delineating boundaries of the saline water intrusion zones for the LCB. From the models it was noted that the western and central parts of the study area were the worst impacted by the seawater incursion, particularly the second aquifer. The eastern limits of the study area essentially contains freshwater in the first and second aquifers because of the increase in distance away from the ocean and increase in the freshness of the surface water further away from the ocean. Therefore, it was established from the models that saline intrusion is a function of distance from the salinity sources, modified by aquifer configuration and aided by human activities. The conceptual models were well in agreement with other methods and conformed to the actual situation in the study area. Hence, it will be useful in decision-making in the search for fresh groundwater around the study area.

9.2 Research contributions to knowledge

The contributions to knowledge are subdivided into two aspects, namely specific contributions (contributions to the study area), and general contributions (contributions to the field of hydrogeology).

9.2.1 Specific contributions

These concern modification and application of the existing methods that were not known to the study area prior to the present doctoral research in the characterisation of the LCB groundwater systems. These are:

i. Pioneer application of the environmental isotope studies (Chapter 6) parts of which has been published in the Elsevier journal *Heliyon* under the title: "Origin and residence time of shallow groundwater resources in LCB, south-west Nigeria: An isotopic approach" (Appendix K).

ii. Application of a geochemical model to the study area delineating boundaries between freshwater and saline water zones for potential drillers and users (Chapter 7: section 7.7), parts of the work is under review in the Elsevier journal *Heliyon* under the title: "Hydrogeochemical and salinity appraisal of the surficial lens of freshwater aquifer along Lagos coastal belt, southwest, Nigeria" (Appendix L).

iii. The proposition of a general conceptual model for the study area (Chapter 6), part of which had been published in the Elsevier journal *Heliyon* under the title: "Origin and residence time of shallow groundwater resources in LCB, southwest Nigeria: An isotopic approach" (Appendix K).

iv. Derivation of the mathematical relationship between ambient temperature and ^{18}O ($\delta^{18}O = 0.54 * t - 17.6$ ‰) for the region towards deducing recharge temperature of an aquifer (Chapter 6, Equation 6.8), part of which is under review in the Elsevier journal *Groundwater for Sustainable Development*, under the title: "Application of environmental isotopes in sustainability assessment of the groundwater resources of Lagos coastal basin, south-west, Nigeria". This has a regional application beyond the study area and it may be adopted by all the countries bordering the Dahomey basin across West Africa, among which are the Benin Republic, Togo and Ghana (Appendix L).

9.3 General contributions

These contributions consist of the application of formula or methods proposed in this research for global use in the field of hydrogeology. These contributions are useful at any comparable sites around the world and they are listed as follows:

i. Proposed formula or methods for identification and differentiation between carbonate weathering, silicate weathering and evaporate dissolution. The two proposed methods are:

   - Cationic contribution evaluation method [$Ca^{2+} + Mg^{2+}$ vs Total cation (TZ^{+})].
   - Ionic ratio bivariate plots method (HCO_3^-/Ca^{2+} vs Ca^{2+}/Mg^{2+} and HCO_3^-/Ca^{2+} vs Ca^{2+}/Na^{+}).

ii. Proposed ionic ratio plot vs TDS to deduce recharge temperature (modern or humid climate) as written below:

   (Ca^{2+} / (Ca^{2+} +HCO_3^-) vs TDS).

iii. Proposed ionic ratio to evaluate marine impact in an aquifer:

   ($Ca^{2+} + Mg^{2+}$) vs Cl^- and Ca^{2+}/Mg^{2+} ratios against Cl^-.

The above methods have proved useful for the purpose of which they were proposed in this study. Therefore, they may be applied not only in sub-Saharan Africa and Africa but also across the world where similar investigations are demanded.

However, since there are no methods without their limitations and shortcomings, the herein presented conceptual models and the proposed methods were based on limited available data; they may be improved upon with more data accessibility.

Chapter 10
CONCLUSIONS AND RECOMMENDATIONS

10.1 Conclusions

Prior to this study, sparse and isolated data regarding geophysical, geostatistical and hydrochemical assessment of the aquifer systems in the LCB were available. Besides, aquifer assessments based on geochemical modelling and environmental isotopes towards enabling improved the groundwater characterisation are largely unavailable, if not completely lacking. Considering the heterogeneous nature of the LCB aquifer systems, it is important to note that this research was propelled at a local scale and conclusions were thus drawn. Similarly, the report on intrusion represents its status at the time of undertaking this study. Nevertheless, the presented approaches in this study produced a good idea about the hydrochemical processes and hydrogeological conditions in the LCB. Many findings are well in agreement with those of previous researchers at comparable sites. Having achieved the aim and objectives of the research through geophysical and hydrochemical methods in a general sense, the conclusions are, therefore, presented as follows:

The subsurface lithological units comprised an alternating sequence of clay, sandy clay/clayey sand, sand, and foreign materials, while sand and clayey sand are the major hosts of the aquifer systems in the basin. Four multilayered aquifer systems were reported for the LCB, two of which were mostly exploited by the inhabitants due to ease of assessment dictated by depths of occurrence. However, the surficial freshwater aquifer is more vulnerable to contaminants from the surface than the underlying aquifers.

Hydrochemical signatures showed slight differences in the composition of the lens of a freshwater aquifer between the dry and wet seasons due to the mixing of water from various sources with the shallow groundwater through flash floods and surface run-off. The interactions were further confirmed by high concentrations of some trace metals, microbial counts and NO_3^- in the sampled shallow groundwater. The major water types characterising the phreatic aquifer are Ca-HCO_3, Ca-Mg-HCO_3 and Ca-Mg-Cl-SO_4 water types for both seasons, while the lagoon and ocean waters are characterised by Mg-Cl and Na-Cl water facies, respectively. Interpretation from the Durov diagram, Gibbs diagram, geochemical model, ionic ratios, and plots, suggested that water–rock interactions and ion exchange

processes are the dominant factors controlling the shallow groundwater hydrogeochemistry. The proposed formula revealed carbonate weathering as the dominant chemical process controlling groundwater chemistry.

Reasons for concern are the saline intrusion and sustainability of the coastal aquifer systems. Regarding the occurrence of saline intrusion, the second aquifer at a depth of ≥20 m was severely impacted and this part of the subsurface may be regarded as the main zone of saline intrusion, where interaction between surface water and groundwater becomes imminent. Seawater intrusion above this specified depth (near-surface with a depth of <15 m) was attributed to groundwater over-exploitation. Direct evidence of upward migration of fluid reflected by the localised occurrence of saltwater intrusion at the base of the first aquifer as shown in the conceptual models and borehole logs, was a justification for pressure on the groundwater systems.

The extent and thicknesses of the intrusion revealed by the geophysical models and borehole logs affirmed that the western and central parts of the study in proximity to the salinity sources suffered more acute saline water intrusions than the eastern region; therefore, saltwater intrusion is found to be a function of distance to the ocean. The spread patterns of saline invasion as observed in the ERT sections suggested an active saline incursion into the shallow aquifer from the ocean and the brackish waters, respectively. The boundaries between the freshwater–saltwater interface and zones of intrusion have been clearly established by this study and, except for minor users, a reliable target in the quest for potential fresh groundwater, though varied, may conservatively drill deeper beyond a depth of 170 m. However, the limited available data is a reminder that the presented models are only a simplified starting point for improved future modelling.

Concerning the sustainability of the aquifer systems, which is essential for effective management of the basin water resource, the stable isotope results revealed that the LCB aquifer system contain water from a meteoric origin. The tritium analysis showed that post-1952 precipitation is an important source to the shallow aquifer but did not have a significant effect on the deep groundwater. The shallow aquifer recharge took place in the Holocene (modern climatic condition), with an MRT ranging from 4350±10 to 1050±10 years, whereas the deep aquifers are old water, the recharge of which occurred in the Late Pleistocene (humid temperature) with an MRT ranging between 12030±10 and 7400±10 years. Therefore, the shallow aquifer is being actively recharged and thus sustainable, while the

deep aquifer is being mined or depleted with increased groundwater exploitation due to rare or non-replenishment to the aquifer at this horizon.

10.2 Recommendations

Based on the present study, the following recommendations are proposed:

- There is a need for government to have an up-to-date database from where meteorology, hydrology, hydrogeology (e.g. permeability and resistivity values) and other related data may be accessed with ease for scientific research.
- The collection of continuous piezometric and groundwater level measurements, at least on a monthly or bi-monthly basis, should be undertaken by relevant government agencies such as Ministry of Environment, Lagos State Water Corporation (LSWC), Federal Environmental protection Agency (FEPA) etc. The maps generated from such data will allow and improve the accurate analysis of the hydrodynamic groundwater flow systems.
- There is a need to develop an improved hydrogeological conceptual model for the study area and the region at large, which will take into consideration input factors such as rate of withdrawal (various water uses), rate of recharge, precipitation, evaporation, evapotranspiration, groundwater outflow to the surface water and surface run-off.
- The saline intrusion resulted from a combination of climate change and over-exploitation of groundwater resources; hence, adequate policies and regulations, coupled with necessary enforcement, are urgently required from the government to ensure the sustainability of coastal fresh aquifers, otherwise, possible mismanagement might soil the whole study area.
- The occurrence of saline intrusion in the shallow aquifers necessitates adequate measures to be put in place in the design of boreholes by drillers in the affected areas, to shield saltwater zones from the coastal freshwater zones. This could be achieved by adequate delineation of the saltwater zone using geophysical techniques, followed by the standard grouting using cement and bentonite, allow 4-5 days for solidification before drilling through the grouted saline water zone to the fresh water aquifer. This procedure is expected to eliminate the saline water from the borehole to tap only the fresh water

- The groundwater resource managers should establish monitoring wells or boreholes along the coastline from the west to the east and at every one kilometre or less, up to 10 km away from the coastline in a north–south direction, from where periodic scientific surveys should be carried out to monitor the progression of saline water intrusion into the fresh groundwater resource around the study area.
- The debate on the mode of saline intrusion in the basin on "whether saline intrusion is recent or upconing from the seawater trapped (connate water) in miogeoclinal depressions during the regression and transgression period" could be put to rest through systematic isotope analyses of the intruded zones from the upper interface to the lower interface.
- Due to invaluable contributions of environmental isotopes to hydrologic and hydrogeologic studies, this research is strongly recommending GNIP–IAEA stations to be established in Lagos by the government, considering her strategic location along the West African transboundary coastal basin.
- Lastly, it is hoped that this research has contributed to the improved understanding of the groundwater systems in parts of the Dahomey basin and hydrogeology field at large; therefore, forming the basis on which government, corporate and individual decisions could be relied upon. Furthermore, future research around the study area could be built on this study and the proposed formula may be applied at every comparable site globally.

REFERENCE LIST

Abdalla, F., Al-Turki, A. and Al Amri, A. (2014) Evaluation of groundwater resources in the Southern Tihama plain, Saudi Arabia. *Arabian Journal of Geosciences*, vol. 8, pp. 3299-3310. doi:10.1007/s12517-014-1401-3

Abiola, O., Enikanselu, P.A. and Oladapo, M.I. (2009) Groundwater potential and aquifer protective capacity of overburden Units in Ado-Ekiti, Southwestern Nigeria. *International Journal of Physical Sciences*, vol. 4, no. 3, pp. 120-132.

Abiye, T.A. (2011) Provenance of groundwater in the crystalline aquifer of Johannesburg area, South Africa. *International Journal of the Physical Sciences*, vol. 6, no, 1, pp. 98-111. doi:10.5897/IJPS10.119

Abiye, T.A., Mengistu, H., Demlie, M.B (2011). Groundwater resource in the crystalline rocks of the Johannesburg area, South Africa. *Journal of Water Resources and Protection* 3(4): 199-212.

Abiye, T.A. (2013). Surface water and groundwater interaction in the upper Crocodile River basin. In T. Abiye, ed., *The use of isotope hydrology to characterize and assess water resources in South(ern) Africa*, pp. 141-163. Pretoria: Water Research Commission. (WRC Report No TT 570/13). http://www.wrc.org.za/wp-content/uploads/mdocs/TT%20570-13.pdf

Acheampong, S.Y. and Hess, J.M. (2000) Origin of the shallow groundwater system in the Southern Voltaian Sedimentary Basin of Ghana: An isotopic approach. *Journal of Hydrology*, vol. 233, , no. 1-4, pp. 37-53. doi:10.1016/S0022-1694(00)00221-3

Adebo, B.A. and Adetoyinbo, A.A. (2009) Assessment of groundwater quality in unconsolidated Sedimentary coasted aquifer of Lagos. *Scientific Research and Essay*, vol. 4, pp.314-319.

Adegoke, O.S. (1969) Eocene stratigraphy of Southern Nigeria. *Bur. Rech. Geol. Min., Mem*. vol. 69, pp. 23-47

Adegoke, O.S., Adeleye, D.R., Ejeagba, D.M., Odebode, M.O. and Petters, S.W. (1980) Geological guide to some Nigerian Cretaceous–Recent localities Shagamu quarry and

bituminous sands of Ondo and Ogun States, Nigeria. *Journal of Mining and Geology*, pp 1-44.

Adekeye, O.A. (2005) *Aspects of sedimentology, geochemistry and hydrocarbon potentials of cretaceous-tertiary sediments in the Dahomey Basin, Southwestern Nigeria*. Unpublished Ph.D. thesis, University of Ilorin.

Adekeye, O.A., Akande, S.O., Bale, R.B. and Erdtmann, B.D. (2005) Carbon and oxygen isotopic compositions and diagenesis of the Ewekoro Formation in the eastern Dahomey Basin, southwestern Nigeria. *Journal of Mining and Geology*, vol. 41, pp. 87-95.

Adelana, S.M.A. and Olasehinde, P.I. (2004) Assessment of aquifer system in parts of South-western Nigeria using isotope techniques. *Proceedings of the International Workshop on the Application of Isotope Techniques in Hydrological and Environmental Studies* held in UNESCO, Paris, France, September 6-8, 2004.

Adelana, S.M.A., Olasehinde, P.I. and Vrbka, P. (2003) Isotopes and geochemical characterization of surface and subsurface waters in the semi-arid Sokoto Basin, Nigeria. *African Journal of Science and Technology*, vol. 4, no. 2, pp.76-85. doi:10.4314/ajst.v4i2.15298

Adelana, S.M.A., Bale, R.B., Olasehinde, P.I. & Wu, M. (2005). The impact of anthropogenic activities over groundwater quality of a coastal aquifer in southwestern Nigeria. *Aquifer vulnerability and risk*. 2nd international Workshop and 4th Congress on the Protection and Management of Groundwater, Reggia di Colomo-Parma, 21-23 September 2005.

Adelana, S.M.A., Olasehinde, P.I., Bale, R.B., Vrba, P., Edet, A.E. and Goni, I.B. (2008) An overview of the geology and hydrogeology of Nigeria. In S.M.A. Adelana & A.M. MacDonald eds., *Applied Groundwater Studies in Africa*, IAH Special Publications in Hydrogeology, vol. 13. Leiden: CRC Press/Balkema, pp. 171-197.

Adeleye, D.R. (1975) Nigerian late Cretaceous stratigraphy and paleogeography, *AAPG Bulletin*, vol. 59/12, pp. 2302-2313.

Adeoti, L., Alile, O.M. and Uchegbulam, O. (2010) Geophysical investigation of saline water intrusion into freshwater aquifers: A case Study of Oniru, Lagos State. *Scientific Research and Essays*, vol. 5, no. 3, pp. 248-259.

Adepelumi, A.A., Ako, B.D., Ajayi, T.R., Afolabi, O. and Omotoso, E.J. (2008) Delineation of saltwater intrusion into the freshwater aquifer of Lekki Peninsula, Lagos. *Nigerian Journal of Environmental Geology*, vol. 56, no. 5, pp. 927-933.

Aderogba, K. (2012) Climate change and sustainable growth and development in Lagos Metropolis, Nigeria. *International Journal of Social Science & Education*, vol. 2, pp. 2223-4934.

Adewuyi, G.O., Oputu, O.U. and Opasina, M.A. (2010) Assessment of groundwater quality and saline intrusions in coastal aquifers of Lagos Metropolis, Nigeria. *Journal of Water Resources and Protection*, vol. 2. doi:10.4236/jwarp.2010.210100

Agagu, O.K. (1985) *A geological guide to bituminous sediments in southwestern Nigeria*. M.Phil. dissertation (unpublished), Department of Geology, University of Ibadan.

Ako, B.D., Adegoke, O.S. and Petters, S.W. (1981) Stratigraphy of the Oshosun Formation in southwestern Nigeria. *Journal of Mining Geology*, vol. 17, no. 1, pp. 97-106.

Ako, A.A., Shimada, J., Hosono, T., Kagabu, M., Ayuk, A.R., Nkeng, G.E., Eyong, G.E.T. and Takounjou, A.L.F. (2012) Spring water quality and usability in the Mount Cameroon area revealed by hydrogeochemistry. *Environmental Geochemistry and Health*, vol. 34, no. 5, pp. 615-639.

Akoteyon, I.S. (2013) Hydrochemical studies of groundwater in parts of Lagos, southwestern Nigeria. *Bulletin of Geography*, vol. 6, pp. 27-42. doi:10.2478/bgeo-2013-0002

Akoteyon, I.S., Mbata, U.A. and Olalude, G.A. (2011) Investigation of heavy metal contamination in groundwater landfill site in a typical sub-urban settlement in Alimosho, Lagos, Nigeria. *Journal of Applied Sciences in Environmental Sanitation*, vol. 6, no. 2, pp. 155-163.

Akouvi, A., Dray, M., Violette, S., de Marsily, G., Zuppi, G.M. (2008) The sedimentary coastal plain of Togo: example of a multilayered aquifer still influenced by a palaeo-seawater intrusion. Journal of Hydrology vol. 16, pp. 419-436.

Alegba, G. (2019) Govt. repairs roads, cleans Lagos highway drains to avert flooding. *Enviro News Nigeria*, 14 April. Available at https://www.environewsnigeria.com/govt-repairs-roads-cleans-lagos-highway-drains-to-avert-flooding/

Amadi, A.N. (2010) Effects of urbanization on groundwater quality: A case study of Port-Harcourt, Southern Nigeria. *Natural and Applied Sciences Journal*, vol. 11, no. 2, pp. 143-152.

Amadi, A.N. (2011) Assessing the effects of Aladimma dumpsite on soil and groundwater using water quality index. *Australian Journal of Basic and Applied Sciences*, vol. 5, no. 11, pp. 736-770

Amadi, A.N., Olasehinde, P.I., Yisa, J., Okosun, E.A., Nwankwoala, H.O. and Alkali, Y.B. (2012) Geostatistical Assessment of Groundwater Quality from Coastal Aquifers of Eastern Niger Delta, Nigeria. *Geosciences*, vol. 2, no. 3, pp. 51-59 doi:10.5923/j.geo.20120203.03

Anderson, M.P., Woessner, W.W. and Hunt, R.J. (2002) *Applied groundwater modelling: Simulation of flow and advective transport*. London: Academic Press.

Appelo, C.A.J. and Postma, D. (2005) *Geochemistry, groundwater and pollution*. 2nd edition. Balkema, Rotterdam.

Atakpo, E.A., Akpoborie, A. and Ayolabi, E. (2011) Evaluation of aquifer contamination using 2D geoelectric imaging at Ikeja, Lagos, Nigeria. *Journal of Environmental Hydrology*, vol. 19, paper 19. http://hydroweb.com/jehabs/atakpoabs.html

Avtar, R., Kumar, P., Singh, C.K., Sahu, N., Verma, R.L., Thakur, J.K., Mukherjee, S. (2013) *Hydrogeochemical assessment of ground-water quality of Bundelkhand, India using statistical approach, water quality exposure and health*. doi:10.1007/s12403-013-0094-2

Awosika, L., Adekoya, E.A., Adekanmbi, M.A., Dublin-Green, C.O., Folorunsho, R. & Jim-Saiki, L. (2000) *Study of Main drainage channels of Victoria and Ikoyi Islands in Lagos, Nigeria and their responses to tidal and sea level changes*. UNESCO-CSI: Environment and Development in Coastal Regions and Small Islands (p. 108). http://www.unesco.org/csi/act/lagos/drains2.htm

Ayolabi, E.A., Atakpo, E.A., Adeoti, L., Otobor, E.C. and Arerin, T. (2009) Groundwater quality assessment using predrilling electrical measurements. *Journal of Environmental Hydrology*, vol. 17, pp. 1-12.

Ayolabi, E.A., Folorunso, A.F., Odukoya, M.A. & Adeniran, A.E. (2013). Mapping the saline water intrusion into the coastal aquifer with geophysical and geochemical techniques: The university of Lagos campus case (Nigeria). *Springplus*, vol. 2, p. 433.

Babatunde, A.L., Okolue, M., Oyelola, O.T. and Odunlade, A.K. (2009) Pollution of groundwater through surface input from domestic, agriculture and industrial sources in FESTAC town Lagos, Nigeria. *International Journal of Applied Science*, vol. 3, no. 2, pp.19-59

Balogun, I.I. and Akoteyon, I.S. (2012) Assessment of groundwater quality in the lower coastal plain sand aquifer for varied uses. *Special Publication of the Nigerian Association of Hydrological Sciences*, pp. 299-315.

Banoeng-Yakubo, B., Yidana, S. M and Nti, E. (2009), An evaluation of the genesis and suitability of groundwater for irrigation in the Volta region, Ghana; Environ. Geol. 57, 1005–1010.

Barbecot, F., Marlin, C., Gibert, E. and Dever, L. (2000) Hydrochemical and isotopic characterisation of the Bathonian and Bajocian coastal aquifer of the Caen area (northern France). *Applied Geochemistry*, vol. 15, no. 6, pp. 791-805. doi:10.1016/s0883-2927(99)00088-8

Barrett, B., Heinson, G., Hatch, M., Telfer, A., 2002. Geophysical methods in saline groundwater studies: locating perched water tables and fresh-water lenses. Explor. Geophys. 33, 115–121.

Batayneh, A.T. (2006) Use of electrical resistivity methods for detecting subsurface fresh a saline water and delineating their interfacial configuration: A case study of the Eastern dead sea coastal aquifers. *Jordan Hydrogeology Journal*, vol. 14, no. 7, pp. 1277-1283.

Batayneh A.T. (2013) The estimation and significance of Dar-Zarrouk parameters in the exploration of quality affecting the gulf Aqaba coastal aquifer systems. *Journal of Coastal Conservation*, vol. 17, pp. 623-635.

Batayneh, A., Zaman, H., Zumlot, T., Ghrefat, H., Mogren, S., Nazzal, Y., Al-Taani, A. et al (2014) Hydrochemical facies and ionic ratios of the coastal groundwater aquifer of Saudi Gulf of Aqaba: implication for seawater intrusion. *Journal of Coastal Research*, vol. 293, pp. 75-87. doi:10.2112/jcoastres-d-13-00021.1

Belkhiri, L., Mouni, L. and Boudoukha, A. (2012) Geochemical evolution of groundwater in an alluvial aquifer: case of El Eulma aquifer, East Algeria. *Journal of African Earth Science*, vol. 66, pp. 46-55.

Billman, H.G. (1976) Offshore stratigraphy and palaeontology of the Dahomey Embayment, *Proc. 7th Micropaleontology Colloquim*, Ile-Ife, Nigeria, pp. 21-46.

Bloch, R., Fox, S., Monroy, J. and Ojo, A. (2015) *Urbanisation and urban expansion in Nigeria*. Urbanisation Research Nigeria (URN) Research Report. London: ICF International, Creative Commons Attribution-Non-Commercial-ShareAlike CC-BY-NC-SA https://core.ac.uk/ download/ pdf/ 96701289.pdf

Boomie, O. (2001) *Population of Lagos*. Motherland Nigeria (Online publication)

Buckley, D.K., Hinsby, K. and Manzano, M. (2001) Application of geophysical borehole logging techniques to examine coastal aquifer palaeohydrogeology. In: W.M. Edmunds and C.J. Milne, eds., *Palaeowaters in Coastal Europe: Evolution of Groundwater since the Late Pleistocene*. London: Geological Society. Special Publication 189, pp. 251-270.

Burger, H.R. (1992) *Exploration geophysics of the shallow subsurface*. Englewood Cliffs, NJ: Prentice Hall.

Cerling, T.E., Pedrson, B.L. and Damm, K.L.V. (1989) Sodium-calcium ionexchange in weathering of shales. Implications for global weathering budgets. *Geology*, 17, pp. 552-554.

Chen Z., Nie, Z., Zhang, G., Wan, L. and Mei, J. (2006) Environmental isotopic study on the recharge and residence time of groundwater in the Heihe River Basin, North Western China. *Hydrogeology Journal*, vol. 14, pp. 1635-1651.

Chidambaram, S., Kumar, G.S., Prasanna, M.V., Peter A.J., Ramanathan, A.L. and Srinivasamoorthy, K. (2009) A study on the hydrogeology and hydrogeochemistry of

groundwater from different depths in a coastal aquifers: Annamalai Nagar, Tamilnadu, India. *Environmental Geology*, vol. 57, pp. 59-73.

Clark, I.D. and Fritz, P. (1997) *Environmental isotopes in hydrogeology*. New York: Lewis. http://www.scirp.org

Coetsiers, M. and Walravens, K. (2006), Chemical characterization of the Noegene Aquifer, Belgium; Hydrogeol. 14, 1556–1568. Sci. 121(2), 491–507

Coode Blizard, Oteri, A.U. and Rofe, K.L. (1996) *Hydrogeological investigation of Lagos State*. Final Report, Vol. I & II.

Cook and Herczeg (2000)

Craig, H. (1961) Standard for reporting concentrations of deuterium and oxygen-18 in Natural waters. *Science*, vol. 133, pp. 1833-1834. doi:10.1126/science.133.3467.1833

Dalton, M.G. and Upchurch, S.B (1978) Interpretation of hydro-chemical facies by factor analysis. *Groundwater*, vol. 16 no. 4, pp. 228-233.

Dansgaard, W.F. (1964) Stable isotopes in precipitation. *Tellus*, vol. 16, pp. 436-468. doi:10.3402/tellusa.v16i4.8993

DeGroot-Hedlin, C. and Constable, S.C. (1990) Occam's inversion to generate smooth dimensional models from magnetotelluric data. *Geophysics* 55, pp. 1613-1624

Dorr, H., Sonntag, W. and Regenberg, W. (1987) Field study on the initial 14C content as a limiting factor in 14C groundwater dating (IEAA-SM-299/38). *Isotope techniques in water resources development*, Proceedings of a symposium, Vienna, 30 March-3 April, International Atomic Energy Agency, Vienna.

Doveton, J.H. and Prensky, S.E. (1992) Geological applications of wireline logs: A synopsis of developments and trends. *The Log Analyst*, vol. 33, no. 3, pp. 286-303.

Drever, J.I. (1997) *The geochemistry of natural waters: Surface and groundwater environments*. Englewood Cliffs, NJ: Prentice-Hall.

Durov, S.A. (1948) Classification of natural waters and graphical representation of their composition. *Doklady Akademii Nauk SSSR*, vol. 59, no. 1, pp. 87-90.

Edet, A., Nganje, T.N., Ukpong, A.J. and Ekwere, A.S. (2011) Groundwater chemistry and quality of Nigeria: A status review. African Journal of Environmental Science and Technology vol. 5, no. 13, pp. 1152-1169. doi:10.5897/AJESTX11.011

Echinger, L., Forster, M., Rast, H., Rauert, W. and Wolf, M. (1981) Experience gathered in low-level measurement of tritium in water. In: *Low-Level Tritium Measurement (IAEA-TECDOC–246)*. International Anatomic Energy Agency, pp. 43-65. http://www-naweb.iaea.org/napc/ih/documents/TECDOCS/TECDOC%200246%20Low%20level%20tritium%20measurement%201981.PDF

Edet, A., Nganje, T.N., Ukpong, A.J. and Ekwere, A.S. (2011) Groundwater chemistry and quality of Nigeria: A status review. *African Journal of Environmental Science and Technology*, vol. 5, no. 13, pp. 1152-1169. doi:10.5897/AJESTX11.011

Elueze, A.A. and Nton, M. (2004). Organic geochemical appraisal of limestones and shales in part of eastern Dahomey basin, southwestern Nigeria. *Journal of Mining and Geology*, vol. 40, no. 1, pp. 29-40. doi:10.4314/jmg.v40i1.18806

Emmanuel, B.E. and Chukwu, L.O. (2010) spatial distribution of saline water and possible sources of intrusion into a tropical freshwater lagoon and the transitional effects on the lacustrine ichthyofaunal diversity. *African Journal of Environmental Science and Technology*, vol. 4, no. 7, pp. 480-491.

Expectant Leaders Fundaytion (2014) *Lagos State*. [Online] https://raregeminitiatives.wordpress.com/tag/lagos-state/

Fasona, M., Omojola, A., Odunuga, S., Tejuoso, O, and Amogu, N. (2005) An appraisal of sustainable water management solutions for large cities in developing countries through GIS: the case of Lagos, Nigeria. *Sustainable Water Management Solutions for Large Cities*, Proceedings of symposium S2 held during the Seventh IAHS Scientific Assembly at Foz do Iguaçu, Brazil, April 2005. IAHS Publ. 293

Federal Environmental Protection Agency (1997) *Large marine ecosystem project for the Gulf of Guinea: Coastal profile of Nigeria*. Ceda Center for Environment and Development in Africa.

Fetter, C.W. (2001) *Applied hydrogeology*. 4th edition. Upper Saddle River, NJ: Prentice Hall.

Fisher, S.R. and Mullican, W.F. (1997) Hydrogeochemical evolution of sodium-sulfate and sodium-chloride groundwater beneath the northern Chihuahua desert, Trans-Pecos, Texas, U.S.A.: *Hydrogeology Journal*, vol. 5, no. 2, pp. 4-16.

Fitterman, D.V. and Deszcz-Pan, M. (2001) *Geophysical mapping of saltwater intrusion in Everglades National Park*. First International Conference on Saltwater Intrusion and Coastal Aquifers Monitoring, Modelling and Management, Morocco.

Fontes J.Ch. (1971) Un ensemble destine a la mesure de l'activite du radiocarbon naturel par scintillation liquide. *Revue de Geographie Physique et de Geologie Dynamiqu*e 2, XIII, fasc. 1, pp. 67-86.

Fontes, S.J.Ch. (1980) Environmental isotopes in groundwater hydrology. In: P. Fritz and J.Ch. Fontes, eds., *Environmental Isotope Geochemistry*, vol. I. New York: Elsevier, pp. 75-140.

Fontes, J.Ch. and Edmunds, W.M. (1989) *The use of environmental isotope techniques in arid zone hydrology – A critical review*. IHP-III Project 5.2. UNESCO, Paris, p. 75.

Frohlich, R.K., Urish, D.W., Fuller, J., Reilly, M.O (1994) Use of geoelectrical method in pollution surveys in a coastal environment. Journal of Applied Geophysics, 32, pp. 139–154.

Frohlich, R.K., and Urish, D.W (2002) The use of geoelectrics and test wells for the assessment of groundwater quality of a coastal industrial site. Journal of Applied Geophysics, 50, pp. 261–278.

Gabriel, H.F. and Khan, S. (2010) Climate responsive urban groundwater management options in a stressed aquifer system. Hydrocomplexity: New tools for solving wicked water problems. *Kovacs Colloquium*, July 2010. IAHS-AISH publication, pp. 166-168. Available at: https://iahs.info/uploads/dms/15058.39-166-168-Gabriel---Khan.pdf

Garrels, R.M. (1976) A survey of low temperature water mineral relations. In: *Interpretation of Environmental Isotope and Hydrogeochemical Data in Groundwater Hydrology* International Atomic Energy Agency, Vienna, pp. 65-84.

In: Stable isotope Hydrology, Deutrium and oxygen-18 in the water cycle, IAEA Technical reports series 210, pp.21-34

Gat, J.R. (1996) Oxygen and hydrogen isotopes in hydrologic cycle. *Annual Review of Earth and Planetary Sciences*, vol. 24, pp. 225-262. doi:10.1146/annurev.earth.24.1.225

Gat, J.R. (1981). Isotopic fractionation. In: J.R. Gat and R. Gonfiantini, eds. (1981) *Stable isotope hydrology: Deuterium and oxygen-18 in the water cycle*. IAEA Technical Reports Series No. 210. https://inis.iaea.org/collection/NCLCollectionStore/_Public/13/677/13677657.pdf?r=1

George, C.K. (2009) *The challenges of urbanisation in Nigerian urban centres: The Lagos mega city situation –A town planner's perspective*. Lagos: Libro-Gem Books.

Geyh, M. (2000) Environmental isotopes in the hydrological cycle. *Principles and applications. Groundwater – Saturated and unsaturated zone*. Technical documents in hydrology. UNESCO, vol. 6, p. 36.

Gibbs, R.J. (1970) Mechanisms controlling world water chemistry, *Science*, vol. 170, pp. 1088-1090.

Goldman, M., Gilad, D., Ronen, A. and Melloul, A. (1991) Mapping of seawater intrusion into the coastal aquifer of Israel by the time domain electromagnetic method. *Journal of Applied Geophysics*, vol. 28, no. 2, pp. 153-174.

Gonfiantini, R. (1978) Standards for stable isotope measurements in natural compounds. *Nature*, vol. 271, pp. 534-536.

Gonfiantini, R. (1986) Environmental isotopes in lake studies. In: P. Fritz and J.Ch. Fontes, eds., *Handbook of environmental isotope geochemistry*, vol. 2, The Terrestrial Environment. Amsterdam: Elsevier, pp. 113-168.

Goni, I.B. and Edmunds, W.M. (2001) The use of unsaturated zone solutes and deuterium profiles in the study of groundwater recharge in the semi-arid zone of Nigeria. Isotope-based assessment of groundwater renewal in water-scarce regions. In: *Low-*

Level Tritium Measurement (IAEA-TECDOC–246). International Anatomic Energy Agency, pp. 85-99. http://www-naweb.iaea.org/napc/ih/documents/TECDOCS/TECDOC%200246%20Low%20level%20tritium%20measurement%201981.PDF

Guan, H., Love, A.J., Simmons, C.T., Makhnin, O. and Kayaalp, A.S. (2010) Factors influencing chloride deposition in a coastal hilly area and application to chloride deposition mapping, Hydrology and Earth Systems Science Discussions, vol. 14, no. 5, pp. 801-813.

Habbeijam, G.M. (1972) The effect of anisotropy on square array resistivity measurements. *Geophysical Prospecting*, vol. 20, no. 2, pp. 249-266.

Hainsworth, L.J., Mignerey, A.C, Helz, G.R., Sharma, P. and Kubik, P.W. (1994) Modern chlorine-36 deposition in southern Maryland, USA. Nuclear Instruments and Methods in Physics Research. Section B: Beam Interactions with Materials and Atoms, vol. 92, issues 1-4, pp. 345-349.

Hallenburg, J.K. (1987) *Geophysical logging for mineral and engineering applications*. Tulsa, Oklahoma: Penn Well Books.

Hallenburg, J.K. (1992) Nonhydrocarbon logging. *The Log Analyst*, vol. 33, no. 3, pp. 259-269.

Han, D.M., Song, X.F., Currell, M.J., Yang J.L. and Xiao, G.Q. (2014) Chemical and isotopic constraints on evolution of groundwater salinization in the coastal plain aquifer of Laizhou Bay, China. *Journal of Hydrology*, vol. 508, pp. 12-27

Harikrishna, K., Ramprasad, D.N., Venkateswara, T.R., Jaisankar, G. and Venkateswara, V.R. (2012) A study on saltwater intrusion around Kolleru Lake, Andhra Pradesh, India. *International Journal of Engineering and Technology*, vol. 4, no. 3, pp. 133-139. 13.

Harter, T. (2015) Basic Concepts of Groundwater Hydrology , ANR Publication 8083 , FWQP Reference Sheet 11.1, University of California.

Hearst, J.R., Nelson, P.H. and Paillet, F.L. (2000) *Well logging for physical properties*. 2nd Edition. Chichester: Wiley.

Hem, J.D. (1985) Study and interpretation of the chemical characteristics of natural water. US Geological Survey Water-Supply Paper, 3rd. edition. https://pubs.usgs.gov/wsp/wsp2254/pdf/wsp2254a.pdf

Henriet, J.P. (1976) Direct application of Dar-Zarrouk parameters in ground water surveys. *Geophysical Prospecting*, vol. 24, no. 2, pp. 344-353. doi:10.1111/j.1365-2478.1976.tb00931.x

Herczeg, A.L., Barnes, C.J., Macumber, P.G. and Olley, J.M. (1992) A stable isotope investigation of groundwater–surface water interactions at Lake Tyrrell, Victoria, Australia. *Chemical Geology*, vol. 96, issues 1-2, pp. 19-32.

Hobday, D.K. (1979) Geological evolution and geomorphology of the Zululand coastal plain. In: B.R. Allanson, ed., *Lake Sibaya. Monographiae Biologicae*. London: Dr. Junk Publications.

Hwang, S., Shin, J., Park, I. and Lee, S. (2004) Assessment of seawater intrusion using geophysical well logging and electrical soundings in a coastal aquifer, Youngkwang-gun, Korea. *Geophysics and Geophysical Exploration*, vol. 35, no. 1, pp. 99-104.

IAEA (International Atomic Energy Agency). (1992) *Statistical treatment of data on environmental isotopes in precipitation*. Technical Reports Series, No. 331. http://www-naweb.iaea.org/napc/ih/documents/IAEA%20Monographs/TRS%20331%20Statistical%20Treatment%20of%20GNIP%20Data%201992.pdf

IAEA (International Atomic Energy Agency). (2000) *Global Network of Isotopes in Precipitation (GNIP*). The GNIP Database. http://www-naweb.iaea.org/napc/ih/IHS_resources_gnip.html

Ibrahim, E. (2008) Identification of groundwater spreading by using geoelectrical resistivity method. *International Journal of Engineering, Science and Technology*, 1, pp. 55-59.

Ikem, A., Osibanjo, O., Sridhar, M.K.C. and Sobande, A. (2002) Evaluation of groundwater quality characteristics near two wastes sites in Ibadan and Lagos, Nigeria. *Journal of Water, Air and Soil Pollution*, vol. 140, no. 1-4, pp. 307-333.

Isife, F.A. and Obasi, R.A. (2012) Electrical anisotropy of crystalline basement/sediment rock around Ifon, south-western Nigeria: Implications in geologic mapping and groundwater investigation. *ARPN Journal of Engineering and Applied Sciences*, vol. 7, no. 5, pp. 634-640.

Jackson, R.B., Carpenter, S.R., Dahm, C.N., McKnight, D.M., Naiman, R.J., Postel, S.L. and Running, S.W. (2001) Water in a changing world. Issues in Econology. Technical Report. *Ecological Applications, Ecological Society of America,* vol. 11, no. 4, pp. 1027-1045. doi:10.1890/1051-0761(2001)011[1027:WIACW]2.0.CO;2

Jankowski, J., Acworth, R.I. and Shekarforoush, S. (1998) Reverse ion exchange in a deeply weathered porphyritic dacite fractured aquifer system, Yass, in New South Wales Australia. In: G.B. Arehart and J.R. Hulston, eds., *Proceedings of 9th International Symposium on Water–Rock Interaction*, Taupo, New Zealand, pp. 243-246.

Japan International Cooperation Agency. (1999) The study on the national water resources master plan of the Federal Republic of Nigeria, March 1992 to March 1995 by Japan International Cooperation Agency.

Johansen, H.K. (1977) A man/computer interpretation system for resistivity soundings over a horizontal strafified [sic] earth. *Geophysical Prospecting*, vol. 25, no. 4, pp. 667-691. doi:10.1111/j.1365-2478.1977.tb01196.x

Jones, H.A. and Hockey, R.D. (1964) The geology of part of southwestern Nigeria. *Geological Survey of Nigeria Bulletin*, 31, pp. 1-101.

Jorgensen, N.O. and Banoeng-Yakubo, B.K. (2001) Environmental Isotopes (18O, 2H, and 87Sr/86Sr) as a tool in groundwater investigations in the Keta Basin, Ghana. *Hydrology Journal*, vol. 9, pp. 190-201. https://link.springer.com/article/10.1007/s100400000122

Jorgensen, D.G. and Petricola, M. (1995) Research borehole-geophysical logging in determining geohydrologic properties. *Ground Water*, vol. 33, no. 4, pp. 589-596.

Kalu, U. (2011) Lagos floods: Residents, Senate blame Fashola, Jonathan. *News*, 15 July. Vanguard Media Ltd. http://www.vanguardngr.com/2011/07/lagos-floods-residents-senate-blame-fashola-jonathan/ (Accessed 16/07/2020).

Kampsax-Kruger and Sshwed Associates (1977) *Underground water resources of the Metropolitan Lagos*. Final Report to Lagos State Ministry of Works.

Karanth, K.R. (1987) *Assessment, development and management of groundwaters*. New Delhi: Tata McGraw Hill.

Kehinde, M.O. (1993) Preliminary isotopic studies in the Bida Basin, Central Nigeria. *Environmental Geology*, 22, pp. 212-217. doi:10.1007/BF00767406

Kendall, C. and McDonell, J.J. eds. (1998) *Isotope tracers in catchment hydrology*. Amsterdam, The Netherlands: Elsevier Science B.V.

Kelle, G.V. and Frischknecht, F.C. (1966) *Electrical methods in geophysical prospecting*. Oxford: Pergamon.

Keys, W.S. (1990) Borehole geophysics applied to ground-water investigations. *Techniques of Water-resources Investigations of the United States Geological Survey*, Book 2, Chapter E2. Washington.

Keys, W.S. (1997) *A practical guide to borehole geophysics in environmental investigations*. Boca Raton, Florida: Lewis.

Kim, J., Kim, R, Lee, J. and Chang H. (2003) Hydrogeochemical characterization of major factors affecting the quality of shallow groundwater in the coastal area at Kimje in South Korea. Environmental Geology, vol. 44, pp. 478-489.

Kingston, D.R., Dishroon, C.P. and Williams, P.A. (1983) Global basin classification system. *AAPG. Bulletin*, vol. 67, pp. 2175-2193.

Klovan, J.E. (1975) R-mode and Q-mode factor analysis: In R.B. McCammaon, ed., *Concepts in geostatistics*. New York: Springer Verlag.

Kobr, M., Mares, S. and Paillet, F. (2005) Geophysical well logging – Borehole geophysics for hydrogeological studies: Principles and applications. In: Y. Rubin & S.S. Hubbard, eds., *Hydrogeophysics*, pp. 291-331. Amsterdam: Springer.

Kogbe, C.A. (1974) Paleo-ecologic significance of vertebrate fossil in the Dukamaje and Dange Formations (Maastrichtian and Paleocene) of northwestern Nigeria. *Journal of Mining and Geology (Nigeria)*, vol. 8, pp. 49-55.

Kpegli, K.A.R; Alassane, A; van der Zee, S.E.A.T.M; Boukari, M.; Mama, D. (2018) Development of a conceptual groundwater flow model using a combined hydrogeological, hydrochemical and isotopic approach: A case study from southern Benin: Journal of Hydrology: Regional studies vol.18, pp. 50 - 67

Krammer, K. (1997) Geophysikalische Bohrlochmessungen bei der Erkundung von Deponiestandorten. In: M. Beblo, ed., *Umweltgeophysik*. Berlin: Ernst.

Kulessa, B. (2007) A critical review of the low-frequency electrical properties of ice sheets and glaciers. *Journal of Environmental and Engineering Geophysics,* vol. 12, no. 1, pp. 23-36. doi:10 .2113/JEEG12.1.23

Lawrence, F.W and Upchurch, S.B (1982) Identification of recharge areas using geochemical factor analysis. *Groundwater,* vol. 20, pp. 680-687.

Lee, J.S., Chon, H.T., Kim, J.S., Kim, K.W. and Moon, H.S. (1998) Enrichment of potentially toxic elements in areas underlain by black shales and slates in Korea. *Environmental Geochemistry and Health*, vol. 20, pp. 135-147.

Lee, J.Y., Song, S.H., 2007. Evaluation of groundwater quality in coastal areas: implications for sustainable agriculture. Environ. Geol. 52 (7), 1231–1242.

Le Gal La Salle, C., Marlin, C., Leduce, C., Taupin J.D., Massault, M. and Favreau, G. (2001) Renewal rate estimation of groundwater based on radioactive tracers (3H, 14C) in an unconfined aquifer in a semi-arid area, Illumeden Basin, Niger. *Journal of Hydrology*, vol. 254, pp. 145-156. doi:10.1016/S0022-1694(01)00491-7

Li, P., Qian, H., Wu, J., Zhang, Y. and Zhang, H. (2013) Major ion chemistry of shallow groundwater in the Dongsheng coalfield, ordos basin, China. *Mine Water and the Environment*, vol. 32, 195-206. https://doi.org/10.1007/s10230-013-0234-8

Li, P., Wu, J. and Qian, H. (2016) Hydrochemical appraisal of groundwater quality for drinking and irrigation purposes and the major influencing factors: A case study in and around Hua County, China. *Arab Journal of Geoscience*, vol. 9, p. 15. doi:10.1007/s12517-015-2059-1.

Liu, W.X., Li, X.D., Shen, Z.G., Wang, D.C., Wai, O.W.H., Li, Y.S. (2003) Multivariate statistical study of heavy metal enrichment in sediments of the Pearl River Estuary. *Environmental Pollution*, vol. 121, pp. 377-388.

Liu, C.W., Jang, C.H., Chen, C.P., Lin, C.N., Lou, K.L., 2008. Characterization of groundwater quality in Kinmen Island using multivariate analysis and geochemical modeling. Hydrol. Process. 22, 376–

Lloyd, J.A. and Heathcote, J.A. (1985) *Natural inorganic hydrochemistry in relation to groundwater: An introduction*. New York: Oxford University Press.

Loehnert, E.P. (1988) Major chemical and isotope variations in surface and subsurface waters of West Africa. *Journal of African Earth Sciences*, vol. 7, pp. 588-589. doi:10.1016/0899-5362(88)90047-4

Loke, M.H. (2004) *Tutorial: 2-D and 3-D Electrical Imaging Surveys*. Revised Edition., Retrieved from www.gps.caltech.edu/classes/ge111/Docs DCResistivity_Notes.pdf

Loke, M.H. and Barker, R.D. (1996) Rapid least-squares inversion of apparent resistivity pseudosections by a Quasi- Newton method. *Geophysic Prospect*, vol. 44, pp. 131-152.

Longe, E.O. (2011) Groundwater Resources Potential in the Coastal Plain Sands Aquifers, Lagos, Nigeria. *Research Journal of Environmental and Earth Sciences*, vol. 3, vol. 1, pp. 1-7.

Longe, E.O., Malomo, S. and Olorunniwo, M.A. (1987) Hydrogeology of Lagos Metropolis. *Journal of African Earth Science*, vol. 6, no. 2, pp. 163-174. doi:10.1016/0899-5362 (87)90058-3

LWC (Lagos Water Corporation). (2009) We will soon deliver 15 new water works, Lagos State Water Corporation Alausa Alert, Dec. 30th, 2008 to Jan. 18th, 2009. Retrieved from: http://www.lagosstate.gov.ng

LWC (Lagos Water Corporation). (2011) LWC targets 733 millions daily by 2020. http://www.lagoswater.org/news.php?page=45

Majolagbe, A.O. and Osinbajo, O. (2012) Physicochemical quality assessment of groundwater based on land use in Lagos city, Southwest, Nigeria: *Chemistry Journal*, vol. 2, no. 2, pp. 79-86.

Maillet, R. (1947) The fundamental equation of electrical prospecting. *Geophysics* 12, pp. 529-556.

Mann, W.B., Urterweger, M.P. and Coursey, B.M. (1982) Comments of the NBS tritiated water standards and their use. *International Journal of Applied Radiation and Isotopes*, vol. 33, pp. 383-386.

Martinez, D.E. and Bocanegra, E.M. (2002) Hydrogeochemistry and cation exchange processes in the coastal aquifer of Mar Del Plata, Argentina. *Hydrogeology Journal*, vol. 10, pp. 393-408.

Martins, O. (2001) *Water resources management and development in Nigeria: Issues and challenges in a new millennium*. Paper Presented at the University of Abeokuta, Nigeria.

Martos, S.F., Bosch, P.A. and Calaforra, J.M. (1998) Hydrogeochemical processes in arid region of Europe (Almeria, SE Spain). *Applied Geochemistry*, vol. 14, pp. 735-745.

Masindi, K. and Abiye, T. (2018) Assessment of natural and anthropogenic influences on regional groundwater chemistry in a highly industrialized and urbanized region: a case study of the Vaal River Basin, South Africa. *Environmental Earth Sciences*, vol. 77, article 722 doi:10.1007/s12665-018-7907-3

Mazor, E. (1991) *Applied chemical and isotopic groundwater hydrology*. New York: Wiley.

Mohan, S.V., Nithila, P. and Reddy, S.J. (1996) Estimation of heavy metals in drinking water and development of heavy metal pollution index. *Journal of Environmental Science, Health Part A*, vol. 31, pp. 283-289. doi:10.1080/10934529609376357.

Mook, W.G. (1976). The dissolution-exchange model for dating groundwater with carbon-14: In *Interpretation of Environmental Isotope and Hydrochemical Data in Groundwater Hydrology*, Vienna, 27-31 January 1975, International Atomic Energy Agency, pp. 213-225.

Morse, J.W. and Mackenzie, F.T., eds. (1990) Geochemistry of sedimentary carbonates. *Developments in Sedimentology*, vol. 48. Elsevier.

Moujabber, M.E., Samra, B.B., Darwish, T. and Atallah, T. (2006) Comparison of different indicators for groundwater contamination by seawater intrusion on the Lebanese Coast. *Water Resources Management*, vol. 20, pp. 161-180.

Murat R.C. (1972) Stratigraphy and paleogeography of the Cretaceous and Lower Tertiary Sediments in Southern Nigeria. In: T.J.F. Dessauvagie and A.J. Whiteman, eds., *African Geology*. Ibadan: Ibadan University Press, pp. 251-266.

Murray, R. (E.C.), Swana, K., Miller, J., Talma, S. (A,S.), Tredoux, G., Vengosh, A, and Darreh, T. (2015) *The chemistry, isotopes and gases as indicators of deeper circulating groundwater in the Main Karoo Basin*. Report submitted to the Water Research Commission (WRC) of South Africa; WRC Report No. 2254/1/15. http://www.wrc.org.za/wp-content/uploads/mdocs/2254-1-15.pdf

National Emergency Management Agency

National Institute of Environmental Research (2007) *Investigation of the impact of mine discharges on Han-river watershed*, 1st year's report. Ministry of Environment, Seoul, Korea.

Nigeria Institute of Oceanography and Marine Research (year)

Nton, M.E. (2001) *Sedimentological and geochemical studies of rock units in the eastern Dahomey Basin, southwestern Nigeria*. Unpublished Ph.D, thesis, University of Ibadan.

Nwagwu, I. and Oni, T. (2015) *Lagos and its potentials for economic growth*. https://ng.boell.org/2015/07/02/lagos-and-its-potentials-economic-growth

Nwankwoala, H.O. and Udom, G.J. (2011) Hydrochemical facies and ionic ratios of groundwater in Port Harcourt, Southern Nigeria. *Research Journal Chemical Sciences*, vol. 1, no. 3, pp. 87-101. http://www.isca.in/rjcs/Archives/v1/i3/12.pdf

Nowroozi, A. A., Horrocks, S. B and Henderson, P (1999) Saltwater intrusion into the freshwater aquifer in the eastern shore of Virginia: a reconnaissance electrical resistivity survey. Journal of Applied Geophysics, 42, pp. 1–22.

Obaje, N.G. (2009) *Geology and mineral resources of Nigeria*. New York: Springer. doi:10.1007/978-3-540-92685-6

Obiefuna, J.N., Nwilo, P.C., Atagbaza, A.O. and Okolie, C.J. (2013) Land Cover Dynamics Associated with The Spatial Changes in the Wetlands of Lagos/Lekki Lagoon System of Lagos, Nigeria. *Journal of Coastal Research*, vol. 29, no. 3, pp. 671-679. doi:10.2112/JCOASTRES-D-12-00038.1

Odukoya, A.M. and Abimbola, A.F. (2010) Contamination assessment of surface and groundwater within and around two dumpsites. *International Journal of Environmental Science and Technology*, vol. 7, pp. 367-376.

Odukoya, A.M., Folorunso, A.F., Ayolabi, E.A. and Adeniran, E.A. (2013) Groundwater quality and identification of hydrochemical processes within University of Lagos, Nigeria. *Journal of Water Resources and Protection*, vol. 5, pp. 930-940.

Odumosu, T., Balogun, Y. and Ojo, K. (1999) *Lagos State in maps*. Ibadan: Rex Charles Publication.

Ogbe, F.G.A. (1970) Stratigraphy of strata exposed in the Ewekoro quarry, western Nigeria. In: T.J.F. Dessauvagie and A.J. Whiteman, eds., *African Geology*. Ibadan: Ibadan University Press, pp. 305-322.

Ogundele, F.O. (2012) Variation in the physico-chemical properties of Badagry and Ikorodu Soils, Lagos Nigeria. International Journal of Humanities and Social Science, vol. 2, no. 8, pp. 244-258. ijhssnet.com/journals/Vol_2_No_8_Special_Issue_April_2012/30.pdf

Okagbue, C.O. (1988) Hydrology and chemical characteristics of surface and groundwater resources of Okigwe area and environs, Imo state, Nigeria. In C.O. Ofoegbu, ed., *Groundwater and mineral resources of Nigeria* (Earth evolution science series), Brauschweig, Wisbadan: Vieweg & Teubner Verlag, pp. 3-14.

Oke, S.A. (2015) *Evaluation of the vulnerability of selected aquifer systems in the eastern Dahomey basin, south western Nigeria*. Unpublished Ph.D. thesis, Institute for Groundwater Studies, University of Free State, South Africa.

Oke, S.A., Vermeulen, D. and Gomo, D. (2016) Aquifer culnerability assessment of Dahomey basin using the RTt method. *Environmental Earth Science*, vol. 75, pp. 1-9

Okonkwo, A.C. and Ugwu, G.Z. (2015) Determination of Dar-Zarrouk parameters for prediction of aquifer protective capacity: A case of Agbani Sandstone Aquifer, Enugu State, Southeastern Nigeria. *International Research Journal of Geology and Mining*, (2276-6618), vol. 5, pp. 12-19.

Okosun, E.A. (1998) Review of the early tertiary stratigraphy of southwestern Nigeria. *Journal of Mining and Geology*, vol. 34, no. 1, pp. 27-35.

Okosun, E.A. (1990) A review of the Cretaceous stratigraphy of the Dahomey Embayment West Africa. *Cretaceous Research*, vol. 11, pp. 17-27.

Oladapo, M.I. and Akintorinwa, O.J. (2007) Hydrogeophysical study of Ogbese, Southwestern Nigeria. *Global Journal of Pure and Applied Science*, vol. 13, no. 1, pp. 55-61.

Oladapo, M.I., Ilori, O.B. and Adeoye-Oladapo, O.O. (2013) Geophysical study of saline water intrusion in Lagos municipality; *African Journal of Environmental Science and Technology*, vol. 8, no. 1, pp. 16-30.

Olorunfemi, M.O., Ojo, J.S. and Akintunde, O.M. (1999) Hydrogeophysical evaluation of the groundwater potential of Akure Metropolis, South-Western Nigeria. *Journal of Mining and Geology*, vol. 35, no. 2, 207-228.

Omatsola, M.E. and Adegoke, O.S. (1981) Tectonic evolution of the Cretaceous stratigragphy of the Dahomey Basin. *Journal of Mining and Geology*, vol 15, no. 2, pp. 78-83.

Omosuyi, G.O., Ojo, J.S. and Olorunfemi, M.O. (1999) Borehole lithologic correlation and aquifer delineation in parts of the coastal basin of SW Nigeria-implication for groundwater development. *Journal of Applied Science*, vol. 2, no. 2, pp. 617-626.

Onwuka, M.O., and Amadi, U.M.P. (1987) *Borehole design against saltwater intrusion in the coastal areas of Lagos State, Nigeria*. Proceedings of the NIWASA Symposium, Port Harcourt, 19-21 October, pp. 1-17.

Oteri, A.U. (1977) *Application of surface geophysics in hydrogeology*. University of London and Diploma Imperial College, London.

Oteri, A.U. (1981) Geoelectric investigation of saline contamination of a chalk aquifer by mine drainage water at Tilmanstone, England. *Geoexploration*, vol. 19, no. 3, pp. 179-192.

Oteri, A.U. (1986) Interpretation of electric logs in aquifers of the Dahomey Basin of Nigeria. *African Journal of Science and Technology*, Series B 2, pp. 54-61.

Oteri, A.U. and Atolagbe, F.P. (2003) *Saltwater intrusion into coastal aquifers in Nigeria*. Paper presented in the 2nd International Conference on Saltwater Intrusion and Coastal Aquifers: Monitoring, Modelling and Management, Merida, Yucatain, Mexico, March 30–April 2, 2003.

Oyedele, K.F. (2001) Hydrogeophysical and Hydrogeochemical investigation of groundwater quality in some parts of Lagos, Nigeria. African Journal of Environmental Studies, vol. 2, no. 1, pp. 31-37.

Oyedele, K.F. and Momoh, E.I. (2009) Evaluation of sea water intrusion in freshwater aquifers in a Lagoon Coast: A case study of the University of Lagos Lagoon, Akoka, Nigeria. *New York Science Journal*, vol. 2, pp. 32-42.

Oyeku, O.T. and Eludoyin, O.A. (2010) Heavy metal contamination of groundwater resources in a Nigerian Urban Settlement. *Africa Journal of Environmental Science and Technology*, vol. 4, no. 4, pp. 201-214.

Oyeyemi, K.D., Aizebeokhai, A.P. and Oladunjoye, M.A. (2015) Integrated and geochemical investigations of saline water intrusion in a coastal alluvial terrain, Southwestern Nigeria. *International Journal of Applied Environmental Sciences*, vol. 10, no. 4, pp. 1275-1288.

Parkhurst, D.L. and Appelo, C.A.J. (1999) User's guide to PHREEQC (version 2): A computer program for speciation, batch-reaction, one-dimensional transport, and inverse geochemical calculations. *USGS Water Resources Investigation Report* 99-4259. https://doi.org/10.3133/wri994259

Piper, A.M. (1944) A graphical procedure in the chemical interpretation of ground water analyses transactions. *American Geophysical Union*, vol. 25, pp. 914-923. doi:10.1029/TR025i006p00914

Prasanna, M.V., Chidambaram, S., Hameed, A.S and Srinivasamoorthy, K. (2010) Study of evaluation of groundwater in Gadilam basin using hydrogeochemical and isotope data. *Environmental Monitoring and Assessment*, vol. 168, pp. 63-90.

Repsold, H. (1989) Well logging in groundwater development. *International Contributions to Hydrogeology 9*. Hannover: Verlag Heinz Heise.

Reyment, R.A. (1965) *Aspects of the geology of Nigeria*. Ibadan: Ibadan University Press.

Rozanski, K., Johnsen, S.J., Schotterer, U. and Thompson, L.G. (1997) Reconstruction of past climates from stable isotopes records of palaeo-precipitation preserved in continental archives. *Hydrological Sciences Journal*, vol. 42, pp. 725-745.

Rubin, Y. and Hubbard, S.S., eds. (2005) *Hydrogeophysics*. Springer, Dordrecht (Water Science and Technology Library 50)

Russ, W. (1924) The geology of part of Niger, Zaria and Sokoto provinces with special reference to the occurrence of gold, Nigeria. *Geology Survey* Bulletin, No 27, p. 42.

Saad, M. and Turgeon, A. (1988) Application of principal component analysis to long-term reservoir management. *Water Resources*, vol. 24, no. 7, pp. 907-912.

Sacks, L.A. and Tihansky, A.B. (1996) Geochemical and isotopic composition of ground water, with emphasis on sources of sulfate, in the Upper Floridan Aquifer and Intermediate Aquifer System in Southwest Florida. *USGS Water Resources Investment Report 96-4146*.

Sample, E.D., Awopetu, M.S. & Harou, J. (2013) Modelling urban water use in developing countries. A preliminary application to Lagos Metropolitan Area of Nigeria. *International Journal of Engineering Research & Technology*, vol. 2, no. 11.

Samworth J.R. (1992) *Quantitative open-hole logging with very small diameter wireline tools*. SPWLA 33rd Annual Logging Symposium, Paper NN.

Schoeller, H. (1967) Qualitative evaluation of groundwater resources In *Methods and Techniques of Groundwater Investigation and Development*. *Water Resource Series*, vol. 33, pp. 44-52.

Schwartz, F.W. and Zhang, H. (2003). *Fundamentals of groundwater*. New York: Wiley.

Sheppard, S.M.F. (1986) Characterization and isotopic variations in natural waters. In J.W. Valley, H.P. Taylor and J.R. O'Neill, eds., *Stable isotopes in high-temperature geological processes*. Mineralogical Society of America, Reviews in Mineralogy, vol. 16, 165-183.

Shilaja, G., Laxminarayana, M., Patil, J.D., Erram, V.C., Suryawanshi, R.A. and Gupta, G. (2016) Efficacy of anisotropic properties in groundwater exploration from geoelectric sounding over trap covered terrain. *Journal of Indian Geophysical Union*, vol. 20, no. 5, pp. 453-461.

Slansky, M. (1962) Contributional etude Geological du Basin sedimentative corfell all Dahomey at du too Bearaeu du Kuchercher, *Geologue at Mounever memoir*, pp. 11-12.

Slaughter, A. and Odume, N. (2017) Why flooding in Nigeria is an increasingly serious problem. *The Conversation*, 15 August. Available at https://theconversation.com/why-flooding-in-nigeria-is-an-increasingly-serious-problem-82272

Sojobi, A.O., Balogun, I.I. and Salami, A.W. (2016) Climate change in Lagos State, Nigeria: What really changed. *Environmental Monitoring and Assessment*, vol. 188, no. 556, pp. 1-42.

Soladoye, O. and Ajibade, L.T. (2014) A groundwater quality study of Lagos State, Nigeria: *International Journal of Applied Science and Technology*, vol. 4, pp. 271-282.

SON (Standard Organization of Nigeria). (2007) *Nigerian Standard for Drinking Water Quality* NIS 554:2007 Standard Organization of Nigeria, Abuja, Nigeria Sujatha.

Sridharan M. and Nathan, M.D (2017) Hydrochemical facies and ionic exchange in coastal aquifers of Puducherry region, India: Implications for Seawater Intrusion. *Journal of Earth Systems and Environment*, vol. 1, Article 5. doi:10.1007/s41748-017-0006-x

Starinsky, A., Bielski, M., Lazar, B., Steinitz, G. and Raab, M. (1983) Strontium isotope evidence on the history of oilfield brines, Mediterranean coastal plains, Israel. *Geochimica et Cosmochimica Acta*, vol. 47, pp. 687-695. doi:10.1016/0016-7037(83)90103-5

Statistical Package for the Social Sciences SPSS-16. (2009) Chicago, USA: SPSS Inc.

Stearns, S. (2011) Lagos governor orders demolition of illegal buildings. *VOA News* (Voice of America), 12 July 2011. https://www.voanews.com/africa/lagos-governor-orders-demolition-illegal-buildings (Accessed 14/07/2011).

Stumm, W. and Morgan, J.J. (1981) *Aquatic chemistry: An introduction emphasizing chemical equilibria in natural waters*. 2nd edition. (Environmental Science and Technology: A Wiley-Interscience Series of Texts and Monographs). New York: Wiley.

Sunkari, E.D., Abu, M., Bayowobie, P.S. and Dokuz, U.E. (2019) Hydrogeochemical appraisal of groundwater quality in the Ga west municipality, Ghana: Implication for domestic and irrigation purposes. *Groundwater for Sustainable Development*, vol. 8, pp. 501-511.

Taylor, K., Hess, J. and Wheatcraft, S. (1990) *Evaluation of selected borehole geophysical methods for hazardous waste site investigations and monitoring*. Final Report, United States Environmental Protection Agency, EPA/600/490/029, Las Vegas, Nevada.

Teikeu, W.W., Njandjock, P.N., Bisso, D. and Atangana, Q.Y. (2012) Hydrogeophysical parameters estimation for aquifer characterization in hardrock environment: A case study from Yaounde, Cameroon. *Journal of Water Resources and Protection*, vol. 4, pp. 944-953. doi:10.4236/jwarp.2012.411110

Tijani, M.N., Loehnert, E.P. and Uma, K.O. (1996) Origin of saline groundwaters in the Ogoja area, Lower Benue Trough, Nigeria. *Journal of African Earth Sciences*, vol. 23, no. 2, pp. 237-252.

Ugada, U., Okpara, A.I., Emberga, T.T., Ibim, F.D., Omenikoro, A.I. and Womuru, E.N. (2013) Delineation of Shallow Aquifers of Umuahia and Environs, Imo River Basin, Nigeria, Using Geo-Sounding Data. *Journal of Water Resource and Protection*, vol. 5, pp. 1097-1109. doi:10.4236/jwarp.2013.511115

United Nations (1988) *Ground water in north and West Africa*. Natural Resources Water Series No. 18. New York: United Nations Department of Technical Co-operation for Development.

Urish, D. and Frohlich, R. (1990) Surface electrical resistivity in coastal groundwater exploration. *Geoexploration*, vol. 26, pp. 267-289.

Usunoff, E.J. and Guzman, A. (1989) Multivariate analysis in hydro- chemistry: An example of the use of factor and correspondence analysis. *Groundwater*, vol. 27, no. 1, pp. 27-34.

Van Nostrand, R.E. and Cook, K.L. (1966) *Interpretation of resistivity data*. U.S. Geological Survey Professional Paper 499, Washington, D.C.

Vereecken, H., Binley, A., Cassiani, G., Revil, A. and Titov, K. (2006) *Applied hydrogeophysics*. Dordrecht: Springer (NATO Science Series: Earth and Environmental Sciences IV 71)

Vogel, J.C. and Ehhalt, D. (1963) the use of the carbon isotopes in ground water studies. *Radio Isotopes in Hydrology*, Iaea, Vienna, pp. 383-395.

Walton, W.C. (1970) *Groundwater resource evaluation*. New York: McGraw Hill.

Watson, K.A. and Barker, R.D. (1999) Differentiating anisotropy and lateral effects using azimuthal resistivity offset Wenner soundings. *Geophysics*, vol. 64, no. 3, pp. 1-7

Weaver, J.M.C., Cave, L. and Talma, S. (2007) *Groundwater sampling a comprehensive guide for sampling methods*. Water Research Commission. Report No TT 303/07.

Werner, D. and Gallagher, M.R (2012) Characterisation of sea-water intrusion in the Pioneer valley, Australia using hydrochemistry and three-dimensional numerical modelling. *Hydrogeology Journal*, vol. 14, pp. 1452-1459.

Whiteman, A. (1982) *Nigeria: Its petroleum geology resources and potential*. Graham and Trotman, 1, pp. 166.

WHO (World Health Organization). (2017). *Guidelines for drinking water quality*. 4th edition. Geneva, Switzerland.

https://www.who.int/water_sanitation_health/publications/drinking-water-quality-guidelines-4-including-1st-addendum/en/

WHO (World Health Organisation). (2018) *A global overview of national regulations and standards for drinking-water quality*. Geneva, Switzerland. http://apps.who.int/iris/bitstream/handle/10665/272345/9789241513760-eng.pdf?ua=1

Yearsley, L.E. and Crowder, R.E. (1990) State-of-the-art borehole geophysics applied to hydrology. *Canadian/American Conference on Hydrology*, 18-20 September.

Yidana, S.M., Banoeng-Yakubo, B. and Sakyi, P.A. (2012).Identifying key processes in the

Hydrochemistry of a basin through the combined use of factor and regression models. J. Earth Syst.

Yusuf, M.A. & Abiye, T.A. (2019) Risks of groundwater pollution in the areas of Lagos, south western Nigeria. *Groundwater for Sustainable Development*, vol. 9, pp. 100-222. doi:10.1016/j.gsd.2019.100222

Yusuf, M.A., Bale, R.B. & Ibrahim, K.O. (2014) Hydrogeochemical characterization of surface water around canal and lagoon in parts of Lagos, Southwestern, Nigeria. *Science Focus*, vol. 19, pp. 119-128.

Yusuf, M.A., Abiye, T.A., Butler, M.J., Ibrahim, K.O. (2018) Origin and residence time of shallow groundwater resources in Lagos coastal basin, south-west Nigeria: An isotopic approach. *Heliyon*, vol. 4, e00932. doi: 10.1018/j.heliyon.2018.e00932

Zohdy, A.R. (1974) Use of Dar-Zarrouk curves in the interpretation of vertical electrical sounding data. *United States Geological Survey Bullettin*, 1313-D, vol. 41, no. 4.

Zohdy, A.R. (1989) A new method for automatic interpretation of Schlumberger and Werner sounding curves. *Geophysics*, vol. 54, pp. 245-253.

Zohdy, A.A.R., Martin, P.M. and Bisdorf, R.J. (1993) *A study of seawater intrusion using direct-current soundings in the southern part of the Oxnard Plain, California*. Open-File Report 93-524. U.S. Geological Survey. https://doi.org/10.3133/ofr93524

Zohdy, A.A.R., Eaton, G.P. and Mabey, D.R. (1990) *Application of surface geophysics to groundwater investigation*. 4th edition. USGS Publications.

Appendix A:

SAMPLING OF WATER FROM THE LAGOONS



Field photography showing surface water sampling at Lagos Lagoon



Field photography showing surface water sampling at Ajah Lagoon

Appendix B:

GROUNDWATER SAMPLING FROM WELLS



Field photography showing surface water sampling at Apapa



Field photography showing surface water sampling at Lekki

Appendix C:

CARBON SAMPLING STEPS, STABLE ISOTOPES OF OXYGEN-18 AND DEUTERIUM







Field photography water sampling for carbon dating

Appendix D:

I-GEOPHYSICAL PROFILING





Field photographyshoeing the process of geophysical data acquistion

II-Geophysical Data Interpretations showing Resistivity Curves

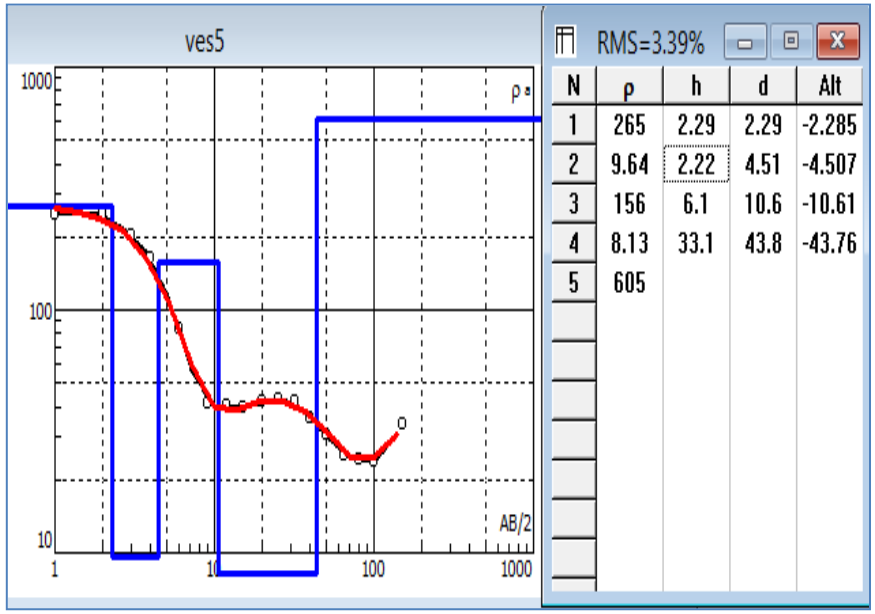

N	ρ	h	d	Alt
1	265	2.29	2.29	-2.285
2	9.64	2.22	4.51	-4.507
3	156	6.1	10.6	-10.61
4	8.13	33.1	43.8	-43.76
5	605			

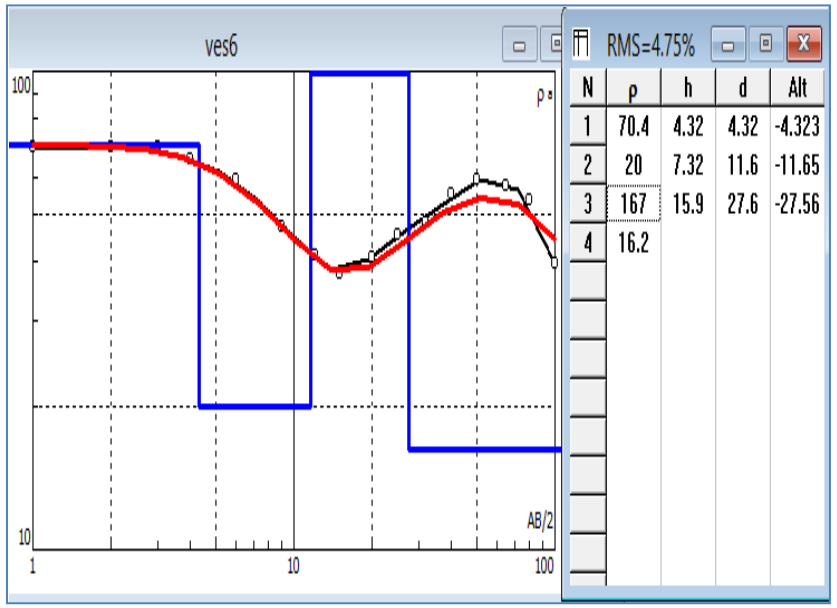

N	ρ	h	d	Alt
1	70.4	4.32	4.32	-4.323
2	20	7.32	11.6	-11.65
3	167	15.9	27.6	-27.56
4	16.2			

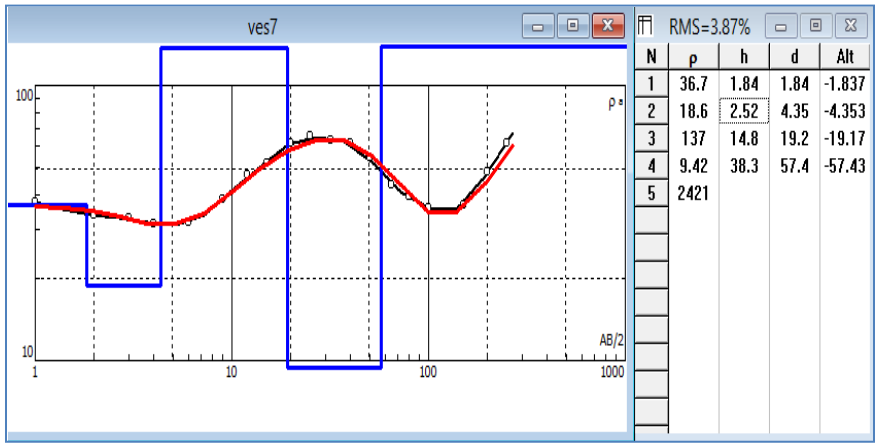

N	ρ	h	d	Alt
1	36.7	1.84	1.84	-1.837
2	18.6	2.52	4.35	-4.353
3	137	14.8	19.2	-19.17
4	9.42	38.3	57.4	-57.43
5	2421			

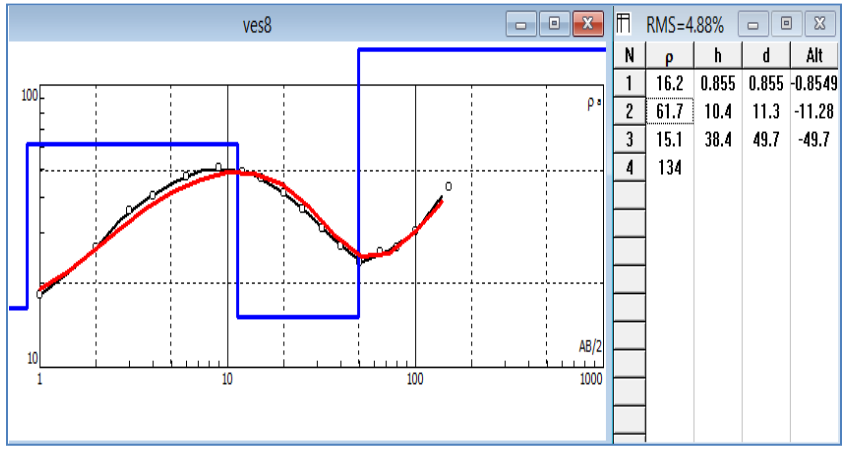

N	ρ	h	d	Alt
1	16.2	0.855	0.855	-0.8549
2	61.7	10.4	11.3	-11.28
3	15.1	38.4	49.7	-49.7
4	134			

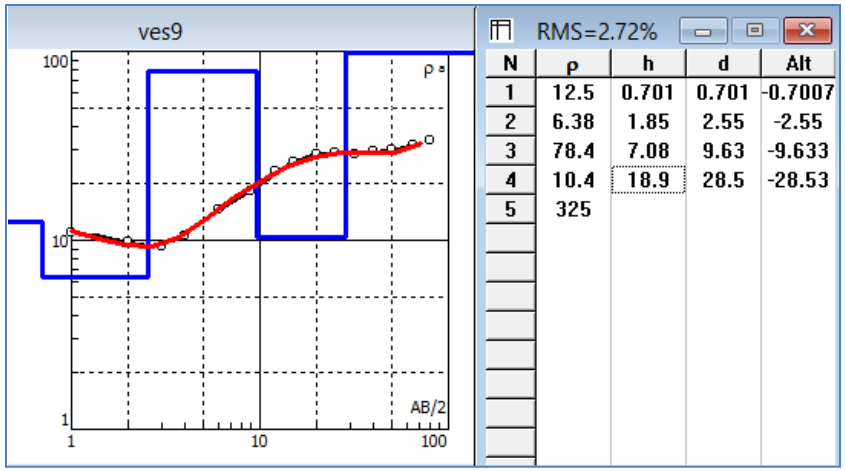

N	ρ	h	d	Alt
1	12.5	0.701	0.701	-0.7007
2	6.38	1.85	2.55	-2.55
3	78.4	7.08	9.63	-9.633
4	10.4	18.9	28.5	-28.53
5	325			

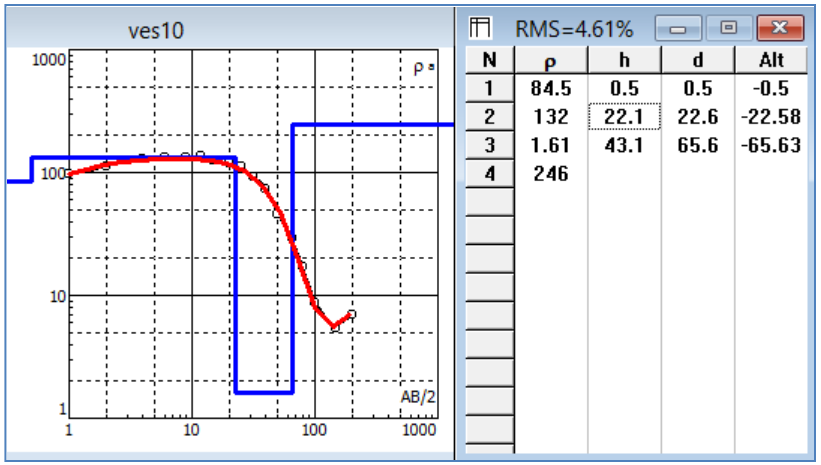

N	ρ	h	d	Alt
1	84.5	0.5	0.5	-0.5
2	132	22.1	22.6	-22.58
3	1.61	43.1	65.6	-65.63
4	246			

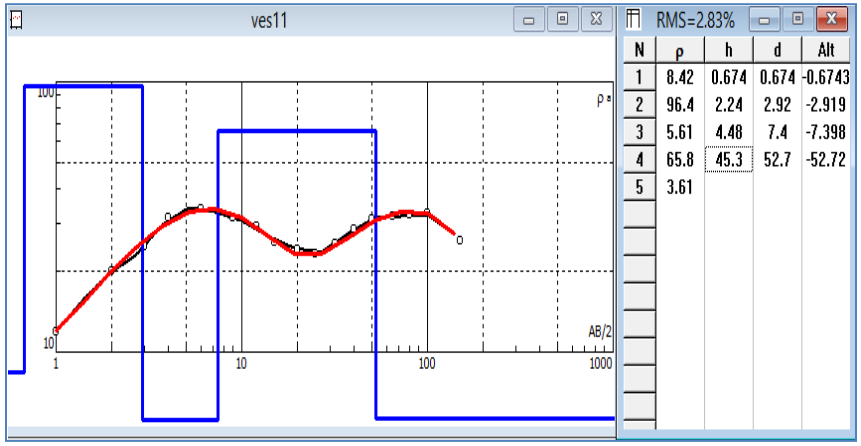

N	ρ	h	d	Alt
1	8.42	0.674	0.674	-0.6743
2	96.4	2.24	2.92	-2.919
3	5.61	4.48	7.4	-7.398
4	65.8	45.3	52.7	-52.72
5	3.61			

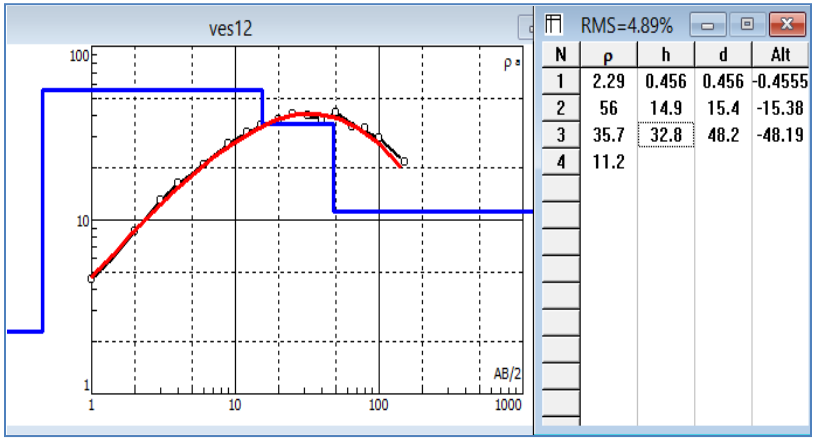

N	ρ	h	d	Alt
1	2.29	0.456	0.456	-0.4555
2	56	14.9	15.4	-15.38
3	35.7	32.8	48.2	-48.19
4	11.2			

III-Borehole Logs

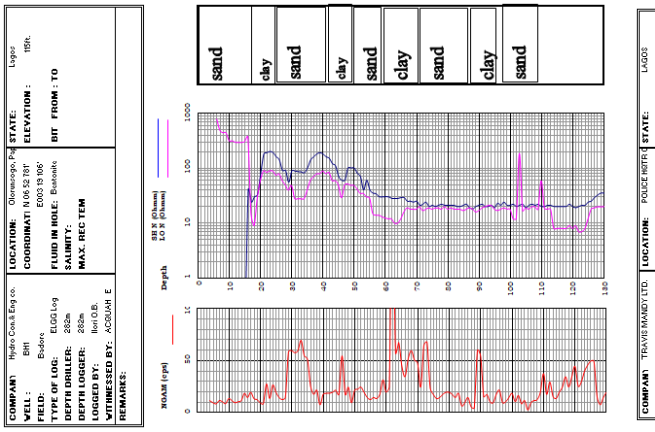

BH1

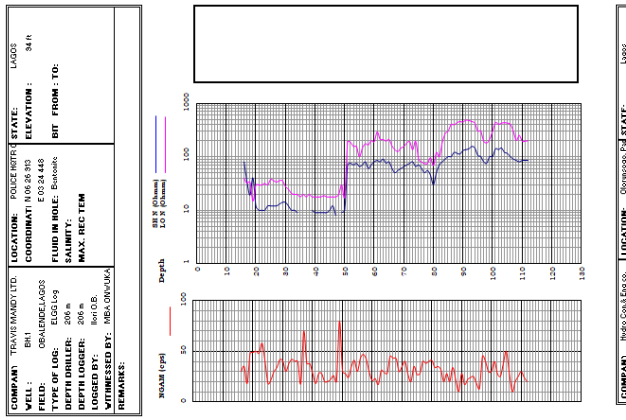

BH3

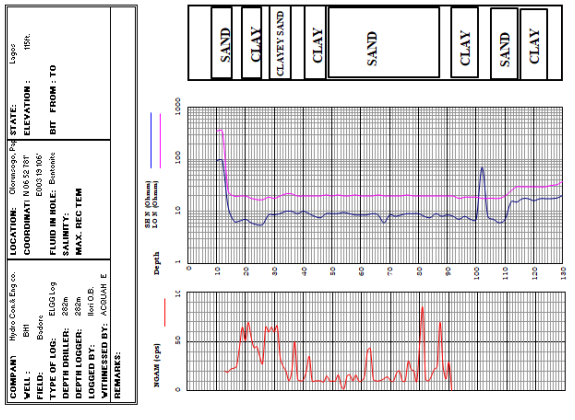

BH4

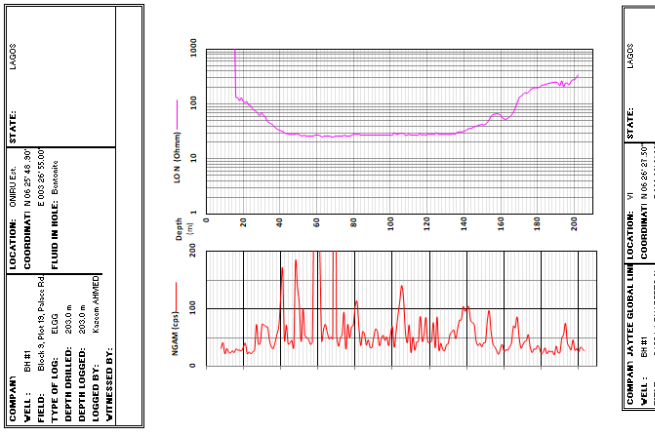

BH10

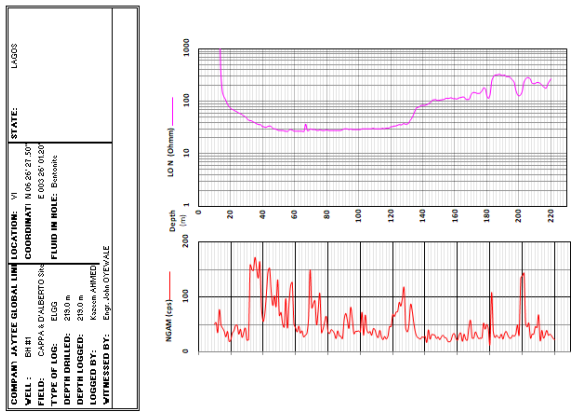

BH11

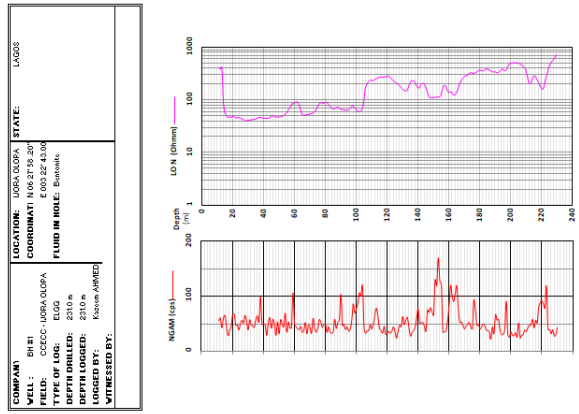

BH12

BH18

COMPANY	LOCATION: VICTORIA ISLA	STATE: LAGOS
WELL : BH #1	COORDINATI N 06 25' 38 .90"	
FIELD: 6 AJ MARINHO Street	E 003 25' 59.40"	
TYPE OF LOG: ELGG	FLUID IN HOLE: Bentonite	
DEPTH DRILLED: 272.0 m		
DEPTH LOGGED: 272.0 m		
LOGGED BY: Kazeem AHMED		
WITNESSED BY: Akudo DINMAH, Chucks ORJI		

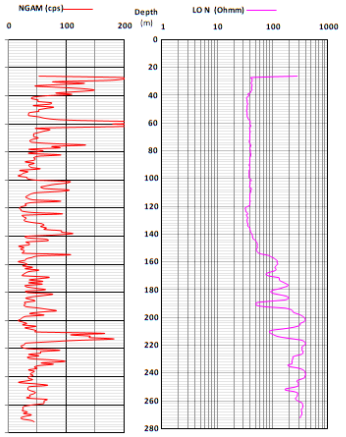

BH14

COMPANY	LOCATION: LEKKI	STATE: LAGOS
WELL : BH #1	COORDINATI N 06 25' 50 .10"	
FIELD: CLOVER COURT	E 003 30' 49.50	
TYPE OF LOG: ELGG	FLUID IN HOLE: Bentonite	
DEPTH DRILLED: 248.0 m		
DEPTH LOGGED: 248.0 m		
LOGGED BY: Kazeem AHMED		
WITNESSED BY:		

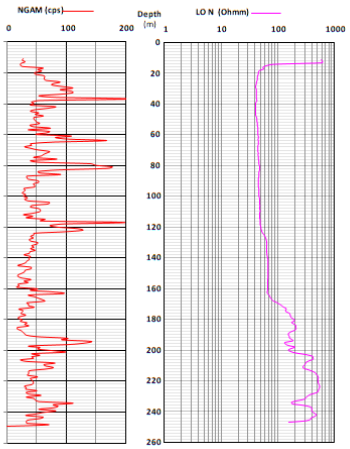

BH20

COMPANY	LOCATION: Ajah	STATE: LAGOS
WELL : Bh. 1	COORDINATI N 06 26.813	ELEVATION : 2m
FIELD: ITB Construction Limite	E 003 32.365	
TYPE OF LOG: ELGG	FLUID IN HOLE: Bentonite	BIT FROM : TO
DEPTH DRILLED: 212m		15" 0m 212m
DEPTH LOGGED: 212m		
LOGGED BY: AHMED Kazeem		
WITNESSED BY:		

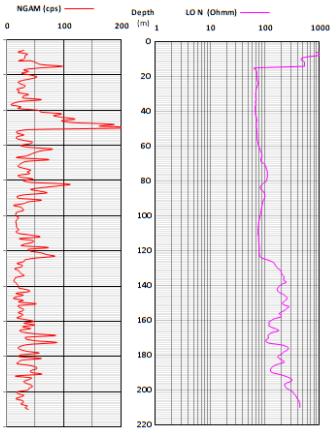

BH15

COMPANY	LOCATION: APAPA Wharf	STATE: LAGOS
WELL : BH #1	COORDINATI N 06 26' 15.4"	
FIELD: DANGOTE FLOUR Mill	E 003 22' 46.2"	
TYPE OF LOG: ELGG	FLUID IN HOLE: Bentonite	
DEPTH DRILLED: 236.0 m		
DEPTH LOGGED: 171.0 m		
LOGGED BY: Gbengs ILORI		
WITNESSED BY: Abuchi EKEJIOFOR		

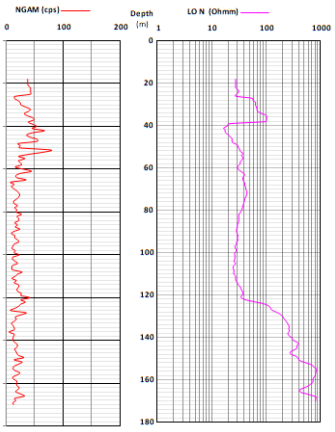

BH21

COMPANY	LOCATION: LEKKI	STATE: LAGOS
WELL : BH #2	COORDINATI N 06 27' 48 .10"	
FIELD: JAMES PINNOCK Estate	E 003 30' 40.10"	
TYPE OF LOG: ELGG	FLUID IN HOLE: Bentonite	
DEPTH DRILLED: 231.0 m		
DEPTH LOGGED: 230.0 m		
LOGGED BY: Kazeem AHMED		
WITNESSED BY: Lucas OLUWATOSIN, Shakiru SARO		

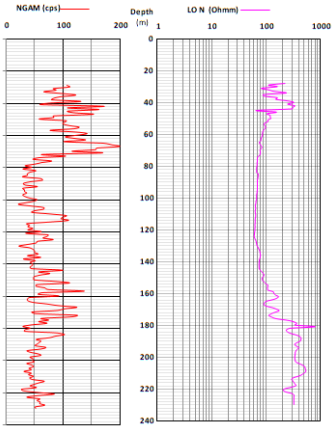

BH16

COMPANY	LOCATION: DTV, Apapa	STATE: LAGOS
WELL : Bh. 1	COORDINATI N 06 26.386	ELEVATION : 7m
FIELD: DTV Nigeria Limited	E 003 19.614	
TYPE OF LOG: ELGG	FLUID IN HOLE: Bentonite	BIT FROM : TO
DEPTH DRILLED: 200m		15" 0m 173m
DEPTH LOGGED: 173m		
LOGGED BY: AHMED Kazeem		
WITNESSED BY: OGUNNAIKE B.		

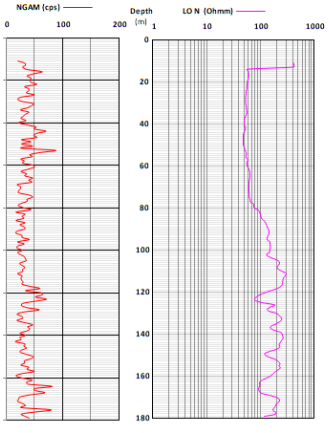

BH28

COMPANY	LOCATION: VICTORIA Island	STATE: LAGOS
WELL : BH #1	COORDINATI N 06 25' 20.736"	
FIELD: PRODECO Guest House	E 003 24' 43.62"	
TYPE OF LOG: ELGG	FLUID IN HOLE: Bentonite	
DEPTH DRILLED: 223.0 m		
DEPTH LOGGED: 216.0 m		
LOGGED BY: AHMED Kazeem		
WITNESSED BY: JONAH Udoeyi		

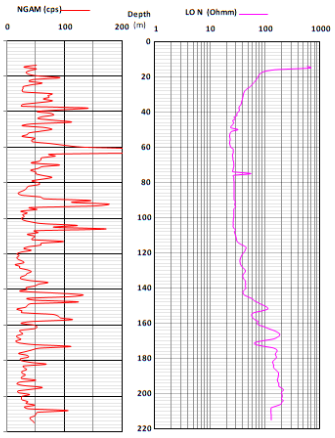

BH22

COMPANY	LOCATION: VICTORIA Island	STATE: LAGOS
WELL : BH #1	COORDINATI N 06 25' 33.00"	
FIELD: JOSEPH NAHMAN Close	E 003 25' 32.40"	
TYPE OF LOG: ELGG	FLUID IN HOLE: Bentonite	
DEPTH DRILLED: 236.0 m		
DEPTH LOGGED: 236.0 m		
LOGGED BY: Kazeem AHMED		
WITNESSED BY:		

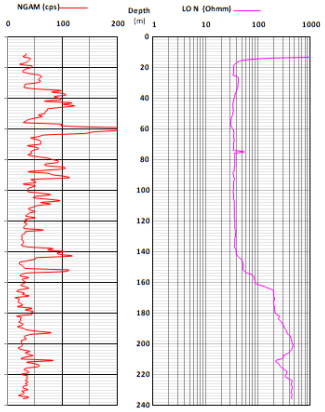

BH30

COMPANY	LOCATION: LEKKI	STATE: LAGOS
WELL : BH #1	COORDINATI N 06 26' 33.30"	
FIELD: The address - femi okunnu	E 003 30' 26.30"	
TYPE OF LOG: ELGG	FLUID IN HOLE: Bentonite	
DEPTH DRILLED: 220.0 m		
DEPTH LOGGED: 220.0 m		
LOGGED BY: Kazeem AHMED		
WITNESSED BY: Adeyinka OTENAIKE		

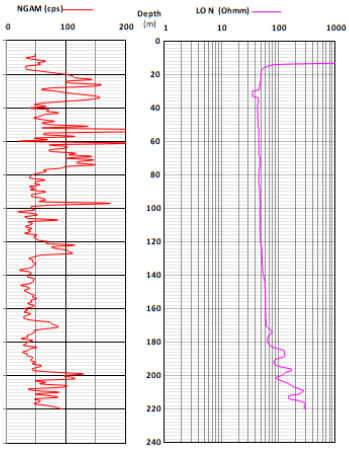

BH25

COMPANY	LOCATION: LEKKI	STATE: LAGOS
WELL : BH #1	COORDINATI N 06 26' 11.30"	
FIELD: OMORIRE JOHNSON Stree	E 003 27' 32.40"	
TYPE OF LOG: ELGG	FLUID IN HOLE: Bentonite	
DEPTH DRILLED: 236.0 m		
DEPTH LOGGED: 236.0 m		
LOGGED BY: Kazeem AHMED		
WITNESSED BY:		

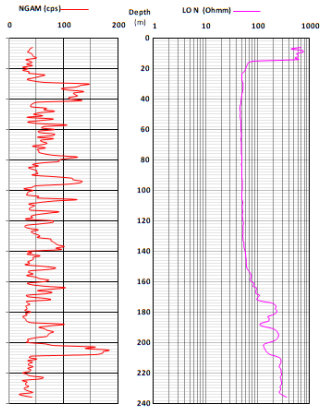

BH31

COMPANY	LOCATION: LEKKI	STATE: LAGOS
WELL : BH #2	COORDINATI N 06 26' 55.70"	
FIELD: WILLOW GREENS Estate	E 003 30' 38.60"	
TYPE OF LOG: ELGG	FLUID IN HOLE: Bentonite	
DEPTH DRILLED: 248.0 m		
DEPTH LOGGED: 248.0 m		
LOGGED BY: Kazeem AHMED		
WITNESSED BY:		

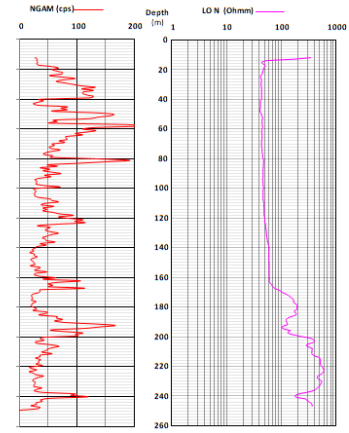

BH26

COMPANY AQUAFLO UNIV. SERVIC	LOCATION: VICTORIA ISLA	STATE: LAGOS
WELL : Bh # 1	COORDINATI N 06 26' 11.28"	
FIELD: OZUMBA NBADIWE	E 003 25' 05.39"	
TYPE OF LOG: ELGG	FLUID IN HOLE: Bentonite	
DEPTH DRILLED: 230m		
DEPTH LOGGED: 225m		
LOGGED BY: AHMED Kazeem		
WITNESSED BY:		

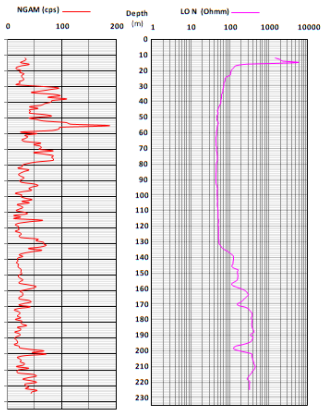

BH37

COMPANY	CHINA GEO LTD	LOCATION:	Akodo	STATE:	Lagos
WELL :	Bh 1	COORDINATES	N 06° 25.451	ELEVATION :	62ft
FIELD:	Ibeju Lekki Secretariat		E 003° 25.705		
TYPE OF LOG:	ELGG Log	FLUID IN HOLE:	Bentonite	BIT FROM : TO	
DEPTH DRILLER:	240m	SALINITY:			
DEPTH LOGGER:	240m	MAX. REC TEM			
LOGGED BY:	Braimoh				
WITHNESSED BY:	Eduno J.				
REMARKS:					

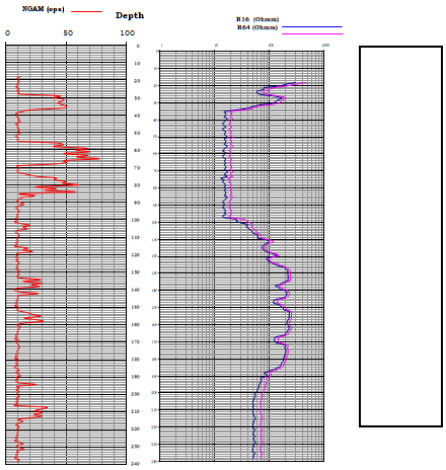

BH32

COMPANY		LOCATION:	VICTORIA Island	STATE:	LAGOS
WELL :	BH #1	COORDINATES	N 06 25' 48 .20"		
FIELD:	Zenith Bank Head Office		E 003 26' 04.60		
TYPE OF LOG:	ELGG	FLUID IN HOLE:	Bentonite		
DEPTH DRILLED:	240.0 m				
DEPTH LOGGED:	240.0 m				
LOGGED BY:	Kazeem AHMED				
WITNESSED BY:	Engr. Joseph, Mr. Akodo DINMAH				
REMARKS:					

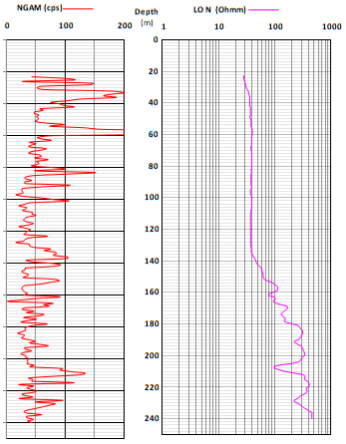

BH39

COMPANY	HYDROCON & ENGINEERI	LOCATION:	NIGERDOCK,SN	STATE:	Lagos
WELL :	BH 1	COORDINATES	N06 25 528	ELEVATION :	ft
FIELD:	NIGERDOCK,SNAKE IS		E003 20 422		
TYPE OF LOG:	ELGG Log	FLUID IN HOLE:	Bentonite	BIT FROM : TO:	
DEPTH DRILLER:	110m	SALINITY:			
DEPTH LOGGER:	110m	MAX. REC TEM			
LOGGED BY:	Ilori O.B.				
WITHNESSED BY:	ACQUAH E				
REMARKS:					

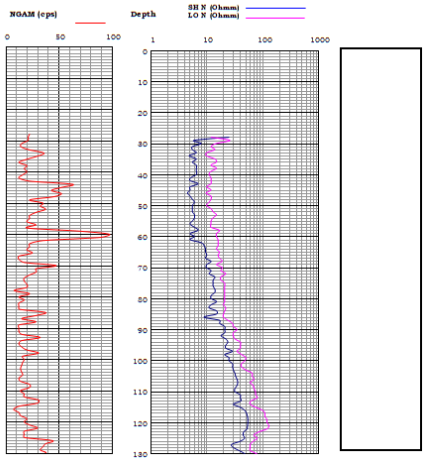

BH34

COMPANY	Hydro Con.& Eng co.	LOCATION:	Oloruncogo, Pap	STATE:	Lagos
WELL :	BH1	COORDINATES	N 06 52 781'	ELEVATION :	115ft.
FIELD:	Badore		E003 19 106'		
TYPE OF LOG:	ELGG Log	FLUID IN HOLE:	Bentonite	BIT FROM : TO	
DEPTH DRILLER:	282m	SALINITY:			
DEPTH LOGGER:	282m	MAX. REC TEM			
LOGGED BY:	Ilori O.B.				
WITHNESSED BY:	ACQUAH E				
REMARKS:					

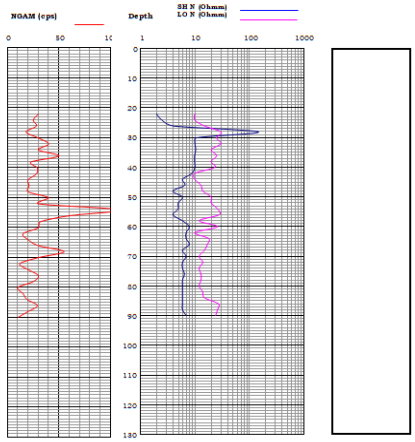

BH40

COMPANY	Hydro Con.& Eng co.	LOCATION:	Oloruncogo, Pap	STATE:	Lagos
WELL :	BH1	COORDINATES	N 06 52 781'	ELEVATION :	115ft.
FIELD:	Badore		E003 19 106'		
TYPE OF LOG:	ELGG Log	FLUID IN HOLE:	Bentonite	BIT FROM : TO	
DEPTH DRILLER:	282m	SALINITY:			
DEPTH LOGGER:	282m	MAX. REC TEM			
LOGGED BY:	Ilori O.B.				
WITHNESSED BY:	ACQUAH E				
REMARKS:					

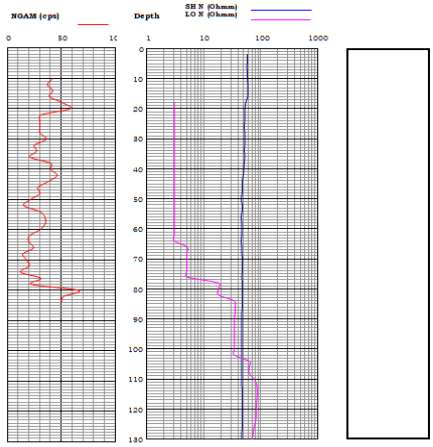

BH36

COMPANY	Hydro Construction	LOCATION:	Federal Palace H	STATE:	Lagos
WELL :	BH1	COORDINATES	N 06 25 736	ELEVATION :	50 ft
FIELD:	Federal Palace Hotel		E 003 24 431		
TYPE OF LOG:	ELGG Log	FLUID IN HOLE:	Bentonite	BIT FROM : TO	
DEPTH DRILLER:	230 m	SALINITY:			
DEPTH LOGGER:	230 m	MAX. REC TEM			
LOGGED BY:	Akinyemi E.B.				
WITHNESSED BY:	Acquah. E.				
REMARKS:					

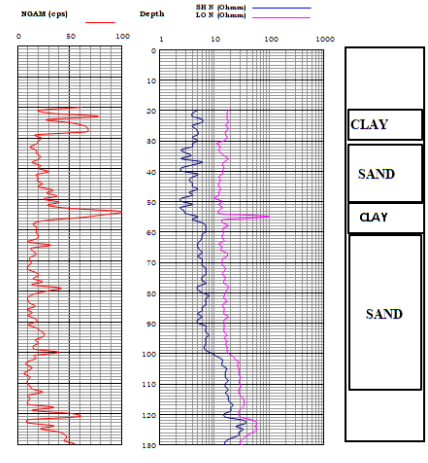

BH43

COMPANY	TRAVIS MANDY LTD.	LOCATION:	POLICE HQTR C	STATE:	LAGOS
WELL :	BH.1	COORDINATI	N 06 26 313	ELEVATION :	34 ft
FIELD:	OBALENDE,LAGOS		E 03 24 448		
TYPE OF LOG:	ELGG Log	FLUID IN HOLE:	Bentonite	BIT FROM : TO:	
DEPTH DRILLER:	206 m	SALINITY:			
DEPTH LOGGER:	206 m	MAX. REC TEM			
LOGGED BY:	Ilori O.B.				
WITHNESSED BY:	MBA ONWUKA				
REMARKS:					

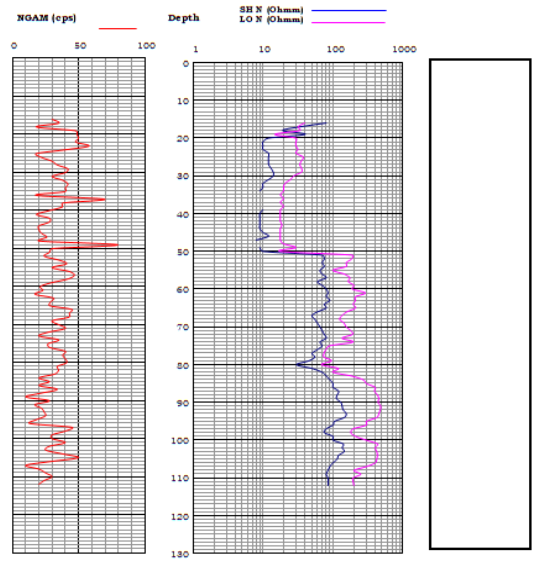

BH41

COMPANY	Hydro Con.& Eng co.	LOCATION:	Olorunsogo, Pap	STATE:	Lagos
WELL :	BH1	COORDINATI	N 06 52 781'	ELEVATION :	115ft.
FIELD:	Badore		E003 13 106'		
TYPE OF LOG:	ELGG Log	FLUID IN HOLE:	Bentonite	BIT FROM : TO	
DEPTH DRILLER:	282m	SALINITY:			
DEPTH LOGGER:	282m	MAX. REC TEM			
LOGGED BY:	Ilori O.B.				
WITHNESSED BY:	ACQUAH E				
REMARKS:					

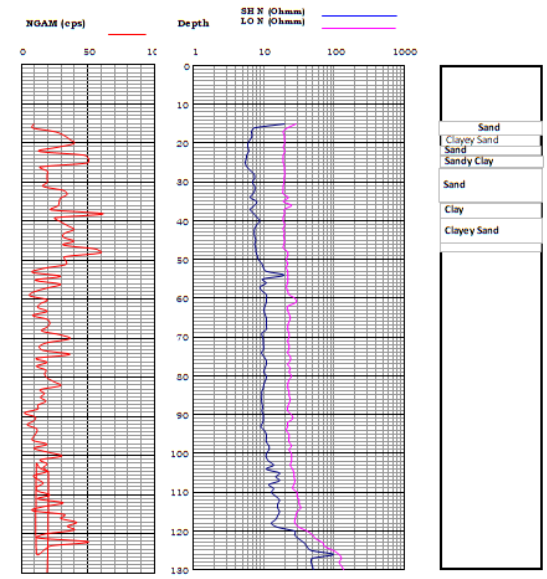

BH44

COMPANY	HYDRO CON. LTD	LOCATION:	Apapa	STATE:	Lagos
WELL :	Bh. 1	COORDINATI	N 06° 25.783	ELEVATION :	34ft
FIELD:	Takwa Bay Island		E 003° 23.304		
TYPE OF LOG:	ELGG Log	FLUID IN HOLE:	Bentonite	BIT FROM : TO	
DEPTH DRILLER:	240m	SALINITY:			
DEPTH LOGGER:	240m	MAX. REC TEM			
LOGGED BY:	Ilori O.B.				
WITHNESSED BY:	Acqush C.				
REMARKS:					

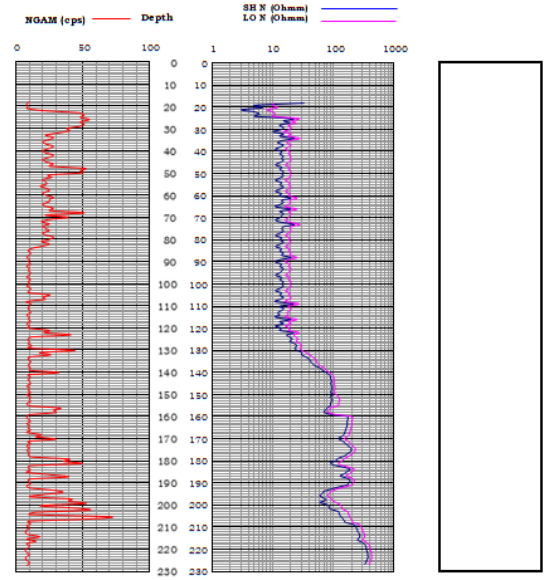

BH42

COMPANY	AQUADRILL LTD	LOCATION:	Ikoyi	STATE:	Lagos
WELL :	Bh. 2	COORDINATI		ELEVATION :	
FIELD:	Osborne Est, Ikoyi				
TYPE OF LOG:	ELGG Log	FLUID IN HOLE:	Bentonite	BIT FROM : TO	
DEPTH DRILLER:	220m	SALINITY:			
DEPTH LOGGER:	220m	MAX. REC. TEM			
LOGGED BY:	Ilori O.B.				
WITHNESSED BY:	Adebayo B.				
REMARKS:					

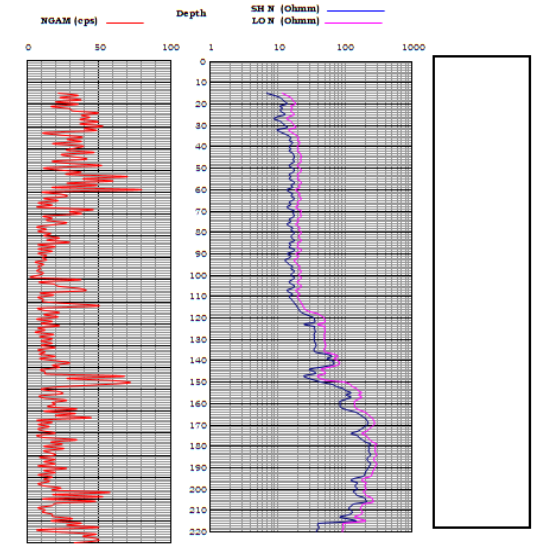

Appendix E:

COMPLETE ANALYTICAL RESULTS FOR THE PHYSICOCHEMICAL PARAMETERS FOR THE WET SEASON

Sample ID	Site	X	Y	PH	WL	EC	Hardn.	TDS	Ca^{2+}	Mg^{2+}	Na^{+}	K^{+}	Cl^{-}	$SO4^{2+}$	$NO3^{-}$	$CO3^{2+}$	$HCO3^{-}$	f. coli
GW1	App	06˚26.520'	003˚19.876'	7.5	1.2	1563	312	772	78.74	13.28	14.77	23.77	178	31	2.9	135	274.5	>201
GW2	App	06˚26.631'	003˚19.775'	7.7	0.7	736	332	399	97.13	5.57	11.46	15.65	36	58	16.8	45	91.5	>201
GW3	App	06˚27.854'	003˚20.315'	7.6	5.3	849	196	465	27.76	3.61	13.03	16.49	90	43	29.9	15	30.5	>201
GW4	App	06˚28.163'	003˚21.560'	6.7	3	1133	248	589	30.78	6.28	13.83	21.29	156	44	4.5	37.5	76.25	>201
GW5	App	06˚27.899'	003˚21.561'	7.7	1.85	760	240	670	44.72	10.57	14.60	12.08	315	26	3.8	60	122	>201
GW6	App	06˚26.555'	003˚22.017'	7.4	1.3	2172	668	971	7.70	9.56	1.29	1.77	315	3	10.3	165	335.51	>201
GW7(BH1)	App	06˚26.899'	003˚19.837'	6.8	2.2	1232	364	650	8.05	6.7	1.25	1.68	129	78	73.6	30	61.01	>201
GW8	Isl	06˚27.196'	003˚23.052'	8.2	3.04	3284	524	1642	11.76	14.9	1.57	1.93	720	88	15.1	135.5	274.5	>201
GW9	Isl	06˚26.908'	003˚24.627'	7.3	2.27	1076	216	546	4.54	5.9	1.01	1.38	105	72	71.3	45	91.5	201
GW10	Isl	06˚27.483'	003˚23.925'	7.8	1	1200	212	602	10.74	7.5	1.23	1.32	134	64	59.9	105	213.5	>201
GW11	Isl	06˚27.322'	003˚23.600'	7.8	0.9	1360	188	672	6.74	8.46	0.78	1.06	114	<0.01	2.2	120	244.01	>201
GW12	Isl	06˚27.815'	003˚23.259'	7.9	2	779	236	419	6.17	5.14	0.79	1.17	59	57	22.1	81.34	183	201
GW13(BH2)	Isl	06˚27.464'	003˚22.938'	7.5	4.25	1393	116	704	10.22	8.27	0.70	1.15	110	63	61.1	120	244	>25
GW14	Isl	06˚25.891'	003˚24.590'	7.6	1.3	342	182	102	7.36	2.68	0.80	0.65	46	13	13.6	22.5	45.75	>201
GW15	Isl	06˚26.629'	003˚25.243'	7.7	2.62	715	322	380	7.46	5.85	1.11	1.10	62	29	1.4	60	122	36
GW16	Isl	06˚26.648'	003˚24.640'	7.8	1.3	442	238	252	8.03	3.33	0.84	0.58	58	35	6.5	30	61	>201
GW17	Isl	06˚26.213'	003˚24.317'	8.6	0.8	112	92	070	3.27	1.87	0.20	0.19	18	5	5.3	15.5	32.05	>201
GW18	Isl	06˚26.341'	003˚28.077'	7.5	1.6	897	272	448	14.48	6.55	0.90	0.74	42	45	7.7	75	152.5	>201
GW19	Isl	06˚26.218'	003˚29.444'	8.4		2908	304	1454	0.78	16.77	1.65	1.95	533	64	5.7	210	284.67	6
GW20	Eti	06˚26.268'	003˚31.209'	7.7	0.71	512	196	288	5.47	5.13	1.12	1.55	21	19	5.8	75	152.5	>201
GW21	Eti	06˚25.884'	003˚32.618'	6.2	1.4	251	52	160	0.05	2.66	0.71	0.52	85	16	4.5	15	30.5	18
GW22	Eti	06˚28.161'	003˚34.789'	7	1.9	525	206	296	3.36	4.57	1.03	0.87	21	59	23.3	30	61	>201
GW23(BH3)	Eti	06˚29.328'	003˚34.864'	6.8	2.7	862	190	385	1.88	7.98	1.27	1.56	91	48	23.9	45	91.5	>201
GW24	Eti	06˚29.861'	003˚35.154'	7.2	0.5	972	162	502	4.62	9.26	1.26	1.56	105	79	8.7	60	122	>201
GW25	Eti	06˚30.124'	003˚36.007'	7	0.4	751	246	401	5.34	6.59	0.92	1.02	123	48	6.8	45	91.5	>201
GW26	Eti	06˚27.307'	003˚35.201'	7	0.31	417	140	237	3.07	3.92	0.55	0.14	69	15	3.6	15	30.5	70
GW27	Eti	06˚27.820'	003˚40.300'	7	1.72	418	98	209	1.75	5.24	0.55	0.16	11	22	29.1	30	61	10

GW28(BH4)	Eti	06˚28.139'	003˚42.195'	5.4	1.13	341	48	170	0.14	2.01	0.46	0.23	11	55	16.8	15.02	30.54	2
GW29	Eti	06˚28.427'	003˚48.325'	6.8	0.8	111	72	69	1.10	1.33	0.15	0.16	1	15	3.2	6	12.2	>201
GW30	Eti	06˚29.103'	003˚53.303'	7	0.2	254	120	151	2.27	1.29	0.49	0.21	9	33	6.7	7.5	15.25	>201
GW31	Eti	06˚28.014'	003˚47.801'	6.7	2.4	258	94	152	2.05	1.85	0.45	0.38	3	0.36	50	6.6	13.42	>201
GW32	Eti	06˚28.415'	003˚38.133'	6.1	3.7	701	110	380	1.26	2.88	0.71	0.92	80	0.65	67.7	14.1	28.67	>201
GW33(BH5)	Eti	06˚28.466'	003˚34.616'	6.3	1.3	300	118	175	1.27	3.53	0.69	0.45	2	0.06	11.6	7.8	15.86	>201
GW34	Eti	06˚30.265'	003˚34.796'	7.4	0.2	1041	96	537	5.75	7.91	0.68	0.83	106	1.35	1.3	38.1	77.46	>201
GW35	Eti	06˚29.888'	003˚34.940'	6.9	1.5	1883	116	891	5.04	9.86	1.17	1.59	236	69	108.7	21.1	42.9	>201
GW36	Eti	06˚28.121'	003˚33.873'	7.3	3.25	310	116	192	2.33	5.03	0.51	0.67	26	32	36.7	7.8	15.86	>201
GW37	Eti	06˚26.380'	003˚31.305'	7.2	1	514	76	291	4.00	4.34	0.59	0.63	36	0	0	37.5	76.24	>201
GW38	Eti	06˚26.016'	003˚31.395'	7.4	0.75	922	250	480	4.65	2.34	0.81	1.20	86	37	31.5	9	18.3	>201
GW39	Eti	06˚25.958'	003˚30.443'	7.2	1	935	132	368	1.88	4.59	0.56	0.74	74	64	13.7	66	134.18	>201
GW40	Eti	06˚26.959'	003˚32.928'	7.4	2.12	183	78	112	1.07	1.3	0.42	0.36	10	18	26.8	3	6.1	>201
P-SW1*	Lagoon			7.83	-	3999	-	2000	430	1313.00	1750	44.00	2327	465	245	60.00	80.00	1733**
P-SW2*	Lagoon			7.86	-	3999	-	2000	1625	4275.00	6500	163.00	8643	1728	230	30.00	40.00	-
P-SW3*	Lagoon			8.25	-	3999	-	2000	1750	4850.00	7000	175.00	9308	1862	218	36.00	48.00	34**
SW4	Ocean			8.4	-	48000	-	35040	321.28	5036.23	8674.52	294.67	15582	102	9.6	180	365.94	173

***NB: P-SW1 to P-SW3 are retrieved data from previous study and** all **measurements are in mg/L; ** measured by present study**

Appendix F:

COMPLETE ANALYTICAL RESULTS OF HEAVY METAL ANALYSIS IN THE WET SEASON

Sample ID	Site	Location	X	Y	Zn^{2+}	Cu^{2+}	Mn^{2+}	Fe^{2+}	Ni^{2+}	Cd^{2+}	Ag^{+}	Pb^{2+}	Cr^{2+}
GW1	App	Coconut	06˚26.520'	003˚19.876'	<0.0001	0.1103	0.1588	0.2143	0.3937	<0.0001	0.0349	<0.0001	<0.0001
GW2	App	Coconut	06˚26.631'	003˚19.775'	0.0205	0.1377	<0.0001	0.2173	0.3506	<0.0001	<0.0001	<0.0001	<0.0001
GW3	App	Amukoko	06˚27.854'	003˚20.315'	0.004	0.1359	<0.0001	1.5821	0.1493	0.0038	<0.0001	<0.0001	<0.0001
GW4	App	Badia	06˚28.163'	003˚21.560'	0.239	0.0524	0.0231	0.2047	0.4945	<0.0001	0.02	<0.0001	<0.0001
GW5	App	Ijora	06˚27.899'	003˚21.561'	0.0323	1.3343	<0.0001	0.3258	0.566	<0.0001	0.0224	0.0266	<0.0001
GW6	App	Wharf	06˚26.555'	003˚22.017'	0.0011	<0.0001	149	0.0136	<0.0001	<0.0001	0.0015	0.003	0.0218
GW7	App	Kirikiri Rd	06˚26.899'	003˚19.837'	0.0007	<0.0001	0.0044	0.0008	<0.0001	<0.0001	0.0021	0.0001	0.021
GW8	Isl	Marina	06˚27.196'	003˚23.052'	0.0009	<0.0001	0.022	0.0292	<0.0001	<0.0001	0.0045	0.0026	0.0445
GW9	Isl	Obalende	06˚26.908'	003˚24.627'	0.0004	<0.0001	<0.0001	0.0021	<0.0001	0.0006	0.0023	0.0036	0.0179
GW10	Isl	Adeniji	06˚27.483'	003˚23.925'	0.0014	<0.0001	0.0015	0.0021	<0.0001	<0.0001	0.0043	0.0059	0.0039
GW11	Isl	Olopade	06˚27.322'	003˚23.600'	0.0001	<0.0001	0.0122	0.0393	<0.0001	0.0001	0.0005	0.003	0.0223
GW12	Isl	Isale eko	06˚27.815'	003˚23.259'	0.0017	<0.0001	0.0058	<0.0001	<0.0001	0.0001	0.0007	0.0023	0.0299
GW13	Isl	Bankole	06˚27.464'	003˚22.938'	0.0011	<0.0001	0.0033	0.0046	<0.0001	0.0001	0.0016	0.0021	0.0104
GW14	Isl	Abdu Smith	06˚25.891'	003˚24.590'	0.0023	0.025	0.003	0.0052	<0.0001	<0.0001	0.0004	0.0017	0.0177
GW15	Isl	Off Ribadu	06˚26.629'	003˚25.243'	0.0013	0.0104	0.0102	0.3235	<0.0001	<0.0001	0.0003	0.0045	0.0297
GW16	Isl	Awolowo Rd	06˚26.648'	003˚24.640'	<0.0001	0.0147	0.0004	0.0025	<0.0001	<0.0001	<0.0001	0.0001	0.0086
GW17	Isl	Aboyade C.	06˚26.213'	003˚24.317'	0.0095	0.0259	0.0083	0.1851	<0.0001	<0.0001	0.0015	0.0038	0.0247
GW18	Isl	Lekki Ph1	06˚26.341'	003˚28.077'	<0.0001	<0.0001	0.0078	0.0083	<0.0001	0.0007	0.001	0.0032	0.0467
GW19	Isl	Ikate	06˚26.218'	003˚29.444'	<0.0001	0.022	0.0067	0.0002	<0.0001	<0.0001	0.001	<0.0001	0.0319
GW20	Eti	Alpha plaza	06˚26.268'	003˚31.209'	<0.0001	0.0076	0.0151	0.0635	<0.0001	<0.0001	0.0008	0.0007	0.0469
GW21	Eti	Elesan	06˚25.884'	003˚32.618'	<0.0001	0.0256	0.0057	0.2776	<0.0001	<0.0001	0.0007	<0.0001	0.0163
GW22	Eti	Good Motor	06˚28.161'	003˚34.789'	<0.0001	<0.0001	0.0038	<0.0001	<0.0001	<0.0001	0.0002	0.0024	0.0256
GW23	Eti	Ado Rd	06˚29.328'	003˚34.864'	<0.0001	0.0078	0.0075	0.0106	<0.0001	0.0006	<0.0001	0.0047	0.0286

Sample ID	Site	Location	X	Y	Zn^{2+}	Cu^{2+}	Mn^{2+}	Fe^{2+}	Ni^{2+}	Cd^{2+}	Ag^{+}	Pb^{2+}	Cr^{2+}
GW24	Eti	Badore Rd	06˚29.861'	003˚35.154'	<0.0001	0.0003	0.0045	0.0257	<0.0001	0.0003	0.0006	0.0036	0.0307
GW25	Eti	Badore	06˚30.124'	003˚36.007'	<0.0001	<0.0001	0.0041	0.0544	<0.0001	<0.0001	<0.0001	0.0014	0.0254
GW26	Eti	Abraham	06˚27.307'	003˚35.201'	0.0001	0.0001	0.0063	0.0881	<0.0001	0.0008	0.0004	0.0016	0.0084
GW27	Eti	Abijo	06˚27.820'	003˚40.300'	<0.0001	0.0002	0.0059	0.0002	<0.0001	0.0007	0.001	<0.0001	0.0105
GW28	Eti	Awoyaya	06˚28.139'	003˚42.195'	0.0007	0.0026	0.0052	0.0029	<0.0001	<0.0001	0.0005	0.0006	0.0127
GW29	Eti	Igando town	06˚28.427'	003˚48.325'	<0.0001	0.0051	0.0028	0.0346	<0.0001	<0.0001	0.0005	0.0007	0.0104
GW30	Eti	Lekki town	06˚29.103'	003˚53.303'	0.0001	0.0022	0.0039	0.0034	<0.0001	0.0008	0.0012	<0.0001	0.0111
GW31	Eti	Alatishe twn	06˚28.014'	003˚47.801'	<0.0001	0.0023	0.0018	<0.0001	<0.0001	<0.0001	0.0011	<0.0001	0.0163
GW32	Eti	Sangotedo	06˚28.415'	003˚38.133'	0.0012	<0.0001	0.0067	0.0003	<0.0001	<0.0001	0.0002	0.0002	<0.0001
GW33	Eti	Thomas Est.	06˚28.466'	003˚34.616'	0.0011	<0.0001	0.0129	0.0104	<0.0001	<0.0001	<0.0001	0.0014	<0.0001
GW34	Eti	Langbasa	06˚30.265'	003˚34.796'	0.0007	<0.0001	0.0143	0.1735	<0.0001	<0.0001	<0.0001	<0.0001	<0.0001
GW35	Eti	Addo town	06˚29.888'	003˚34.940'	0.0016	<0.0001	0.0003	<0.0001	<0.0001	<0.0001	<0.0001	0.002	<0.0001
GW36	Eti	Ajah Mosq.	06˚28.121'	003˚33.873'	0.0033	<0.0001	0.0001	0.0109	<0.0001	<0.0001	0.0001	<0.0001	<0.0001
GW37	Eti	Idado town	06˚26.380'	003˚31.305'	0.0049	<0.0001	0.0113	0.3632	<0.0001	<0.0001	<0.0001	0.0007	<0.0001
GW38	Eti	Igboefon	06˚26.016'	003˚31.395'	0.0048	<0.0001	0.0027	0.0017	<0.0001	<0.0001	<0.0001	0.0002	<0.0001
GW39	Eti	Jakande Est.	06˚25.958'	003˚30.443'	0.002	0.0007	0.0121	0.44	<0.0001	0.0002	<0.0001	0.0002	<0.0001
GW40	Eti	Ikota	06˚26.959'	003˚32.928'	0.0006	<0.0001	0.0004	<0.0001	<0.0001	0.0001	<0.0001	<0.0001	<0.0001
SW1	Lagoon	Ebute-ero			<0.0001	<0.0001	0.6435	0.1752	<0.0001	0.1888	24.98	<0.0001	.0681
SW2	Ocean	Oniru			.0199	<0.0001	.0871	.1045	.0024	.0216	24.9745	.4535	.127
SW3	Lagoon	Ajah			.0002	<0.0001	.0041	.2409	<0.0001	<0.0001	<0.0001	<0.0001	.0005

*All measurements are in mg/L

Appendix G:

COMPLETE ANALYTICAL RESULTS OF THE PHYSICOCHEMICAL PARAMETERS IN THE DRY SEASON

Sample ID	Site	X	Y	PH	Temp.	Water level	EC	TDS	Elev.	Ca^{2+}	Mg^{2+}	Na^{+}	K^{+}	Cl^{-}	$SO4^{2-}$	$NO3^{-}$	$CO3^{2-}$	$HCO3^{-}$
GW1	Apapa	06˚26.520'	003˚19.876'	7.5	29.2	3	1542	785	32	10.6	4.14	5.86	5.24	6.24	0.01	0.057	4	50
GW2	Apapa	06˚26.631'	003˚19.775'	7.4	28.7	1.69	949	536	144	11.8	3.4	4.2	6.35	5.21	0.13	0.011	4	90
GW4	Apapa	06˚28.163'	003˚21.560'	5.1	28.7	4.44	1912	1020	51	11.6	3.3	5.7	5.44	9.73	0.21	0.033	4	70
GW5	Apapa	06˚27.899'	003˚21.561'	7.3	29	1.71	1880	1034	30	11.6	2.5	5.22	3.99	3.33	0.12	0.002	4	92
GW6	Apapa	06˚26.555'	003˚22.017'	7.6	29.8	1.15	3089	1637	25	9.4	3.45	5.7	6.35	5.12	0.12	0.024	3	17
GW7	Apapa	06˚26.899'	003˚19.837'	7	29.6	6.16	1360	728	43	10.4	4.55	4.16	8.99	4.1	0.01	0.004	0.9	97
GW8	Island	06˚27.196'	003˚23.052'	8.5	30.6	3.06	3832	1916	38	8.6	4.43	5.2	5.49	5.23	0.01	0.040	2	69
GW9	Island	06˚26.908'	003˚24.627'	7.2	29.2	2.88	1023	558	4	10.8	6.23	4.2	6.35	2.5	0.21	0.011	4	94
GW10	Island	06˚27.483'	003˚23.925'	7.6	29	0.65	1681	862	65	12.2	3.3	6.3	5.51	9.65	0.01	0.025	5	70
GW11	Island	06˚27.322'	003˚23.600'	7.6	29.4	0.49	1119	621	59	12.1	3.2	5.2	9.01	4.3	0.03	0.015	4	53
GW12	Island	06˚27.815'	003˚23.259'	7.6	28.6	1.71	1150	641	8	12.3	2.5	4.2	4.75	3.12	0.01	0.033	1	62
GW13	Island	06˚27.464'	003˚22.938'	7.6	30	5	1250	685	123	10.9	4.5	6.4	3.95	3.35	0.12	0.054	4	92
GW14	V/I	06˚25.891'	003˚24.590'	7.6	29	1.84	982	537	70	9.6	3.3	8.3	4.99	5.2	0.13	0.015	4	17
GW15	Ikoyi	06˚26.629'	003˚25.243'	7.6	28.2	1.79	643	387	20	9.8	4.11	5.7	3.99	3.12	0.01	0.033	2	95
GW17	V/I	06˚26.213'	003˚24.317'	7.6	30.1	1.54	418	263	82	10.6	3.44	5.78	6.35	3.33	0.02	0.054	4	70
GW18	Lekki	06˚26.341'	003˚28.077'	7.7	30.2	2.16	809	505	59	12.3	4.3	5.72	4.99	5.12	0.20	0.003	6	55
GW19	Lekki	06˚26.218'	003˚29.444'	8.5	31.5	AD	2648	1324	42	12.2	3.2	9.05	3.99	4.1	0.20	0.002	4	64
GW20	Igboefon	06˚26.268'	003˚31.209'	8.3	28	1.41	620	375	51	10.8	4.11	5.25	6.35	5.23	0.02	0.024	4	90
GW21	Lafiaji	06˚25.884'	003˚32.618'	8.7	29.2	2.36	275	114	32	11.9	5.24	4.1	8.99	2.54	0.12	0.004	3	17
GW22	Ajiwe	06˚28.161'	003˚34.789'	7.5	28.8	2.69	354	177	37	12.6	4.4	5.15	5.49	9.65	0.12	0.040	4	95
GW23	Etiosa	06˚29.328'	003˚34.864'	8.6	29.6	AD	693	412	170	10.8	3.24	4.2	6.35	4.3	0.01	0.011	5	69

Sample ID	Site	X	Y	PH	Temp.	Water level	EC	TDS	Elev.	Ca^{2+}	Mg^{2+}	Na^{+}	K^{+}	Cl^{-}	$SO4^{2-}$	$NO3^{-}$	$CO3^{2-}$	$HCO3^{-}$
GW24	Etiosa	06˚29.861'	003˚35.154'	7	28	2.22	908	528	52	8.8	3.44	7.24	5.51	3.13	0.01	0.025	4	94
GW25	Etiosa	06˚30.124'	003˚36.007'	6.3	28.9	2.06	588	368	55	10.9	2.66	5.65	9.01	3.35	0.21	0.015	1	70
GW26	Etiosa	06˚27.307'	003˚35.201'	7.4	29.2	0.89	266	171	19	9.8	4.3	4.25	5.44	5.2	0.01	0.015	4	53
GW27	Ibeju/L	06˚27.820'	003˚40.300'	7.6	29.2	3.82	142	123	35	12.1	4.22	5.2	3.95	3.12	0.03	0.033	4	62
GW28	Ibeju/L	06˚28.139'	003˚42.195'	7.2	29.9	2.85	268	134	52	11.9	3.4	4.25	3.99	3.33	0.20	0.054	2	69
GW29	Ibeju/L	06˚28.427'	003˚48.325'	7.3	28.3	1.64	338	169	38	12.4	4.14	5.7	3.99	5.12	0.20	0.015	4	94
GW31	Ibeju/L	06˚28.014'	003˚47.801'	5.9	28.4	2.16	201	132	63	8.2	2.5	6.22	9.01	4.1	0.02	0.033	4	70
GW32	Etiosa	06˚28.415'	003˚38.133'	5.6	29.3	3.27	553	314	67	12.2	2.45	5.72	4.75	5.2	0.12	0.054	2	53
GW33	Etiosa	06˚28.466'	003˚34.616'	6.7	29.6	3.13	340	225	62	10.8	3.6	9.1	4.36	2.54	0.12	0.003	4	62
GW34	Etiosa	06˚30.265'	003˚34.796'	7.4	28	0.68	1170	663	42	10.4	3.2	4.12	4.98	9.65	0.01	0.002	6	92
GW35	Etiosa	06˚29.888'	003˚34.940'	7.5	27.6	2.32	1629	878	73	9.6	4.5	6.45	4.04	4.3	0.12	0.054	4	17
GW36	Ajah	06˚28.121'	003˚33.873'	8.4	28.3	4.54	555	345	38	12.8	3.3	5.13	5.49	3.12	0.01	0.015	4	95
GW37	Etiosa	06˚26.380'	003˚31.305'	7.4	29.9	1.37	530	323	32	12.3	3.36	5.2	6.49	3.35	0.01	0.033	3	70
GW38	Etiosa	06˚26.016'	003˚31.395'	7.6	30.7	1.95	1051	591	63	11.9	3.45	4.1	5.51	5.2	0.21	0.054	0.8	55
GW39	Etiosa	06˚25.958'	003˚30.443'	7.1	28.2	1.08	951	549	37	10.4	2.44	5.2	8.84	3.12	0.01	0.003	1	64
GW40	Etiosa	06˚26.959'	003˚32.928'	nm	29.5	2.95	323	162	58	12.8	2.48	5.7	5.39	3.33	0.03	0.002	6	90
GW41	Ogombo	06˚26'58.6"	006˚36'45.2"	7.5	28.3	1.92	447	278	28	12.2	3.45	4.4	3.89	5.12	0.20	0.024	4	17
GW42	Ibeju/L	06˚29'21.1"	003˚53'46.2"	8.6	28.4	3.23	357	270	46	11.6	3.44	4.8	3.99	4.1	0.20	0.002	6	95
GW43	Eleko town	06˚26'26.0"	003˚51'21.6"	7.1	29.9	4.25	388	247	64	12.6	3.67	6.1	4.09	5.23	0.02	0.054	4	69
GW44	Lakowe	06˚28'27.3"	003˚43'49.2"	6.8	28.9	1.97	845	507	49	11.9	5.04	4.58	6.59	2.54	0.12	0.015	6	94
GW45	Awoyaya	06˚28'40.7"	003˚42'40.9"	6.9	30.1	3.1	477	348	62	9.6	4.3	5.02	5.49	9.65	0.12	0.033	6	42

All measurements are in mg/L

Appendix H:

WET SEASON HYDROCHEMICAL FACIES AND SOME IONIC RATIOS OF A SHALLOW UNCONFINED AQUIFER IN THE LAGOS COASTAL BASIN

Sample ID	Facies	Ca^{2+}/Mg^{2+}	Ca^{2+}/Na^{+}	Na^{+}/Cl^{-}	Mg^{2+}/Cl^{-}	HCO_3^{-}/Cl^{-}	SO_4^{2+}/Cl^{-}	$HCO3^{-}/Ca^{2+}$	$Na^{+}+K^{+}/Cl^{-}$	$Ca^{2+}/Ca^{2+}+HCO3^{-}$	Total Cations	$Ca^{2+}+Mg^{2+}$	$Ca^{2+}+Mg^{2+}/HCO3^{-}+SO4^{2-}$	$Na^{+}/Na^{+}+Ca^{2+}$
GW1	Ca-Cl-HCO_3	3.6	6.13	0.13	0.22	0.89	0	1.14	0.25	0.47	6.28	8.44	1.12	0.16
GW2	Ca-HCO_3- SO_4-Cl	10.59	9.75	0.49	0.45	1.48	1.19	0.31	0.88	0.76	6.21	6.36	1.96	0.11
GW3	Ca-Cl-SO_4	4.67	2.45	0.22	0.12	0.2	0.35	0.36	0.39	0.74	2.67	1.89	1.21	0.32
GW4	Ca-Cl-HCO_3	2.98	2.56	0.14	0.12	0.28	0.21	0.81	0.26	0.55	3.20	2.79	0.95	0.31
GW5	Ca-Cl-HCO_3	2.57	3.52	0.07	0.1	0.22	0.06	0.89	0.11	0.53	4.05	4.24	1.22	0.25
GW6	Cl-HCO_3	0.48	6.87	0.01	0.09	0.62	0.01	14.28	0.01	0.07	1.27	5.89	0.21	0.14
GW7	Cl-SO_4-HCO_3	0.73	7.42	0.01	0.15	0.27	0.45	2.48	0.03	0.29	1.05	1.40	0.36	0.13
GW8	Cl-HCO_3	0.48	8.62	0	0.06	0.22	0.09	7.65	0.01	0.12	1.93	5.09	0.29	0.12
GW9	Cl-HCO_3-SO_4	0.47	5.17	0.01	0.16	0.51	0.51	6.61	0.03	0.13	0.79	1.73	0.24	0.18
GW10	Cl-HCO_3-SO_4	0.87	10.07	0.01	0.16	0.92	0.35	6.52	0.02	0.13	1.24	4.04	0.24	0.10
GW11	HCO_3-Cl	0.48	9.89	0.01	0.22	1.24	0	11.88	0.02	0.08	1.09	4.34	0.26	0.10
GW12	HCO_3-Cl-SO_4	0.73	8.96	0.02	0.25	1.8	0.71	9.72	0.04	0.09	0.80	3.31	0.17	0.11
GW13	HCO_3-Cl-SO_4	0.75	16.67	0.01	0.22	1.29	0.42	7.83	0.02	0.11	1.25	4.51	0.22	0.06
GW14	Ca-Cl-HCO_3	1.67	10.59	0.03	0.17	0.58	0.21	2.04	0.04	0.33	0.64	1.12	0.58	0.10
GW15	HCO_3-Cl-SO_4	0.78	7.76	0.03	0.27	1.14	0.34	5.36	0.04	0.16	0.93	2.37	0.33	0.13
GW16	Cl-HCO_3-SO_4	1.47	11	0.02	0.17	0.61	0.45	2.49	0.03	0.29	0.73	1.40	0.39	0.09
GW17	Ca-Mg-HCO_3-Cl	1.06	18.58	0.02	0.3	1.03	0.2	3.21	0.03	0.24	0.33	0.69	0.50	0.06
GW18	Ca-HCO_3-ClSO_4	1.34	18.56	0.03	0.45	2.11	0.79	3.45	0.05	0.22	1.32	3.22	0.37	0.06
GW19	Cl-HCO_3	0.03	0.55	0	0.09	0.31	0.09	119.11	0.01	0.01	1.54	4.71	0.24	0.68
GW20	HCO_3-Cl	0.65	5.61	0.08	0.71	4.21	0.67	9.14	0.15	0.10	0.78	2.77	0.24	0.17
GW21	Cl-HCO_3	0.01	0.09	0.01	0.09	0.21	0.14	187.97	0.02	0.01	0.27	0.50	0.27	0.93
GW22	Mg-SO4-HCO_3-Cl	0.45	3.77	0.08	0.63	1.69	2.07	5.95	0.11	0.14	0.61	1.17	0.24	0.23
GW23	Mg-Cl-HCO_3-SO4	0.14	1.7	0.02	0.26	0.58	0.39	15.95	0.04	0.06	0.85	1.59	0.30	0.40
GW24	Cl-HCO_3-SO_4	0.3	4.22	0.02	0.26	0.67	0.55	8.66	0.03	0.10	1.09	2.23	0.27	0.21
GW25	Cl-HCO_3-SO_4	0.49	6.66	0.01	0.16	0.43	0.29	5.61	0.02	0.15	0.88	1.77	0.32	0.15
GW26	Cl-HCO_3	0.48	6.43	0.01	0.17	0.26	0.16	3.26	0.01	0.23	0.50	0.65	0.59	0.15
GW27	Mg-HCO_3-SO_4-Cl	0.2	3.64	0.08	1.39	3.22	1.48	11.41	0.09	0.08	0.55	1.09	0.36	0.24

Sample ID	Facies	Ca^{2+}/Mg^{2+}	Ca^{2+}/Na^{+}	Na^{+}/Cl^{-}	Mg^{2+}/Cl^{-}	HCO_3^{-}/Cl^{-}	SO_4^{2+}/Cl^{-}	$HCO3^{-}/Ca^{2+}$	$Na^{+}+K^{+}/Cl^{-}$	$Ca^{2+}/Ca^{2+}+HCO3^{-}$	Total Cations	$Ca^{2+}+Mg^{2+}$	$Ca^{2+}+Mg^{2+}/HCO3^{-}+SO4^{2-}$	$Na^{+}/Na^{+}+Ca^{2+}$
GW28	SO4-HCO_3-Cl	0.04	0.35	0.06	0.53	1.61	3.69	71.93	0.08	0.01	0.20	0.51	0.10	0.77
GW29	Mg-SO4-HCO_3	0.5	8.5	0.23	3.88	7.08	11.06	3.65	0.37	0.22	0.17	0.25	0.32	0.12
GW30	SO_4-Cl-HCO_3	1.07	5.29	0.08	0.42	0.98	2.7	2.2	0.11	0.31	0.25	0.36	0.23	0.18
GW31	Mg-Ca-HCO_3-Cl	0.67	5.21	0.23	1.8	2.6	0.09	2.14	0.35	0.32	0.28	0.32	1.12	0.18
GW32	Cl-HCO_3	0.26	2.03	0.01	0.1	0.21	0.01	7.49	0.02	0.12	0.35	0.53	0.62	0.36
GW33	Mg-HCO_3	0.22	2.13	0.53	5.14	4.6	0.02	4.08	0.73	0.20	0.40	0.32	1.36	0.35
GW34	Mg-Cl-HCO_3	0.44	9.77	0.01	0.22	0.42	0.01	4.42	0.02	0.18	0.99	1.56	0.72	0.11
GW35	Cl-SO_4	0.31	4.95	0.01	0.12	0.11	0.22	2.79	0.01	0.26	1.15	0.96	0.50	0.19
GW36	Mg-Cl-SO_4-HCO_3	0.28	5.22	0.03	0.56	0.35	0.91	2.23	0.05	0.31	0.57	0.38	0.57	0.18
GW37	Mg-HCO_3-Cl	0.56	7.75	0.03	0.35	1.23	0	6.26	0.04	0.14	0.60	1.45	0.45	0.13
GW38	Cl-SO_4	1.21	6.56	0.01	0.08	0.12	0.32	1.29	0.03	0.44	0.49	0.53	0.40	0.15
GW39	HCO_3-Cl-SO_4	0.25	3.83	0.01	0.18	1.05	0.64	23.42	0.02	0.04	0.52	2.29	0.13	0.23
GW40	Mg-SO_4-Cl-HCO_3	0.5	2.94	0.06	0.38	0.35	1.33	1.88	0.1	0.35	0.19	0.15	0.34	0.28
SW1	Mg-Cl	-	-	-	-	-	-	-	-	-	-	-	-	-
SW2	Mg-Cl	-	-	-	-	-	-	-	-	-	-	-	-	-
SW3	Mg-Cl	-	-	-	-	-	-	-	-	-	-	-	-	-
SW4	Na-Cl	-	-	-	-	-	-	-	-					

Appendix I:

DRY SEASON HYDROCHEMICAL FACIES AND SOME IONIC RATIOS OF A SHALLOW UNCONFINED AQUIFER IN THE LAGOS COASTAL BASIN

Sample ID	Facies	Ca^{2+}/Mg^{2+}	Ca^{2+}/Na^{+}	Na^{+}/Cl^{-}	Mg^{2+}/Cl^{-}	HCO_3^{-}/Cl^{-}	SO_4^{2+}/Cl^{-}	$HCO3^{-}/Ca^{2+}$	$Na^{+}+K^{+}/Cl^{-}$	$Ca^{2+}/Ca^{2+}+HCO3^{-}$	Total Cations	$Ca^{2+}+Mg^{2+}$	$Ca^{2+}+Mg^{2+}/HCO3^{-}+SO4^{2-}$	$Na^{+}/Na^{+}+Ca^{2+}$
GW1	Ca-Mg-Na HCO_3	1.56	2.08	1.45	1.93	4.65	0	1.55	2.21	0.17	1.26	0.87	1.06	0.36
GW2	Ca-HCO_3	2.11	3.23	1.24	1.9	10.02	0.02	2.5	2.35	0.12	1.22	0.87	0.59	0.26
GW4	Ca-Mg-HCO_3-Cl	2.14	2.34	0.9	0.99	4.18	0.02	1.98	1.41	0.12	1.24	0.85	0.74	0.33
GW5	Ca-HCO_3	2.82	2.56	2.41	2.19	16.03	0.03	2.6	3.5	0.14	1.12	0.79	0.52	0.31
GW6	Ca-Mg-Na-HCO_3	1.66	1.9	1.71	1.96	1.93	0.02	0.59	2.84	0.11	1.16	0.75	2.71	0.38
GW7	Ca-Mg-HCO_3	1.39	2.88	1.56	3.23	13.73	0	3.06	3.55	0.36	1.31	0.89	0.56	0.29
GW8	Ca-Mg-HCO_3	1.18	1.9	1.53	2.47	7.66	0	2.63	2.48	0.10	1.16	0.79	0.70	0.38
GW9	Ca-Mg-HCO_3	1.05	2.96	2.59	7.26	21.82	0.06	2.85	4.89	0.11	1.40	1.05	0.68	0.28
GW10	Ca-HCO_3	2.25	2.23	1	1	4.21	0	1.88	1.52	0.10	1.30	0.88	0.77	0.34
GW11	Ca-Mg-Na-HCO_3	2.3	2.68	1.86	2.17	7.15	0	1.44	3.76	0.15	1.33	0.87	1.00	0.30
GW12	Ca-HCO_3	2.99	3.37	2.07	2.33	11.53	0	1.65	3.45	0.19	1.13	0.82	0.81	0.25
GW13	Ca-Mg-HCO_3	1.47	1.96	2.94	3.91	15.94	0.03	2.77	4.01	0.17	1.29	0.92	0.61	0.37
GW14	Ca-Na-Mg-HCO_3	1.77	1.33	2.46	1.85	1.9	0.02	0.58	3.33	0.11	1.24	0.75	2.70	0.46
GW15	Ca-Mg-HCO_3	1.45	1.98	2.81	3.84	17.67	0	3.18	3.97	0.36	1.18	0.83	0.53	0.37
GW17	Ca-Mg-Na-HCO_3	1.87	2.11	2.67	3.01	12.2	0	2.17	4.4	0.09	1.23	0.81	0.71	0.35
GW18	Ca-Mg-Na-HCO_3	1.74	2.47	1.72	2.45	6.23	0.03	1.47	2.6	0.13	1.35	0.97	1.07	0.32
GW19	Ca-Na-Mg-HCO_3	2.32	1.55	3.4	2.27	9.06	0.04	1.72	4.28	0.18	1.37	0.87	0.83	0.43
GW20	Ca-Mg-HCO_3	1.6	2.37	1.55	2.29	9.99	0	2.73	2.65	0.16	1.27	0.88	0.60	0.33
GW21	Ca-Mg-Na-HCO_3	1.38	3.34	2.48	6.01	3.88	0.03	0.47	5.7	0.11	1.44	1.03	3.68	0.26
GW22	Ca-Mg-HCO_3	2.9	2.81	0.82	1.33	5.71	0.01	2.47	1.34	0.41	1.36	0.99	0.64	0.29
GW23	Ca-Mg-HCO_3	1.74	2.96	1.5	2.2	9.31	0	2.09	2.84	0.12	1.15	0.81	0.71	0.28
GW24	Ca-Na-HCO_3	2.03	1.4	3.56	3.2	17.43	0	3.5	5.16	0.14	1.18	0.72	0.47	0.45
GW25	Ca-Na-HCO_3	1.55	2.22	2.6	2.31	12.13	0.05	2.11	5.04	0.09	1.24	0.76	0.67	0.34

Sample ID	Facies	Ca^{2+}/Mg^{2+}	Ca^{2+}/Na^{+}	Na^{+}/Cl^{-}	Mg^{2+}/Cl^{-}	HCO_3^{-}/Cl^{-}	SO_4^{2+}/Cl^{-}	$HCO3^{-}/Ca^{2+}$	$Na^{+}+K^{+}/Cl^{-}$	$Ca^{2+}/Ca^{2+}+HCO3^{-}$	Total Cations	$Ca^{2+}+Mg^{2+}$	$Ca^{2+}+Mg^{2+}/HCO3^{-}+SO4^{2-}$	$Na^{+}/Na^{+}+Ca^{2+}$
GW26	Ca-Mg-HCO_3	2.49	2.65	1.26	2.41	5.91	0	1.77	2.21	0.13	1.17	0.84	0.97	0.30
GW27	Ca-Mg-HCO_3	1.38	2.68	2.57	3.94	11.53	0.01	1.68	3.71	0.16	1.28	0.95	0.94	0.30
GW28	Ca-Mg-HCO_3	1.74	3.22	1.96	2.97	12.02	0.04	1.9	3.05	0.16	1.16	0.87	0.77	0.26
GW29	Ca-Mg-HCO_3	2.13	2.5	1.71	2.36	10.65	0.03	2.49	2.42	0.15	1.31	0.96	0.62	0.31
GW31	Ca-Mg-HCO_3	1.82	1.52	2.33	1.78	9.91	0	2.8	4.33	0.12	1.12	0.62	0.54	0.43
GW32	Ca-Na-HCO_3	1.99	2.45	1.69	1.37	5.91	0.02	1.42	2.52	0.10	1.18	0.81	0.93	0.32
GW33	Ca-HCO_3	3.03	1.36	5.51	4.13	14.17	0.03	1.88	7.07	0.19	1.34	0.84	0.82	0.46
GW34	Ca-HCO_3	1.82	2.9	0.66	0.97	5.53	0	2.9	1.13	0.15	1.09	0.78	0.52	0.28
GW35	Ca-Mg-Na-HCO_3	1.97	1.71	2.31	3.05	2.29	0.02	0.58	3.16	0.10	1.23	0.85	3.05	0.40
GW36	Ca-Na-HCO_3	1.3	2.87	2.53	3.08	17.67	0	2.43	4.13	0.36	1.28	0.91	0.59	0.29
GW37	Ca-Mg-HCO_3	2.36	2.72	2.39	2.92	12.13	0	1.87	4.15	0.12	1.28	0.89	0.78	0.30
GW38	Ca-Mg-HCO_3	2.22	3.34	1.21	1.93	6.14	0.03	1.52	2.18	0.15	1.20	0.88	0.97	0.26
GW39	Ca-HCO_3	2.1	2.3	2.57	2.28	11.9	0	2.02	5.14	0.18	1.17	0.72	0.69	0.33
GW40	Ca-HCO_3	2.59	2.58	2.63	2.17	15.68	0.01	2.31	4.1	0.14	1.23	0.84	0.57	0.31
GW41	Ca-HCO_3	3.14	3.19	1.32	1.96	1.93	0.03	0.46	2.01	0.12	1.18	0.89	3.21	0.27
GW42	Ca-Mg-Na-HCO_3	2.15	2.78	1.8	2.44	13.45	0.04	2.69	2.69	0.42	1.17	0.86	0.55	0.29
GW43	Ca-Mg-Na-HCO_3	2.05	2.38	1.8	2.04	7.66	0	1.8	2.51	0.11	1.30	0.93	0.82	0.33
GW44	Ca-Mg-HCO_3	2.09	2.99	2.78	5.78	21.48	0.03	2.59	5.13	0.15	1.38	1.01	0.66	0.28
GW45	Ca-Mg-HCO_3	1.43	2.2	0.8	1.3	2.53	0.01	1.43	1.32	0.11	1.19	0.83	1.21	0.34

Appendix J:

DISTRIBUTION OF WATER TYPES IN THE LAGOS COASTAL BASIN

Serial No.	Water type	No. of Samples
Wet season		
1	Ca-Cl water	3
2	Mg-Cl water	11
3	Mg-SO_4 water	2
4	Mg-HCO_3 water	5
5	Mixed cationic 'Ca' dominating bicarbonate water	1
6	Mixed cationic 'Ca' dominating sulphate water	1
7	Mixed cationic 'Ca' dominating chloride water	2
8	Mixed cationic and anionic 'Ca' dominating bicarbonate water	1
9	Mixed cationic and anionic 'Ca' dominating chloride water	1
10	Mixed anionic 'Ca' dominating bicarbonate water	1
	Mixed anionic 'Ca' dominating chloride water	1
11	Mixed anionic 'Mg' dominating bicarbonate water	2
12	Mixed anionic 'Mg' dominating chloride water	3
13	Mixed anionic 'Mg' dominating sulphate water	2
14	Mixed cationic and anionic 'Mg' dominating bicarbonate water	3
15	Mixed cationic and anionic 'Mg' dominating chloride water	1
Dry season		
1	Ca-HCO_3 water	8
2	Mixed cationic 'Ca' dominating bicarbonate water	34

Appendix K:

PUBLISHED ARTICLES

PUBLICATION 1: V4, issue 11, doi: 10.1016/j.heliyon.2018.e00932

Heliyon

ELSEVIER

Received:
3 August 2018
Revised:
4 October 2018
Accepted:
8 November 2018

Cite as: M. A. Yusuf, T. A. Abiye, M. J. Butler, K. O. Ibrahim. Origin and residence time of shallow groundwater resources in Lagos coastal basin, south-west Nigeria: An isotopic approach. Heliyon 4 (2018) e00932. doi: 10.1016/j.heliyon.2018.e00932



Review Article

Origin and residence time of shallow groundwater resources in Lagos coastal basin, south-west Nigeria: An isotopic approach

M. A. Yusuf [a,b,*], **T. A. Abiye** [b], **M. J. Butler** [c], **K. O. Ibrahim** [d]

[a] *Department of Geology and Mineral Sciences, University of Ilorin, Ilorin, Nigeria*

[b] *School of Geosciences, University of the Witwatersrand, Johannesburg, South Africa*

[c] *i-Themba Labs, Gauteng, Johannesburg, South Africa*

[d] *Institute of Groundwater Studies, University of the Free State, Bloemfontein, South Africa*

* Corresponding author.

E-mail address: ajijolakewu@yahoo.com (M.A. Yusuf).

Abstract

Knowledge of the source of water in the Lagos coastal basin (LCB) groundwater system was to be found vital to the future development and management of the system. Stable and radioactive isotopic measurements have been employed to unravel the source of recharge and residence time of the shallow groundwater system, based on the sampling conducted in 2016 and 2017 on groundwater, surface water and rainfall. The concentration of tritium in the groundwater samples were very low and ranged from less than 1 to 2.8 TU, while measured ^{14}C contents ranged from 59.1 to 88 pMC. The $\delta^{18}O$ values of groundwater samples ranged from 4.81 and 3.98 ‰, while the $\delta^{2}H$ values ranged from -24.75 and -19.70 ‰ for the wet and dry seasons, respectively. The obtained results indicated non-existence of paleo recharge; rather all groundwater in the basin were found to be essentially of meteoric origin with intermittent surface water contributions. Moreover, shallow groundwater and surface water have

https://doi.org/10.1016/j.heliyon.2018.e00932
2405-8440/© 2018 The Authors. Published by Elsevier Ltd. This is an open access article under the CC BY-NC-ND license (http://creativecommons.org/licenses/by-nc-nd/4.0/).

PUBLICATION 2: doi/10.1016/j.gsd.2019.100222

Groundwater for Sustainable Development 9 (2019) 100222

Contents lists available at ScienceDirect

Groundwater for Sustainable Development

journal homepage: www.elsevier.com/locate/gsd

Research paper

Risks of groundwater pollution in the coastal areas of Lagos, southwestern Nigeria

M.A. Yusuf[a,b,*], T.A. Abiye[b]

[a] Department of Geology and Mineral Sciences, University of Ilorin, Ilorin, Nigeria
[b] School of Geosciences, University of the Witwatersrand, Johannesburg, South Africa

ARTICLE INFO

Keywords:
Groundwater
Pollution
Dar-zarrouk parameters
Protective capacity

ABSTRACT

Saltwater intrusion is a common problem associated with every coastal region all over the globe, and Lagos state is not an exception. This study was carried out in the coastal belt of Lagos, Southwestern Nigeria with the main objective of assessing the risk of shallow groundwater and its susceptibility to contamination. In this research, geophysical and geochemical techniques coupled with the concepts of Dar- Zarrouk (D-Z) parameters were employed. Resistivity measurements were taken at twelve vertical electrical sounding (VES) stations and eight 2-D resistivity profiles using the Schlumberger, dipole-dipole and pole-dipole arrays were analyzed and interpreted respectively. The D-Z parameters such as longitudinal conductance (S_L), transverse resistance (Tr), longitudinal resistivity (??L) and transverse resistivity (??T) data were computed from the qualitative interpretation of VES data to reveal the aquifer hydraulic characteristics. The 2-D sections display the lateral invasion of saline water within the aquifer systems and variations in resistivity of the subsurface being the geo-electric property that differentiates lithologies. The geo-electric model interpretation supported with available geologic information revealed four/five geo-electric layers namely; top sandy layer, clayey sand/sandy clay, clay and sand. Two aquifers (Upper and Lower) were delineated within the depth of investigation hosted mainly by sand and sandy clay/clayey sand. Furthermore, the longitudinal conductance data was used to predict the protective capacity of the coastal aquifer. Generally, the water table aquifer falls within the poor/weak protective capacity, while the lower semi-confined to confined aquifer is within the zone of good to excellent protective capacity. The lower aquifer is essentially impacted with saline intrusion while the phreatic aquifer contaminations are both from saline and anthropogenic sources. These assertions corroborate the geochemical results and previous findings in the study area. Hence, geophysical method with the use of D-Z parameters proved to be useful tool in the pollution assessment of groundwater.

1. Introduction

In Lagos state of Nigeria, especially in the coastal terrain, salt water intrusion is a common occurrence. The southwestern Nigeria, where Lagos is situated is characterized by two principal climatic seasons: the dry and wet seasons. The dry season usually extends from November to March while the wet season starts from April to October, with a brief break in August. The aquifer is adequately recharged with high annual rainfall (mean of over 2000 mm) while the depth to groundwater table are generally below 5.0 m in the coastal area (Offodile, 1992). Most rivers from south-western Nigeria drain into the Lagos lagoon. The occurrence of brackish/saline water is a major feature that characterizes the alluvium and underlying coastal plain sands aquifer contrary to what is obtainable in areas in the mainland of Lagos state.

The city can be accessed through road, rail, air and sea ports. Like every other coastal belt, it experiences various degrees of saline incursion especially along the coastline as a result of its sole reliance on the groundwater as the major source of potable water for domestic and industrial purposes, so as to compensate for inadequate supply of piped water (Adeoti et al., 2010). Groundwater availability however is unevenly distributed while the resource that is available has been polluted. Quality of groundwater drops when anthropogenic chemicals that threaten human health enter a water body through run-off, weathering or when concentration of natural elements fall short of required standard (Anudu et al., 2011). The sources of groundwater contaminants in the area under study may be classified into two; surface contaminants which migrate as leachates into groundwater and subsurface pollutants in the form of saline water intrusion. Increasing

* Corresponding author. Department of Geology and Mineral Sciences, University of Ilorin, Ilorin, Nigeria.
E-mail addresses: ajijolakewu@yahoo.com, asiribo.ma@unilorin.edu.ng (M.A. Yusuf), tamiru.abiye@wits.ac.za (T.A. Abiye).

https://doi.org/10.1016/j.gsd.2019.100222
Received 14 November 2017; Received in revised form 1 May 2019; Accepted 3 May 2019
Available online 04 May 2019
2352-801X/ © 2019 Published by Elsevier B.V.

APPENDIX L:

SUBMITTED MANUSCRIPTS

MANUSCRIPT 1: SUBMITTED TO SPRINGER JOURNAL OF ENVIRONMENTAL HEALTH SCIENCES (ENGE-D-18-02360R2)

Geo-environmental Studies from Borehole Logs in the Lagos Coastal Region, Nigeria.

M.A. Yusuf[1, 2*], T.A. Abiye[2], K.O. Ibrahim[1, 3] and B.A. Ojulari[4]

[1]Department of Geology and Mineral Sciences, University of Ilorin,
Ilorin, Nigeria; email:ajijolakewu@yahoo.com [2]School of Geosciences, University of the Witwatersrand,
Johannesburg, South Africa; Tamiru.Abiye@wits.ac.za
[3]Institute for Groundwater Studies (IGS), University of the Free State, Bloemfontein, South Africa
[4] Department of Chemical, Geological and Physical Sciences, Kwara State University, Nigeria
[1]Corresponding author: ajijolakewu@yahoo.com/ +2348035522483

Acknowledgements:

The authors would like to thank Mr. Oyebade, Mr. Kuseju, Mr. Adeogun and Mr. Agbalaya of Lagos state ministry of energy and mineral resources for providing geophysical logs. We are very grateful to the groundwater and geophysical services (GGS) limited for also providing parts of the geophysical logs. The logistic support and useful discussions provided by Mr. Ilori of Lagos state water corporation, is highly appreciated. The anonymous reviewers whose comments helped to significantly improve this manuscript are highly acknowledged.

ABSTRACT

Analysis of borehole logs with hydro-physical data from Lagos coastal belt, Southwestern Nigeria was carried out to facilitate lithological and geo-environmental assessment in the area. Forty-five (45) borehole logs and hydro-physical parameters from the study area were analyzed. The qualitative interpretation natural gamma ray (NGAM) shows the variations in lithology with depth. The shallow aquifer is made up of coastal plain sands and essentially unconfined aquifer with perched characteristics in places while the deep aquifer systems are made up of alternating sequence of sand and clayey sand is confined. The study revealed that the subsurface was intruded by saline water. The fresh/saline water boundaries from west to east (Victoria Island, Lekki, Ajah and Awoyaya) occur at depth ranges between 15 m and 355 m and truncated by extensive clay column at Sangotedo. Meanwhile, along Apapa-Ikoyi-Badore-Lakowe (west to east) fresh/saline water interface occurs at depth ranges of 14 m-112 m. Vast majority of the abandoned boreholes

MANUSCRIPT 2: SUBMITTED TO ELSEVIER JOURNAL OF HELIYON (HELIYON-2020-02205R2)

HYDROGEOCHEMICAL AND SALINITY APPRAISAL OF SURFICIAL LENS OF FRESHWATER AQUIFER ALONG LAGOS COASTAL BELT, SOUTH WEST, NIGERIA

M.A. Yusuf[1, 2], T.A. Abiye[2], K.O. Ibrahim[1] and H.O. Abubakar[1]

[1]Department of Geology and Mineral Sciences, University of Ilorin, Ilorin, Nigeria; email:ajijolakewu@yahoo.com
[2]School of Geosciences, University of the Witwatersrand, Johannesburg, South Africa; Tamiru.Abiye@wits.ac.za

ABSTRACT

In order to determine the hydrogeochemical model and salinity status of the surficial lens of freshwater aquifer in the Lagos coastal basin, physicochemical parameters and hydrogeochemical tools were employed. The geochemical tools include: Ionic ratio (s), Piper diagram, Durov diagram, Gibb's diagram and Phreeqc software. A total of eighty-two (82) groundwater samples were collected from shallow aquifers in the study area during dry and wet seasons to reveal the seasonal variation. The physicochemical parameters in groundwater are within the WHO acceptable limit for drinking water with the exception of TDS and EC resulting from carbonate dissolution and marine influence. The water samples revealed chemical facies rich in (Ca, Mg, HCO_3 and Cl) and (Ca and HCO_3) for wet and dry seasons respectively, while Mg-Cl and Na-Cl water types characterised the lagoon and the ocean. The chemical facies indicated recently recharged groundwater and this assertion is substantiated by the ionic ratios estimation. The ionic constituents of the groundwater are essentially derived from the carbonate rock dissolution evident from abundant Ca^{2+} and HCO_3^- concentration. In a descending order, water-rock interaction, ion exchange, leaching and evaporation are the geochemical processes controlling the groundwater quality in the area. In addition, the equilibrium specification

MANUSCRIPT 3: SUBMITTED TO JOURNAL OF GROUNDWATER FOR SUSTAINABLE DEVELOPMENT (GSD-20-357R1)

Application of environmental isotopes in sustainability assessment of the groundwater resources of Lagos Coastal Basin (LCB), south-west, Nigeria

Mumeen .A. Yusuf[1, 2*], Tamiru .A. Abiye[2], and Michael .J. Butler[2]

[1]Department of Geology and Mineral Sciences, University of Ilorin, Ilorin, Nigeria
email:ajijolakewu@yahoo.com, ORCID: https://orcid.org/0000-0002- 4849-3508
*Corresponding author
[2]School of Geosciences, University of the Witwatersrand, Johannesburg, South Africa
email:Tamiru.Abiye@wits.ac.za, ORCID: https://orcid.org/0000-0002-9327-1955
[3]Environmental Isotope Group, i-Themba Labs, Private Bags X11, P.O. Box Wits 250, Johannesburg, South Africa

Abstract

Owning to the fact that groundwater is the main source of water supply for both domestic and commercial activities by the inhabitants of the Lagos Coastal Basin (LCB) in Lagos, Nigeria, detailed study with respect to recharge and Mean Residence Time (MRT) of both shallow aquifer and deep groundwater samples across the area was carried out to enable proper management of this resource. The study used environmental isotopes of water particularly carbon (^{14}C) and tritium (^{3}H) contents in the groundwater to determine the mean residence time, and stable isotope of ^{2}H, ^{18}O and $^{13}C$to reveal source of recharging water. The stable Isotope of $\delta^{18}O$ and $\delta^{2}H$ plot around and along the local meteoric water line with mixing line represented by $\delta^{2}H = 6.8^{*}\ \delta^{18}O + 6.9$ ‰; $\delta^{2}H = 3.48^{*}\ \delta^{18}O + 2.8$ ‰, for deep and shallow aquifer, respectively, indicating meteoric origin. The tritium results revealed evidence of mixture of recent recharge with low ^{14}C content water. The low ^{14}C resulted in the MRT between 1050 ±10 and 4350±10 in shallow groundwater, while the deep aquifer are old recharged water with MRT range from 7400 ±10 to 12030 ±10 years. Integrated results from the mean annual temperature correlation, ^{18}O, ^{14}C activity and ^{14}C age showed that the shallow aquifer was recharged in Holocene to present (modern climatic condition),whereas the confined deep groundwater recharge took place during Late Pleistocene (more humid condition than present). Consequently, the unconfined shallow aquifer is considered